

ENANTIOMERIC SEPARATIONS AND NEW CHIRAL STATIONARY PHASES

by

CHUNLEI WANG

Presented to the Faculty of the Graduate School of
The University of Texas at Arlington in Partial Fulfillment
of the Requirements for the Degree of

DOCTOR OF PHILOSOPHY

The University of Texas at Arlington

December 2009

Copyright © by Chunlei Wang 2009

All Rights Reserved

This dissertation is dedicated to those:

who raised me and supported me,

who educated me and molded me,

who directed me and encouraged me,

who challenged me and inspired me,

and who loved me and delighted me.

ACKNOWLEDGEMENTS

I would like to gratefully thank my research advisor, Dr. Daniel Armstrong, for his support and guidance during my graduate studies. Dr. Armstrong inspired me not only as a pioneering scientist in the area of enantiomeric separations, but also as a person effusing his excellence from every aspect. I consider myself extremely fortunate to have the opportunity to learn from him.

I would also like to thank Dr. Sandy Dasgupta and Dr. Richard Guan for their help and service on my research committee. It has been a great honor to have you serve on my committee.

I would especially like to thank my parents and my aunt for their unconditional support for my best education and general well being. I would also like to thank my wife Xinghua for her countless sacrifices for our family, and my little one Sophie for the joy she brought to our family.

I greatly appreciate the assistance of all faculty and staff in the Department of Chemistry and Biochemistry at the University of Texas at Arlington, especially Barbara for taking care of my orders and paperwork, and Brian for helping me to set up the LC column packing station. I also thank my fellow group members and other colleagues in the Chemistry Department (Adam, Cliff, Molly, Max, Xinxin, Renee, BaoYe, Rongfang, Ping, Violet, Koko, Xiaotong, Zach, Eranda, Sophie, Qing, Yasith, Sarantha, Jonathon, Edra, Eva, Nilusha, Tharanga, Dilani, Aruna, Sam, David, Jianguang, Mr. Risely, Dr. Cintron, Dr. Berthod, Dr. Schug, and Dr. Kroll) for their help and friendship.

November 24, 2009

ABSTRACT

ENANTIOMERIC SEPARATIONS AND NEW CHIRAL STATIONARY PHASES

Chunlei Wang, PhD

The University of Texas at Arlington, 2009

Supervising Professor: Daniel W. Armstrong

Chirality is an important concern for biological activity because asymmetry dominates biological processes at a molecular level. After nearly thirty years of development, liquid chromatographic separations on chiral stationary phases (CSPs) have become the state-of-art technology for resolution of enantiomeric compounds. However, with the trend in the pharmaceutical industry to replace racemate drugs with their single enantiomer forms, chiral methods are in ever increasing demand. The efficient development of enantiomeric separation methods is still challenging and time consuming. In this thesis, we present new approaches for the enantiomeric separation of two important pharmaceutical compounds, the development of three new CSPs, and mechanistic studies of the cyclofructan-based CSPs.

Part one discusses the enantiomeric separation of β -lactams and astaxanthin on cyclodextrin- and cellulose-based CSPs, respectively. Part two presents three types of new CSPs, i.e., the boromycin CSP, the cyclofructan-based CSP, and a synthetic polymer-based CSP. Supercritical fluid chromatography (SFC) separations on polymeric CSPs are also discussed in detail. Part three examines the host-guest complexation between cyclofructans and metal cations, application of its host-guest complexation for the purification of cyclofructans, and possible chiral recognition mechanisms of cyclofructans.

TABLE OF CONTENTS

ACKNOWLEDGEMENT	iv
ABSTRACT	v
LIST OF ILLUSTRATIONS	viii
LIST OF TABLES	xvi
Chapter	Page
1. INTRODUCTION	1
2. SEPARATION OF ENANTIOMERS OF B-LACTAMS BY HPLC USING CYCLODEXTRIN-BASED CHIRAL STATIONARY PHASES	4
3. RAPID BASELINE SEPARATION OF ENANTIOMERIC AND MESO FORMS OF ALL- <i>TRANS</i> -ASTAXANTHIN, 13- <i>CIS</i> -ASTAXANTHIN, ADONIRUBIN, AND ADONIXANTHIN IN STANDARDS AND COMMERCIAL SUPPLEMENTS	16
4. EMPIRICAL OBSERVATIONS AND MECHANICAL INSIGHTS ON THE FIRST BORON-CONTAINING CHIRAL SELECTOR FOR LC AND SFC	31
5. DEVELOPMENT OF NEW HPLC/SFC CHIRAL STATIONARY PHASES BASED ON NATIVE AND DERIVATIZED CYCLOFRUCTANS	53
6. PREPARATION AND EVALUATION OF A NEW SYNTHETIC POLYMERIC CHIRAL STATIONARY PHASE FOR HPLC BASED ON THE <i>TRANS</i> -9, 10-DIHYDRO-9, 10-ETHANOANTHRACENE- (11 <i>S</i> , 12 <i>S</i>)-11, 12-DICARBOXYLIC ACID BIS-4-VINYLPHENYLAMIDE MONOMER	83
7. SUPER/SUBCRITICAL FLUID CHROMATOGRAPHY SEPARATIONS WITH FOUR SYNTHETIC POLYMERIC CHIRAL STATIONARY PHASES.....	105
8. STUDY OF COMPLEXATION BETWEEN CYCLOFRUCTANS AND ALKALI METAL CATIONS BY ELECTROSPRAY IONIZATION MASS SPECTROMETRY AND DENSITY FUNCTIONAL THEORY CALCULATIONS	128
9. SEPARATIONS OF CYCLOINULOOOLIGOSACCHARIDES VIA HYDROPHILIC INTERACTION CHROMATOGRAPHY (HILIC) AND LIGAND-EXCHANGE CHROMATOGRAPHY	143

10. CYCLOFRUCTANS, A NEW CLASS OF CHIRAL STATIONARY PHASE	154
11. CONCLUSIONS AND REMARKS	175
REFERENCES	180
BIOGRAPHICAL INFORMATION	186

LIST OF ILLUSTRATIONS

Figure	Page
2.1 Selected chromatograms showing the best (top two), medium (middle two) and worst (bottom two) enantioseparation for the substituted β -lactams	9
2.2 Performance of different cyclodextrin-based CSPs in different separation modes: (A) Overall Enantioseparation results for 9 CSPs in all separation modes; (B) Different enantioseparation results in three separation modes on the three aromatic derivatized cyclodextrin CSPs	10
2.3 Comparison of separations resulting from the use of different organic modifiers. Compound 10 was separated on the Cyclobond I 2000 DMP column using the following mobile phases: A) 70/30 water/methanol and B) 85/15 water/acetonitrile	10
2.4 Retention times of 13 β -lactams on four Cyclodextrin-based CSPs (α , β , γ , and DM). Note: the mobile phase for α , β , γ -cyclodextrin CSPs is acetonitrile-water (1/99), while it is acetonitrile-water (5/95) for Cyclobond I-2000 DM CSP	14
3.1 Structure of astaxanthin geometrical isomers (A) all- <i>trans</i> -astaxanthin, (B) 9- <i>cis</i> -astaxanthin, (C) 13- <i>cis</i> -astaxanthin, and stereoisomers of all- <i>trans</i> -astaxanthin: (D) (3S,3'S)-all- <i>trans</i> -astaxanthin, (E) (3R,3'S)-all- <i>trans</i> -astaxanthin, and (F) (3R,3'R)-all- <i>trans</i> -astaxanthin	18
3.2 Monomer structures of the CSPs used in this study	18
3.3 Comparison of retention, selectivity, efficiency, and resolution of the all- <i>trans</i> -astaxanthin separations with mobile phases of different acetonitrile/methyl t-butyl ether compositions. k_1 is the retention capacity of the first eluted isomer (SS); α is the selectivity between the RR and SS isomer; N is the number of plates for the second eluted isomer (meso); R_s is the resolution between RR and SS isomers	24
3.4 Separations of all- <i>trans</i> -astaxanthin on Chiralpak IC CSP. Mobile phases: (A), MtBE/ACN 50/50; (B), MtBE/ACN 95/5; and (C) ACN 100%	24
3.5 Separation of (A) all- <i>trans</i> -astaxanthin, (B) adonrubin, and (C) adonixanthin on Chiralpak IC CSP with MtBE/ACN 50/50 mobile phase. Peak 1, 2, and 3: (3S,3'S), (3S,3'R), and (3R,3'R)-astaxanthin; peak 4, 5: undetermined (3R/S)-adonrubin; peak 6, and 7*: (3S, 3'S), and (3R, 3'R)-adonixanthin. *The split in peak 7 is due to impurities in (3R,3'R)-adonixanthin sample from CaroteNature (Lupsingen, Switzerland)	26
3.6 Separation of astaxanthin isomers. (A,D), isomerized mixtures of <i>cis</i> and <i>trans</i> -astaxanthin obtained by exposing all- <i>trans</i> -astaxanthin to daylight for 6 days; (B,E), all- <i>trans</i> -astaxanthin purified from isomerized mixtures by preparative	

C18 separation; (C,F) <i>cis</i> -astaxanthin (mainly 13- <i>cis</i>) purified from isomerized mixtures by preparative C18 separation. (A-C), analytical C18 stationary phase from Astec, MeOH/ACN/DCM/H ₂ O 85/5/5.5/4.5; (D-E), Chiralpak IC CSP, MtBE/ACN 50/50	28
3.7 Chromatograms obtained with Circular Dichroism (CD) detector on Chiralpak IC CSP. (A) all- <i>trans</i> -astaxanthin, and (B) 13- <i>cis</i> -astaxanthin. Top chromatograms were obtained using chiroptical detector (see Experimental), are the bottom chromatograms utilized UV detector (330 nm). Mobile phase: MtBE/ACN 50/50	30
3.8 Separation of all four stereoisomers (peak 1-4) of 13- <i>cis</i> -astaxanthin on Chiralpak IB CSP. Mobile phase: heptane/aceton 95/5. Note: small peaks in the chromatogram are possibly other forms of <i>cis</i> isomers of astaxanthin co-eluted with 13- <i>cis</i> -astaxanthin on the preparative C18 column	30
4.1 (A) Molecular structure of boromycin . (B) Face view and (C) side view of <i>des</i> -val-boromycin ball and stick model. (D) Space filling model of <i>des</i> -val-boromycin: side view. Color code: carbon: black, hydrogen: white, oxygen: red and boron: green	35
4.2 Chromatograms showing typical separations on the boromycin CSP: (A) <i>cis</i> -1-amino-2-indanol, (B) 4-chlorophenylalanine ethyl ester hydrochloride, (C) 1-(2-naphthyl)ethylamine and (D) phenethylsulfamic acid. Mobile phases: (A), methanol/1,4-dioxane/tetramethylammonium nitrate (TMAN) 80/20/5 mM; (B), (C) and (D), methanol/acetonitrile/TMAN 70/30/30 mM. Note that chromatogram D is a separation of the only compound in this study that wasn't a primary amine	46
4.3 Effects of organic modifiers in a methanol mobile phase on the separation of: A, B & C = methionine beta-naphthylamide and D, E & F = tyrosinol hydrochloride. Mobile phases: (A), methanol/acetonitrile/TMAN 80/20/10 mM; (D), methanol/acetonitrile/TMAN 60/40/10 mM; (B), (E), methanol/ethyl acetate/TMAN 70/30/5 mM; (C), (F), methanol/1,4-dioxane/TMAN 80/20/5 mM	46
4.4 Separations of <i>trans</i> -1-amino-2-indanol using a methanol mobile phase: (A) without and (B) with 10 mM TMAN (see Results and Discussion for details.) (A): $k'_1=14.0$, $\alpha=1.24$, $R_s=1.3$; (B): $k'_1=0.553$, $\alpha=1.29$, $R_s=1.6$	47
4.5 Separations of <i>trans</i> -1-amino-2-indanol using methanol as the mobile phase with 10mM additives of: (A) ammonium nitrate, (B) tetramethylammonium nitrate (TMAN), (C) tetraethylammonium nitrate (TEAN), (D) tetrapropylammonium chloride (TPAC) and (E) tetrabutylammonium nitrate (TBAN)	47
4.6 (A), Retention of the first eluted (k'_1) and the second eluted (k'_2) enantiomers of homocysteine thiolactone hydrochloride as the function of mobile phase organic modifier composition. Mobile phases: methanol/acetonitrile/TMAN (100-x)/x/10 mM. (B), Retention of the first eluted (k'_1) and the second eluted (k'_2) enantiomers of <i>trans</i> -1-amino-2-indanol as the function of the tetramethylammonium nitrate additive concentration. Mobile phases: methanol with various amount of TMAN	49
4.7 Supercritical Fluid Chromatography (SFC) enantiomeric separations of (A) DL-tryptophan benzyl ester , (B) DL-methionine beta-naphthylamide, and	

(C) DL-tryptophan methyl ester hydrochloride on the 15 cm boromycin CSP column. Mobile phase, CO ₂ /methanol(20 mM TMAN) 70/30; flow rate, 4 mL/min; temperaturer, 40 °C ; and column back pressure, 100 bar	49
4.8 Comparison of retention behavior of an achiral primary amine (2-phenethylamine) in its free base form (A), and in the hydrochloride salt form (B) on the boromycin CSP. Mobile phase: 100% methanol	51
5.1 Structure of cyclofructan. (A) Molecular structure of CF6, CF7 and CF8; (B-D) Crystal structure of CF6: B. side view; C. hydrophobic side up; D. hydrophilic side up. Color scheme: oxygen atoms are red and carbons are black. Hydrogens are not shown	55
5.2 Scheme of chemically-bonded CF6 stationary phase and derivatized-CF6 CSPs and chemical structure of all derivatizing groups	59
5.3 Separation of primary amines on derivatized-CF6 stationary phases with different substitution degrees. Analytes and mobile phases are: (A) normetanephrine hydrochloride, 75ACN/25MEOH/0.3AA/0.2TEA (top), 60ACN/40MEOH/0.3AA/0.2TEA (bottom); (B) 1-aminoindan, 60ACN/40MEOH/0.3AA/0.2TEA (top and bottom)	64
5.4 Edge view of CF6 derivatized with (A) six methyl carbamate groups and (B) eighteen R-naphthylethyl carbamate groups. The color coding is: oxygen atoms are red, carbon atoms are black and nitrogen atoms are blue. Hydrogen atoms are not shown. Compare these edge views with that of native cyclofructans in Figure 5.1B	65
5.5 Comparison between aromatic- and aliphatic-derivatized-CF6 CSPs. The analyte is DL-tryptophanol. The chromatographic data and mobile phases are: (A) $k_1=4.66$, $\alpha=1.12$, $R_s=1.4$, 75ACN/25MEOH/0.3AA/0.2TEA; (B) $k_1=3.39$, $\alpha=1.15$, $R_s=2.7$, 60ACN/40MEOH/0.3AA/0.2TEA; (C) $k_1=3.03$, $\alpha=1.12$, $R_s=1.7$, 60ACN/40MEOH/0.3AA/0.2TEA	66
5.6 Comparison between native- and aromatic-functionalized CF6 chiral columns. The analytes is N-(3,5-dinitrobenzoyl)-DL-leucine. Mobile phases: (A) 90heptane/10ETOH/0.1TFA; (B) 70heptane/30ETOH/0.1TFA	66
5.7 Comparison between methyl carbamate- and methyl thiocarbamate-CF6 CSPs. The analyte and mobile phase are cis-1-amino-2-indanol, and 60ACN/40MEOH/0.3AA/0.2TEA, respectively	70
5.8 Separation of 1,2,2-triphenylethylamine on the IP-CF6 column. The chromatographic data and mobile phases are: (A) $k_1=2.09$, $\alpha=1.25$, $R_s=1.4$, 70heptane/30ETOH/0.1TFA; (B) $k_1=1.14$, $\alpha=1.16$, $R_s=1.6$, 75ACN/25MEOH/0.3AA/0.2TEA	70
5.9 Selected chromatograms showing enantioseparations of various analytes on different derivatized-CF6 columns. The analytes and mobile phases are: (A) Bis-[(R/S)-1-phenylethyl]amine, 90H10E0.1TFA; (B) α -Methyl-9-anthracenemethanol, 98heptane/2IPA/0.1TFA; (C) Tröger's base, 70heptane/30ETOH; (D) Thalidomide, 70heptane/30ETOH/0.1TFA	77
5.10 Complimentary character of the aromatic-derivatized CF6 CSPs. The analyte	

is 3,5-dinitro-N-(1-phenylethyl)benzamide. The CSPs and mobile phases are: (A) 3,5-dimethylphenyl carbamate-CF6 CSP, 70heptane/30ETOH/0.1TFA; (B) R-naphthylethyl carbamate-CF6 CSP, 50heptane/50ETOH/0.1TFA; (C) S- α - methylphenyl carbamate-CF6 CSP, 70heptane/30ETOH/0.1TFA	79
5.11 Separation of 6,6'-dibromo-1,1'-bi-2-naphthol in the normal phase mode and reversed phase mode on the DMP-CF6 column. The chromatographic data and mobile phases are: (A) $k_1=0.74$, $\alpha=1.58$, $R_s=4.7$, 70heptane/30ETOH; (B) $k_1=2.51$, $\alpha=1.03$, $R_s=0.6$, 50ACN/50water	79
5.12 Effect of alcohol modifier on enantioseparation in the normal phase mode on the DMP-CF6 column. The mobile phase is 90heptane/10 alcohol modifier. The analyte is N-benzoyl-DL-phenylalanine β -naphthyl ester. The chromatographic data are: (A) $k_1=3.23$, $\alpha=1.05$, $R_s=0.8$; (B) $k_1=4.00$, $\alpha=1.10$, $R_s=1.7$	80
5.13 Temperature effect on separation of trans-stilbene oxide on the IP-CF6 column. The mobile phase is 100% heptane. The chromatographic data: (A) $k_1=0.62$, $\alpha=1.10$, $R_s=1.3$; (B) $k_1=0.80$, $\alpha=1.16$, $R_s=2.0$	80
5.14 Loading test on the RN-CF6 column. The analyte is N-(3,5-dinitrobenzoyl)-DL- phenylglycine. The mobile phase is 85ACN/15MEOH/0.3AA/0.2TEA. Injection volumes are: 5 μ L (top) and 100 μ L (bottom). UV detection: 350 nm	81
5.15 SFC chromatogram of althiazide on the RN-CF6 column. The gradient mobile phase is as described in EXPERIMENTAL SECTION	81
5.16 Separation of dansyl-norleucine cyclohexylammonium salt on the dimethylphenyl carbamate-CF7 CSP. The mobile phase is 80heptane/20ETOH/0.1TFA	81
6.1 Preparation of the poly-DEABV chiral stationary phase	89
6.2 Summary of the number of observable and baseline separations achieved on the poly-DEABV CSP	100
6.3 The effect of polar modifier on the enantiomeric separations of compounds 6 (a, b)) and 24 (c, d)) in the normal phase mode. Mobile phase: a) Heptane/Ethanol/TFA = 90/10/0.1, b) Heptane/Isopropanol/TFA = 90/10/0.1, c) Heptane/Ethanol/TFA = 60/40/0.1, d) Heptane/Isopropanol/TFA = 50/50/0.1. Enantioselectivity α : a) $\alpha = 1.30$, b) $\alpha = 1.39$, c) $\alpha = 1.49$, d) $\alpha = 1.67$. Resolution R_s : a) $R_s = 2.7$, b) $R_s = 1.8$, c) $R_s = 1.8$, d) $R_s = 1.4$. Number of theoretical plates of the first peak N_1 : a) $N_1 = 2600$, b) $N_1 = 700$, c) $N_1 = 800$, d) $N_1 = 200$	100
6.4 The effect of the acidic additive on the enantiomeric separations of compound 33 (a, b)) and 31 (c, d)) in the normal phase mode. Mobile phase: a), c) Heptane/ Ethanol/TFA = 60/40/0.1, b), d) Heptane/Isopropanol/TFA = 60/40. Enantioselectivity α : a), b) $\alpha = 1.30$, c) $\alpha = 1.87$, d) $\alpha = 1.54$. Resolution R_s : a), b) $R_s = 1.8$, c) $R_s = 2.8$, d) $R_s = 1.4$	102
6.5 The effect of sample loading on the enantiomeric separation of compound 30 with a) 1.0 μ g and b) 1000 μ g of compound injected on the poly DEABV CSP. Mobile phases: a), b) Heptane/Ethanol/TFA = 60/40/0.1. Enantioselectivity α : a) $\alpha = 4.11$, b) $\alpha = 2.94$. Resolution R_s : a) $R_s = 5.1$, b) $R_s = 2.4$	102

6.6 Comparison of the enantiomeric separations of compound 13 (a, b, c) and 30 (d, e, f) on the P-CAP (a, d), poly-DPEDA (b, e), and poly-DEABV (c, f) CSPs. Mobile phase: a) Heptane/Ethanol/TFA = 90/10/0.1, b) Heptane/Isopropanol = 80/20, c) Heptane/Isopropanol = 50/50, d) Heptane/Ethanol/TFA = 80/20/0.1, e) Heptane/Isopropanol/TFA = 70/30/0.1, f) Heptane/Ethanol/TFA = 60/40/0.1. Enantioselectivity α : a) $\alpha = 1.36$, b) $\alpha = 1.23$, c) $\alpha = 1.07$, d) $\alpha = 1.07$, e) $\alpha = 1.41$, f) $\alpha = 3.93$	104
7.1 The monomer of the polymeric chiral stationary phases used. a- P-CAP (<i>trans</i> -1,2-cyclohexanediyl-bis acrylamide) , b- P-CAP-DP (N,N'-[(1R,2R)-1,2-diphenyl-1,2-ethanediyl] bis-2-propenamide), c-DEABV (<i>trans</i> -9,10-dihydro-9,10-ethanoanthracene-(11S,12S)-11,12-dicarboxylic acid bis-4-vinylphenylamide), d-DPEVB (N,N'-[(1R,2R)-1,2-diphenyl-1,2-ethanediyl] bis[4-vinylbenzamide]	108
7.2 Overall results obtained with the four synthetic polymeric chiral stationary phases in subcritical mode. Top diagram: number of separations obtained on each CSPs. Bottom diagram: the number of compounds that were separated only by one single CSP or 2 or 3 or all 4 CSPs. The percentages refer to the number of compounds from the 88 compound set shown in Table 7.1	120
7.3 Overview of the results obtained on the four polymeric CSPs with the 88 chiral compounds evaluated in subcritical mode with CO ₂ /methanol/trifluoroacetic acid mobile phases, see Table 1 for full details. A solid dark vertical bar over the compound number indicates an observable separation ($R_s > 0.3$). A vertical bar with horizontal stripes doubling a bar indicates a baseline separation ($R_s > 1.4$) and a light vertical bar with wave lines indicates that the compound was only separated on that particular CSP	121
7.4 Enantioseparation of DNB-leucine (3 left chromatograms) and DNB-phenylglycine (3 right chromatograms) on the indicated polymeric chiral stationary phases. Column 250 x 4.6 mm with 5 μ m silica particles bonded by the indicated selector, subcritical mobile phase with CO ₂ + methanol (+ 0.2% v/v TFA) (proportion in Table 7.1, Compounds 63 and 64), 100 bar, 4 ml/min, 31°C, UV detection 254 nm	123
7.5 Separation of the enantiomers of N-(α -methylbenzyl) phthalic acid monoamide (16) on the DEABV CSP. Chromatogram A: normal phase heptane/EtOH 70%/30% (+0.1% v/v TFA), 1 ml/min, $\alpha = 1.13$, $R_s = 1.2$; Chromatogram B: SFC CO ₂ /MeOH 75/25% v/v (+0.2% v/v TFA), 100 bar, 4 ml/min, 31°C, $\alpha = 1.14$, $R_s = 1.4$; Chromatogram C: SFC CO ₂ /MeOH 70/30% v/v (+0.2% v/v TFA), 100 bar, 4 ml/min, 31°C, $\alpha = 1.12$, $R_s = 1.3$. Separation of the enantiomers of Furoin (13) on the polymeric P-CAP-DP CSP. Chromatogram D: normal phase mode, mobile phase heptane/IPA 80/20 %v/v (with 0.1% TFA), 1 ml/min, $\alpha = 1.69$, $R_s = 3.7$; Chromatogram E: SFC CO ₂ /MeOH 90/10% v/v (+0.2% v/v TFA), 100 bar, 4 ml/min, 31°C, $\alpha = 1.25$, $R_s = 2.0$, detection UV 254 nm	125
7.6 Efficiency variations on the P-CAP-DP chiral stationary phase. Left chromatogram: separation of the enantiomers of 1,5-dihydroxy-1,2,3,4-tetrahydronaphthalene (28), mobile phase, CO ₂ + 15% v/v (MeOH + 0.2% v/v TFA); right chromatogram: enantioseparation of Chlorthalidone (45), mobile phase, CO ₂ + 40% v/v (MeOH + 0.2% v/v TFA). Total flow rate 4 mL/min, 31°C, 100 bar, UV detection 254 nm	126
8.1 (A) Molecular structure of CF6. (B) 3-D structure of CF6 with only 18-crown-6	

skeleton and two neighboring fructofuranose units: one is “inward-inclined” and the other is “outward-inclined”. All hydrogen atoms have been removed for visual clarity. Color coding: carbon, gray; oxygen, red	130
8.2 Sample mass spectrum obtained by electrospraying 50% aqueous methanol solution of 1:1 (1.0×10^{-4} M each) CF6 and NaCl	133
8.3 The linear fit of ESI-MS peak intensity vs. concentration of 1:1 CF6 and NaCl in 50% aqueous methanol solution. Error bars represent one standard deviation from the mean	133
8.4 Comparison of ESI-MS spectra between the β -CD and CF7 when complexing with Li^+ and Na^+ . (A) 1:2 complexes is more favorable for Li^+ than for Na^+ ; (B) CF7 gives the opposite trend, i.e., 1:2 complexes is more favorable for Na^+ than for Li^+ . Figure A is reprinted from reference 88 with permission	136
8.5 Competitive binding of (A) CF6 and (B) CF7 with all alkali metal cation and ammonium chlorides	137
8.6 Collision induced dissociation mass spectra of complexes formed by ESI-MS: (A) $(\text{CF}_6 + \text{Na} + \text{K})^{2+}$ and (B) $(\text{CF}_6 + \text{Rb} + \text{Cs} + \text{Cl})^+$	139
8.7 Ball and stick model of optimized CF6- Na^+ complex: (A) side view; (B) top view. Color coding: sodium, blue; carbon, gray; oxygen, red; hydrogen, white. The plane defined by three O-3(<i>i</i>) atoms is shaded light gray. The size of sodium is enlarged in order to differentiate from C, H, and O atoms. Hydrogen atoms attached to the carbons have been removed for visual clarity	141
9.1 Chemical structure of (A) cyclofructans and (B) cyclodextrins	145
9.2 Separation of (A) CFs and (B) CFs and CDs on the β -cyclodextrin column. Mobile phases: (A), ACN/water 70/30; (B) ACN/water 72/28	148
9.3 Plots of retention time of (A) CFs and (B) CDs vs. water percentage in the aqueous ACN mobile phases on the β -cyclodextrin column	148
9.4 (A) Separation of CFs on the Li-SCX column using an ACN/water 65/35 mobile phase. (B) Plot of retention time of CFs vs. water percentage in the aqueous ACN mobile phases on the Li-SCX column	150
9.5 Separations of CFs on (A) the Ba-SCX column and (B) the Ag-SCX column. Mobile phases: (A) water; (B) MeOH/water 80/20	150
9.6 Separation of CFs on the Rb-SCX column using an ACN/water 65/35 mobile phase	151
9.7 Separation of CFs on the K-SCX column using different mobile phases: (A) ACN/water 40/60; (B) ACN/water 65/35	151
9.8 Separation of CDs under various tested conditions: (A) β -cyclodextrin column, ACN/water 65/35; (B) Li-SCX column, ACN/water 65/35; (C) Ba-SCX column, ACN/water 55/45; (D) Ag-SCX column, MeOH/water 97/3; (E) Ag-SCX column, ACN/water 70/30; (F) Rb-SCX column, ACN/water 65/35; and (G) K-SCX column, ACN/water 65/35	152

10.1 Molecular structure of cyclofructans	155
10.2 Inward and outward included fructofuranose units on the crown ether rim of CF6. The angle $O_{center}-C2-C3$ is 92° and 139° for inward and outward included fructofuranose units, respectively. O_{center} is the average position of six oxygen atoms on the crown ether rim, and is colored pink. Only two fructosefuranose units and part of the crown ether rim are shown for clarity reason. Carbon atoms are colored gray, oxygen atoms red. The suffix “(i)” and “(o)” are included in atom labels to indicate that the atom is in the “inward” inclined and “outward” inclined fructofuranose units, respectively	155
10.3 Comparison of the macrocycle in CF6 with that in 18-crown-6: (A) the oxygen atoms are in the gggggg conformation in 18-crown-6 and K^+ complexes. (B) the oxygen atoms are alternatively in the gtgtgt conformation in the macrocycle in CF6; Color coding: carbon, gray, oxygen, red. Hydrogen atoms are left out for clarity purpose	157
10.4 Space filling model of CF6: (A) view from the hydrophobic side; (B) view from the hydrophilic side. Color coding: carbon, gray, oxygen, red; oxygen on the crown ether ring, pink; hydrogen, white.....	157
10.5 Two out of a few enantiomeric separations observed on a native CF6 CSP: (A) primary amine type compound; (B) binaphthyl type compound. Mobile phases: (A) heptane/ethanol/trifluoroacetic acid 70/30/0.1; (B) heptane 100	159
10.6 Possible tripodal hydrogen bonding sites for ammonium cations: (A) alternating oxygen atoms in 18-crown-6; (B) three alternating O3 on inward-included fructofuranose units (O3(i) atoms); (C) O4(i), O3'(o) and O3''(i) on three neighboring fructofuranose units; (D) O3(o), O6(o) and O4'(i) on two neighboring fructofuranose units. The distance between those oxygen atoms are labeled on the figures in the unit of Å. The binding energy of potassium cation (having similar size as ammonium cation) at these sites (calculated at B3LYP/6-31g level) are -364, -195, -261, and -210 kJ mol^{-1} , respectively. Color coding: carbon, gray, oxygen, red. Hydrogen atoms are left out for clarity purpose	161
10.7 The polar organic mode (A) and the normal phase (B) mode separations of a chiral primary amine on a methylated CF6 CSP. Chromatographic parameters: (A) acetonitrile/methanol/acetic acid/triethylamine 60/40/0.3/0.2, $k_1 = 1.77$, $\alpha = 1.19$, $N = 8750$, $R_s = 2.8$; (B) heptane/ethanol/trifluoroacetic acid 70/30/0.1, $k_1 = 4.33$, $\alpha = 1.22$, $N = 3110$, $R_s = 2.2$	163
10.8 Separation of <i>trans</i> -1-amino-2-indanol on a methyl carbamate CF6 CSP in a heptanes/ethanol 70/30 mobile phase with different additives: (A) 0.1% trifluoroacetic acid; (B) 0.1% triethylamine	163
10.9 Separation of <i>trans</i> -1-amino-2-indanol (left) and Troger's base (right) on CF6 CSPs derivatized in three different ways: (A) and (D), low degree methyl carbamate derivatization; (B) and (E), low degree 3,5-dimethylphenyl carbamate derivatization; (C) and (F), high degree 3,5-dimethylphenyl carbamate derivatization. Mobile phases: left, acetonitrile/methanol/acetic acid/triethylamine 60/40/0.3/0.2 (70/30/0.3/0.2 for (C)); right, heptane/ethanol 70/30	165

10.10 Space filling model of all-O-3,5-dimethylphenyl carbamate CF6 calculated at HF/6-31g level: (A) top view from the hydrophilic side of CF6; (B) side view	167
10.11 Separation of different class of compounds on aromatic-derivatized CF6 CSPs. Aromatic derivatization groups: (A) 3,5-dichlorophenyl carbamate; (B) 3,5-bis(trifluoromethyl)phenyl carbamate; (C), and (D) R-naphthylethyl carbamate. Mobile phases: (A) heptane/ethanol 80/20; (B) acetonitrile/methanol/acetic acid/triethylamine 75/25/0.3/0.2; (C) heptane/isopropanol/trifluoroacetic acid 98/2/0.1; (D) acetonitrile/methanol 40/60 with 25 mM ammonium nitrate	167
10.12 Effect of MeOH addition (in volume percentages) on the separation of <i>p</i> -chloroamphetamine using 5 mM sulfated cyclofructan as the chiral selector. CE conditions: buffer, 20 mM ammonium acetate; pH, 4.7; voltage, +25 kV; capillary length, 30/40 cm; capillary i.d., 50 μ m. First peak is EOF marker. The unit for the time axis (horizontal axis) is minute. Reprinted from reference 104 with permission	169
10.13 Top view of native and alkylated CF6: (A) and (B), native CF6 optimized at B3LYP/6-31g level; (C) and (D), permethylated CF6 optimized at HF/6-31g level; (E) and (F), all-4-O-all-6-O-pentylated CF6 optimized at HF/6-31g level. Figures on the right side are displaying relative positions of O3 atoms on each fructofuranose units. The distance between neighboring oxygen atoms are labeled in the unit of Å. Color coding: gray, carbon; oxygen, red; O3 oxygen atoms, purple. Hydrogen atoms are left out for clarity purpose	170
10.14 ESI-MS spectrum showing adduct ions of one CF6 with multiple sodium cations (see reference 127 for detail experimental conditions)	171
10.15 Loading test of a methyl carbamate CF6 CSP in the polar organic mode. (A) 13.5 μ g and (B) 3.37 mg of <i>trans</i> -1-amino-2-indanol were injected on a 250 x 4.6 mm column. Mobile phase: acetonitrile/methanol/acetic acid/triethylamine 75/25/0.3/0.2	173

LIST OF TABLES

Table	Page
2.1 Summary of the optimized enantioseparation results	7
2.2 Effect of concentration of organic modifier on the separation parameters for compound 10 on the Cyclobond I 2000 SN column	12
2.3 Effect of the flow rate of the mobile phase on the separation of compound 12 on Cyclobond I 2000SN column using 1% tetrahydrofuran (aq) solvent	13
3.1 Example of the separations of all- <i>trans</i> -astaxanthin on three polymeric CSPs	21
3.2 Organic modifier effects on the separation of all- <i>trans</i> -astaxanthin on Chiralpak IC CSP using methyl t-butyl ether (MtBE) mobile phases	23
4.1 Physicochemical properties of boromycin	37
4.2 Chromatographic data for enantiomeric separation of amino alcohol enantiomers on the boromycin CSP	38
4.3 Chromatographic data for enantiomeric separation of amino acid ester/amide enantiomers on the boromycin CSP	41
4.4 Chromatographic data for enantiomeric separation of other primary amine enantiomers on the boromycin CSP	42
4.5 Comparison of enantiomeric Sseparations of amino alcohols and their related amino acid esters on the boromycin CSP	51
5.1 Elemental analysis results of three representative CF6-based stationary phases	60
5.2 Physical properties of cyclofructans 6-8	60
5.3 Chromatographic data of primary amines separated on derivatized-CF6 stationary phases in optimized conditions	68
5.4 Additive effect of separation of (\pm) <i>trans</i> -1-amino-2-indanol (primary amine type) in the polar organic mode on the IP-CF6 column	72
5.5 Chromatographic data of other compounds separated on six derivatized-CF6 stationary phases in optimized conditions	73
6.1 Retention factor of the first peak (k_1), enantioselectivity (α), and enantioresolution (R_s) of separated racemic compounds on the poly-DPAAS column in the normal phase mode	90

6.2 Retention factor of the first peak (k_1), enantioselectivity (α), and enantioresolution (R_s) of separated racemic compounds on the poly-DPAAS column in the polar organic mode	95
6.3 Retention factor of the first peak (k_1), enantioselectivity (α), and enantioresolution (R_s) of separated racemic compounds on the poly-DPEDA column in the normal -phase mode with halogenated solvent	97
7.1 Enantiomeric separations on four polymeric CSPs by SFC	110
8.1 The ratios between 1:2 and 1:1 cyclofructan-metal cation complexes electrosprayed form 1:1 solutions of cyclofructan and metal chloride salts. The peak intensities are scaled relative to the 1:1 cyclofructan-metal complexes within each set. "NA" represents less than 1% of 1:2 complexes observed. Standard deviation for three measurements are given	135
8.2 Relative abundance of cyclofructan-alkali metal cation complexes obtained from ESI-MS experiment for the equimolar (10^{-4} M) solution of cyclofructan, alkali metal and ammonium chloride salts (refer to Figure 5 for mass spectra). Standard deviation for three measurements are given	135
8.3 Binding energy (kJ mol^{-1}) between alkali metal cations and crown ethers and CF6. Values for crown ethers are obtained from threshold CID experiments, ⁹⁸ and values for CF6 are obtained from DFT calculations	141
8.4 Optimized structural parameters for complexes between CF6 and alkali metal cations	141
9.1 Complexation coefficients between CFs and different metal cations (summarized from reference 84e)	150
10.1 The effect of acidic and basic additives on the chromatographic separation of (\pm) <i>trans</i> -1-amino-2-indanol in the polar organic mode on an isopropyl carbamate derivatized CF6 column	165
10.2 O_{center} -C2-C3 angles (as shown in Figure 10.2) for each of the six fructofuranose ring in native and derivatized CF6. a, X-ray structure of CF6 (obtained from reference 60g); b, structures calculated at B3LYP/cc-pVDZ level; c, X-ray structure of permethylated CF6 when crystallized with Ba(SCN)2 (obtained from reference 84d); d, structures calculated at HF/b-31g level; e, all-4-O-all-6-O-pentylated CF6	169
10.3 Chromatographic data for three structurally similar compounds on permethylated-CF6 chiral GLC phase at the same chromatographic condition. Data from reference 126	171

CHAPTER 1

INTRODUCTION

There is a remarkable discrepancy between, on one hand, the high requirements for purity as laid down in the various pharmacopoeias and, on the other hand, the indiscriminate use of racemic mixtures; that is, the neglect of the extremely high degrees of impurity-the "isomeric ballast"-that they actually contain. There is no reason why the distomer should not contribute to the toxic action.¹

Ariëns, 1984

1.1 Importance and Challenges of Enantiomeric Separations

Chirality is one of the most fundamental and fascinating aspects of life. Most biomolecules are chiral, such as sugars, amino acids, proteins, the nucleic acids, DNA and RNA. More interestingly, chiral biomolecules exist dominantly in one enantiomeric form in living organisms, i.e., D-sugars and L-amino acids. A group of molecules possessing the same sense of chirality is known as homochiral. Homochirality is considered "the signature of life",² and the origin of homochirality is listed as one of the top 125 questions facing scientific inquiry over the next quarter-century by the Science magazine in 2005.³ An understanding in homochirality could even provide crucial knowledge as to the origin of life. If research on homochirality is simply to cater to ones curiosity, chirality does draw probably the most practical concerns: the health and well-being of our lives.⁴ Since countless biological pathways of the life cycle are so intricately enantioselective, the ability to discriminate between chiral molecules holds vast importance in biochemical development. Chiral selection plays an even more critical role in matters dealing with extraneously introduced substances (from food additives to drugs) that affect these metabolic pathways, of which is an area that garners special consideration from regulatory agencies worldwide.⁵

The ability to analyze and/or separate enantiomers is usually a prerequisite for almost all avenues of research involving chirality. Many non-chromatographic techniques have been used for enantiomeric analysis, e.g., polarimetry, nuclear magnetic resonance, isotopic dilution, calorimetry, and enzyme techniques. Unfortunately, these techniques require enantiomeric pure samples as standards or references.

On the other hand, chromatographic methods, especially enantiomeric separations by high performance liquid chromatography (HPLC), have become the method of choice due to the wide availability of chromatographic instruments, high extent of automation, as well as its high reproducibility and transferability. In addition to their application in enantiomeric analysis, HPLC and supercritical fluid chromatography (SFC) also can be employed to purify targeted enantiomers in large quantities via preparative scale separations. As a matter of fact, the development and maturity of chiral HPLC methods played an active role in driving the pharmaceutical industry towards producing single enantiomer drugs.⁶ Developing an enantioselective chromatographic method is not always easy. The most challenging aspect for chiral method development is to choose the right chiral stationary phase (CSP). Currently, there are over a hundred CSPs available commercially.⁷ On one hand, more CSPs provide more “degrees of freedom” for researchers. On the other hand, one might have to undertake an arduous path of searching through multiple manufacture’s brochures when faced with a limited time and budget. Fortunately, Most of the chiral separations can be achieved on relatively few CSPs (e.g., macrocyclic glycopeptides CSPs and polysaccharide CSPs).⁷ “It is only when these few ‘mainstays’ don’t work that the sometimes arduous task of surveying the vast array of other columns presents itself.”⁷ However, even with those “mainstay” CSPs, it is not usually an easy task to find the right chromatographic conditions for certain compounds.

1.2 Research Objectives and Organization of the Thesis

My general research goal is to advance chiral HPLC method development via three approaches, which corresponds to the three parts in this thesis.

Although accumulated trial-and-error knowledge or simply experience does not sound scientific, these provide the main source of information when selecting the right chromatographic columns and conditions for enantiomeric separations nowadays. The first part of my research focuses on expanding the general knowledge database of enantiomeric separations on the most useful CSPs for important classes of chiral compounds. Chapter one discusses the separation of β -lactams on cyclodextrin based CSPs; Chapter two reports the first baseline separation of astaxanthin on cellulosic based CSPs. Those are important separations that have immediate applications in the pharmaceutical industry. Indeed, the chromatographic

method for the separation of astaxanthin stereoisomers was directly transferred to a pharmaceutical company and used for both analytical and preparative separations.

The second part of my research involves the development of new CSPs. Instead of focusing on broad selectivity, we developed CSPs with high specificity, i.e., having almost universal enantioselectivity for certain classes of compounds. Chapter three presents the performance of the boromycin-based CSP, which shows a 98% success rate for enantiomeric separation of primary amine compounds. Chapter four discusses the cyclofructan family CSPs, which display different chiral recognition ability when derivatized with different groups. Certain types of derivatized cyclofructan CSPs showed high chiral selectivity for amine containing compounds, whereas differently derivatized cyclofructan CSPs produced broader chiral selectivity for other types of compounds. Chapter five outlines the development of a synthetic polymeric CSP, which is believed to have good preparative capabilities given the high loading ability of polymeric chiral selectors. Chapter six reports the performance of polymeric CSPs in SFC, which is considered a green technique of increasing popularity especially for preparative separations.

The last part of my research is dedicated to understanding of the separation mechanism of cyclofructan family of CSPs. The “holy grail” of the chiral separation research is to be able to predict whether or not a specific CSP can separate certain enantiomers. This is possible only with a full understanding of the chiral selector. There are limited studies of cyclofructans since its discovery in 1989, and more basic host-guest studies are needed for a better understanding of cyclofructan CSPs. Chapter seven describes an electrospray ionization mass spectrometry (ESI-MS) study of the complexation of cyclofructans with metal cations. Chapter eight takes advantage of the host-guest chemistry of cyclofructans and presents an efficient separation method for the homologous series of cyclofructans in the hydrophilic chromatography (HILIC) mode. Chapter nine discusses the operation mechanism of cyclofructan CSPs with the aid of computational methods.

CHAPTER 2

SEPARATION OF ENANTIOMERS OF B-LACTAMS BY HPLC USING CYCLODEXTRIN-BASED CHIRAL STATIONARY PHASES

2.1 Abstract

The enantiomeric separation of 12 β -lactam compounds on 3 native cyclodextrin and 6 derivatized β -cyclodextrin stationary phases was evaluated using high performance liquid chromatography (HPLC). The dimethylphenyl carbamate functionalized chiral stationary phase (CSP) (Cyclobond I 2000 DMP) separated 11 of the 12 β -lactams in the reversed phase mode. The dimethylated β -cyclodextrin column (Cyclobond I 2000 DM) was the second most effective CSP and it separated 8 of the 12 compounds. The reversed phase separation mode was the most effective approach. The effects of the composition and the flow rate on enantioseparations were studied. The effect of the structure of the substituents on the β -lactams was examined. P. Sun, C. Wang, A. Péter, and D. W. Armstrong. *Journal of Liquid Chromatography & Related Technologies* (2006), 29(13), 1847-1860. Copyright © 2006 with permission from the Taylor & Francis Group, LLC.

2.2 Introduction

β -Lactams, including penicillins and cephalosporins, are one of the most widely used types of antibiotics. Their antibacterial function results from the four-membered β -lactam ring inhibiting the formation of bacterial cell walls.¹ Many synthetic methods have been developed to construct β -lactams with functional groups and defined stereochemistry.⁸ In addition, β -lactams have been used as important building blocks in the synthesis of other compounds of biological importance, such as amino acid, peptides, and heterocyclic molecules.⁹

Stereochemistry greatly affects the synthetic approach, as well as the biological activity of these compounds, so there is a great need for obtaining enantiomerically pure β -lactams. Due to its flexibility, broad selectivity and high efficiency, liquid chromatography with chiral stationary phases (CSPs) has been

widely used for enantioseparations.¹⁰ Some enantiomers of β -lactams with aromatic substituents in the 3- or 4-position were separated on an amino acid-derived CSP ((S)-N-3,5-dinitrobenzoylleucine).^{10f} It was reported that a C3, C4-substituted β -lactamic cholesterol absorption inhibitor was separated on an amylose-based chiral stationary phases (Chiralpak AD and AS).^{10a} The enantiomers of 12 β -lactams were separated on two types of CSPs, one of which was a cellulose-tris-3,5-dimethylphenyl carbamate, and the other of which was a macrocyclic glycopeptide antibiotic teicoplanin or teicoplanin aglycone CSP.^{10c} Cyclodextrin-based CSPs have been widely used to separate chiral compounds,¹¹ especially those with aromatic moieties. This class of chiral stationary phases has not been used for separating bicyclic and tricyclic β -lactams to our knowledge. In this work, the enantioseparation of 12 chiral β -lactams is evaluated by comparing 3 native and 6 derivatized cyclodextrin based CSPs in different chromatographic modes. The effects of the composition of the mobile phase and flow rate on enantioseparation are studied. The effects of the structure of the analytes on retention and selectivity also are discussed.

2.3 Experimental

2.3.1 Materials

2-Azetidinone was purchased from Aldrich (Milwaukee, WI, USA). The twelve β -lactams were given by Antal Péter. They are dissolved in either ethanol or acetonitrile. Ethanol (200 proof) was obtained from Aaper Alcohol and Chemical Company (Shelbyville, KY, USA). Acetonitrile, methanol, tetrahydrofuran (THF), isopropanol and heptane of HPLC grade were purchased from Fisher Scientific (Fairlawn, NJ, USA). Water was deionized and filtered through active charcoal and a 5- μ m filter. Cyclobond I (β -cyclodextrin), II (γ -cyclodextrin), III (α -cyclodextrin), AC (acetylated β -cyclodextrin), DM (dimethylated β -cyclodextrin), RSP (hydroxypropyl ether β -cyclodextrin), DMP (dimethylphenyl carbamate β -cyclodextrin), RN and SN (naphthylethyl carbamate) CSPs were obtained from Advanced Separation Technologies (Whippany, NJ, USA).

2.3.2 Equipment

Chromatographic separations were carried out in three HPLC systems. The first system was a HP (Agilent Technologies, Palo Alto, CA, USA) 1050 system with a UV VWD detector, an autosampler, a quaternary

pump and Chemstation software. The second system consisted of a UV detector (SPD-6A, Shimadzu, Kyoto, Japan), a pump (LC-6A, Shimadzu), a system controller (SCL-10A, Shimadzu) and a chromatographic integrator (SPD-6A, Shimadzu). The third one included a pump (LC-10A, Shimadzu), a UV detector (SPD-10A, Shimadzu) and an integrator (SPD-6A, Shimadzu). In these systems, the samples were injected via a six-port injection valve with a 10 μ L sample loop (Rheodyne, Cotati, CA, USA). Mobile phase was degassed by ultrasonication under vacuum for 5 min. All compounds are detected at 210 nm.

2.3.3 Column Evaluation

All CSPs were evaluated in the reversed phase mode using acetonitrile-water, methanol-water, and tetrahydrofuran-water. Except DM, all CSPs were also evaluated in the polar organic mode using acetonitrile/methanol. Aromatic derivatized CSPs (DMP, SN and RN) were evaluated in the normal phase mode with isopropanol-heptane mobile phase. All separations were carried out at room temperature with the mobile phase flow rate of 1.0 mL/ min.

2.3.4 Calculations

The retention factor (k) was calculated using the equation $k = (t_r - t_0)/t_0$, where t_r is the retention time, and t_0 is the dead time which is determined by the peak of the refractive index change due to the sample solvent. Selectivity (α) was calculated by $\alpha = k_2/k_1$, where k_1 and k_2 are the retention factors of the first and second eluted enantiomers, respectively. The resolution (R_s) was determined using $R_s = 2 \times (t_{r2} - t_{r1}) / (w_1 + w_2)$, where w is the base peak width. The efficiency (the number of theoretical plates, N) was calculated by $N = 16 \times (t_r / w)^2$.

2.4 Results and Discussion

2.4.1 Evaluation

In this work, nine cyclodextrin-based CSPs were evaluated for their ability to separate 12 chiral bicyclic or tricyclic β -lactam compounds in the reversed phase mode. Because these β -lactams have no ionizable groups, the pH of the mobile phase does not greatly affect the enantioseparation. Three types of organic modifier were used: methanol, acetonitrile, and tetrahydrofuran. Except for the Cyclobond I 2000 DM CSP, the other eight columns were evaluated in the polar organic mode with acetonitrile/methanol as the mobile

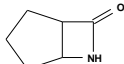
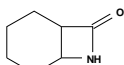
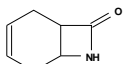
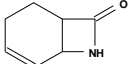
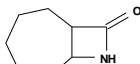
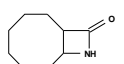
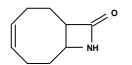
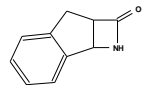
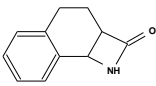
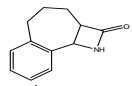
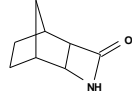
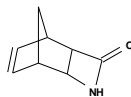
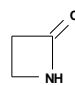
phase. In the normal phase mode, the main attractive interactions between analytes and the chiral stationary phase are of the π - π and dipolar types, so only the aromatic derivatized cyclodextrin-based CSPs (DMP, RN, and SN) were used in the normal phase mode with heptane /2-propanol as the mobile phase.

In the reversed phase mode, enantioselectivity ($\alpha \geq 1.02$) was observed for all the 12 β -lactams. Table 2.1 shows the compound structure and the separation results (including k_1' , α , R_s , and the mobile phase composition) under optimized conditions. If the chiral analytes are partially separated ($0.3 < R_s < 1.5$), the condition with the largest R_s was selected. When baseline separation occurred ($R_s \geq 1.5$), the conditions that produced the smallest k' are given. The results show that seven β -lactams (Compounds 4, 5, 6, 7, 8, 9, and 10) are baseline separated and five (Compounds 1, 2, 3, 11, and 12) are partially separated. Decreasing the flow rate from 1.0 mL/min to 0.5 ml/min improved all the enantioseparations. At the lower flow rate compounds 4, 5, and 7 were baseline separated, while at higher flow rates, they were not.

In order to illustrate the effect of the analyte structure on the enantioseparation, Table 2.1 also includes the chromatographic retention data of compound **13** (2-azetidinone, a nonchiral compound). This compound has greater retention in the polar organic mode (methanol/acetonitrile=1/99) than in the reversed phase mode (acetonitrile/water =1/99). It is most strongly retained on the γ -cyclodextrin CSP, with a $k' = 0.91$, shown in Table 2.1. Enantioresolution varied for different β -lactams and Figure 2.1 shows selected chromatograms for the best (compounds **9** and **10**), moderate (compounds **5** and **12**), and the worst resolutions (compounds **1** and **3**).

Different columns have different selectivities for these β -lactams. Figure 2.2A shows the performance of nine CSPs. The dimethylphenyl functionalized β -cyclodextrin (Cyclobond I 2000 DMP) is the most effective column for separating these β -lactam enantiomers. It showed enantioselectivity for eleven of the β -lactams (all except compound **12**), including five baseline separations and six partial separations. The dimethylated β -cyclodextrin (Cyclobond I 2000 DM) is the second effective column with two baseline and six partial separations. For the native cyclodextrin CSPs, only γ -cyclodextrin showed any enantioselectivity for these compounds (e.g. for two of the chiral β -lactam compounds). It is apparent that the different functional groups of the derivatized cyclodextrin CSPs provide enhanced enantioselectivity and expand the

Table 2.1 Summary of the optimized enantioseparation results.

Number	Structure	CSP ^a	k ₁	α	Rs ^b	Rs* ^c	Mobile Phase (v/v)
1		DMP	3.14	1.06	0.8	0.9	ACN/H ₂ O=1/99
2		DMP	7.85	1.07	0.9	0.9	ACN/H ₂ O=1/99
3		DMP	3.88	1.08	0.9	1.0	ACN/H ₂ O=1/99
4		DMP	4.70	1.11	1.3	1.5	ACN/H ₂ O=1/99
5		DMP	3.96	1.10	1.2	1.5	MeOH/H ₂ O=30/70
6		DMP	7.40	1.08	1.5	1.6	ACN/H ₂ O=15/85
7		DM	2.68	1.14	1.4	1.5	THF/H ₂ O=0.1/100
8		DMP	4.20	1.10	1.5	1.9	ACN/H ₂ O=15/85
9		DMP	5.20	1.13	1.9	2.4	ACN/H ₂ O=15/85
10		DM	2.13	1.20	1.6	2.0	ACN/H ₂ O=5/95
11		SN	7.34	1.07	1.2	1.2	ACN/H ₂ O=5/95
12		DM	1.24	1.11	1.2	1.3	THF/H ₂ O=0.1/99.9
13 ^d		II	0.91				MeOH/ACN=1/99

^afor the CSP designated by the abbreviations, see Experimental sections.

^bobtained at 1.0 mL/min; ^cobtained at 0.5 mL/min.

^dk' on α, β, DMP, DM, RSP, RN, SN, and AC in the reversed phase (acetonitrile/water =1/99) and polar organic mode (acetonitrile/methanol=99/1) are 0.19 and 0.47, 0.07 and 0.41, 0.23 and 0.57, 0.09, 0.17 and 0.44, 0.22 and 0.42, 0.20 and 0.52, 0.13 and 0.42, respectively.

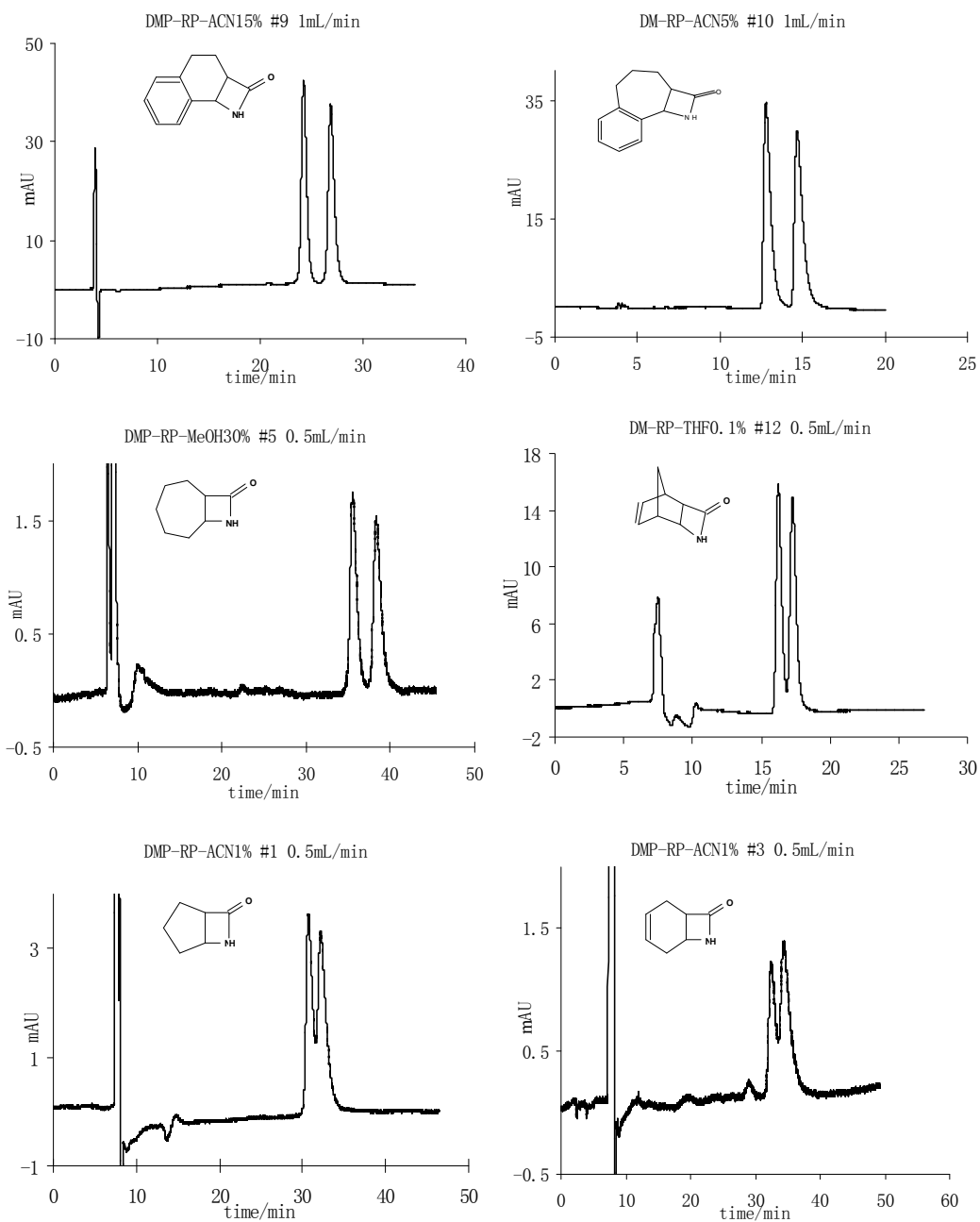


Figure 2.1 Selected chromatograms showing the best (top two), medium (middle two) and worst (bottom two) enantioseparation for the substituted β -lactams.

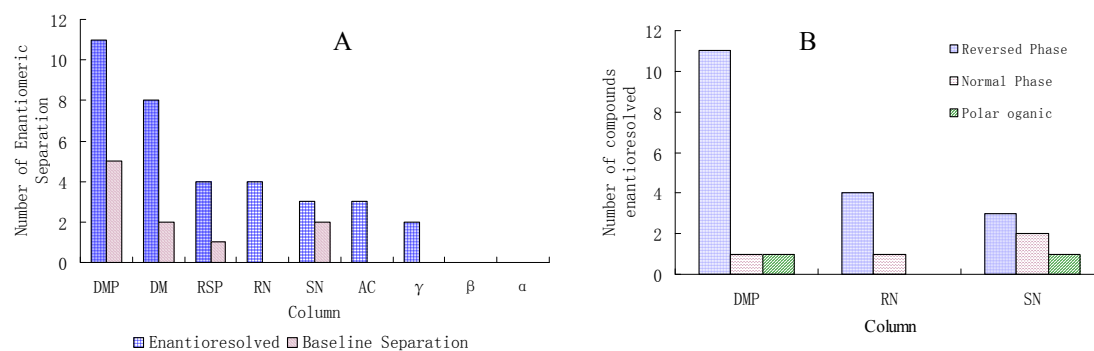


Figure 2.2 Performance of different cyclodextrin-based CSPs in different separation modes: (A) Overall Enantioseparation results for 9 CSPs in all separation modes; (B) Different enantioseparation results in three separation modes on the three aromatic derivatized cyclodextrin CSPs

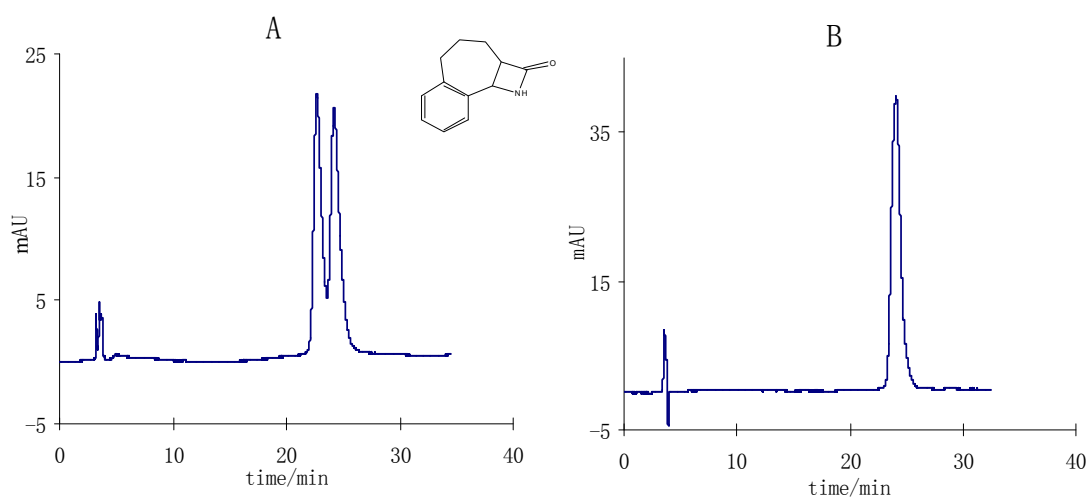


Figure 2.3 Comparison of separations resulting from the use of different organic modifiers. Compound 10 was separated on the Cyclobond I 2000 DMP column using the following mobile phases: A) 70/30 water/methanol and B) 85/15 water/acetonitrile.

usefulness of CSPs based on cyclodextrin.

Only the aromatic derivatized cyclodextrin CSPs (DMP, SN and RN) can be used to separate enantiomers in all three chromatographic modes (shown in Figure 2.2B). Eleven compounds are separated in the reversed phase mode on the Cyclobond DMP compared to four on the RN and three on the SN column. In the normal phase mode, the DMP, RN, and SN columns can separate one, one, and two compounds, respectively. In the polar organic mode, only compound **10** was separated on the DMP and SN columns, while the RN column did not achieve any enantioseparations. The separation efficiencies in the reversed phase mode are significantly greater than in the other two modes. Comparing the resolution (R_s) achieved in different modes for the same compound, the reversed phase separations consistently produced larger R_s values for these compounds. The separation of compound **10** on the Cyclobond I-2000 SN is a good example. With acetonitrile/water (20/80), the R_s is 2.0, while in 100% acetonitrile and 2-propanol/heptane (5/95) the values are 0.5 and 1.0 respectively. The change in enantioresolution in different chromatographic modes depends on the retention mechanism. In the reversed phase mode, inclusion complexation is the dominant retentive interaction while CSPs form dipolar and π -complexes in the normal phase mode. The hydrogen bonding interactions are the most important in the polar organic mode.

2.4.2 Effect of Mobile Phase on Enantioseparation

2.4.2.1 Type of Organic Modifier

In the reversed phase mode on Cyclobond CSPs, acetonitrile and methanol are more commonly used than tetrahydrofuran as organic modifiers. The optimized separations for ten of twelve compounds were achieved with acetonitrile or methanol and water as the mobile phase (Table 2.1). The best separations for compounds **7** and **12** were achieved with tetrahydrofuran (THF)-water mobile phases. Comparing acetonitrile and methanol as organic modifiers, acetonitrile is more successful mainly due to the higher chromatographic efficiencies produced the selectivity was similar for most compounds. In some specific cases, changing from acetonitrile to methanol has a notable effect on enantioselectivity. For example, using acetonitrile/water as the mobile phase, no selectivity for compound **10** was seen on the Cyclobond I 2000 DMP column, while it was partially separated with a methanol-water mobile phase, as shown in Figure 2.3.

2.4.2.2 Concentration of Organic Modifier

When operating in the reversed phase mode, an important interaction between the CSPs and analytes is the hydrophobic inclusion complex. Organic solvents compete with the analytes for the nonpolar cavity of the cyclodextrin, so the analytes are more strongly retained when the concentration of the organic modifier is decreased. Changing the concentration of organic modifier changes the retention, selectivity and resolution. Table 2.2 lists the separation results for compound **10** as separated on the Cyclobond I 2000 SN column. When the percentage of acetonitrile is below 80%, decreasing the concentration of acetonitrile increases the retention, enantioselectivity, and resolution of the analytes. However, when the percentage of acetonitrile is above 80%, the reverse trend is obtained. In pure acetonitrile (the polar organic mode), a partial separation ($R_s=0.6$, $\alpha=1.08$) was obtained.

2.4.2.3 Flow Rate of the Mobile Phase

Changing the flow rate of the mobile phase affects the efficiency of liquid chromatography. Table 2.3 shows the separation results for compound **12** on the Cyclobond I 2000 SN column with a THF/water (1/99) mobile phase. When decreasing the flow rate from 1.0 ml/min to 0.2 ml/min, the selectivity (in the range of 1.128-1.130) and the retention factor (0.64) are the same within experimental error. The main factor contributing the change of resolution is efficiency (N_1 , the number of theoretical plates of the first peak). Decreasing the flow rate from 1.0 to 0.2 mL/min improved the efficiency (N increased from 7040 to 8200) and resolution slightly (R_s changed from 0.99 to 1.14). In some cases, the flow rate shows larger effect on chromatographic separation. In Table 2.1, decreasing the flow rate from 1.0 mL/min to 0.5 mL/min improve the resolution of compound **9** from 1.9 to 2.4.

2.4.2.1 Effect of Analyte Structure

It was found that the simple, unsubstituted lactam (compound **13**) has very little retention on any column and under any of the mobile phase conditions (Table 2.1). Clearly the hydrophobicity provided by the cyclic or bicyclic hydrocarbon substituent is essential for retention in the reversed phase mode and this substituent structure affects enantioselectivity as well.

In the reversed phase mode, solute retention results from an inclusion complex formation with the cyclodextrin cavity, and this is affected by the hydrophobicity of the solutes. Figure 2.4 indicates that the

Table 2.2 Effect of concentration of organic modifier on the separation parameters for compound 10 on the Cyclobond I 2000 SN column.

Percent of Acetonitrile	k_1	α	R_s
0	20.78	1.39	3.4
5	7.40	1.27	2.2
10	5.04	1.25	2.1
15	3.33	1.19	1.8
20	2.23	1.15	1.4
30	0.92	1.10	1.1
40	0.73	1.05	0.6
50	0.59	1.00	0
60	0.46	1.00	0
70	0.23	1.00	0
80	0.18	1.00	0
90	0.25	1.00	0
100	0.63	1.08	0.6

Table 2.3 Effect of the flow rate of the mobile phase on the separation of compound 12 on Cyclobond I 2000SN column using 1% tetrahydrofuran (aq) solvent.

Fow rate (mL/min)	k_1	α	R_s	2.4.3	N
1.0	0.64	1.13	0.99		7040
0.9	0.64	1.13	1.06		7530
0.8	0.64	1.13	1.09		7620
0.7	0.64	1.13	1.10		7940
0.6	0.64	1.13	1.12		8080
0.5	0.64	1.13	1.13		8110
0.4	0.64	1.13	1.13		8160
0.3	0.64	1.13	1.13		8140
0.2	0.64	1.13	1.14		8170

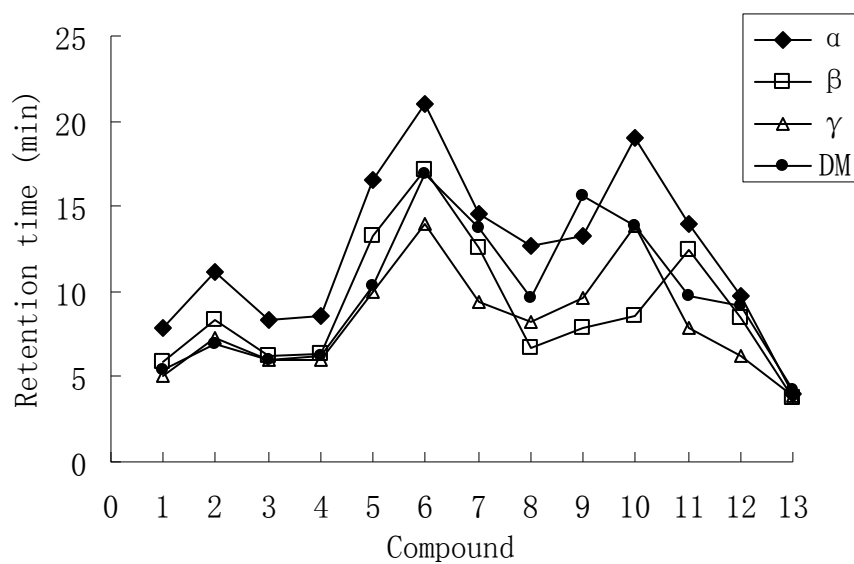


Figure 2.4 Retention times of 13 β -lactams on four Cyclodextrin-based CSPs (α , β , γ , and DM). Note: the mobile phase for α , β , γ -cyclodextrin CSPs is acetonitrile-water (1/99), while it is acetonitrile-water (5/95) for Cyclobond I-2000 DM CSP.

size of the substituent ring of the β -lactams affects the retention greatly. An examination of the retention results of compounds **1**, **2**, **5**, and **6** on the Cyclobond DM column reveals that the size increase from a five-membered to eight-membered ring enhances the retention due to higher hydrophobicity.

The presence of an aromatic ring is beneficial to chiral recognition on Cyclobond-based CSP as well.

Comparison of compounds **1** and **8**, **2** and **9** on the Cyclobond I 2000 DMP column (shown in Table 2.1) shows the effect of addition of an aromatic ring. The Cyclobond DMP CSP shows baseline resolution for compounds **8** ($R_s^* = 1.9$) and **9** ($R_s^* = 2.4$), but not for **1** ($R_s^* = 0.9$) and **2** ($R_s^* = 0.9$) under optimized conditions.

The presence of double-bond also shows a beneficial effect on enantioseparation. Comparison of the chromatographic results of compounds **2**, **3** and **4** on the Cyclobond DM column is a good example.

Compared to **2**, compounds **3** and **4** have a double-bond, which are positioned differently in the ring. It was observed that adding a double-bond decreased the retention (shown in Figure 2.4) while enhancing selectivity. Cyclobond DM CSP shows enantioselectivity for compound **4**, but not for compounds **2** and **3**.

2.5 Conclusions

Enantioseparation of 12 β -lactams was achieved on nine cyclodextrin-based CSPs. Baseline separation was observed for seven compounds. The Cyclobond DMP column was the most effective stationary phase in that it separated 11 of 12 substituted β -lactams. Cyclobond DM also is effective and separated 8 of 12 β -lactams. Cyclobond RSP, RN, SN, AC, and γ cyclodextrin CSPs show enantioselectivity for a few β -lactams, while the native α and β -cyclodextrin CSPs do not show any enantioselectivity for these analytes. The reversed phase mode was the most effective approach and only two separations were observed in the normal phase and polar organic modes. The composition of organic modifier and the flow rate affect all enantioseparations. The substituents on the β -lactams contribute much to retention and enantioselectivity. In particular more rigid aromatic and tricyclic compounds produced the greatest separation factors and resolutions.

CHAPTER 3

RAPID BASELINE SEPARATION OF ENANTIOMERIC AND MESO FORMS OF ALL-*TRANS*-ASTAXANTHIN, 13-*CIS*-ASTAXANTHIN, ADONIRUBIN, AND ADONIXANTHIN IN STANDARDS AND COMMERCIAL SUPPLEMENTS

3.1 Abstract

Astaxanthin, 3,3'-dihydroxy- β,β -carotene-4,4'-dione, is widely used as important colorant in the aquaculture feed industry, and as nutraceuticals in human health products. Synthetic all-*trans*-astaxanthin consists of a mixture of a pair of enantiomers (3R,3'R and 3S,3'S) and a meso form (3R, 3'S). An HPLC method for direct, rapid, and baseline separation of three stereoisomers of all-*trans*-astaxanthin is described for the first time on a immobilized cellulosic column (Chiralpak IC). Enantiomers of two important precursors in the biosynthetic pathway of astaxanthin, adonirubin and adonixanthin, were also directly separated. In addition, the major *cis* form of astaxanthin (13-*cis*-astaxanthin) resulted from isomerization was isolated with preparative C18 separation, and the separation of all four stereoisomers of 13-*cis*-astaxanthin is achieved. Finally, the stereoisomeric purity test of commercial astaxanthin supplements confirmed that they were from a natural source, although their levels were quite low. Chunlei Wang, Daniel W. Armstrong, and Chau-Dung Chang. Journal of Chromatography A (2008), 1194(2), 172-177. Copyright © 2008 with permission from the ScienceDirect.

3.2 Introduction

Astaxanthin (3,3'-dihydroxy- β,β -carotene-4,4'-dione), adonirubin (3-hydroxy- β,β -carotene-4,4'-dione) and adonixanthin (3,3'-dihydroxy- β,β -carotene-4-one) belong to the xanthophylls family of oxygenated derivatives of carotenoids. Astaxanthin is an important colorant in the salmonid and crustacean aquaculture feed industry to provide the desirable pink color characteristic of these species.¹² Astaxanthin also is used as a human nutraceutical. Its major health benefits arises from its outstanding antioxidant activity, several fold higher than that of vitamin E and other carotenoids.¹³ Hence, astaxanthin is a potential candidate as a

protective agent against a wide range of ailments that may be either triggered or aggravated by oxidative stress. These include cardiovascular problems, inflammation, ulcerous infections, and UV-light damage.¹² Other benefits such as immunomodulating¹⁴ and anti-cancer properties¹⁵ of astaxanthin have been reported in literature. Adonirubin and adonixanthin are direct precursors along the biosynthetic pathway of astaxanthin,¹⁶ and often are present in the final product, in various percentages.¹⁷

Astaxanthin has two ionone rings held together by a long chain of conjugated double bonds (Figure 3.1), indicating many possible geometrical isomeric forms (*cis* and *trans*). Thermodynamically, the all-*trans*-astaxanthin is more stable than other *cis* isomers,¹⁸ but they may be isomerized from one to another when heated or exposed to light.¹⁹ Due to the presence of two stereogenic carbon atoms at the C-3 and C-3' position, there are three stereoisomers for astaxanthin: a pair of enantiomers (3R,3'R- and 3S,3'S-astaxanthin) and an optically inactive meso form (3R,3'S-astaxanthin). Synthetic formed astaxanthin has a stereoisomeric ratio of 1:2:1 for the 3R,3'R/meso/3S,3'S isomers. However, in nature, 3S,3'S-astaxanthin is the most abundant isomer,²⁰ and different biologic sources produce astaxanthin of different stereoisomeric ratios.²¹ Artificial racemic astaxanthin (e.g., from BASF, Roche) are widely used as additives in fish feed, whereas the natural source of optically active astaxanthin (usually (3S,3'S)-isomer) is utilized by fish in the wild. A knowledge of the stereoisomeric ratios may help to identify the source of the aquaculture product (whether wild or farmed).²² In addition, the U.S. Food and Drug Administration (FDA) requires a characterization of the stereoisomer from API (active pharmaceutical ingredient) manufacturing, and an evaluation of the pharmacology and toxicology of stereoisomer could be needed.^{5a} As studies of astaxanthin's health benefits proliferate, a method to separate, identify, and quantitate the stereoisomers is necessary.

The current method to determine the astaxanthin stereoisomer ratio is based on the separation of corresponding diastereomeric astaxanthin di-(-)-camphanates by high performance liquid chromatography (HPLC) on a Spherisorb S-5CN stationary.²³ Many attempts have been made to separate astaxanthin stereoisomers directly without pre-column derivatization. These include normal phase separations on: a Sumipax OA-2000 column,²⁴ a D-phenylglycine based CSP; a 3,5-dinitrobenzoyl derivatized L-leucine based CSP,^{24b, 25} and a reversed phase separation on Chiralcel OD-RH, a coated cellulosic CSP.²¹ In none

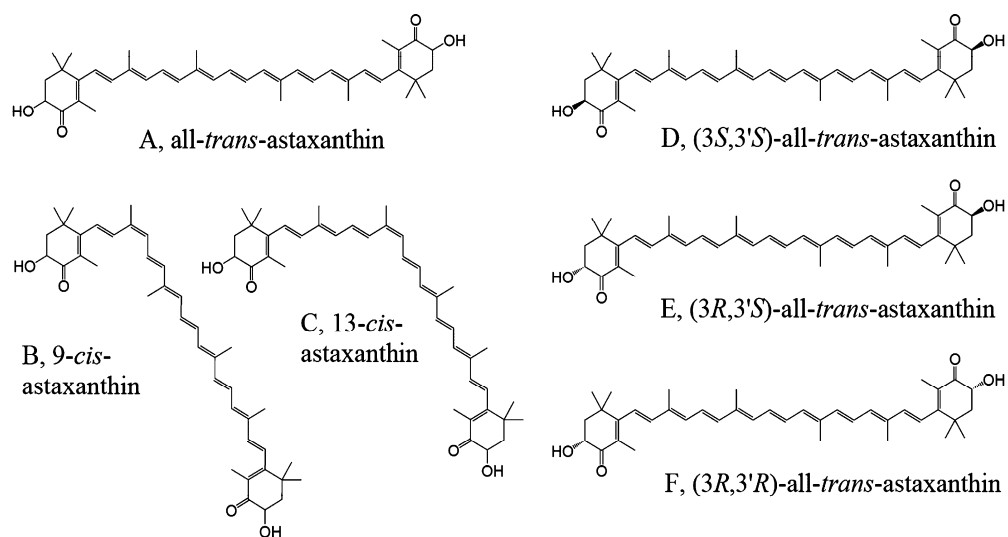


Figure 3.1 Structure of astaxanthin geometrical isomers (A) all-*trans*-astaxanthin, (B) 9-*cis*-astaxanthin, (C) 13-*cis*-astaxanthin, and stereoisomers of all-*trans*-astaxanthin: (D) (3*S*,3'*S*)-all-*trans*-astaxanthin, (E) (3*R*,3'*S*)-all-*trans*-astaxanthin, and (F) (3*R*,3'*R*)-all-*trans*-astaxanthin.

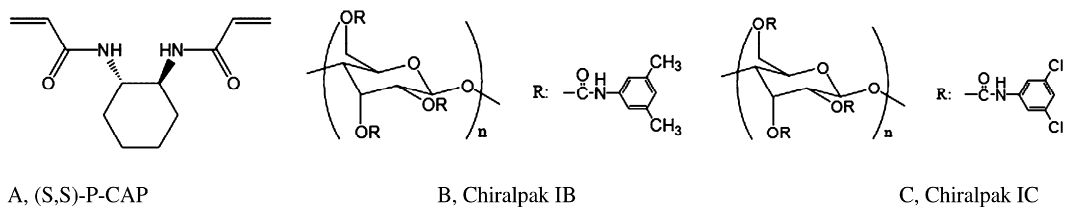


Figure 3.2 Monomer structures of the CSPs used in this study.

of these cases were the three stereoisomers of all-*trans*-astaxanthin baseline separated ($R_s \geq 1.5$) from each other. Furthermore, the analysis times were usually 30 min or longer. Finally, no direct enantiomeric separations have been reported for the closely related precursor molecules adonirubin and adonixanthin. In this study, we report a direct, fast and baseline separation method for all stereoisomers of the all-*trans*-astaxanthin, and structurally related carotenoids. Successful separations were found on three immobilized polymeric CSPs. The effects of mobile phase composition on the separations are discussed in detail. All four stereoisomers of 13-*cis*-astaxanthin were successfully separated as well. Finally, all-*trans*-astaxanthin from commercial nutraceutical supplements were analyzed for their stereoisomeric purity.

3.3 Experimental

3.3.1 Materials

All-*trans*-astaxanthin was purchased from Sigma-Aldrich (Milwaukee, WI). Racemic adonirubin, (3R,3'R)-adonixanthin, and (3S,3'S)-adonixanthin were purchased from CaroteNature (Lupsingen, Switzerland). All commercial astaxanthin supplements were purchased from vitacost.com. The analytical (25 cm x 4.6 mm) and preparative (25 cm x 21.2 mm) C18 stationary phases, and the (S,S)-P-CAP (25 cm x 4.6 mm) chiral stationary phase (CSP) were obtained from Astec (Whippany, NJ). The Chiralpak IB (25 cm x 4.6 mm) and Chiralpak IC (25 cm x 4.6 mm) CSPs were purchased from Chiral Technologies, Inc. (West Chester, PA). HPLC grade acetonitrile, dichloromethane, ethanol, ethyl acetate, isopropanol, methanol, methyl t-butyl ether (MtBE), tetrahydrofuran were purchased from VWR (Bridgeport, NJ).

3.3.2 Instrumentation

The analytical scale separations were achieved on an HP 1050 HPLC with an autosampler, a quaternary pump, a UV VWD detector, and ChemStation. The preparative separations were obtained with a self assembled Shimadzu system: Shimadzu LC-10AD pump, Shimadzu SPD-6A UV VWD detector, and Shimadzu CR601 chart recorder. The diode array detection was achieved with an Agilent 1100 HPLC, equipped with an autosampler, micro vacuum degasser, binary pump, diode array detector, and Agilent ChemStation for data processing. The JASCO CD-2095 circular dichroism detector together with Shimadzu LC-10AD pump was used for chiroptical detection analysis.

3.3.3 Methods

Samples were prepared by dissolving 0.5 mg of the analytes in either MtBE, acetonitrile or the mobile phases. All separations were monitored at 476 nm at room temperature (~22 °C). The flow rates for analytical and preparative separations were 1.0 mL/min and 10.0 mL/min respectively. The detection wavelength used for circular dichroism detector is 330 nm.

3.4 Results and Discussion

3.4.1 Separation of all-*trans*-Astaxanthin

Among all of the tested chiral stationary phases (CSPs), three bonded polymeric CSPs showed enantioselectivity towards astaxanthin enantiomers. They were: the (S,S)-P-CAP (Astec, Whippany, NJ), Chiralpak IB and IC (Chiral Technologies, West Chester, PA). The structures of monomeric unit for each of these three polymeric CSPs are shown in Figure 3.2.

Typical separation conditions of all-*trans*-astaxanthin on these three CSPs are listed in Table 3.1. The (S,S)-P-CAP column partially separates the astaxanthin stereoisomers with a heptane/ethanol 90/10 mobile phase (Table 3.1, entry 1). Although the enantiomers are well separated, there is some overlap between the meso compound and each of the enantiomers. The isomers' elution order on the (S,S)-P-CAP CSP is opposite to that on the immobilized cellulose based CSPs. Since this is the only totally synthetic CSP (of the three), it is possible to produce the opposite retention order using a (R,R)-P-CAP column.

Recently, Grewe et al reported the reversed phase separation of all-*trans*-astaxanthin on a coated cellulose tris(3,5-dimethylphenyl-carbamate) CSP(Chiralcel OD-RH).²¹ Chiralpak IB is the immobilized version of the Chiralcel OD CSP. The reported separation was reproduced on the Chiralpak IB CSP with slightly worse selectivity and resolution (Table 3.1, entry 2). In the normal phase mode, the separation is also achieved using a heptane/ethanol mobile phase (Table 3.1, entry 3), which is compatible with the coated Chiralcel OD CSP, but was not reported. The best separation on the Chiralpak IB is obtained with a heptane/acetone 90/10 mobile phase (Table 3.1, entry 4). In both the reversed and normal phase mode, the elution order of the all-*trans*-astaxanthin isomers on the IB CSP is the same as that reported on the reversed phase OD CSP.

In none of the above cases are all three stereoisomers baseline separated from each other. The Chiralpak IC

Table 3.1 Example of the separations of all-*trans*-astaxanthin on three polymeric CSPs.

No.	CSPs	Mobile Phases ^a	kI' ^b	$\alpha(1,2)$ ^c	$\alpha(1,3)$	$\alpha(2,3)$	$Rs(1,2)$ ^d	$Rs(1,3)$	$Rs(2,3)$	First eluted
1	(S,S)-P-CAP	Hept/EtOH 90/10	4.70	1.08	1.16	1.07	0.8	1.5	0.7	(R, R)
2	Chiralpak IB	ACN/H ₂ O 70/30	9.70	1.05	1.12	1.07	1.1	2.2	1.1	(S, S)
3		Hept/EtOH 90/10	2.90	1.06	1.13	1.07	0.8	1.9	1.1	(S, S)
4		Hept/ACT 90/10	5.37	1.07	1.16	1.09	1.2	2.6	1.4	(S, S)
5		MtBE/EtOH 98/2 ^e	0.77	--	--	--	--	--	--	--
6	chiralpak IC	Hept/EtOH 90/10	no elution within 60 min							
7		Hept/EtOH 50/50	14.30	1.09	1.29	1.19	1.1	3.3	2.2	(S, S)
8		MtBE/EtOH 98/2	7.90	1.27	1.62	1.27	2.0	4.1	2.1	(S, S)

^a Mobile phases: Hept, heptanes; EtOH, ethanol; ACN, acetonitrile; ACT, acetone; MtBE, methyl t-butyl ether. ^b kI' is the k' of the first eluted isomer. ^c $\alpha(1,2)$ is the selectivity between the first and second eluted isomers. ^d $Rs(1,2)$ is the resolution between the first and second eluted isomers. ^e There is no separation of the isomers at this particular condition.

CSP is based on cellulose tris(3,5-dichlorophenyl-carbamate) polymer. By changing the derivatization group from 3,5-dimethylphenyl to 3,5-dichlorophenyl, the Chiralpak IC CSP retains astaxanthin more strongly than the Chiralpak IB CSP using the same mobile phase (compare Table 3.1, entries 3, 5 with entries 6, 8). The increased retention, or solute-CSP interaction, proved to be key to the enantiomeric separation of astaxanthin.

The stereoselectivity for astaxanthin is maintained on the Chiralpak IC CSP with a variety of normal phase solvent compositions. Because of the aforementioned stronger interaction between the astaxanthin and Chiralpak IC CSP, heptane cannot be used to effectively elute the solute in a reasonable time period (Table 3.1, entry 6 and 7). Therefore methyl t-butyl ether (MtBE) is used as the major component of the mobile phase. The nature of the stronger mobile phase solvent modifier greatly affects the selectivity and efficiency of the astaxanthin separations. Table 3.2 compares the selectivity, efficiency, and the resolution of the separations achieved at similar retention times using different organic modifiers in the MtBE main solvent. Regardless of the type of organic modifier, astaxanthin is separated using MtBE based mobile phase on the Chiralpak IC CSP with greater selectivity than anything previously reported. Generally, the selectivity and resolution of the separations are better when using organic additives that have hydrogen bond accepting capabilities but not hydrogen bond donating properties, e.g., tetrahydrofuran, ethyl acetate, acetone, and acetonitrile (Table 3.2, entries 4-7) versus alcohols (Table 3.2, entries 1-3). Using a halogenated solvent, dichloromethane, as the organic modifier results in the highest efficiency, but the resolution is sacrificed somewhat due to the decreased selectivity, compared to other organic solvents (Table 3.2, entry 8). Compared with all other the mobile phase compositions in Table 3.2, the MtBE/acetonitrile mobile phase separates astaxanthin with the highest selectivity and resolution, and it produces short analysis times. Hence this solvent combination was used for the rest of the study.

Figure 3.3 shows plots of the capacity factor, selectivity, efficiency, and resolution of all-*trans*-astaxanthin on the Chiralpak IC CSP as a function of acetonitrile volume percentage in the mobile phase. The capacity factor decreased quickly as acetonitrile increased from 5% to 20% (by volume), reached a minimum and leveled off between 20% and 40%, and gradually increased as the acetonitrile concentration went from 40% to 100%. The selectivity (α) between R,R- and S,S-astaxanthin decreased from 1.81 to 1.49 as the

Table 3.2 Organic modifier effects on the separation of all-*trans*-astaxanthin on Chiralpak IC CSP using methyl t-butyl ether (MtBE) mobile phases.

No.	Modifiers in MtBE ^a	N (meso)	<i>k</i> ' (SS)	α (meso,SS)	α (RR,SS)	α (RR,meso)	<i>R</i> _s (meso,SS)	<i>R</i> _s (RR,SS)	<i>R</i> _s (RR,meso)
1	5% IPA	1573	6.03	1.27	1.62	1.27	1.7	3.6	1.9
2	5% EtOH	2172	4.60	1.23	1.53	1.24	1.8	3.7	1.9
3	2% MeOH	2200	6.43	1.21	1.47	1.21	1.8	3.4	1.7
4	5% THF	1653	4.87	1.27	1.64	1.29	1.8	3.6	1.8
5	10% EtAc	2055	5.20	1.31	1.73	1.32	2.2	4.6	2.4
6	5% ACT	2316	3.47	1.29	1.67	1.30	2.0	4.4	2.4
7	5% ACN	2531	4.17	1.34	1.81	1.35	2.7	5.6	2.8
8	50% DCM	3187	6.73	1.15	1.32	1.15	1.4	3.0	1.6

^a Modifiers: IPA, isopropanol; EtOH, ethanol; MeOH, methanol; THF, tetrahydrofuran; EtAc, ethyl acetate; ACT, acetone; ACN, acetonitrile; DCM, dichloromethane.

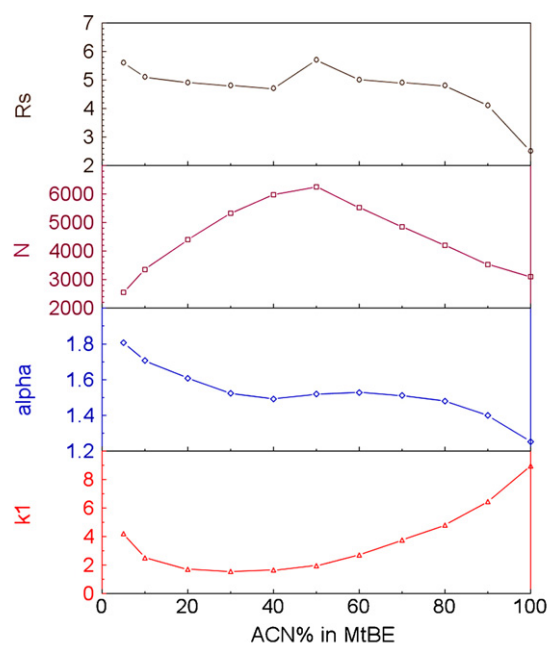


Figure 3.3 Comparison of retention, selectivity, efficiency, and resolution of the all-*trans*-astaxanthin separations with mobile phases of different acetonitrile/methyl *t*-butyl ether compositions. k_1 is the retention capacity of the first eluted isomer (SS); α is the selectivity between the RR and SS isomer; N is the number of plates for the second eluted isomer (meso); R_s is the resolution between RR and SS isomers.

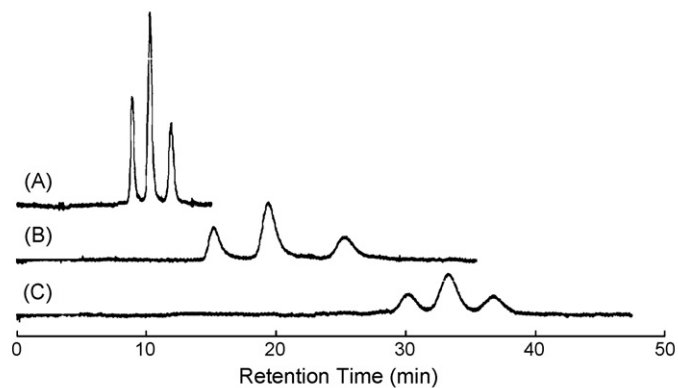


Figure 3.4 Separations of all-*trans*-astaxanthin on Chiralpak IC CSP. Mobile phases: (A), MtBE/ACN 50/50; (B), MtBE/ACN 95/5; and (C) ACN 100%.

acetonitrile increased from 5% to 40%, leveled off at ~1.50 between 40% and 80% acetonitrile in MtBE, and continued to decrease to 1.25 when a pure acetonitrile mobile phase was used. The efficiency of the meso-astaxanthin peak showed a maximum of 6230 at a 50/50 MtBE/acetonitrile mobile phase composition, and decreased rapidly when either the acetonitrile or MtBE volume percentage increased. The resolution profile paralleled the selectivity curve, with an exception of the 50/50 v/v MtBE/acetonitrile mobile phase composition, where the separation reached the highest resolution due to the highest efficiency. Figure 3.4 shows separations with mobile phases of (A) MtBE/acetonitrile 50/50, (B) MtBE/acetonitrile 95/5, and (C) 100% acetonitrile.

3.4.2 Separation of Structurally Related Carotenoids

Adonirubin and adonixanthin are precursors along the biosynthetic pathway of astaxanthin.^{16, 26} Compared to astaxanthin, adonirubin has one less hydroxyl group attached to a stereogenic carbon center, and thus has only one stereogenic center and two enantiomers (3R or 3S-adonirubin). Adonixanthin has one less ketone group than astaxanthin. Thus it has two stereogenic centers but no internal plane of symmetry (and therefore no meso compound). Although all-*trans*-adonixanthin has four stereoisomers (two pairs of enantiomers), the sample used for analysis is manually mixed (3R,3'R) and (3S,3'S)-adonixanthin enantiomers. Figure 3.5 compares the enantiomeric separation of these three structurally related carotenoids. The removal of the ketone group significantly reduces the retention, selectivity and overall separation (peak 1 and 3 vs. 6 and 7), whereas the removal of hydroxyl group has virtually no effect on the retention or separation (peak 1 and 2 vs. peak 4 and 5). All enantiomers of these structurally related compounds are baseline separated.

3.4.3 Isolation and Separation of 13-*cis*-Astaxanthin

All-*trans*-astaxanthin is readily isomerized to *cis-trans* mixtures, especially to the 9-*cis* and 13-*cis* isomers for steric reasons.¹⁹ In our study, isomerization was achieved by exposing all-*trans*-astaxanthin to daylight for a week. The separation between all-*trans*, 9-*cis*, and 13-*cis*-astaxanthin was achieved on a C18 column with a methanol/dichloromethane/acetonitrile/water 85/5/5.5/4.5 mobile phase according to literature.²⁷ Figure 3.6A shows the separation of isomerized astaxanthin on an analytical C18 column. The capacity factor is about two times that reported by Yuan et al, which could be the result of the different C18 columns

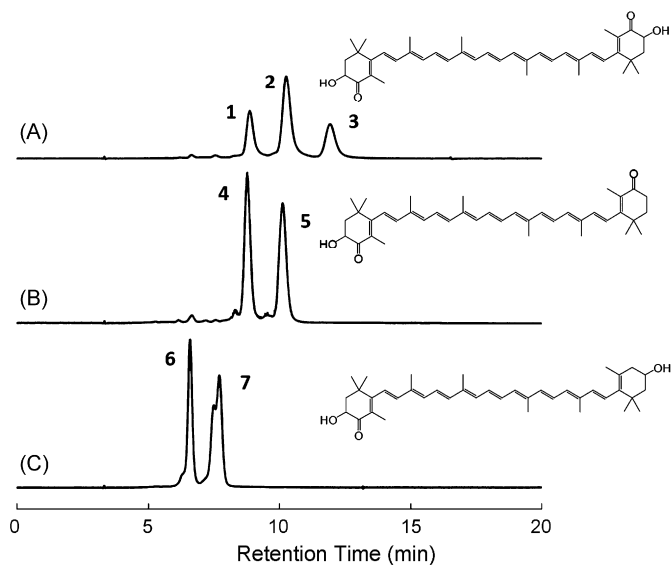


Figure 3.5 Separation of (A) all-*trans*-astaxanthin, (B) adonrubin, and (C) adonixanthin on Chiralpak IC CSP with MtBE/ACN 50/50 mobile phase. Peak 1, 2, and 3: (3*S*,3'*S*), (3*S*,3'*R*), and (3*R*,3'*R*)-astaxanthin; peak 4, 5: undetermined (3*R*/*S*)-adonrubin; peak 6, and 7*: (3*S*, 3'*S*), and (3*R*, 3'*R*)-adonixanthin. *The split in peak 7 is due to impurities in (3*R*,3'*R*)-adonixanthin sample from CaroteNature (Lupsingen, Switzerland).

employed. However, the retention pattern is the same as that reported previously. In addition, the absorption spectra obtained with a diode array detector also confirms the formation and elution of 9-*cis* and 13-*cis*-astaxanthin.²⁷

A preparative C18 column was used to separate and collect isomers of astaxanthin. The eluents collected from the preparative C18 separation were concentrated and subsequently injected into the analytical C18 column to check for purity, and then the Chiralpak IC column for the enantiomeric separations. After purification by preparative HPLC separation, there was no detectable *cis* isomer in the all-*trans* astaxanthin (Figure 3.6B). The enantiomeric separation of the pure all-*trans*-astaxanthin is shown in Figure 3.6 E. However, the 9-*cis* and 13-*cis* isomers cannot be completely separated on the preparative C18 column, and are collected as mixtures. The separation on the analytical C18 reveals that the mixture contains 3.7% of all-*trans*-astaxanthin, 9.7% of 9-*cis*-astaxanthin, and 86.6% of 13-*cis*-astaxanthin (Figure 3.6C). The stereoisomers of ~87% pure 13-*cis*-astaxanthin were also separated at the same chromatographic conditions as the all-*trans*-astaxanthin (Figure 3.6F). Figure 3.7 shows the chromatograms obtained with both UV and circular dichroism (CD) detector for the all-*trans* and 13-*cis*-astaxanthin. Note that the “central eluting” meso compound (all-*trans*- (3R,3'S)-astaxanthin) registers no peak with chiroptical detection (top chromatogram in Figure 3.7A). However, upon the *trans* to *cis* isomerization, the symmetry of the all-*trans*-meso-astaxanthin is lost, and two non-superimposable enantiomers: 13-*cis*-(3R,3'S)-astaxanthin, and 13-*cis*-(3S,3'R)-astaxanthin are generated. Therefore, there are two pairs of enantiomers, or four stereoisomers, of 13-*cis*-astaxanthin. The separation on Chiralpak IC (Figure 3.7B), as well as previously reported separations in literature,^{24a, b, 25} separated only three stereoisomers of 13-*cis*-astaxanthin with stereoisomeric ratio 1:2:1. Separation of all four stereoisomers of 13-*cis*-astaxanthin was achieved on Chiralpak IB with a heptane/acetone 95/5 mobile phase (Figure 3.8).

3.4.4 Stereoisomeric Purity Test of Commercial Nutraceutical Supplements

Astaxanthin supplements from four different manufactures were analyzed. Two of these marked the source as *Haematococcus pluvialis* algae extract, and the other two indicated “natural astaxanthin” on the bottle. The supplement in the liquid state was directly injected into the preparative C18 column with a guard column. The eluent of all-*trans*-astaxanthin was collected, concentrated and subsequently analyzed by

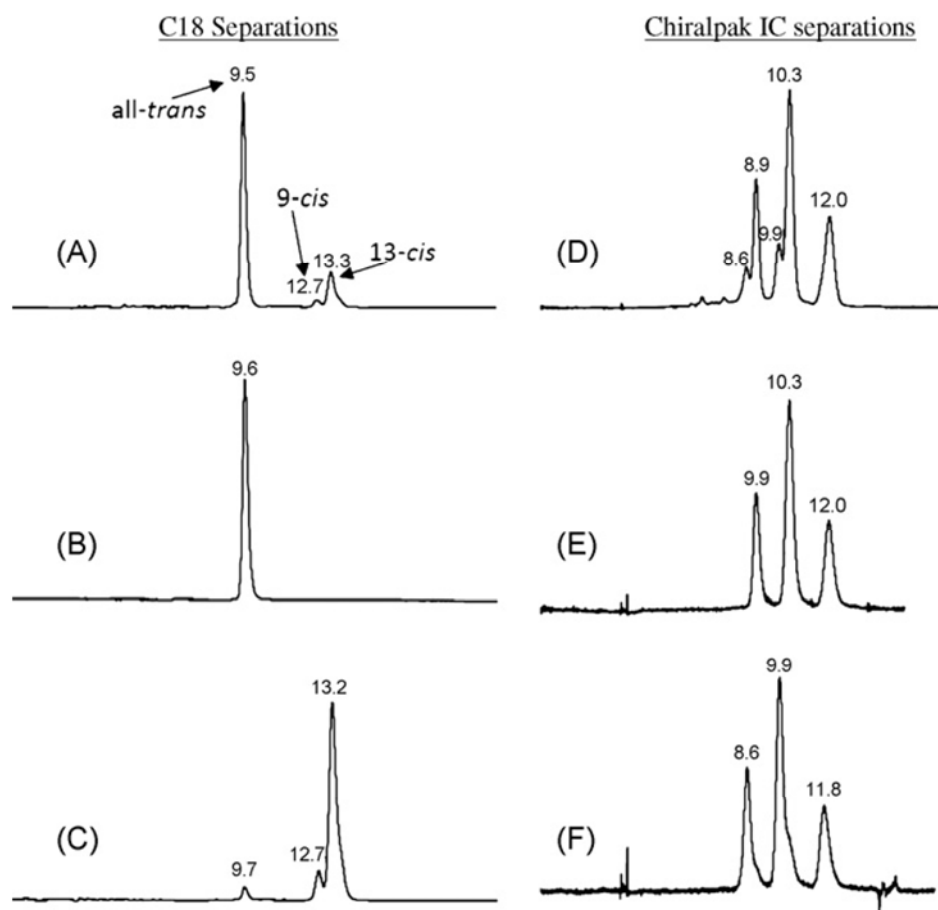


Figure 3.6 Separation of astaxanthin isomers. (A,D), isomerized mixtures of *cis* and *trans*-astaxanthin obtained by exposing all-*trans*-astaxanthin to daylight for 6 days; (B,E), all-*trans*-astaxanthin purified from isomerized mixtures by preparative C18 separation; (C,F) *cis*-astaxanthin (mainly 13-*cis*) purified from isomerized mixtures by preparative C18 separation. (A-C), analytical C18 stationary phase from Astec, MeOH/ACN/DCM/H₂O 85/5/5.5/4.5; (D-E), Chiralpak IC CSP, MtBE/ACN 50/50.

Chiralpak IC using the method described above. All of these tested commercial supplements showed no detectable meso or (3R,3'R) stereoisomer of all-*trans*-astaxanthin, indicating that the (3S,3'S) isomer accounts for more than 99.5% of all-*trans*-astaxanthin in the supplement. Previously, Renstrom et al reported 99% (3S,3'S)-astaxanthin (*trans* + *cis*), and 1% meso-all-*trans*-astaxanthin in *Haematococcus pluvialis* extract.²⁸ The authors also noted that the 1% meso compound was possibly produced during their analysis.²⁸ Our result is in good agreement with that reported by Renstrom et al, and confirms that these commercial astaxanthin supplements are produced from natural source.

3.5 Conclusion

An HPLC method using a chiral stationary phase was developed to directly separate all stereoisomers of all-*trans*-astaxanthin. For the first time, the stereoisomers of all-*trans*-astaxanthin, and its structurally related compounds (adonirubin and adonixanthin) were directly baseline separated from each other. The all-*trans*-astaxanthin was partially isomerized to its *cis* forms after exposure to daylight. The separation of all four stereoisomers of 13-*cis*-astaxanthin was obtained on the Chiralpak IB CSP for the first time. Four natural sourced commercial astaxanthin supplement were analyzed to contain almost exclusively (3S,3'S) isomer of all-*trans*-astaxanthin.

3.6 Acknowledgement

We gratefully acknowledge the National Institutes of Health, General Medical Science NIH RO1 GM53825-12 for support of this work. C.-D. Chang acknowledges the support of Dr. Thomsa H. Goodin.

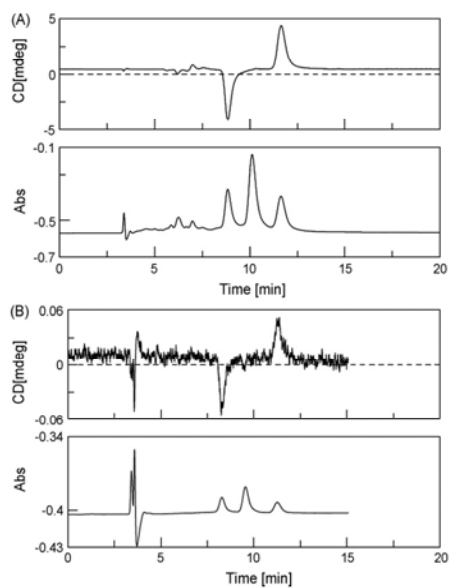


Figure 3.7 Chromatograms obtained with Circular Dichroism (CD) detector on Chiralpak IC CSP. (A) all-*trans*-astaxanthin, and (B) 13-*cis*-astaxanthin. Top chromatograms were obtained using chiroptical detector (see Experimental), are the bottom chromatograms utilized UV detector (330 nm). Mobile phase: MtBE/ACN 50/50.

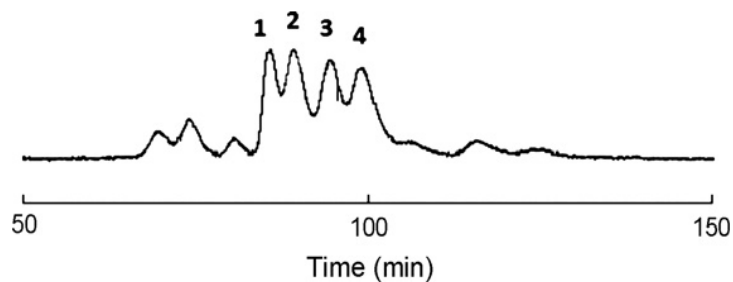


Figure 3.8 Separation of all four stereoisomers (peak 1-4) of 13-*cis*-astaxanthin on Chiralpak IB CSP. Mobile phase: heptane/acetone 95/5. Note: small peaks in the chromatogram are possibly other forms of *cis* isomers of astaxanthin co-eluted with 13-*cis*-astaxanthin on the preparative C18 column.

CHAPTER 4

EMPIRICAL OBSERVATIONS AND MECHANICAL INSIGHTS ON THE FIRST BORON-CONTAINING CHIRAL SELECTOR FOR LC AND SFC

4.1 Abstract

Boromycin is a macrodiolide that exists as a hydrophobic Böeseken complex formed from boric acid and a chiral polyhydroxy macrocyclic ligand. It was covalently bonded to silica gel through a urea linkage to an attached D-valine ester. When evaluated as a chiral stationary phase it shows pronounced enantioselectivity toward primary amine-containing racemates, separating 98% of those tested. The selectivity is most pronounced in the presence of organic solvents and supercritical CO₂ + methanol. The enantioselective binding site and mechanistic factors are examined. Analytes can be complexed as either the free base or their protonated analogues, with the free base being more strongly associated with the chiral selector.

Chunlei Wang, Daniel W. Armstrong, and Donald S. Risley. *Analytical Chemistry* (2007), 79(21), 8125-8135. Copyright © 2007 with permission from the American Chemical Society.

4.2 Introduction

Despite the large number of chiral selectors introduced for modern enantiomeric separations, a few classes tend to dominate the field. The dominant class of chiral selector differs with the separation technique. For example, derivatized cyclodextrins are most often used as chiral stationary phases (CSPs) in gas chromatography.²⁹ Natural and derivatized cyclodextrins are the most frequently used chiral selectors in capillary electrophoresis.³⁰ In liquid chromatography (LC) there is a greater variety and number of chiral selectors available than for other analytical methods.³¹ LC also differs in that it often is used for the preparative separations of enantiomers.³² One's choice of a chiral selector in LC can be strongly affected by factors in addition to enantioselectivity. For example, in pharmacokinetic and pharmacodynamics studies, a reversed phase or polar organic mode CSP often is preferred.³³ For preparative separations a supercritical fluid or normal phase separation can be beneficial given the greater ease of sample recovery and higher

flow rates for these techniques.³⁴ When using ESI-MS detection, a polar organic solvent usually is preferred.³⁵ In order for a new LC-CSP to have a significant impact nowadays it must be either: (a) more broadly applicable than existing CSPs, (b) superior in regard to one or more specific separation properties than existing CSPs (e.g., loadability, separation time, solvent compatibility, specific analyte selectivity, etc.), or (c) fill a separation niche not occupied by any current LC-CSP. Other beneficial aspects of chiral selectors include a reasonable knowledge of their structure and mechanism of action so that they can be utilized and optimized in a logical manner. It is not uncommon that mechanistic studies continue for years after the introduction of chiral selectors. Indeed these studies can be complex, involved and require a variety of experimental and theoretical approaches. The enantioselective separation mechanism of some CSPs remain poorly understood today. Finally, the “holy grail” of CSP understanding is considered to be the ability to predict whether or not a specific CSP can separate enantiomers of a particular compound or group of compounds. This is possible with only a few CSPs.

In this work we introduce a new, highly unusual chiral selector for LC. To our knowledge it is the first effective chiral selector that contains boron. Furthermore, the boron is a stereogenic center and is essential for chiral molecular recognition. We have determined the essential structural characteristics that are required for chiral analytes to be separated. In addition, this CSP fills an important niche in regard to the type of enantiomers separated and their separation mode. Finally information on the separation mechanism will be presented.

4.3 Experimental Section

4.3.1 Materials

HPLC grade Kromasil silica gel (particle size 5 μm , pore size 100 \AA , and surface area 310 m^2/g) was obtained from Akzo Nobel (EKA Chemicals, Bohus, Sweden). All organosilane compounds were obtained from Silar Laboratories (Wilmington, NC). These include: (3-aminopropyl)dimethylethoxysilane, (3-aminopropyl)triethoxysilane, [2-(carbomethoxy)ethyl]trichlorosilane, [1-(carbomethoxy)ethyl]methyldichlorosilane, (3-isocyanatopropyl)triethoxysilane and (3-glycidoxypropyl)triethoxysilane. Anhydrous *N,N*-dimethylformamide (DMF), anhydrous toluene, tetramethylammonium nitrate, tetraethylammonium nitrate, tetrapropylammonium chloride,

tetrabutylammonium nitrate and all chiral analytes tested were obtained from Sigma-Aldrich (Milwaukee, WI). HPLC grade *n*-heptane, 2-propanol, ethanol, methanol, acetonitrile, methylene chloride, 1,4-dioxane, ethyl acetate, tetrahydrofuran were purchased from VWR (Bridgeport, NJ). Boromycin was the generous gift of Eli Lilly and Company (Indianapolis, IN).

Three different linkage chemistries to 5 μ m diameter silica gel particles were attempted as outlined in previous studies.³⁶ A procedure for the successful CSP of the current study is as follows. A 1.3 molar excess of (3-isocyanatopropyl)triethoxysilane was added to 0.5 g of dried boromycin dissolved in 40 mL of dry DMF. This slight excess was sufficient to react with the accessible primary amine of the boromycin but not with the relative inaccessible and less reactive secondary alcohol moieties within its cavity. The reaction was stirred under anhydrous conditions at 95 °C for 5 h. This solution was added to 3.0 g of dry silica gel in a 250-mL three-neck flask. The slurry was heated at 105 °C and stirred for 16 h. The mixture is then cooled, filtered and washed with successive 50 mL portions of DMF, methanol, 50% aqueous methanol and again neat methanol. The elemental analysis for the finished product was: C, 6.6%; H, 1.36%; and N, 0.72%.

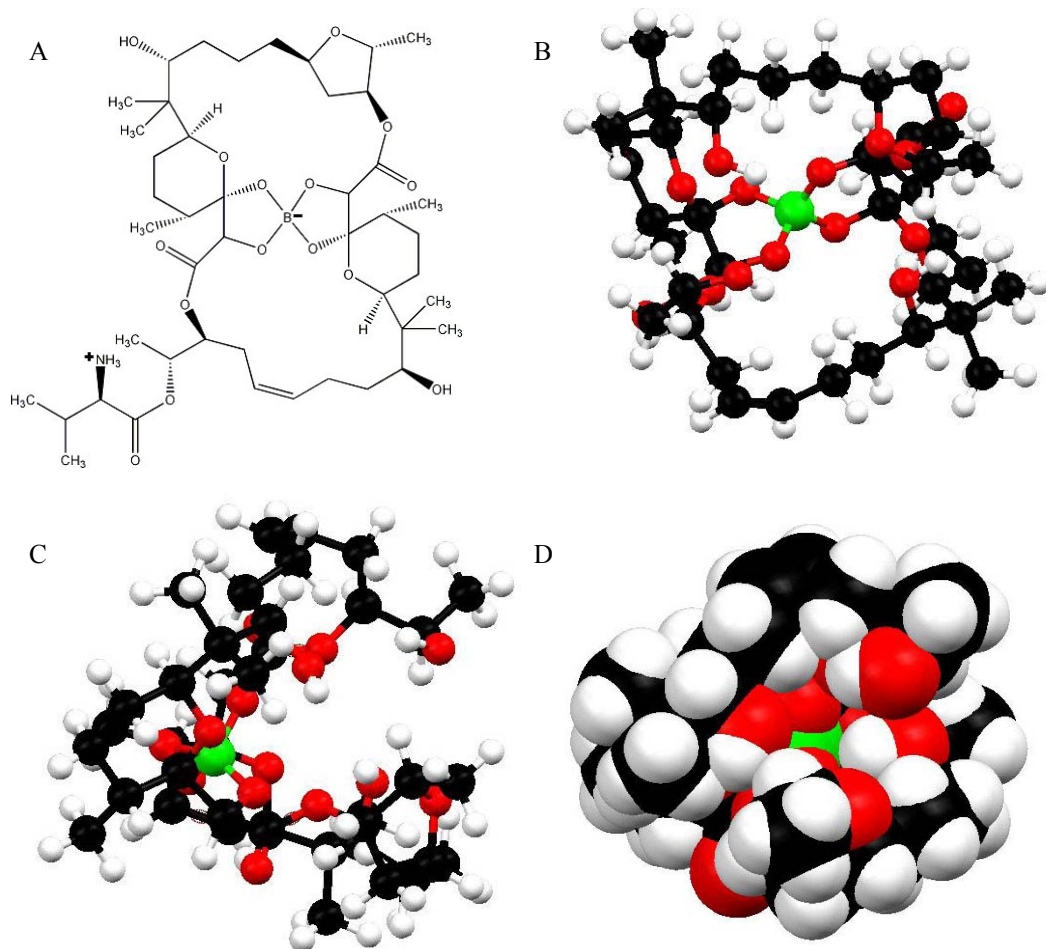
4.3.2 Methods

The CSP was slurry packed into a 15 cm or 25 cm x 0.44 cm (i.d.) stainless steel column. The analytes were dissolved in methanol, ethanol or the appropriate mobile phases. Separations were achieved on an HP 1050 HPLC system with an auto sampler, a UV VWD detector, and computer-controlled HP ChemStation for data processing. The mobile phases were degassed under helium for 10 min. Separations were carried out with 1 mL/min flow rate, 254 nm UV detection wavelength, and at room temperature (~22 °C) unless noted otherwise. The aliphatic amines were detected by Shimadzu (Columbia, MD) RF-10A_{XL} Spectrofluorometric detector after post column derivatization according to the literature.³⁷ In these cases, the mobile phase flow rate was 0.5 mL/min, and the column eluent was mixed with a 0.5 mL/min post-column stream (3.8 g *o*-phthalaldehyde and 2.0 mL 2-mercaptoethanol dissolved in 500 mL methanol). The mixed stream passed a 50 cm PEEK tube (0.25 mm i.d., 1.6 mm o.d.) heated at 45 °C before it reached the detector. The formed adduct fluoresced at 431 nm when excited with 340 nm UV light. Additional mobile phase compositions are listed in the appropriate tables and figures. Note that all solvent mixtures are

given as additive volume percents. The SFC apparatus used for this work was from Thar Technologies, Inc. (Pittsburgh, PA). The SFC system includes a fluid delivery module (liquid CO₂ pump and cosolvent pump), an auto sampler with a 48 sample tray, a column oven with column switching, an auto back pressure regulator, a UV VWD detector, and the SuperChrom software for data processing. The mobile phase for SFC were different compositions of CO₂ and cosolvents (methanol with additives dissolved in it). Separations were carried out with 4 mL/min flow rate, 254 nm UV detection wavelength, and the column was kept at 40 °C, with a 100 bar back pressure. The software used to edit molecular structure of boromycin was Gaussview 3.0 from Gaussian, Inc. (Wallingford, CT) and Mercury 1.4.2 from The Cambridge Crystallographic Data Centre (Cambridge, UK).³⁸

4.4 Results and Discussion

Boromycin is thought to be the first discovered and characterized naturally occurring organic compound that contains boron.³⁹ It is produced via fermentation by a strain of *Streptomyces antibioticus*.⁴⁰ It tends to bind strongly to cell membranes and can act as an ion channel.⁴¹ It can inhibit the growth of gram-positive bacteria and some fungi and protozoae.^{41a} More recently boromycin has been shown to have anti-HIV activity,⁴² to selectively inhibit Ca²⁺ influx in human erythrocytes,⁴³ and to abrogate the bleomycin-induced G2 checkpoint.⁴⁴ Boromycin is a macrodiolide Böeseken complex (named for J. Böeseken who extensively studied boric acid + polyol complexes⁴⁵) containing a D-valine ester as shown in Figure 4.1A. It contains 16 carbon-based stereogenic centers, has two free hydroxyl groups, each attached to a stereogenic center. Boromycin is poorly soluble in water, partly soluble in water-miscible solvents and soluble in many other organic solvents including halocarbons, DMF, DMSO and so forth. A summary of physicochemical properties of boromycin is given in Table 4.1. The valine moiety can be hydrolytically cleaved from boromycin using a dilute solution of a strong base at moderate temperatures.⁴⁶ The x-ray structure of the resulting anion is shown in Figure 4.1B,C, and D.^{46a} Note that the negatively charged “boron-moiety” (in green) is imbedded deep within the C-shaped organic ligand. Except for two carbonyl groups, all oxygens (in red) are inside the C-shaped cavity. The external surface of the macrodiolide is mainly hydrocarbon which make it very nonpolar, despite the charged groups, and helps to explain its solubility. The molecular recognition properties (particularly chiral recognition) of boromycin has not been



considered. No molecule of this type or structure has been evaluated as a chiral selector. After covalently linking boromycin to silica gel (see Experimental) the resulting CSP was evaluated via HPLC by injection of over 250 racemates of most structural types in three mobile phase modes (reversed phase, normal phase and polar organic). The results are summarized in Table 4.2 to Table 4.4. The total number of separated compounds in the three tables is 52, which does not seem to be an extraordinarily high percentage by today's standards. However, a closer examination of the data reveals some rather interesting facts. All the separated compounds are primary amines. In fact 52 out of the 53 primary amine containing compounds tested were easily separated on a 15 cm column – an extraordinarily high percentage. This includes compounds with no other functionality, i.e., simple amino alkanes, that ordinarily can only be separated by gas chromatography (see 2-aminoheptane, Table 4.4, compound 2). Only chiral crown ether-based CSPs have an analogous selectivity for primary amine containing compounds, but even they don't appear to be as broadly applicable for this specific class of compounds as boromycin.⁴⁷ There is another even more significant difference. The boromycin chiral selector works primarily in organic solvents (normal phase and polar organic modes) while chiral crown ether CSPs are used exclusively with acidic, aqueous mobile phases – most often with 0.01 M HClO_{4(aq)}.^{47a-f} This is because the amine must be protonated (ammonium ion form) to form an inclusion complex with 18-crown-6 or similar analogues. In contrast, boromycin does not require protonated amines. It can separate enantiomers of lipophilic amines (that have poor water solubility) or hydrophilic amines as either the free base or the salt (provided they can be solubilized in an organic or polar organic mobile phase). Figure 4.2 shows the types of separations obtained on this CSP. Good efficiencies and separation times <10 minutes are normal. Because of the organic mobile phase composition these separations are amenable to supercritical fluid separations and preparative scale-up as will be discussed in a later section.

The composition of the mobile phase strongly affects retention, efficiency and selectivity. The typical polar organic mobile phase consists of methanol + an organic modifier + a dilute additive (in mM concentration). Figure 4.3 shows the effect of organic modifiers on all three chromatographic parameters for a racemic, free base amino acid amide (methionine- β -naphthylamide, Figure 4.3, A-C) and the hydrochloride salt of an amino alcohol (tyrosinol hydrochloride, Figure 4.3, D-F). The 1,4-dioxane modifier produces the best

Table 4.1 Physicochemical Properties of Boromycin.

Characteristic	
empirical formula	C ₄₅ H ₇₄ BNO ₁₅
molecular weight	879.9
no. of carbon stereogenic centers ^a	16
produced via fermentation from	<i>Streptomyces antibioticus</i>
no. of marocyclic rings	2
no. of hydroxyl groups	2
no. of amine groups	1
no. of charged moieties	2 : boron (-); ammonium (+)
no. of esters	3
no. of ether groups	5
no. of boron moieties	1
solubility	Insoluble in water; partially soluble in methanol, ethanol, acetonitrile; Soluble in <i>N,N</i> -dimethylformamide, dimethylsulfoxide, dichloromethane, chloroform
<i>pI</i> ^b	6.1
acid stability	Acid can remove the boric acid moiety ^c
base stability	Hydrolysis of the valine ester occurs in the presence of dilute solutions of strong base ^d

^a The central boron is also a stereogenic center. ^b The *pI* value was measured using dilute solutions of boromycin in 0.01 M phosphate buffer / methanol (80/20). DMSO was used as the EOF marker. ^c See reference 47. ^d See reference 46.

Table 4.2 Chromatographic Data for Enantiomeric Separation of Amino Alcohol Enantiomers on the Boromycin CSP.

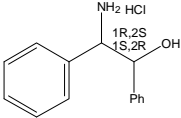
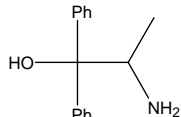
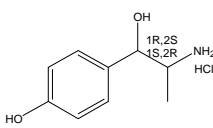
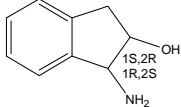
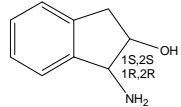
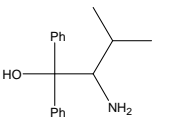
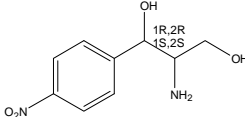
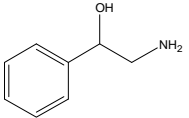
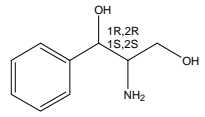
#	COMPOUNDS	$k'{}^a$	α	R_s	Mobile Phase ^b	TMAN ^c
1	2-amino-1,2-diphenylethanol 	0.877	1.36	2.2	MeOH/ACN 70/30	30mM
2	2-amino-1,1-diphenyl-1-propanol 	0.754	1.37	1.8	MeOH/ACN 70/30	10mM
3	α -(1-aminoethyl)4-hydroxybenzyl alcohol hydrochloride 	0.471	1.63	2.4	MeOH/ACN 70/30	30mM
4	<i>cis</i> -1-amino-2-indanol 	0.447	1.99	3.7	MeOH/DiOx 80/20	5mM
5	<i>trans</i> -1-amino-2-indanol 	0.799	1.50	2.4	MeOH/ACN 70/30	30mM
6	2-amino-3-methyl-1,1-diphenyl-1- butanol 	0.935	1.30	2.1	MeOH/DCM 20/80	2.5mM
7	2-amino-1-(4-nitrophenyl)-1,3- propanediol 	1.16	1.31	1.8	MeOH/DiOx 50/50	5mM
8	2-amino-1-phenylethanol 	1.42	1.63	2.8	MeOH/ACN 70/30	30mM
9	2-amino-1-phenyl-1,3-propanediol 	0.998	1.38	2.1	MeOH/DiOx 50/50	5mM

Table 4.2 – Continued

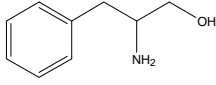
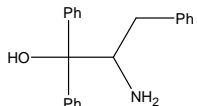
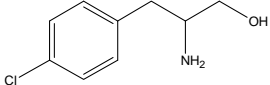
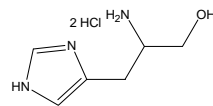
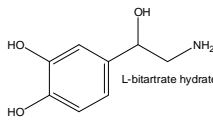
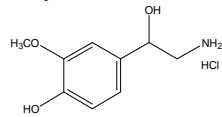
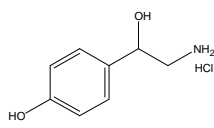
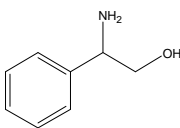
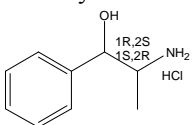
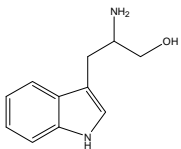
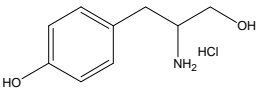
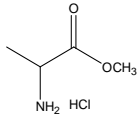
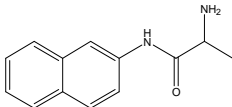
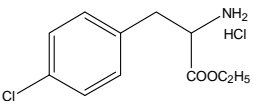
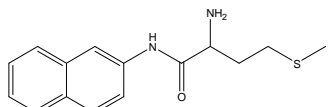
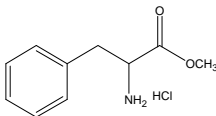
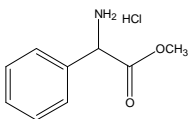
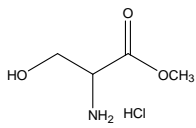
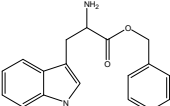
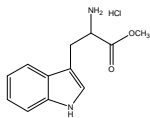
10	2-amino-3-phenyl-1-propanol	0.583	1.43	2.5	MeOH/DiOx 80/20	5mM
						
11	2-amino-1,1,3-triphenyl-1-propanol	0.590	1.80	2.1	EtOH/DCM 10/90	2.5mM
						
12	4-chlorophenyl alaninol	0.687	1.70	3.7	MeOH/DiOx 80/20	5mM
						
13	histidinol dihydrochloride	2.44	1.00	0.0	MeOH 100	10mM
						
14	norepinephrine L-bitartrate hydrate	1.54	1.60	3.8	MeOH/DiOx 80/20	5mM
						
15	normetanephrine hydrochloride	1.39	1.60	3.2	MeOH/ACN 70/30	30mM
						
16	octopamine hydrochloride	1.41	1.59	2.7	MeOH/ACN 70/30	30mM
						
17	2-phenylglycinol	1.94	1.32	1.7	MeOH/DiOx 50/50	5mM
						
18	phenylpropanolamine hydrochloride	0.486	1.62	1.9	MeOH/ACN 70/30	30mM
						

Table 4.2 – *Continued*

19	tryptophanol		1.58	1.29	2.1	MeOH/DiOx 50/50	5mM
20	tyrosinol hydrochloride		0.545	1.33	1.8	MeOH/DiOx 80/20	5mM

^a This is the k' of the first eluted enantiomer. ^b Mobile phases: MeOH for methanol, EtOH for ethanol, ACN for acetonitrile, DCM for dichloromethane, DiOx for 1,4-dioxane. ^c Molarity of additive tetramethylammonium nitrate in the mobile phases.

Table 4.3 Chromatographic Data for Enantiomeric Separation of Amino Acid Ester/Amide Enantiomers on the Boromycin CSP.

#	COMPOUNDS	k' ^a	α	R_s	Mobile Phase ^b	TMAN ^c
1	alanine methyl ester hydrochloride 	0.174	2.32	1.8	MeOH/DiOx 70/30	5mM
2	alanine- β -naphthylamide hydrochloride 	7.19	1.38	3.0	MeOH/ACN 20/80	10mM
3	4-chlorophenylalanine ethyl ester hydrochloride 	0.265	3.53	6.5	MeOH/ACN 70/30	30mM
4	methionine β -naphthylamide 	1.19	1.45	3.8	MeOH/DiOx 80/20	5mM
5	phenylalanine methyl ester hydrochloride 	0.236	2.91	4.1	MeOH/ACN 70/30	30mM
6	2-phenylglycine methyl ester hydrochloride 	0.0777	3.58	2.9	MeOH 100	30mM
7	serine methyl ester hydrochloride 	0.250	2.60	2.6	MeOH/DiOx 70/30	5mM
8	tryptophan benzyl ester 	0.306	2.33	3.5	MeOH/ACN 70/30	30mM
9	tryptophan methyl ester hydrochloride 	0.290	1.73	2.0	MeOH/ACN 70/30	30mM

^a This is the k' of the first eluted enantiomer. ^b Mobile phases (MPs): MeOH for methanol, ACN for acetonitrile, DiOx for 1,4-dioxane. ^c Molarity of tetramethylammonium nitrate in the MPs.

Table 4.4 Chromatographic Data for Enantiomeric Separation of Other Primary Amine Enantiomers on the Boromycin CSP.

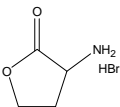
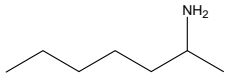
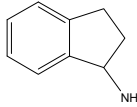
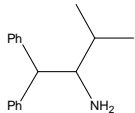
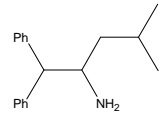
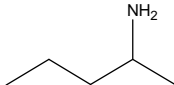
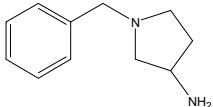
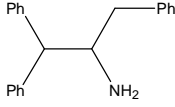
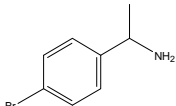
#	COMPOUNDS	k'^a	α	R_s	Mobile Phase ^b	TMAN ^c
1	α -amino- γ -butyrolactone hydrochloride 	0.217	1.18	0.6	MeOH/ACN 70/30	30mM
2 ^d	2-aminoheptane 	7.83	1.20	1.4	MeOH/ACN 10/90	4mM
3	1-aminoindan 	0.793	1.56	2.2	MeOH/ACN 70/30	30mM
4	2-amino-3-methyl-1,1-diphenylbutane 	0.982	1.31	2.2	EtOH/ACN 20/80	5mM
5	2-amino-4-methyl-1,1-diphenylpentane 	2.43	1.33	1.8	MeOH/DiOx 20/80	2.5mM
6 ^d	2-aminopentane 	6.56	1.11	0.6	MeOH/ACN 10/90	4mM
7	1-benzyl-3-aminopyrrolidine 	7.48	1.18	0.8	MeOH/DCM 50/50	10mM
8	1-benzyl-2,2-diphenylethylamine 	0.843	1.33	1.9	EtOH/ACN 20/80	5mM
9	1-(4-borophenyl)ethylamine 	0.438	1.49	2.6	MeOH 100	10mM

Table 4.4 – *Continued*

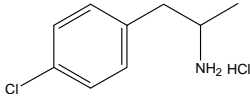
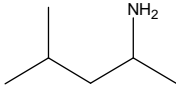
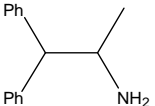
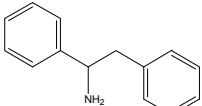
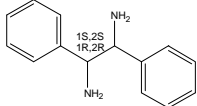
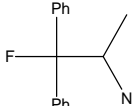
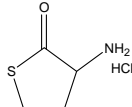
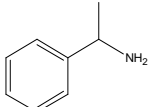
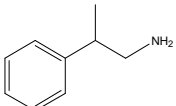
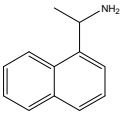
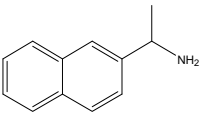
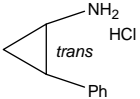
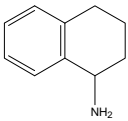
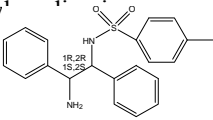
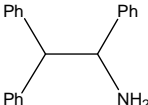
10	<i>p</i> -chloroamphetamine 	1.69	1.38	1.6	EtOH 100	2.5mM
11 ^d	1,3-dimethylbutylamine 	7.98	1.14	0.9	MeOH/ACN 10/90	4mM
12	1,1-diphenyl-2-aminopropane 	0.533	1.47	2.1	MeOH/ACN 50/50	10mM
13	1,2-diphenylethylamine 	3.17	1.20	1.5	MeOH/EtOAc 50/50	5mM
14	1,2-diphenylethylenediamine 	1.08	1.49	3.5	MeOH/DiOx 50/50	5mM
15	1,1-diphenyl-1-fluoro-2-aminopropane 	0.525	1.47	2.4	MeOH/ACN 50/50	10mM
16	homocysteine thiolactone hydrochloride 	0.611	1.35	1.9	MeOH/DiOx 80/20	5mM
17	α -methylbenzylamine 	1.03	1.31	1.9	MeOH/ACN 80/20	2.5mM
18	β -methylphenethylamine 	1.54	1.05	0.6	MeOH/ACN 70/30	10mM

Table 4.4 – Continued

19	1-(1-naphthyl)ethylamine 	0.716	1.61	2.7	MeOH/ACN 70/30	30mM
20	1-(2-naphthyl)ethylamine 	0.764	1.60	3.4	MeOH/ACN 70/30	30mM
21	<i>trans</i> -2-phenylcyclopropylamine hydrochloride 	2.76	1.16	1.3	MeOH/ACN 70/30	30mM
22	1,2,3,4-tetrahydro-1-naphthylamine 	1.09	1.32	2.0	MeOH/THF 70/30	10mM
23	<i>N</i> - <i>p</i> -tosyl-1,2-diphenylethy' 	0.434	1.74	2.9	MeOH/ACN 30/70	5mM
24	1,2,2-triphenylethylamine 	0.268	1.59	2.4	MeOH/ACN 50/50	10mM

^a This is the k' of the first eluted enantiomer. ^b Mobile phases: MeOH for methanol, ACN for acetonitrile, DiOx for 1,4-dioxane. ^c Molarity of additive tetramethylammonium nitrate in the mobile phases. ^d Post column derivatization with *o*-phthalaldehyde/2-mercaptoethanol and the Shimadzu fluorescence detector were used for the detection of aliphatic amines. ³⁷

efficiency, selectivity and shortest retention for tyrosinol hydrochloride as well as the best efficiency for methionine- β -naphthylamide. However, an ethyl acetate modifier produced the shortest retention times and good selectivity for methionine- β -naphthylamide.

The dilute additive (often a quaternary ammonium salt) has a tremendous effect on the retention and efficiency of chiral primary amine containing compounds. This profound effect also provides evidence for the primary enantioselective retention mechanism on these CSPs. This is illustrated in Figure 4.4. With no additive, most analytes have exceeding long retention times and poor efficiencies with substantial tailing peaks (Figure 4.4A). This indicates a very strong interaction with the boromycin with poor mass transfer on the stationary phase. The addition of 10 mM of an appropriate additive can decrease retention by an order of magnitude and increase efficiency by 1-2 orders of magnitude (Figure 4.4B). The selectivity is generally maintained unless much higher additive concentrations are used. The magnitude of this effect changes with the nature and size of the additive. As shown in Figure 4.5, increasing the size of the tetraalkylammonium ion produces less profound effects in regard to decreasing retention time and enhancing efficiency.

However, if the additive competes too effectively with the chiral analyte for the chiral selector (i.e., ammonium ion in Figure 4.5A) then a single unresolved sharp peak is obtained near the dead volume. Since free unprotonated amines bind even more strongly to boromycin than their protonated ammonium analogues, they are not usually effective additives, for the same reason ammonium is not (Figure 4.5A).

Figure 6 shows the effect of added organic modifier (acetonitrile in this case) and added tetramethylammonium nitrate (TMAN) on retention and enantioselectivity. Addition of a poor or non hydrogen bonding modifier to the mobile phase increases retention and enantiomeric separation (Figure 4.6A). Increasing concentrations of the additive salt decreases retention and eventually enantioselectivity (Figure 4.6B).

Packed column supercritical fluid separations (SFC) are playing an increasingly important role in enantiomeric separations.³⁴ Its advantage with respect to separation speed (because of higher flow rates) and analyte recovery (less solvent) have made it particularly advantageous for preparative separations. The ability of CSPs to perform SFC enantiomeric separations is considered an additional advantage, particularly for pharmaceutical applications. Figure 4.7 shows the SFC separation of three racemic analytes on a 15 cm

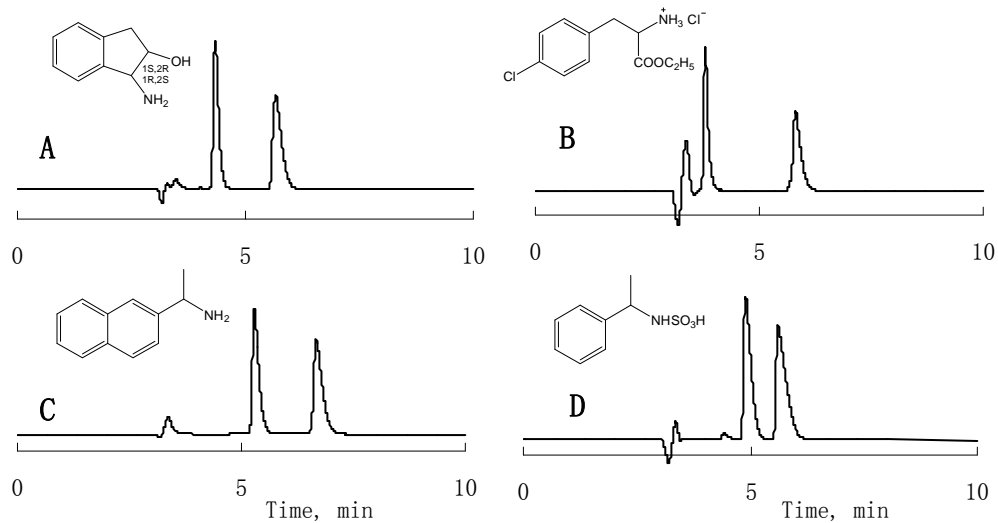


Figure 4.2 Chromatograms showing typical separations on the boromycin CSP: (A) *cis*-1-amino-2-indanol, (B) 4-chlorophenylalanine ethyl ester hydrochloride, (C) 1-(2-naphthyl)ethylamine and (D) phenethylsulfamic acid. Mobile phases: (A), methanol/1,4-dioxane/tetramethylammonium nitrate (TMAN) 80/20/5 mM; (B), (C) and (D), methanol/acetonitrile/TMAN 70/30/30 mM. Note that chromatogram D is a separation of the only compound in this study that wasn't a primary amine.

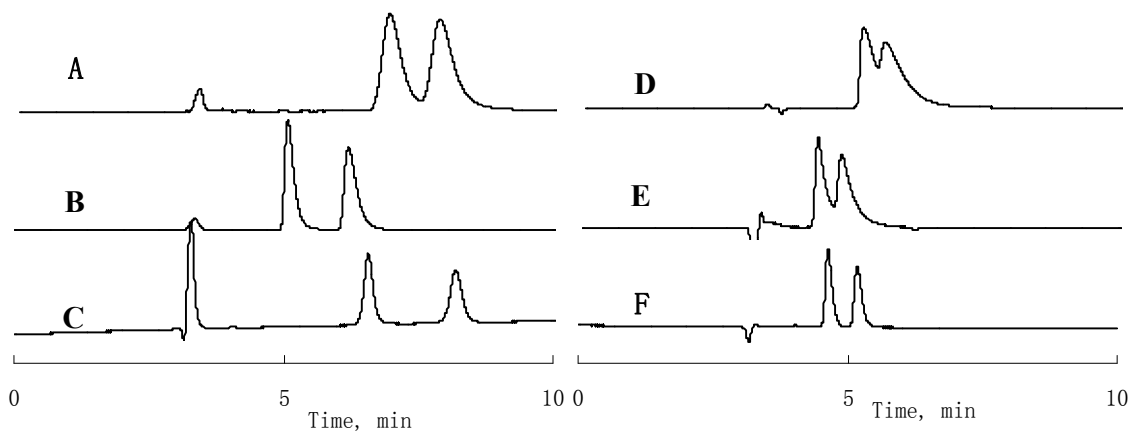


Figure 4.3 Effects of organic modifiers in a methanol mobile phase on the separation of: A, B & C = methionine beta-naphthylamide and D, E & F = tyrosinol hydrochloride. Mobile phases: (A), methanol/acetonitrile/TMAN 80/20/10 mM; (D), methanol/acetonitrile/TMAN 60/40/10 mM; (B), (E), methanol/ethyl acetate/TMAN 70/30/5 mM; (C), (F), methanol/1,4-dioxane/TMAN 80/20/5 mM.

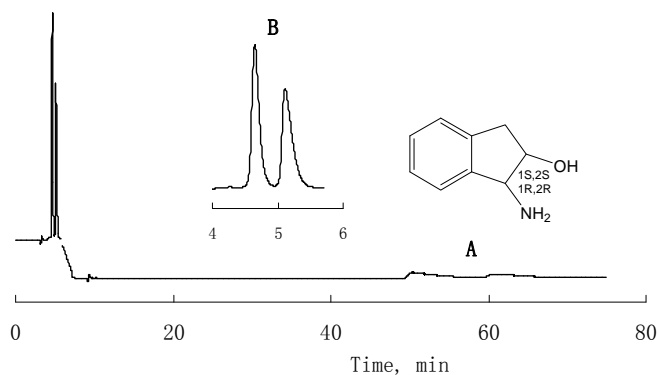


Figure 4.4 Separations of *trans*-1-amino-2-indanol using a methanol mobile phase: (A) without and (B) with 10 mM TMAN (see Results and Discussion for details.) (A): $k_1' = 14.0$, $\alpha = 1.24$, $R_s = 1.3$; (B): $k_1' = 0.553$, $\alpha = 1.29$, $R_s = 1.6$.

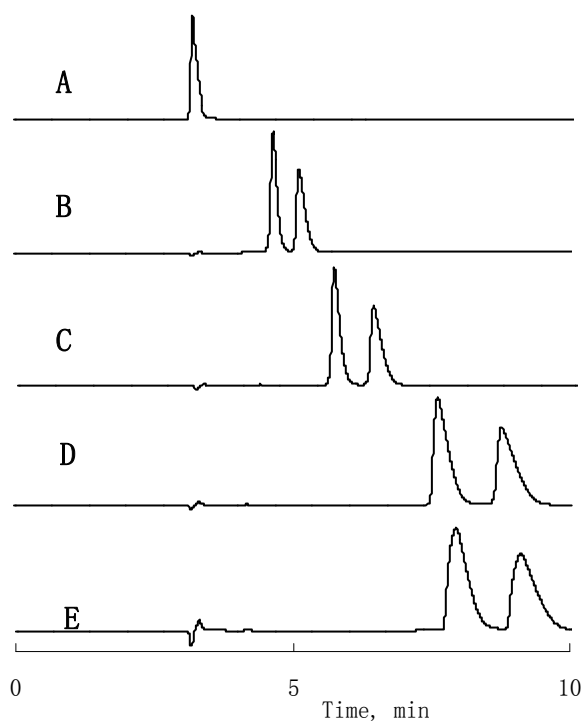


Figure 4.5 Separations of *trans*-1-amino-2-indanol using methanol as the mobile phase with 10mM additives of: (A) ammonium nitrate, (B) tetramethylammonium nitrate (TMAN), (C) tetraethylammonium nitrate (TEAN), (D) tetrapropylammonium chloride (TPAC) and (E) tetrabutylammonium nitrate (TBAN).

boromycin CSP. Typical mobile phase compositions are CO₂ + methanol + a dilute additive. As in the case of HPLC, only primary amine-containing compounds are separated. As can be seen, the separation times are even less than the already short LC separation times (Figure 4.7). The efficiencies are somewhat lower as is sometimes the case with SFC.³⁴ A more exhaustive evaluation of SFC especially in terms of preparative separations and the production of enantiomers is currently under way.

4.5 Enantioselective Retention Mechanism

All previous information on the structure of boromycin and the current data on its association/separation of chiral molecules provide evidence as to the nature and location of its enantioselective binding site. First, the x-ray crystal study of *des*-valine boromycin indicated that the associated rubidium counter cation (not shown in Figure 4.1, B-D) is accommodated within the oxygen-lined cleft (Figure 4.1). When esterified with D-valine (to form boromycin, Figure 4.1A), its ammonium group can be accommodated in the same position.^{46a} Indeed it appears that there are only two possible locations where boromycin can associate with polar functionalities of molecules (chiral or achiral). The first and most obvious is the same oxygen lined cleft that also contains the “buried” negatively charged boron moiety. Oppositely charged ions and free amines most likely insert and bind strongly here. The cleft itself is quite narrow (Figure 4.1C), making it likely that steric interactions are very important for chiral molecular recognition. Indeed, a comparison of the separation of enantiomers for compounds that also are geometrical isomers or differ by only a methyl group support this contention. For example, compare the retention and selectivity for *cis* and *trans*-1-amino-2-indanol (compounds 4&5, Table 4.2), compounds 17&18 in Table 4.2, compounds 4&5 in Table 4.4, and compounds 17&18 in Table 4.4. The importance of “steric bulk” is further indicated in Table 4.5, where the enantiomeric separations of amino acid esters and their related amino alcohol counterparts are compared. Steric bulk that is not alpha to the amine group tends to produce larger selectivities and resolutions. Hence the esters are better separated. Thus it is likely that charge-charge interactions, hydrogen bonding with the cleft oxygens and steric repulsion are largely responsible for chiral recognition by boromycin.

For cations, the size of the ion affects its association with boromycin. For steric reasons, larger cations cannot penetrate the cavity/cleft as easily as smaller cations (Figure 4.5). Hence larger cations cannot

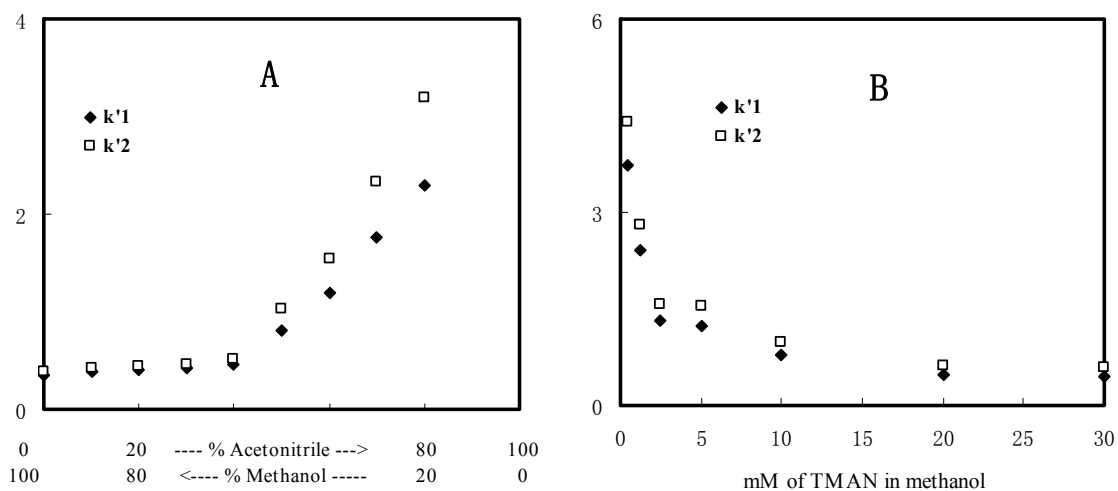


Figure 4.6 (A), Retention of the first eluted (k'1) and the second eluted (k'2) enantiomers of homocysteine thiolactone hydrochloride as the function of mobile phase organic modifier composition. Mobile phases: methanol/acetonitrile/TMAN (100-x)/x/10 mM. (B), Retention of the first eluted (k'1) and the second eluted (k'2) enantiomers of *trans*-1-amino-2-indanol as the function of the tetramethylammonium nitrate additive concentration. Mobile phases: methanol with various amount of TMAN.

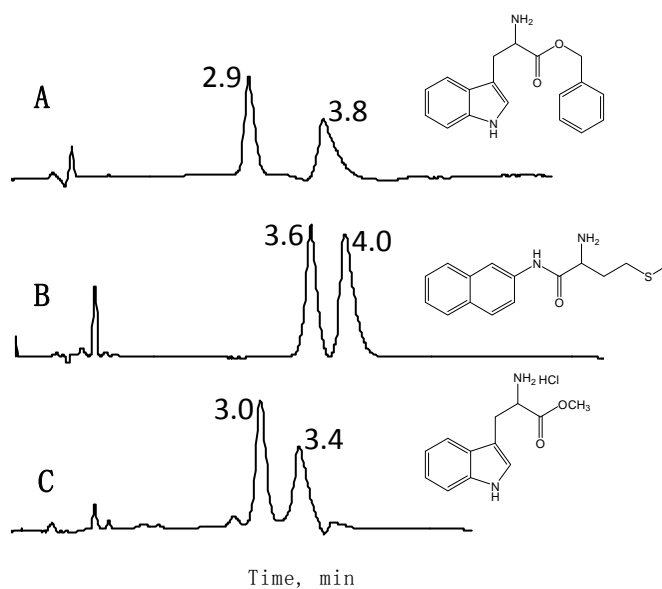


Figure 4.7 Supercritical Fluid Chromatography (SFC) enantiomeric separations of (A) DL-tryptophan benzyl ester, (B) DL-methionine beta-naphthylamide, and (C) DL-tryptophan methyl ester hydrochloride on the 15 cm boromycin CSP column. Mobile phase, CO₂/methanol(20 mM TMAN) 70/30; flow rate, 4 mL/min; temperature, 40 °C; and column back pressure, 100 bar.

compete with and displace primary amine-containing compounds from the boromycin cleft as easily as can smaller cations. Likewise, free primary amines penetrate and are even more strongly retained than cations. The phenomena is clearly illustrated in Figure 4.8, where the free base of 2-phenethylamine is strongly retained and is severely broadened while its hydrochloride salt elutes just after the dead volume as a sharp peak. When 2.5 mM tetramethylammonium nitrate was added in the mobile phase, both the free base and hydrochloride salt forms of 2-phenethylamine elute just after dead volume, with essentially the same retention time as that of the hydrochloride salt in a mobile phase without additives (chromatograms not shown). Certainly the relative mobile phase solubility of the free base versus its protonated ion pair as well as the association with boromycin CSP will affect the separation. Larger racemic secondary and tertiary amines do not bind as strongly or selectively and are not effectively separated in this study.

In order to study the effect of the boron in boromycin, boric acid was removed from the complex via mild acid hydrolysis.^{46b} The remaining ligand is chiral and has a conformation similar to that of boromycin.^{46b} However, no enantiomeric separations of the compounds in Table 4.2 to Table 4.4 were observed, although they were retained. Clearly the anionic boron moiety is essential for chiral molecular recognition.

The only other location on the boromycin molecule that is available for ionic association would be on the backside of the molecule where the boron is close to the outer surface (Figure 4.1). Although an electrostatic association may be possible here, this site is surrounded by hydrocarbon and offers few other interactions possibilities, particularly in the presence of organic solvents (which negate hydrophobic interactions).

4.6 Conclusions

Boromycin is the first effective, boron-containing chiral selector. It strongly retains and selectively separates enantiomers of a wide variety of primary amine-containing compounds. The boromycin CSP is most selective in the presence of organic solvents and supercritical CO₂ + methanol. Unlike crown ether-based CSPs (which require aqueous mobile phases) boromycin can complex unprotonated amines as well as protonated amines. Because of the strength of the CSP-amine complex, mM concentrations of a competitive binding additive profoundly enhances efficiency and decreases retention. Most separations are completed in 4-10 minutes. The amine group of chiral analytes insert in the boromycin's oxygen lined cleft

Table 4.5 Comparison of Enantiomeric Separations of Amino Alcohols and their Related Amino Acid Esters on the Boromycin CSP^a

Amino acid alcohols/esters	<i>k'</i> 1	<i>k'</i> 2	α	<i>R</i> s
4-chlorophenyl alaninol	0.447	0.687	1.44	1.3
4-chlorophenylalanine ethyl ester hydrochloride	0.267	0.936	3.53	6.5
DL-tryptophanol	0.337	0.427	1.27	0.9
DL-tryptophan methyl ester hydrochloride	0.290	0.503	1.73	2.0
DL-tryptophan benzyl ester	0.306	0.712	2.33	3.5

^aMobile phase: methanol/acetonitrile/TMAN 70/30/30 mM.

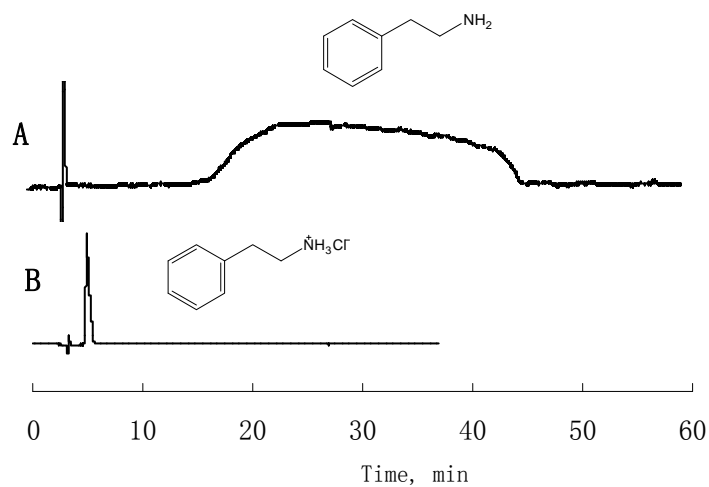


Figure 4.8 Comparison of retention behavior of an achiral primary amine (2-phenethylamine) in its free base form (A), and in the hydrochloride salt form (B) on the boromycin CSP. Mobile phase: 100% methanol.

near the negatively charged boron moiety. The cleft is a sterically restricted space. Consequently “steric bulk” on the analyte plays a major role in chiral molecular recognition. In particular, steric bulk β -, γ - or further from the amine moiety tends to enhance selectivity. Removal of boric acid from the chiral selector produces a chiral ligand with no observed enantioselective behaviors toward any of the chiral amines in this study.

4.7 Acknowledgements

We thank Ye Bao for measuring the pI of boromycin, and Jacquelyn Cole of Thar Technologies Inc. for the use of her SFC instrument and guidance. Finally we gratefully acknowledge the National Institutes of Health, General Medical Science NIH RO1 GM53825-11 for support of this work.

CHAPTER 5

DEVELOPMENT OF NEW HPLC/SFC CHIRAL STATIONARY PHASES BASED ON NATIVE AND DERIVATIZED CYCLOFRUCTANS

5.1 Abstract

An unusual class of chiral selectors, cyclofructans, is introduced for the first time as bonded chiral stationary phases. Compared to native cyclofructans (CFs), which have rather limited capabilities as chiral selectors, aliphatic- and aromatic-functionalized CF6s possess unique and very different enantiomeric selectivities. Indeed, they are shown to separate a very broad range of racemic compounds. In particular, aliphatic-derivatized CF6s with a low substitution degree baseline separate all tested chiral primary amines. It appears that partial derivatization on the CF6 molecule disrupts the molecular internal hydrogen bonding, thereby making the core of the molecule more accessible. In contrast, highly aromatic-functionalized CF6 stationary phases lose most enantioselective capabilities toward primary amines, however they gain broad selectivity for most other types of analytes. This class of stationary phases also demonstrates high “loadability” and therefore has great potential for preparative separations. The variations in enantiomeric selectivity often can be correlated with distinct structural features of the selector. The separations occur predominantly in the presence of organic solvents. Ping Sun, Chunlei Wang, Zachary S. Breitbach, Ying Zhang, Daniel W. Armstrong. *Analytical Chemistry*, in press. Copyright © 2007 with permission from the American Chemical Society.

5.2 Introduction

Enantiomeric separations have attracted great attention in the past few decades. Early enantioselective LC work in the 1980's provided the impetus for the 1992 FDA policy statement on the development of stereoisomeric drugs.^{5a} This was because the facile analysis and preparation of many pharmaceutically active enantiomers became possible for the first time. Such broadly applicable techniques were essential for pharmacokinetic and pharmacodynamic studies, development, quality control and sometimes production of

enantiomeric drugs. HPLC with chiral stationary phases (CSPs) is far and away the most powerful and widely used technique for solvent-based enantiomeric separations at both analytical and preparative scales. Supercritical fluid separations are increasing in importance, particularly for preparative separations. However, they use the same packed columns as those for LC.

Currently, over a hundred CSPs have been reported, and these CSPs are made by coating or bonding the chiral selectors, usually to silica gel supports. Interestingly, only a few types/classes of CSPs dominate the field of enantiomeric separations, for example, polysaccharide-based CSPs,⁴⁸ macrocyclic antibiotic CSPs,⁴⁹ and π complex CSPs.⁵⁰ Researchers continue to make great efforts to develop new HPLC CSPs, which could make a substantial impact on enantiomeric separations. It has been stated that today in order for any new CSPs to have an impact, they must fulfill one or more of the following requirements:⁵¹ (a) broader applicability than existing CSPs; (b) superior separations for specific groups of compounds; or (c) fill an important unfulfilled separation niche. In the present paper, a unique class of CSPs based on cyclofructan (CF) is introduced, and is shown to have the potential to satisfy all of the above-mentioned requirements.

Cyclofructans (CFs) are one of a relatively small group of macrocyclic oligosaccharides.⁵² Cyclodextrins are perhaps the best known member of this class of molecules.^{11a, 53} However, as will be shown, cyclofructans are quite different in both their structure and behavior. Cyclofructans consist of six or more β -(2 \rightarrow 1) linked D-fructofuranose units (see Figure 5.1). Common abbreviations for these compounds are CF6, CF7, CF8, etc, which indicate the number of fructose units in the macrocyclic ring. Cyclofructans were first reported by Karvamura and Uchiyama in 1989.^{52b} Their structures were determined by means of enzymic, spectroscopic, and chromatographic methods. Cyclofructans have been used in a variety of applications mostly as additives to consumer products, such as moderators of food and drink bitterness and astringency,⁵⁴ browning prevention agent,⁵⁵ ink formulation agent,⁵⁶ lubricants⁵⁷ and so on. In addition, cyclofructans have been shown to have cryoprotective effects,⁵⁸ and complexing abilities toward metal ions.⁵⁹ However, to date and to our knowledge, there have been no published reports on HPLC enantiomeric separations using either native cyclofructan or derivatized cyclofructans as chiral selectors. In the present work, we described the unique structure of CF6, synthesis of CF6-based CSPs, chiral

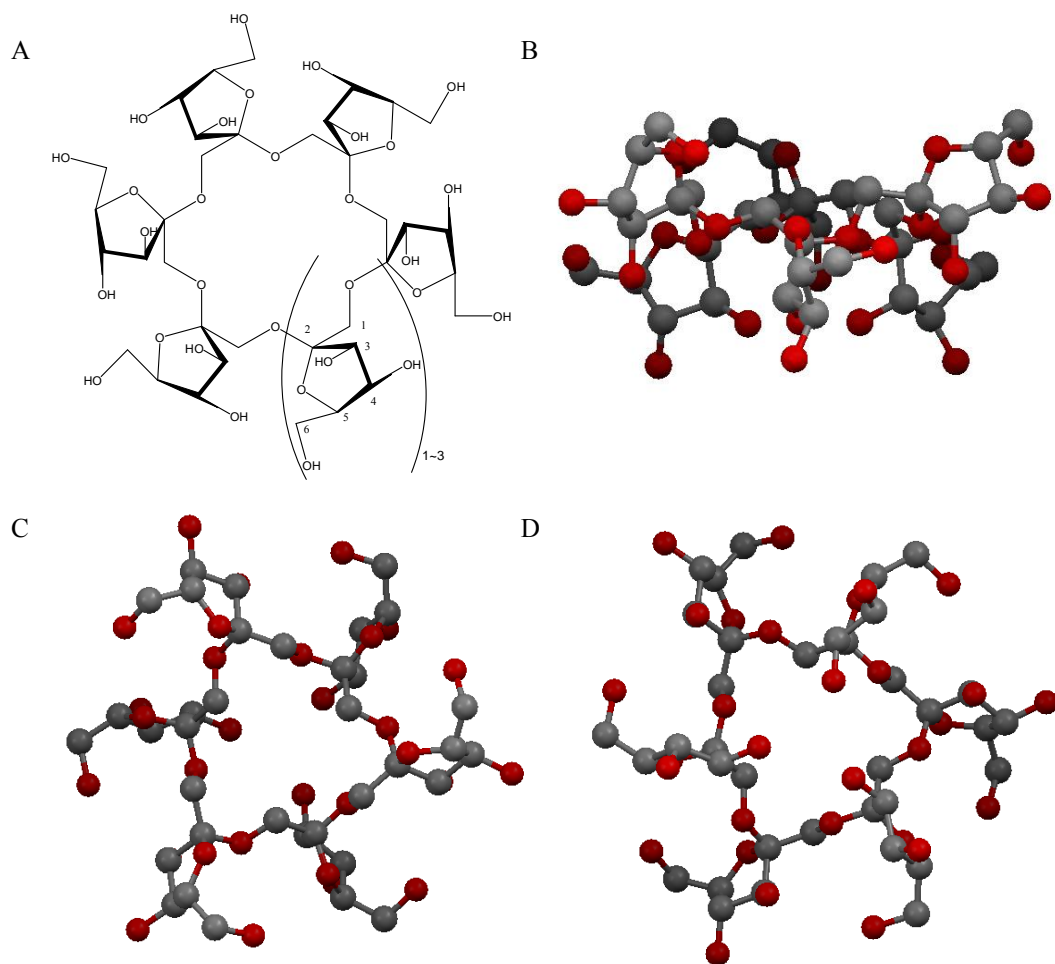


Figure 5.1 Structure of cyclofructan. (A) Molecular structure of CF6, CF7 and CF8; (B-D) Crystal structure of CF6: B. side view; C. hydrophobic side up; D. hydrophilic side up. Color scheme: oxygen atoms are red and carbons are black. Hydrogens are not shown.

separation mechanistic considerations, their chromatographic performance in terms of enantiomeric separations, and the pronounced effect of certain derivatization approaches on CF6 structure and selectivity.

5.3 Experimental Section

5.3.1 Materials

Cyclofructans (CFs) can be produced either by fermentation of inulin via any of five microorganisms (for example, *Bacillus circulans* OKUMZ 31B and *B. circulans* MCI-2554),^{52b, 60} or incubation of inulin with the active enzyme cycloinulo-oligosaccharide fructanotransferase (CFTase).^{52a} Also, the CFTase gene has been isolated, and its sequence has been determined and incorporated into common baker's yeast.^{52a, 60b} Therefore, mass-produced CFs could be available at low cost. CF6, and a mixture of CF7 (80%) + CF6 (20%) were generously donated by Mari Yasuda at Mitsubishi Chemical Group (Tokyo, Japan). Different types of silica (all of 5 μ m spherical diameters) were utilized. They include Daiso silica of 5 μ m spherical diameter (300 Å pore size, 107 m²/g surface area; 200 Å, 170 m²/g; 120 Å, 324 m²/g; 100 Å, 440 m²/g), and Kromasil silica (300 Å, 116 m²/g; 200 Å, 213 m²/g; 100 Å, 305 m²/g). Anhydrous N,N-dimethylformamide (DMF), anhydrous toluene, anhydrous pyridine, acetic acid (AA), triethylamine (TEA), trifluoroacetic acid (TFA), butylamine, sodium hydride, 3-(triethoxysilyl)propyl isocyanate, 1,6-diisocyanatohexane, (3-aminopropyl)triethoxysilane, 3-glycidoxypropyltrimethoxy silane, and all of 81 racemic analytes tested in this study were purchased from Sigma-Aldrich (Milwaukee, WI, USA). All isocyanate and isothiocyanate derivatization reagents were also obtained from Sigma-Aldrich. They include methyl isocyanate, ethyl isocyanate, isopropyl isocyanate, *tert*-butyl isocyanate, methyl isothiocyanate, 3,5-dimethylphenyl isocyanate, 3,5-dichlorophenyl isocyanate, *p*-tolyl isocyanate, 4-chlorophenyl isocyanate, 3,5-bis(trifluoromethyl)phenyl isocyanate, R-1-(1-naphthyl)ethyl isocyanate, S-1-(1-naphthyl)ethyl isocyanate, S- α -methylbenzyl isocyanate. 1-Chloro-3,5-dinitrobenzene, and 4-chloro-2,6-dinitrobenzotrifluoride were obtained from Alfa Aesar (Ward Hill, MA, USA). Acetonitrile (ACN), 2-propanol (IPA), n-heptane, ethanol (ETOH), and methanol (MEOH) of HPLC grade were obtained from EMD (Gibbstown, NJ, USA). Water was obtained from Millipore (Billerica, MA, USA).

5.3.2 Synthesis of CF-based CSPs

Native or derivatized cyclofructan were bonded to silica support by a variety of different methods. Native CF6 is used as an example to describe the procedures for the three binding chemistries tested. In the first method, silica (3 g) was dried at 110 °C for 3 h. Anhydrous toluene was added and any residual water was removed using a Dean-Stark trap for 3h. The mixture was cooled down <40 °C and 1mL of (3-aminopropyl)triethoxysilane was added dropwise to the 3 g silica-toluene slurry. Next the mixture was refluxed for 4 h and then cooled, filtered, washed and dried to obtain amino-functionalized silica (3.3 g). Then, 2 mL of 1,6-diisocyanatohexane was added to the dry amino-silica toluene slurry, which was kept in an ice bath. Next, the slurry mixture was heated to 70°C for 4h. The excess reactant was removed by vacuum filtration and the solid product was washed with anhydrous toluene twice. Lastly, 1 g of dried cyclofructan dissolved in 20 mL of pyridine was added and the mixture was heated to 70°C and allowed to react for 15 h. Finally 3.7 g of product was obtained.

The second binding chemistry also forms the carbamate linker. Cyclofructan (1g) was dissolved in 40 mL of anhydrous pyridine. To this solution, 0.7 mL of 3-(triethoxysilyl)propyl isocyanate was added dropwise under dry argon atmosphere protection. And the mixture was heated at 90 °C for 5h. Next, residual water was removed from silica gel (3g) using a Dean-Stark trap and 150 mL of anhydrous toluene. After the two mixtures were cooled to room temperature, the cyclofructan reaction mixture was added to the silica-toluene slurry and heated at 105 °C overnight. The final mixture was cooled and washed. After drying in vacuum over overnight, 3.4 g of product was obtained.

The third binding chemistry forms an ether linkage. Epoxy-functionalized silica was synthesized as previously described.^{49b} First, CF6 (1g) was dissolved in 30 mL of anhydrous DMF. Then, 0.2 g NaH was added to the solution under dry argon protection and stirred for 10 min. Unreacted NaH was removed by vacuum filtration. Lastly, dry epoxy-functionalized silica (3.3 g) was added to the filtrate, and the mixture was heated at 140 °C for 3 h and subsequently cooled down to room temperature. Then filtered and dried. Syntheses of derivatized cyclofructan chiral stationary phases (CSPs) have been conducted in a variety of ways. For example, native cyclofructan can be chemically bonded to silica, then derivatized; or cyclofructan can be first partially derivatized, then bonded to silica. Figure 5.2 shows the diagram of

covalently-bonded CF6 and the structures of the aliphatic and aromatic derivatization groups used in this study. All derivatization groups were bonded to CF6 via a carbamate or a thiocarbamate linkage, with the exception of dinitrophenyl and dinitrophenyl-trifluoromethyl groups, which are attached to CF6 via an ether linkage.⁶¹ Table 5.1 shows elemental analysis data for the native CF6-CSP, partially-derivatized methyl carbamate-CF6 CSP, and completely-derivatized R-naphthylethyl carbamate-CF6 CSP.

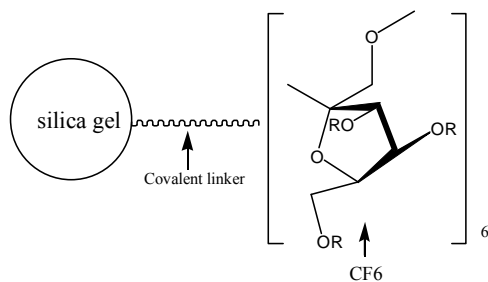
After the cyclofructan derivative is bonded to the support, it can be further derivatized to achieve more complete coverage, or to have two different derivative groups on the cyclofructan (π -acid and π -basic groups).

5.3.3 HPLC method

The HPLC column packing system is composed of an air driven fluid pump (HASKEL, DSTV-122), an air compressor, a pressure regulator, a low pressure gauge, two high pressure gauges (10000 psi and 6000 psi), a slurry chamber, check valves and tubings. The CSP was slurry packed into a 25cm \times 0.46cm (i.d.) stainless steel column.

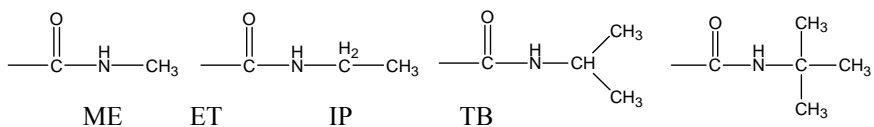
The HPLC system was an Agilent 1100 system (Agilent Technologies, Palo Alto, CA, USA), which consists of a diode array detector, an autosampler, a binary pump and Chemstation software. All chiral analytes were dissolved in ethanol, methanol or appropriate mobile phases. For the LC analysis, the injection volume and the flow rate were 5 μ L and 1mL/min, respectively. Separations were carried out at room temperature (\sim 20 $^{\circ}$ C) if not specified. The mobile phase was degassed by ultrasonication under vacuum for 5 min. Each sample was analyzed in duplicate. Three operation modes (the normal phase mode, polar organic mode, and reversed phase mode) were tested. In the normal phase mode, heptane with ethanol or isopropanol was used as the mobile phase. In some cases, TFA was used as an additive. The mobile phase of the polar organic mode was composed of acetonitrile/methanol and small amounts of acetic acid and triethylamine. Water/acetonitrile or acetonitrile/acetate buffer (20mM, pH=4.1) was used as the mobile phase in the reversed phase mode. Supercritical fluid chromatographic instrument is a Berger SFC unit with an FCM1200 flow control module, a TCM 2100 thermal column module, a dual pump control module, and a column selection valve. The flow rate is 4mL/min. The co-solvent is composed of methanol:ethanol:isopropanol=1:1:1 and 0.2% DEA (diethylamine). The gradient mobile phase

(A) CSP based on chemically-bonded CF6



R=H or derivatization group

(B) Aliphatic derivatization groups



(C) Aromatic derivatization groups

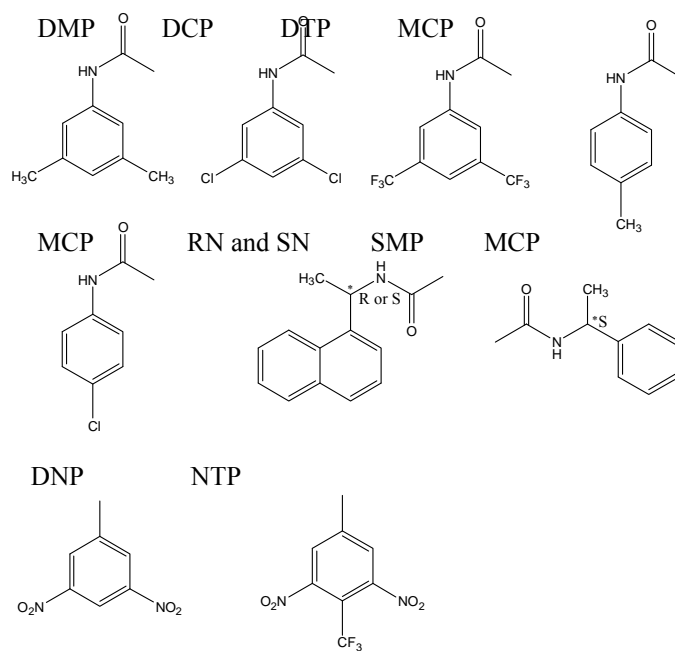


Figure 5.2 Scheme of chemically-bonded CF6 stationary phase and derivatized-CF6 CSPs and chemical structure of all derivatizing groups.

Table 5.1 Elemental analysis results of three representative CF6-based stationary phases

Chiral selector	Degree of substitution	C%	H%	N%
Native CF6	0	10.19	1.78	0.41
Methyl carbamate CF6	Low ^a	12.02	1.90	1.01
R-naphthylethyl carbamate CF6	Very high ^b	19.11	2.52	1.57

^a DS ~ 6.^b Complete derivatization (DS=18).

Table 5.2 Physical properties of cyclofructans 6-8

Macrocycle	Melting Point (°C)	$[\alpha]_D^{20}$ (°) in H ₂ O	Cavity i.d. (Å) ^c	Macrocycle o.d. (Å) ^c	Macrocycle Height (Å) ^c
CF6	210-219 ^a	-64.6 ^b	2.3	14.6	8.7-9.4
	231-233 ^b	-63.5 ^d			
CF7	215-222 ^a	-59.1 ^d	4.1	15.9	8.5-8.9
CF8	N/A	N/A	4.7	16.1	8.5-9.2

^aMelts and decomposes in this range.^bValues taken from Ref. 28.^cValues estimated from Ref. 46. Estimates accounting for van der Waals radii.^dMeasured in our lab.

composition is: 5% co-solvent hold during 0-0.6 min, 5-50% during 0.6-3.6 min, 50% hold during 3.6-4.6 min, 50%-5% during 4.6-5.1min, 5% hold during 5.1-6.6 min.

For the calculations of chromatographic data, t_0 is determined by the peak of the refractive index change due to the sample solvent, or determined by injecting 1,3,5-tri-*tert*-butylbenzene in the normal phase mode. Selectivity (α) was calculated by $\alpha=k_2'/k_1'$, where k_1' and k_2' are the retention factors of the first and second eluted enantiomers, respectively. The molecular structure modeling program is ACD/3D viewer freeware.

5.4 Results and Discussion

5.4.1 Structure and Properties of Cyclofructans

Cyclofructans consist of six or more D-fructofuranose units (Figure 5.1) and each fructofuranose unit contains four stereogenic centers and three hydroxyl groups. Their central skeleton has the same structure as the respective crown ethers. Table 5.2 gives relevant physico-chemical data for CF6, CF7 and CF8. It indicates that the “cavity” inner diameter (i.e., distance between opposing oxygen atoms in the molecular core) increase significantly from 2.3 Å for CF6 to 4.1 Å for CF8.^{60a} And the macrocycle outer diameter of CF6-CF8 demonstrates the same trend. However, the macrocycle heights are all quite similar.

Among cyclofructans, CF6 has attracted the most attention due to its availability in pure form and its highly defined geometry. The crystal structure of CF6 (shown in Figure 5.1B-D) reveals that six fructofuranose rings are arranged in spiral fashion around the crown ether skeleton, either up or down towards the mean plane of the crown ether.^{60f, g} Its symmetry is lowered to C_3 and the molecular energy decreases due to the staggered ring structure that reduces the steric repulsion between adjacent fructofuranose units.^{60a, 60f, g} Six 3-position hydroxyl groups alternate to point towards or away from the molecular center, and three oxygen atoms pointing inside (oxygen in the molecular center of Figure 5.1D) are very close to each other. The distance between them is around 3 Å, which is approximately the sum of van der Waals radius of two oxygen atoms. As a result, access to the 18-crown-6 core on one side of the macrocycle is blocked by the hydrogen bonding between these hydroxyl groups^{60g} (Figure 5.1D). This side of the macrocycle is relatively hydrophilic as the result of the directionality of all its hydroxyl groups (Figure 5.1D). It has been reported that interactions between these 3-OH groups on the CF6 hydrophilic side and metal cations plays an important role in metal complexation.^{60a} The other side of CF6 appears to be more hydrophobic,

resulting from the methylene groups of -O-C-CH₂-O- around the central indentation (Figure 5.1C). A computational lipophilicity pattern of CF6 also confirms that CF6 shows a clear “front/back” regionalization of hydrophilic and hydrophobic surfaces.^{60a} Both the crystal structure and computational modeling studies demonstrate that CF6 appears to have considerable additional internal hydrogen bonding. The fact that three 3-OH groups completely cover one side of the 18-crown-6 ring and the skeleton crown oxygens are almost folded inside the molecule, makes CF6 very different from other 18-crown-6 ether based chiral selectors. It is worth emphasizing that CF6-8 do not possess central hydrophobic cavities, as do cyclodextrins.^{11a, 53} Consequently, hydrophobic inclusion complexation, which plays an important role in the association of organic molecules with cyclodextrins, does not seem to be relevant for cyclofructans. For the above-mentioned structural reasons, native CF6 appears to have limited capabilities to form either hydrophobic inclusion complexes or ion/crown ether inclusion complexes. In order to investigate whether or not CF6 provides any chiral recognition capabilities, we synthesized the covalently bonded native-CF6 stationary phase to investigate its capability for chiral recognition. We also conducted extensive CE experiments investigating CF6 as a chiral run buffer additive. The native CF6-based column was evaluated by injecting a set of 81 analytes with a wide variety of functionalities, including amines, carboxylic acids, alcohols, and so forth. This CSP based on native CF6 only partially separated enantiomers of a few primary amines (Figure 5.3A top) and two binaphthyl compounds [i.e., 1,1'-bi(2-naphthyl diacetate), and 1,1'-bi-2-naphthol bis(trifluoromethanesulfonate)]. It appeared that none of the separations were baseline due to a combination of marginal selectivity, inefficient separations often coupled with poor peak shapes and often long retention. For all of other analytes, the CF6-CSP exhibited negligible enantioselectivity. Furthermore no enantiomeric separations were obtained with native CF6 in CE.

5.4.2 Initial Observations on the Effects of Derivatization of Cyclofructan 6

The hypothesis that extensive intramolecular hydrogen bonding in CF6 (see Figure 5.1D) and its compact configuration has detrimental effects on its enantioselective separation ability could be tested if one could disrupt its internal hydrogen bonding and allow the structure to “relax” or open somewhat. One way to do this is to block a few of the crucial hydrogen bonding groups within the CF6 structure. Interestingly, when CF6 CSPs were made with either aliphatic or aromatic substituted-CF6s (with a low degree of hydroxyl

group substitution), they exhibited tremendous enantioselectivity toward chiral primary amines (see Figure 5.3A). Molecular modeling was performed for the derivatized CF6 (Figure 5.4A) and helps to explain the improved enantiomeric resolution toward primary amines. In this simplest case, it is supposed that initial derivatization with the methyl substituent (ME) occurs with the 6-OH groups. Figure 5.4A shows a side view of the molecular model of ME-carbamate CF6, obtained with ACD/3D viewer freeware program. It suggests that the CF6 intramolecular hydrogen bonding is disrupted after partial derivatization, causing a “relaxation” of the molecular structure. This may expose the crown ether core and/or other previously inaccessible hydrogen bonding sites of the CF6. Substitution of a few of the hydroxyl groups, especially with larger derivatization groups can increase the steric bulk, which can be beneficial for improving peak efficiency (as will be discussed). However, further increases in the substitution degree on the CF6 molecule (Figure 5.3B) results in significantly worse capabilities for separating primary amines. Enantioselectivity for all primary amines was completely lost on the RN-CSP with complete substitution. The reason for this becomes apparent from the structure of CF6 with 18 RN groups (Figure 5.4B), which shows the RN groups are positioned up or down, thus enlarging the depth of the molecule and again sterically blocking the molecular core. The conversion of all hydroxyl groups to carbamate groups also removes all hydrogen bonding donor groups and most oxygens are buried deep inside the molecule. Thus, having many bulky functional groups can sterically hinder the chiral recognition of primary amines. These observations suggest that the substitution degree on CF6 is playing a crucial role in its capability for chiral recognition of primary amines. Also, it is found that aliphatic- and aromatic-functionalized CF6 CSPs provide different capabilities for separating primary amines. Figure 5.5 shows one example, comparing methyl, isopropyl and RN derivatized-CF6 stationary phases of the same substitution degree. The IP- and ME-derivatized columns gave higher enantioselectivity and resolution for tryptophanol. A noticeable improvement in peak efficiency was observed on these aliphatic-functionalized columns. The aliphatic-functionalized CF6 stationary phases separate primary amines more effectively, providing higher selectivity and/or higher efficiency. These results demonstrate that the size of the derivatizing group also plays an important role in the separation of primary amines. Although aliphatic-functionalized CF6 stationary phases with a low substitution degree were highly successful for the separations of primary amines, they show poor

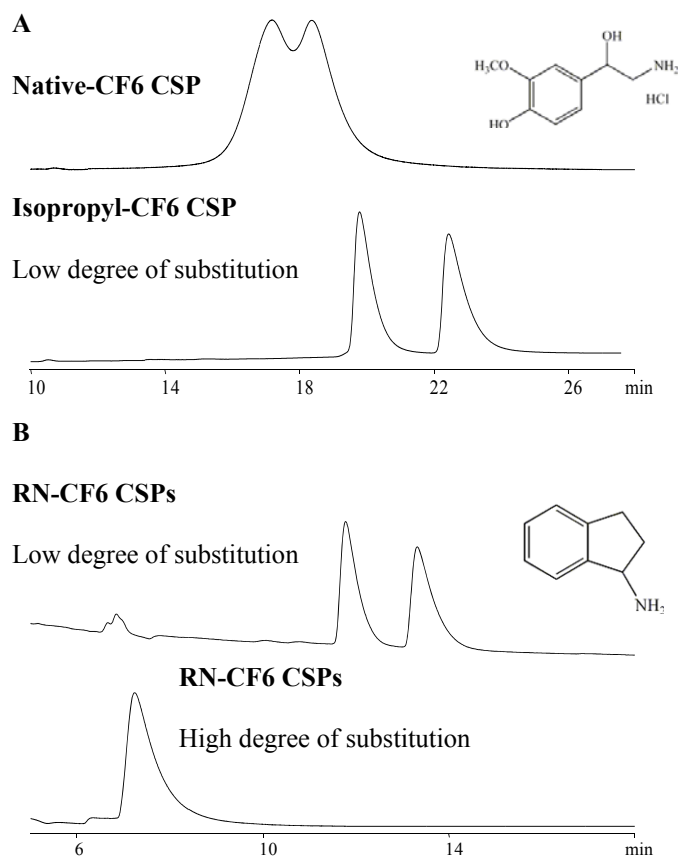
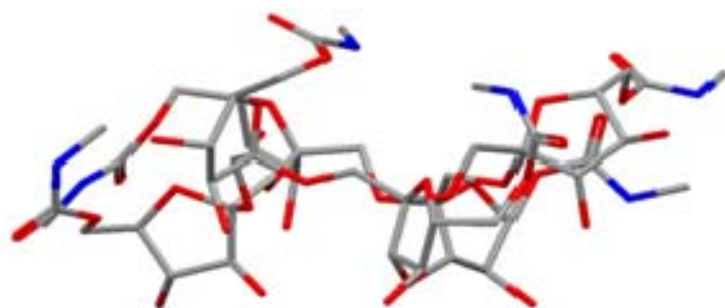


Figure 5.3 Separation of primary amines on derivatized-CF6 stationary phases with different substitution degrees. Analytes and mobile phases are: (A) normetanephrine hydrochloride, 75ACN/25MEOH/0.3AA/0.2TEA (top), 60ACN/40MEOH/0.3AA/0.2TEA (bottom); (B) 1-aminoindan, 60ACN/40MEOH/0.3AA/0.2TEA (top and bottom).

(A)



(B)

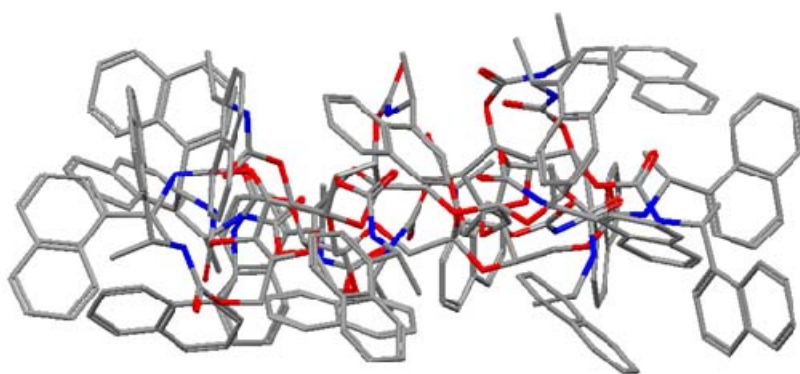


Figure 5.4 Edge view of CF6 derivatized with (A) six methyl carbamate groups and (B) eighteen R-naphthylethyl carbamate groups. The color coding is: oxygen atoms are red, carbon atoms are black and nitrogen atoms are blue. Hydrogen atoms are not shown. Compare these edge views with that of native cyclofructans in Figure 5.1B.

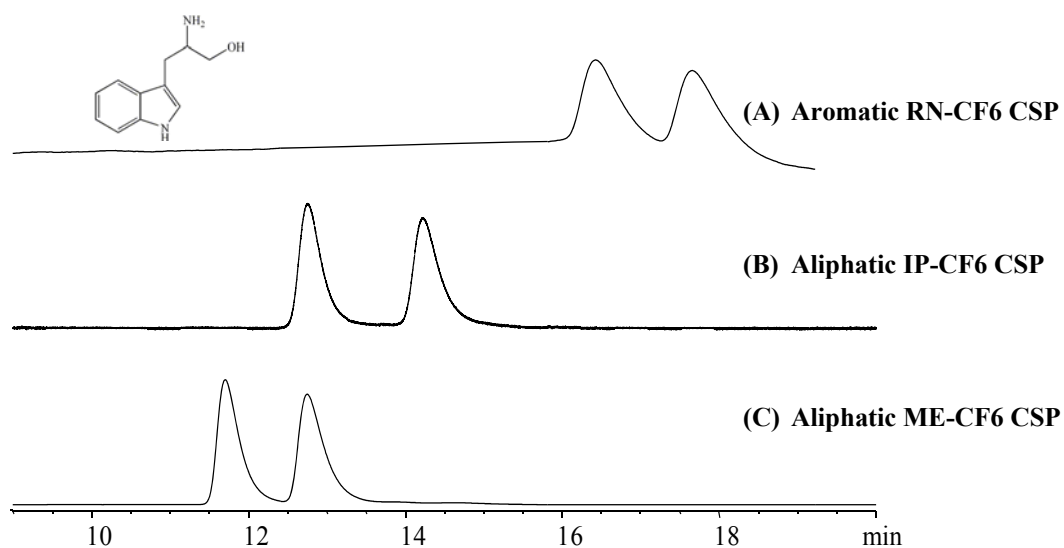


Figure 5.5 Comparison between aromatic- and aliphatic-derivatized-CF6 CSPs. The analyte is DL-tryptophan. The chromatographic data and mobile phases are:
 (A) $k_1=4.66$, $\alpha=1.12$, $R_s=1.4$, 75ACN/25MEOH/0.3AA/0.2TEA;
 (B) $k_1=3.39$, $\alpha=1.15$, $R_s=2.7$, 60ACN/40MEOH/0.3AA/0.2TEA;
 (C) $k_1=3.03$, $\alpha=1.12$, $R_s=1.7$, 60ACN/40MEOH/0.3AA/0.2TEA.

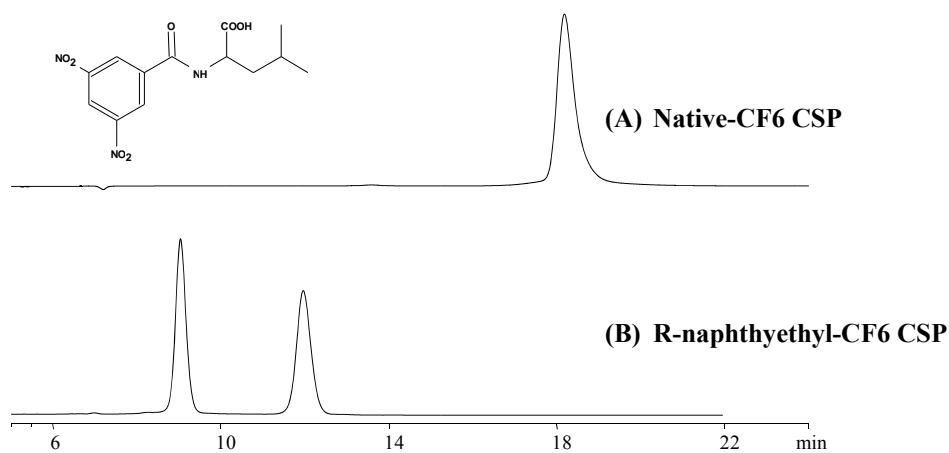


Figure 5.6 Comparison between native- and aromatic-functionalized CF6 chiral columns. The analytes is N-(3,5-dinitrobenzoyl)-DL-leucine. Mobile phases: (A) 90heptane/10ETOH/0.1TFA; (B) 70heptane/30ETOH/0.1TFA.

capabilities for separating most other analytes.

Aromatic-functionalization of a native chiral selector is a common strategy used to develop new chiral stationary phases, such as dimethylphenyl and dichlorophenyl substitution of amylose and cellulose,⁴⁸ and, and dimethylphenyl and naphthylethyl substitution of β -cyclodextrin.⁶² Compared to native chiral selectors, the aromatic derivatized-types provide improved enantioseparation capabilities and separate a wider range of analytes. Therefore it was logical to synthesize aromatic-functionalized CF6 stationary phases with a higher substitution degree. Evaluations of these stationary phases show that highly aromatic-functionalized CSPs negate the previously found almost universal selectivity for chiral primary amines. However, there was a dramatic enhancement in enantiomeric selectivity for most other types of compounds. Figure 5.6 illustrates the enhanced selectivity provided by the RN-carbamate CF6 stationary phase. N-(3,5-dinitrobenzoyl)-DL-leucine was successfully separated ($\alpha=1.91$, $R_s=4.4$) by the RN-CF6 column, while no separation was observed on the CF6-CSP. The aromatic-functionalized CF6 CSPs provide ample opportunities for multiple hydrogen bonding interactions, π - π interaction, and dipole-dipole interaction, aided by steric interactions to obtain effective chiral recognition.

It appears from these initial results, that cyclofructan can be functionalized in such ways as to provide two completely different types of chiral selectors which separate enantiomers via two different mechanisms. The minimally functionalized CF6 (with smaller aliphatic moieties) has a relaxed structure that exposes its crown ether core and additional hydroxyl groups. This allows for interactions with and separation of chiral primary amines in organic solvents for the first time. More highly aromatic derivatized CF6 has a sterically crowded structure (Figure 5.4B) that hinders access to its molecular core, but provides other ample interaction sites about its periphery. It is these sites that provide chiral recognition for a broad range of compounds. In the following sections more detailed examination and optimization of these two functionalized cyclofructan formats are discussed.

5.4.3 Cyclofructan CSPs Based on Aliphatic-functionalized CF6

Initial studies (*supra vide*) showed that aliphatic-CF6 CSPs provide excellent enantiomeric separation abilities for primary amines, so it was necessary to conduct more comprehensive studies on these aliphatic-functionalized stationary phases. Aliquots of CF6 were respectively derivatized with four different aliphatic

Table 5.3 Chromatographic data of primary amines separated on derivatized-CF6 stationary phases in optimized conditions

#	Compound name	CSP ^a	k ₁	α	Rs	Mobile phase ^b
1	trans-1-Amino-2-indanol	IP	2.85	1.31	3.9	60A40M0.3AA0.2T
		ME	2.44	1.28	3.5	60A40M0.3AA0.2T
		RN-L	1.43	1.23	1.6	60A40M0.3AA0.2T
2	cis-1-Amino-2-indanol	IP	2.69	1.12	1.6	60A40M0.3AA0.2T
		ME	2.47	1.10	1.5	60A40M0.3AA0.2T
		RN-L	3.00	1.07	0.8	75A25M0.3AA0.2T
3	Normetanephrine hydrochloride	IP	5.83	1.16	2.6	60A40M0.3AA0.2T
		RN-L	2.84	1.15	1.6	60A40M0.3AA0.2T
		ME	5.24	1.14	2.0	60A40M0.3AA0.2T
4	DL-Octopamine hydrochloride	IP	6.09	1.14	2.1	60A40M0.3AA0.2T
		ME	5.46	1.12	1.8	60A40M0.3AA0.2T
		RN-L	2.74	1.10	1.5	60A40M0.3AA0.2T
5	Phenylpropanolamine hydrochloride	IP	3.64	1.13	2.2	60A40M0.3AA0.2T
		RN-L	1.81	1.13	1.6	60A40M0.3AA0.2T
		ME	3.17	1.11	1.9	60A40M0.3AA0.2T
6	1-Aminoindan	IP	3.90	1.17	3.1	60A40M0.3AA0.3T
		RN-L	3.21	1.17	2.1	60A40M0.3AA0.2T
		ME	3.37	1.15	2.7	60A40M0.3AA0.2T
7	1,1-Diphenyl-2-aminopropane	IP	1.12	1.09	1.5	60A40M0.3AA0.2T
		RN-L	3.31	1.07	1.5	85A15M0.3AA0.2T
		ME	1.94	1.07	1.3	75A25M0.3AA0.2T
8	2-Amino-1-(4-nitrophenyl)-1,3-propanediol	ME	2.40	1.18	1.9	60A40M0.3AA0.2T
		IP	2.16	1.15	2.3	60A40M0.3AA0.2T
		RN-L	6.74	1.14	1.7	85A15M0.3AA0.2T
9	α-Methylbenzylamine	ME	3.07	1.17	1.5	60A40M0.3AA0.2T
		IP	2.77	1.15	1.5	60A40M0.3AA0.2T
		RN-L	8.12	1.09	0.8	85A15M0.3AA0.2T
10	DL-Tryptophanol	IP	3.39	1.15	2.7	60A40M0.3AA0.2T
		ME	3.03	1.12	1.7	60A40M0.3AA0.2T
		RN-L	4.66	1.12	1.4	75A25M0.3AA0.2T
11	1,2,2-Triphenylethylamine	IP	1.14	1.16	1.6	75A25M0.3AA0.2T
		ME	0.48	1.07	0.6	75A25M0.3AA0.2T

^aAbbreviations of CSPs: ME, methyl carbamate-CF6 CSP; IP, isopropyl carbamate-CF6 CSP; RN-L, R-naphthylethyl carbamate-CF6 CSP with a low substitution degree.

^bAbbreviations of mobile phases: A: acetonitrile; M: methanol; AA: acetic acid; T: triethylamine.

moieties: methyl (ME), ethyl (ET), isopropyl (IP), and *tert*-butyl (TB) groups. Among them, IP- and ME-functionalized CF6 appeared to give the best enantiomeric separations of primary amines. Representative chromatographic data are shown in Table 5.3. For comparison, data generated on the aromatic RN-CF6 CSP with a low substitution degree also are included. The IP CSP gave the highest selectivity toward nine primary amines, while slightly higher selectivity was obtained on the methyl-derivatized CF6 column for two of the compounds. However, in those two cases, the IP-CSP gave better or the same resolution, due to its higher efficiency. In most cases the aromatic derivatized RN-CSP gave the poorest enantioselectivities and resolutions. Compared to all other columns (Figure 5.2), the isopropyl-derivatized CF6 CSP provided higher selectivity and/or higher efficiency, and it produced baseline separations of all racemic primary amines tested.

Furthermore, thiocarbamate linkages between CF6 and various functional groups also were tested using the analogous isothiocyanate derivatization reagent. A comparison of the separations obtained from CF6 after derivatization with methyl isocyanate versus methyl isothiocyanate is shown in Figure 5.7. The methyl-functionalized CSP based on the carbamate linkage produced significantly higher selectivity and resolution. For primary amines, enantioresolution was observed in both the polar organic mode and normal phase mode (shown in Figure 5.8). While operating under normal phase conditions, both acidic additives (trifluoroacetic acid) and basic additives (butylamine) were tested. In this instance, the acidic modifier is thought to act to maintain an ion-pair. Fronting asymmetric wide peaks were always observed in the normal phase mode with an acidic additive, due to strong interactions between basic analyte and the weakly acidic silica-based stationary phase. The selectivity of primary amines on the CF6 column was lost in most cases when using a butylamine additive, although symmetric peaks were observed (data not shown). The effect of butylamine in decreasing the retention and selectivity can be attributed to the fact that this basic additive simply competes with basic analytes for the primary interaction sites on the chiral stationary phase. In the polar organic mode, better resolution ($R_s=1.6$) was observed due to good selectivity ($\alpha=1.16$) and highest efficiency (symmetric sharp peaks). However, higher enantioselectivity ($\alpha=1.25$) often was obtained in the normal phase mode. This trend is true for all tested primary amines: better resolution was obtained in the polar organic mode. All primary amines were baseline separated using the same or similar mobile phase

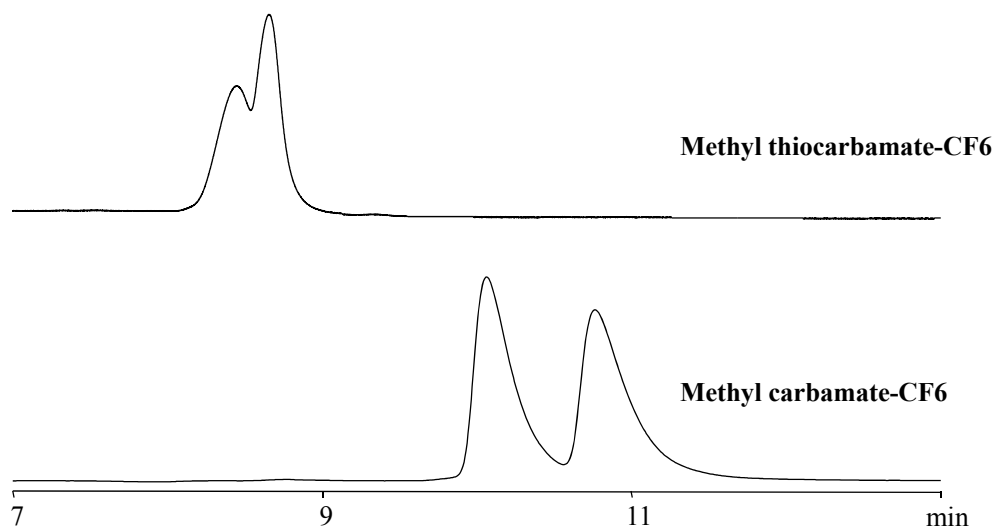


Figure 5.7 Comparison between methyl carbamate- and methyl thiocarbamate-CF6 CSPs. The analyte and mobile phase are cis-1-amino-2-indanol, and 60ACN/40MEOH/0.3AA/0.2TEA, respectively.

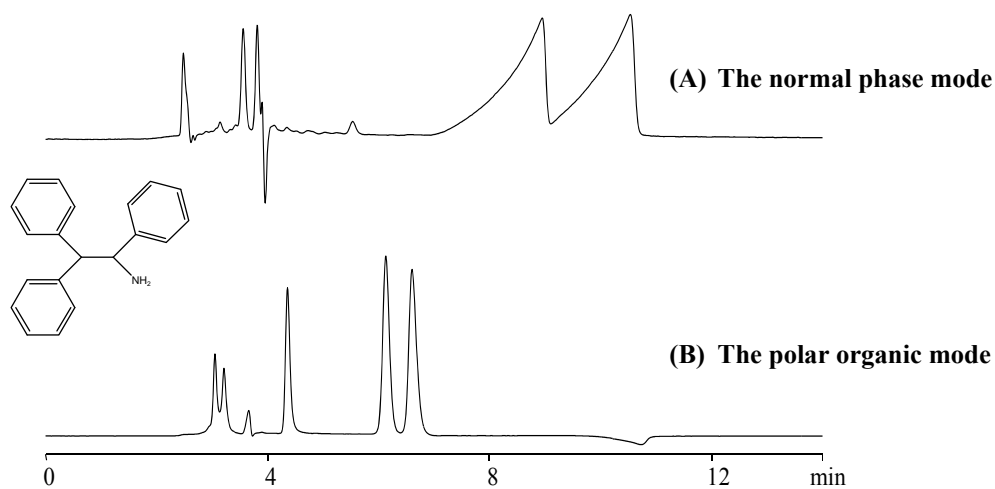


Figure 5.8 Separation of 1,2,2-triphenylethylamine on the IP-CF6 column. The chromatographic data and mobile phases are: (A) $k_1=2.09$, $\alpha=1.25$, $R_s=1.4$, 70heptane/30ETOH/0.1TFA; (B) $k_1=1.14$, $\alpha=1.16$, $R_s=1.6$, 75ACN/25MEOH/0.3AA/0.2TEA.

compositions, which streamlines the method development process. In addition, the polar organic mode offers other advantages, for example, short analysis times, low back-pressure, and better analyte solubility in the mobile phase. In order to evaluate the effects of acidic and basic additives in the polar organic mode on the separation of primary amines, different types and amounts of basic additives were investigated and the results are shown in Table 5.4. The highest enantioselectivity was obtained using the combination of triethylamine and acetic acid as additives. Also, the ratio of acidic/basic additives has been optimized and it was determined that addition of 0.3% acetic acid/0.2% triethylamine commonly results in highest selectivity.

The most important feature of the derivatized-CF6 CSPs is their extremely high success rate for separating primary amines. Indeed, 100% of the tested primary amines were baseline separated. Currently, the most effective CSPs available for separating racemic primary amines are synthetic chiral crown ether-based stationary phases.⁶³ However, their applications are intrinsically restricted to primary amines, with the partial exception of 18-crown-6 tetracarboxylic acid. Furthermore, strong acidic, aqueous mobile phases are always necessary to protonate and separate these primary amines. The derivatized CF6-based CSPs differ significantly from all other crown ether-based ones, in that they work best in polar organic and normal phase solvents for separating primary amines, and their applications are not always limited to primary amines.

5.4.4 *Cyclofructan CSPs based on aromatic-functionalized CF6*

Ten different CSPs were made which consisted of silica bonded cyclofructan, highly functionalized with ten different aromatic moieties (See Figure 5.2). Their respective chromatographic performances were evaluated by injecting all 70 probe molecules (non primary amine types). Among these ten aromatic derivatized-CF6 CSPs, four CSPs appeared to produce superior results. They are: 3,5-dimethylphenyl (DMP), 3,5-dichlorophenyl (DCP), R-1-(1-naphthyl)ethyl (RN), and S- α -methylbenzyl (SMP). The chromatographic data of the 70 probe analytes on these four columns are listed in Table 5.5. If one analyte is separated on more than one columns, the results are listed in descending order of selectivity. If the IP-functionalized CSP showed an enantioseparation, the data also was included for comparison purposes. Chromatograms of four representative separations under optimized conditions are shown in Figure 5.9. In

Table 5.4 Additive effect of separation of (\pm) trans-1-amino-2-indanol (primary amine type) in the polar organic mode on the IP-CF6 column

		k_1	α	R_s
Change basic additive type ^a	triethylamine	2.85	1.31	4.0
	trimethylamine	3.36	1.29	5.3
	ethanolamine	1.97	1.14	2.6
	diethylamine	3.67	1.29	1.6
Change additive amount ratio ^b	0.30AA/0.20TEA	2.85	1.31	4.0
	0.20AA/0.30TEA	2.69	1.24	3.9
	0.25AA/0.25TEA	3.24	1.27	4.4

^aThe mobile phase is composed of 60%acetonitrile/40%methanol/0.3%acetic acid (equals 52mM) /14 mM basic additive. ^bVolume percentage.

Table 5.5 Chromatographic data of other compounds separated on six derivatized-CF6 stationary phases in optimized conditions

#	Compound name	CSP ^a	k ₁	α	R _s	Mobile phase ^b
Acids						
1	O-Acetylmandelic acid	IP	11.00	1.04	1.2	98H2E0.1TFA
		SMP	9.86	1.04	0.9	98H2E0.1TFA
2	2,3-Dibenzoyl-DL-tartaric acid	IP	5.93	1.08	1.0	99A1M0.3AA0.2T
		RN	7.74	1.04	1.2	99.8A0.2M0.3AA0.2T
3	Ketorolac	IP	8.30	1.03	0.9	95H5E0.1TFA
		SMP	4.77	1.03	0.6	90H10E0.1TFA
		RN	4.65	1.03	0.6	90H10E0.1TFA
4	Phenethylsulfamic acid	IP	3.24	1.14	2.6	60A40M0.3AA0.2T
		SMP	3.18	1.13	0.8	70H30E0.1TFA
		RN	5.90	1.10	1.3	80A20M0.3AA0.2T
		DMP	2.03	1.10	0.6	70H30E/0.1TFA
5	1-Methyl-6,7-dihydroxy-1,2,3,4-tetrahydroisoquinoline hydrobromide	RN	8.87	1.16	1.6	70H30E0.1TFA
		SMP	7.19	1.14	2.2	70H30E0.1TFA
		IP	2.74	1.11	1.8	60A40M0.3AA0.2T
		DMP	4.12	1.07	1.2	70H30E0.1TFA
Secondary and tertiary amines						
1	Bis-[(R/S)-1-phenylethyl]amine HCl	RN	4.04	1.16	2.5	90H10E0.1TFA
		SMP	7.07	1.13	1.5	98H2E0.1TFA
2	Bendroflumethiazide	RN	5.50	1.16	2.3	70H30E0.1TFA
		SMP	4.27	1.03	0.5	70H30E0.1TFA
3	Tröger's base	DMP	0.95	1.59	5.7	70H30E
		RN	0.96	1.53	4.2	70H30E
		DCP	1.25	1.28	2.0	80H20E
		SMP	0.94	1.19	1.5	80H20E
		IP	0.62	1.11	0.9	80H20E
4	Orphenadrine citrate salt	DCP	8.28	1.51	3.0	80H20E
5	Diperodon hydrochloride	DCP	2.89	1.21	1.2	80H20E
		SMP	10.36	1.06	0.7	70H30E0.1TFA
Amino acid derivatives						
1	N-(3,5-dinitrobenzoyl)-DL-leucine	RN	0.80	1.91	4.4	50H50E0.1TFA
		DMP	5.54	1.12	2.3	90H10E0.1TFA
		SMP	1.85	1.11	1.5	80H20E0.1TFA
		DCP	7.45	1.06	0.6	80H20E0.1TFA
2	N-(3,5-Dinitrobenzoyl)-DL-phenylglycine	RN	7.22	1.12	1.8	70H30E0.1TFA
		DMP	11.01	1.08	1.5	90H10E0.1TFA
		SMP	10.80	1.05	1.1	90H10E0.1TFA
3	Carbobenzyl-oxy-alanine	SMP	3.83	1.10	1.6	90H10I0.1TFA
		DCP	6.49	1.06	1.3	95H5E0.1TFA
4	N-Benzoyl-DL-phenylalanine β-naphthyl ester	SMP	4.49	1.19	3.2	90H10E0.1TFA
		DMP	4.00	1.10	1.7	90H10I0.1TFA
		IP	6.19	1.08	1.5	95H5E0.1TFA
		RN	10.25	1.06	0.6	95H5E0.1TFA
		DCP	3.63	1.05	0.7	90H10I0.1TFA
5	3,5-Dinitrobenzoyl-tryptophan methyl ester	RN	3.99	1.17	2.2	50H50E0.1TFA
		SMP	2.76	1.10	1.5	70H30E0.1TFA
		DMP	5.19	1.09	1.5	80H20E0.1TFA
6	N-2,4-Dinitrophenyl-DL-norleucine	DMP	5.54	1.10	1.7	95H5I0.1TFA
		RN	10.91	1.07	1.3	95H5E0.1TFA

Table 5.5 – Continued

7	Dansyl-norleucine cyclohexylammonium salt	SMP	6.95	1.07	1.4	90H10E0.1TFA
		DMP	15.05	1.05	1.2	95H5E0.1TFA
		IP	6.93	1.04	0.8	90H10E0.1TFA
Alcohols						
1	α -Methyl-9-anthracenemethanol	RN	5.05	1.08	1.7	98H2I0.1TFA
		DMP	7.61	1.03	0.7	99H1I0.1TFA
		SMP	5.18	1.02	0.5	98H2E0.1TFA
2	Benzoin	DMP	5.91	1.07	1.5	99H1I0.1TFA
		SMP	4.89	1.05	1.3	98H2E0.1TFA
		RN	6.22	1.04	0.8	98H2E0.1TFA
3	N,N'-Dibenzyl-tartramide	DMP	18.03	1.10	1.5	95H5I0.1TFA
		DCP	3.34	1.10	1.2	80H20E0.1TFA
		RN	11.30	1.06	1.3	90H10E0.1TFA
		SMP	9.26	1.05	0.8	90H10E0.1TFA
4	furoin	IP	9.91	1.03	1.3	95H5E0.1TFA
		DMP	9.98	1.03	0.6	98H2E0.1TFA
		SMP	5.64	1.02	0.5	90H10E/0.1TFA
5	Cromakalim	DMP	16.00	1.05	1.5	95H5E0.1TFA
		DCP	8.69	1.05	1.1	90H10E0.1TFA
		RN	8.84	1.02	0.4	90H10E0.1TFA
Others						
1	1,1'-Bi(2-naphthyl diacetate)	IP	0.40	1.35	2.9	70H30E
		DMP	0.74	1.21	1.7	70H30E
		SMP	0.77	1.17	1.9	70H30E
		RN	1.79	1.11	1.6	90H10E0.1TFA
		DCP	1.15	1.08	1.1	90H10E0.1TFA
2	5,5',6,6',7,7',8,8'- Octahydro(1,1'- binaphthalene)-2,2' diol	DMP	5.47	1.18	2.8	99H1I0.1TFA
		RN	5.34	1.11	1.9	98H2E0.1TFA
		SMP	4.47	1.09	1.5	98H2E0.1TFA
3	2,2'-Diamino-1,1'-binaphthalene	DMP	1.43	1.45	5.3	70H30E
		DCP	1.77	1.22	2.0	80H20E
		SMP	1.91	1.20	3.1	70H30E
		RN	2.31	1.18	2.8	70H30E
		IP	2.15	1.16	3.0	80H20E
4	6,6'-Dibromo-1,1'-bi-2-naphthol	DMP	0.74	1.58	4.7	70H30E
		DCP	2.13	1.24	5.0	90H10E
		SMP	0.93	1.19	2.1	70H30E
		RN	1.17	1.15	1.5	70H30E
		IP	3.63	1.07	1.5	90H10E
5	Althiazide	RN	2.83	1.16	1.9	50H50E0.1TFA
		DMP	8.80	1.04	0.7	80H20E0.1TFA
		IP	8.29	1.02	0.8	70H30E0.1TFA
		SMP	7.10	1.02	0.5	70H30E/0.1TFA
6	1,1'-Bi-2-naphthol bis(trifluoromethanesulfonate)	SMP	3.84	1.17	2.0	100H
		IP	1.17	1.08	1.5	100H
		RN	6.13	1.08	1.3	100H
7	cis-4,5-Diphenyl-2- oxazolidinone	DMP	5.41	1.09	1.6	90H10I0.1TFA
		RN	6.82	1.04	0.8	90H10I0.1TFA

Table 5.5 – Continued

8	2,3-Dihydro-7a-methyl-3-phenylpyrrolo[2,1-b]oxazol-5(7aH)-one	RN	3.20	1.12	1.9	85H15I0.1TFA
		DMP	5.13	1.05	1.1	98H2E0.1TFA
		SMP	2.46	1.03	0.7	98H2E0.1TFA
		DCP	2.67	1.02	0.6	90H10E0.1TFA
9	Ethyl 11-cyano-9,10-dihydro-endo-9,10-ethanoanthracene-11-carboxylate	SMP	1.44	1.13	2.0	90H10I0.1TFA
		RN	3.21	1.08	1.5	98H2E0.1TFA
		IP	1.42	1.08	1.5	95H5E0.1TFA
		DMP	2.07	1.03	0.5	98H2E0.1TFA
10	Lormetazepam	SMP	3.87	1.08	1.5	80H20E0.1TFA
		IP	8.46	1.06	1.5	90H10E0.1TFA
		RN	5.02	1.04	0.7	80H20E0.1TFA
11	3a,4,5,6-Tetrahydro-succininido[3,4-b]acenaphthen-10-one	SMP	2.36	1.13	2.2	70H30E0.1TFA
		IP	2.14	1.12	1.9	70H30E0.1TFA
		RN	3.25	1.10	1.5	70H30E0.1TFA
		DMP	7.35	1.08	1.5	90H10E0.1TFA
12	3-(alpha-Acetyl-4-chlorobenzyl)-4-hydroxycoumarin	DMP	5.35	1.17	2.0	90H10I0.1TFA
		SMP	5.16	1.14	2.2	90H10E0.1TFA
13	Warfarin	RN	15.94	1.10	1.6	95H5E0.1TFA
		DCP	4.65	1.10	1.4	90H10E0.1TFA
		IP	4.61	1.09	1.5	90H10E0.1TFA
		DMP	9.87	1.10	1.6	95H5I0.1TFA
		SMP	7.19	1.08	0.9	90H10I0.1TFA
		DCP	4.98	1.07	0.8	90H10E0.1TFA
		RN	11.94	1.05	1.2	95H5E0.1TFA
14	Fipronil	IP	4.60	1.02	0.5	90H10E0.1TFA
		SMP	16.03	1.09	2.0	98H2E0.1TFA
		IP	2.83	1.08	1.5	90H10E0.1TFA
		RN	12.02	1.07	1.5	97H3E0.1TFA
15	trans-Stilbene oxide	DCP	0.55	1.03	0.4	80H20E
		IP	0.62	1.10	1.3	100H
		SMP	2.02	1.09	1.5	100HEP
16	Thalidomide	RN	2.75	1.07	1.0	100HEP
		SMP	5.89	1.10	1.9	70H30E0.1TFA
		DMP	8.03	1.08	1.5	80H20E0.1TFA
		DCP	10.69	1.05	1.0	80H20E
17	3,5-Dinitrobenzoyl-2-aminoheptane	RN	7.85	1.04	0.7	70H30E0.1TFA
		RN	1.68	1.15	2.2	80H20E0.1TFA
18	3,5-Dinitro-N-(1-phenylethyl)-benzamide	RN	1.24	1.92	8.2	50H50E0.1TFA
		SMP	0.93	1.14	1.5	70H30E0.1TFA

^aAbbreviations of CSPs: DMP, dimethylphenyl carbamate-CF6 CSP; DCP, dichlorophenyl carbamate-CF6 CSP; RN, R-naphthylethyl carbamate-CF6 CSP; SMP, S-methylbenzyl carbamate-CF6 CSP. IP, isopropyl carbamate-CF6 CSP; ME, methyl carbamate-CF6 CSP.

^bAbbreviations of mobile phases: H: heptane; I: isopropanol; E: ethanol; A: acetonitrile; M: methanol; AA: acetic acid; T: triethylamine; TFA: trifluoroacetic acid.

summary, 40 analytes out of 70 were separated, including 35 baseline ($R_s \geq 1.5$) and 5 partial resolution ($0.3 < R_s < 1.5$). Table 5.5 clearly demonstrates the aromatic derivatized-CF6 columns show excellent enantioselectivity toward various types of analytes, including acids, secondary amines, tertiary amines, alcohols, and others. Although they are not universally effective for all of the tested enantiomers, the variety of compounds separated by derivatized-CF6 was encouraging. Table 5.5 clearly demonstrates that the nature of the aromatic group plays a major role in chiral recognition. The aromatic-functionalized CF6 CSPs demonstrate complimentary capability of enantiomeric selectivities, in that some analytes were baseline separated on one column, while only a partial separation or no separation was observed on other aromatic functionalized CF6 columns. Figure 5.10 illustrates this complimentary behavior for 3,5-dinitro-N-(1-phenylethyl)benzamide which was well separated ($R_s=8.2$) on the RN-CF6 column with an extremely high selectivity ($\alpha=1.92$), and also baseline separated ($\alpha=1.14$, $R_s=1.5$) on the SMP column. However, a single peak was observed using the DMP-CF6 and DCP-CF6 columns. The stereogenic center of 3,5-dinitro-N-(1-phenylethyl)benzamide is directly attached to a phenyl ring, which participates in π - π interactions with the aromatic moieties of the derivatized CF6. Compared to DMP, both RN and SMP contain a stereogenic center, directly connected to the aromatic ring (phenyl or naphthyl), which may be beneficial for chiral recognition of this analyte. One advantage for all CF6-based CSPs is their excellent stability. These columns are stable in all common organic solvents and no detrimental changes in column performance was observed after more than 1000 injections. The selection of the mobile phase is an important parameter in enantioselective chromatography. Therefore, it was necessary to compare all three operation modes (i.e., the normal phase mode, polar organic mode, and the reversed phase mode) when evaluating these CF6-based columns. Further, the effects of other experimental factors, such as alcohol modifier type in the normal phase mode, and the column temperature on the separations were studied. Such fundamental information offers guidance for methods development. For neutral and acidic compounds, better resolution was typically obtained in the normal phase mode. Figure 5.11 shows one example comparing the reversed phase mode and normal phase mode. 6,6'-Dibromo-1,1'-bi-2-naphthol is baseline separated ($\alpha=1.58$, $R_s=4.7$) using 70%heptane/30%ethanol, while only a tiny peak split ($\alpha=1.03$, $R_s=0.6$) was observed using the reversed phase mode. With the polar organic mobile phase, no retention of this

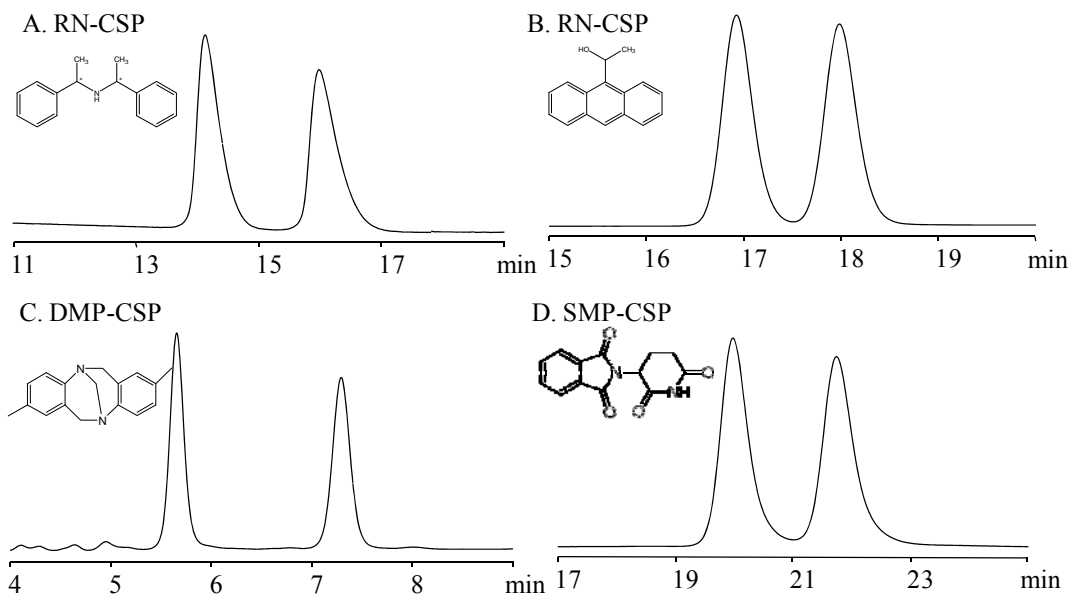


Figure 5.9 Selected chromatograms showing enantioseparations of various analytes on different derivatized-CF6 columns. The analytes and mobile phases are: (A) Bis-[(R/S)-1-phenylethyl]amine, 90H10E0.1TFA; (B) α -Methyl-9-anthracenemethanol, 98heptane/2IPA/0.1TFA; (C) Tröger's base, 70heptane/30ETOH; (D) Thalidomide, 70heptane/30ETOH/0.1TFA.

analyte was obtained. Water in the reversed phase system may compete too effectively for hydrogen bonding sites on the chiral stationary phase, and thus it has a negative effect on the separation of enantiomeric compounds. It is well known that certain interactions are enhanced in less polar solvents.^{50d, 62b, 64} Specifically these are π - π , n- π , dipolar and hydrogen bonding interactions. Since these CSPs are effective mainly in the normal phase mode and polar organic mode, these must be the dominant associative interactions, while steric repulsion is important in all solvent systems.

In the normal phase mode, ethanol and isopropanol are commonly used as alcohol modifiers. Ordinarily, the ethanol modifier yields good enantioselectivity, better peak efficiency, and faster elution, therefore it was chosen as the primary polar organic modifier. Isopropanol also was tested for further optimization, because in some cases higher enantioselectivity is observed using isopropanol rather than ethanol (Figure 5.12). The value of α for the enantioseparation of N-benzoyl-DL-phenylalanine β -naphthyl ester is improved from 1.05 to 1.10, when replacing ethanol with isopropanol.

At lower temperatures, enantioselectivity usually increases, at the expense of efficiency. Figure 5.13 illustrates that reducing the column temperature from 20 °C to 0 °C significantly improves enantioselectivity and resolution. Therefore, lowering the column temperature is another strategy to optimize enantioseparations with these CSPs, as it is with most other CSPs.

In order to assess the potential for preparative HPLC, it is necessary to perform loading tests on any new stationary phases. Sample loading was examined by injecting N-(3,5-dinitrobenzoyl)-phenylglycine on the RN-CF6 column in the polar organic mode. Figure 5.14 shows that 4200 μ g of this racemate has been baseline separated on an analytical column. It should be noted that the injection amount was limited by the solubility of the analyte in the mobile phase. It is clear that more sample could be loaded while maintaining baseline resolution. Currently, all LC studies have been conducted on typical analytical scale columns (250 \times 4.6 mm). Using standard assumptions, scaling to a 5 cm i.d. column could separate 400 mg of N-(3,5-Dinitrobenzoyl)-phenylglycine in a single run (less than 7 min).⁶⁵ As a result, over 3g of the racemic analyte could be separated in one hour. Therefore, these brush-type CSPs based on derivatized-CF6 demonstrate great potential for preparative HPLC. In addition, comprehensive SFC investigations of these cyclofructan-based CSPs are under way and a representative chromatogram is shown in Figure 5.15.

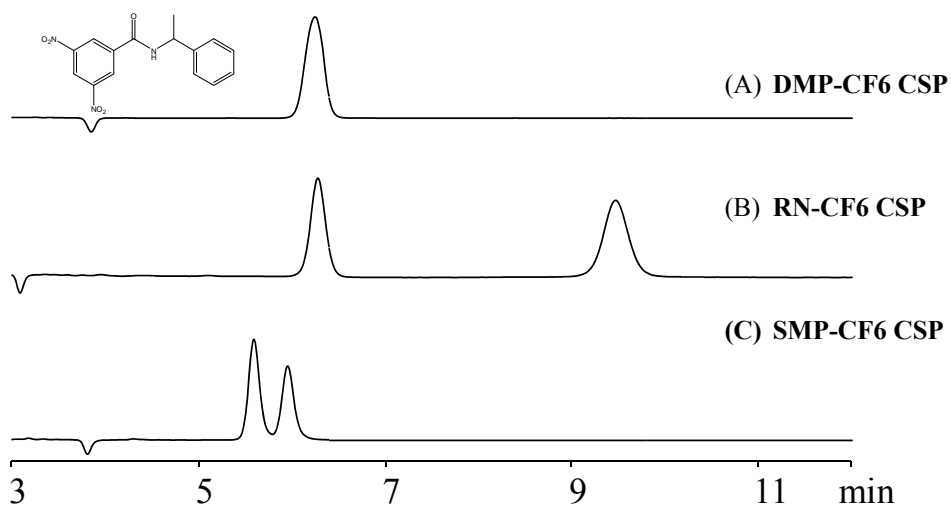


Figure 5.10 Complimentary character of the aromatic-derivatized CF6 CSPs. The analyte is 3,5-dinitro-N-(1-phenylethyl)benzamide. The CSPs and mobile phases are: (A) 3,5-dimethylphenyl carbamate-CF6 CSP, 70heptane/30ETOH/0.1TFA; (B) R-naphthylethyl carbamate-CF6 CSP, 50heptane/50ETOH/0.1TFA; (C) S- α -methylphenyl carbamate-CF6 CSP, 70heptane/30ETOH/0.1TFA.

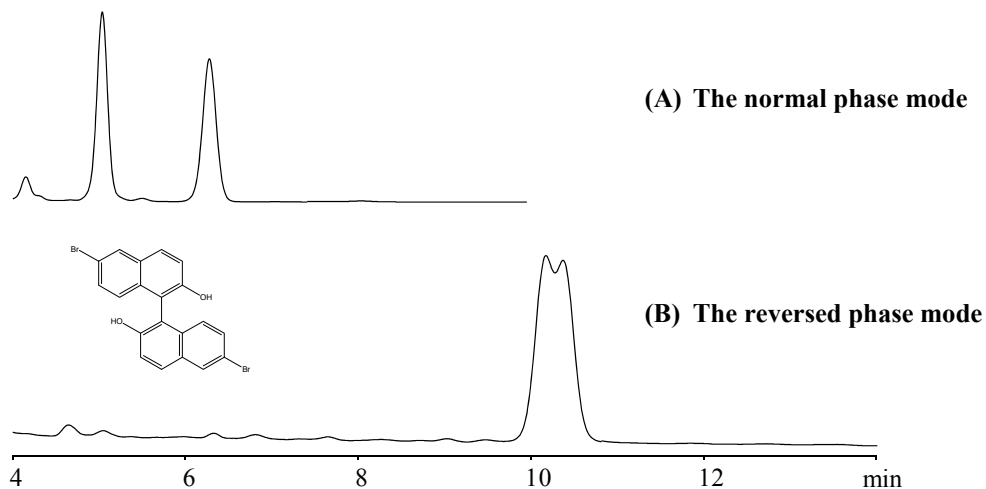


Figure 5.11 Separation of 6,6'-dibromo-1,1'-bi-2-naphthol in the normal phase mode and reversed phase mode on the DMP-CF6 column. The chromatographic data and mobile phases are: (A) $k_1=0.74$, $\alpha=1.58$, $R_s=4.7$, 70heptane/30ETOH; (B) $k_1=2.51$, $\alpha=1.03$, $R_s=0.6$, 50ACN/50water.

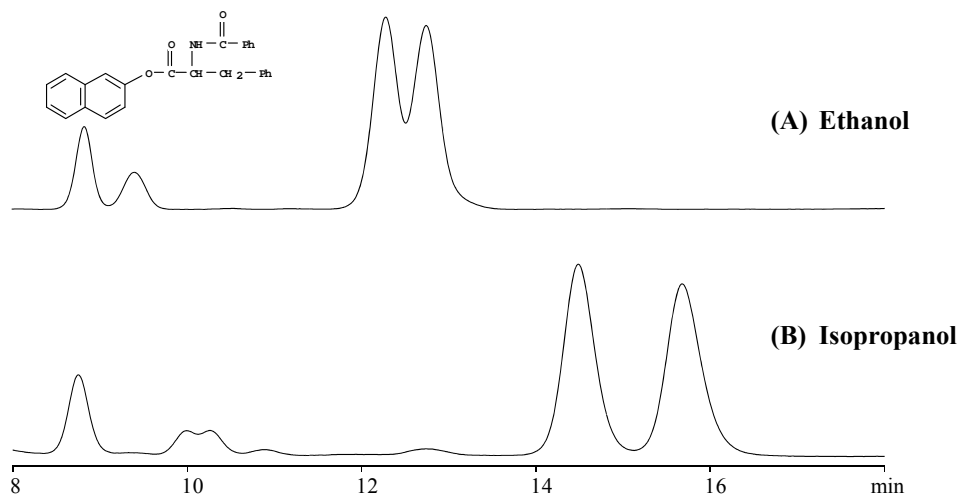


Figure 5.12 Effect of alcohol modifier on enantioseparation in the normal phase mode on the DMP-CF6 column. The mobile phase is 90heptane/10 alcohol modifier. The analyte is N-benzoyl-DL-phenylalanine β-naphthyl ester. The chromatographic data are: (A) $k_1=3.23$, $\alpha=1.05$, $R_s=0.8$; (B) $k_1=4.00$, $\alpha=1.10$, $R_s=1.7$.

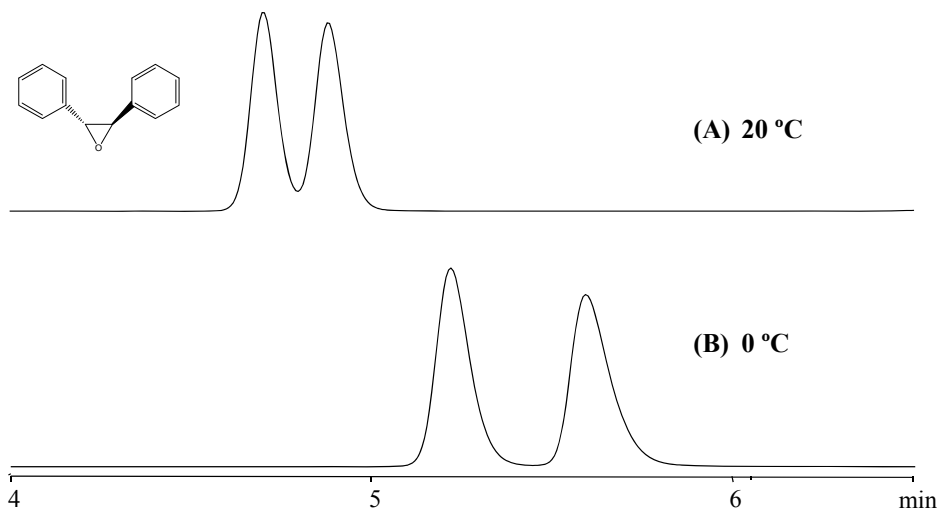


Figure 5.13 Temperature effect on separation of trans-stilbene oxide on the IP-CF6 column. The mobile phase is 100% heptane. The chromatographic data: (A) $k_1=0.62$, $\alpha=1.10$, $R_s=1.3$; (B) $k_1=0.80$, $\alpha=1.16$, $R_s=2.0$.

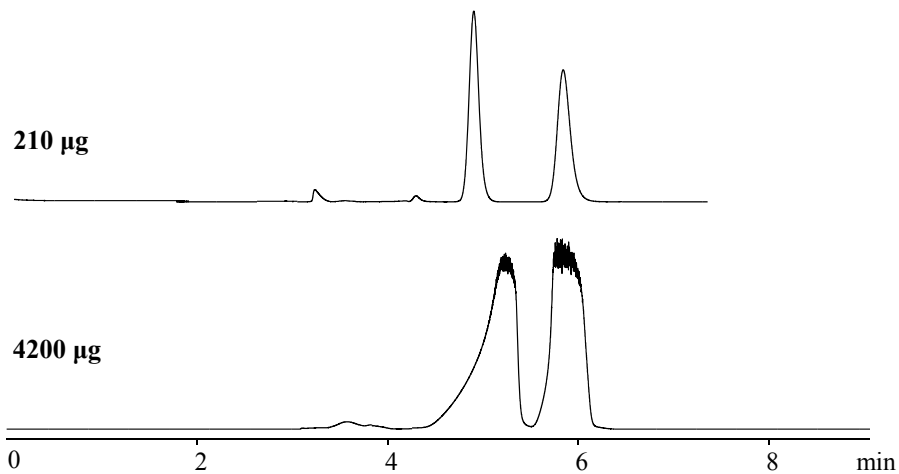


Figure 5.14 Loading test on the RN-CF6 column. The analyte is N-(3,5-dinitrobenzoyl)-DL-phenylglycine. The mobile phase is 85ACN/15MEOH/0.3AA/0.2TEA. Injection volumes are: 5 μ L (top) and 100 μ L (bottom). UV detection: 350 nm.

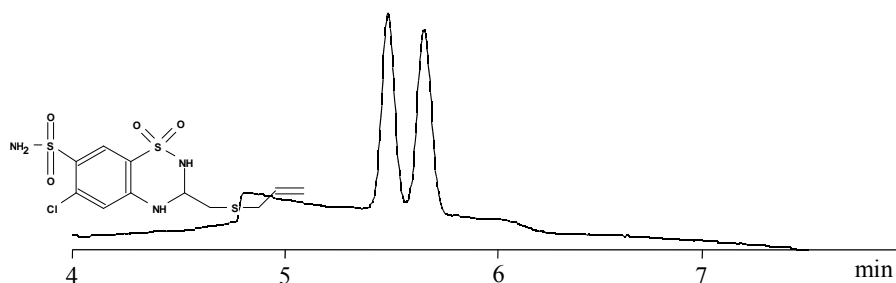


Figure 5.15 SFC chromatogram of althiazide on the RN-CF6 column. The gradient mobile phase is as described in EXPERIMENTAL SECTION.

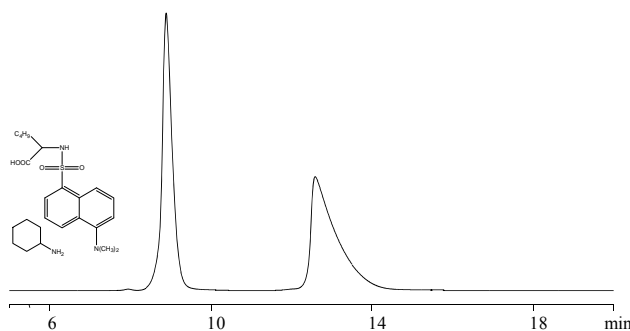


Figure 5.16 Separation of dansyl-norleucine cyclohexylammonium salt on the dimethylphenyl carbamate-CF7 CSP. The mobile phase is 80heptane/20ETOH/0.1TFA.

Most recently, we have begun to study the cyclofructan containing seven units (CF7) as a chiral selector. Preliminary studies show that the derivatized-CF7 CSP also successfully separates various types of analytes and an initial result is shown in Figure 5.16. It is worth mentioning that this analyte was only partially separated by all derivatized-CF6 columns. This demonstrates that the dimethylphenyl carbamate-CF7 likely has somewhat different enantioselectivities. This work is on-going and will be presented in a subsequent publication.

5.5 Conclusions

Cyclofructans are a completely new class of chiral selectors. While native cyclofructan 6 has limited capabilities as a chiral selector, specific, derivatized cyclofructans appear to be exceptional chiral selectors which can be “tuned” to separate enantiomers of different types of molecules. Partial derivatization of the cyclofructan hydroxyl groups appears to disrupt internal hydrogen bonding and “relax” the structure. When “lightly” derivatized with aliphatic functionalities, CF6 becomes exceptionally adept at separating enantiomers of primary amines and does so in organic solvents and supercritical CO₂. This is in contrast to all known chiral crown ether CSPs that work exclusively with aqueous acidic solvents. When CF6 is extensively functionalized with aromatic moieties, it no longer effectively separates primary amine racemates. However, it does separate a broad variety of other enantiomers. Furthermore, its preparative separation capabilities appear to be exceptional and this indicates that it is likely that multiple analytes can associate simultaneously with a single chiral selector. While this class of chiral selectors is in its infancy, it is clear that they will be further developed and play an important role in future enantiomeric separations.

5.6 Acknowledgement

We gratefully acknowledge Mari Yasuda at Mitsubishi Chemical Group for supplying the native cyclofructans and Ke Huang for conducting SFC testing.

CHAPTER 6

PREPARATION AND EVALUATION OF A NEW SYNTHETIC POLYMERIC CHIRAL STATIONARY PHASE FOR HPLC BASED ON THE *TRANS*-9, 10-DIHYDRO-9, 10-ETHANOANTHRACENE-(11S, 12S)-11, 12-DICARBOXYLIC ACID BIS-4-VINYLPHENYLAMIDE MONOMER

6.1 Abstract

A new synthetic polymeric chiral stationary phase for liquid chromatography was prepared via free radical initiated polymerization. The new polymeric chiral stationary phase showed enantiomeric selectivities for many chiral compounds with various structures in multiple mobile phases. High stability and sample loading ability were observed on this new chiral stationary phase. Mobile phase components and additives were important for the chiral separations. The new chiral stationary phase is complementary to commercially available columns such as P-CAP and poly-DPEDA columns and extends the concept of these columns. Xinxin Han, Chunlei Wang, Lingfeng He, Thomas E. Beesley, and Daniel W. Armstrong. *Journal Analytical and Bioanalytical Chemistry* (2007), 387(8), 2681-2697. Copyright © 2007 with permission from the Springer, LLC.

6.2 Introduction

HPLC on chiral stationary phases (CSPs) continues to be the most powerful and versatile method for the separation of racemates in both analytical and preparative scales.^{31a, 66} More than 100 chiral stationary phases have been commercialized.^{31a} Based on the structure of chiral selector, they can be divided into five classes. They are polymeric, macrocyclic, π - π association, ligand exchange, and hybrid chiral stationary phases.^{31a} In general, polymeric CSPs, with the exception of the ones based on proteins, are highly suitable for preparative separation due to their high loading of chiral selectors on the support and the fact a single bonded or adsorbed polymer molecule can interact with and separate several analyte molecules simultaneously along its length. The polymeric chiral selectors can be classified as two types by their

origins.^{66b} One class uses natural polymers such as polysaccharides and proteins or their derivatives as chiral selectors; another class uses purely synthetic polymers as chiral selectors. Chiral stationary phases based on polysaccharide derivatives have been extensively used for the analytical and preparative separations of chiral molecules because of their broad enantioselectivities and high sample loading capacity.^{48e, 66b} Until recently, no synthetic polymeric CSP has achieved comparable success.^{56b} However, research on synthetic polymeric CSPs is also evolving⁶⁷ due to their attractive features such as the richness of the chemical structures, ease of chemical modification of potential chiral selectors, and the possibility of obtaining chiral selectors with opposite absolute configuration. The elution order of the two enantiomers can be easily reversed by using two CSPs with opposite absolute configuration. The change of elution order help the detection of trace enantiomeric impurity when the impurity peak is the latter peak if the first peak is tailing, thus covers the second tiny peak.

Three approaches have been used to make the synthetic polymeric CSPs. The first is the polymerization of chiral monomers. Blaschke and his coworkers reported the first polymeric CSPs.⁶⁸ The CSPs are polymeric beads prepared through copolymerization of chiral acrylamides or methacrylamides with ethylene diacrylate as cross-linking agent. These CSPs could not be used under high pressure and were mainly useful for preparative purposes. The mechanical problem was solved by copolymerization of optically active acrylamides or methacrylamides with methacryloyl silica gel.⁶⁹ These CSPs showed enantioselectivities for some drug molecules including thalidomide. Some other types of polyacrylamide and polymethacrylamide CSPs were also reported.⁷⁰ One type bearing penicillin moieties can separate some aromatic racemates.^{70a} The other one possessing amino acid and menthone or menthol units can separate a few chiral drug molecules.^{70b} A second approach used to prepare chiral polymers uses prochiral monomers via asymmetric catalyzed polymerization.^{66b, 71} Perfectly one-handed helical polymers were prepared from prochiral monomers such as triphenylmethyl methacrylate (TrMA) and diphenyl-2-pyridylmethyl methacrylate (D2PymA) via asymmetric catalyzed anionic polymerization.^{66b, 71} These optically active polymers were either coated or bonded to silica gel to form CSPs. Many chiral compounds were separated on these polymeric CSPs. The last method is copolymerization of chiral monomers with diallyl groups with multifunctional hydrosilane to form network polymeric chiral selectors.⁷² Derivatives of *N, N'*-diallyl-L-

tartradiamide (DATD) [17-18] and derivatives of *trans*-9,10-dihydro-9,10-ethanoanthracene-(11S,12S)-11,12-dicarboxylic acid^{72a} have been used as monomers. These chiral selectors were then bonded to the vinyl-functional silica gel as CSPs. Resolution of many compounds has been reported on these CSPs. In fact, the small molecular chiral selectors are just incorporated into the network of an organosilane matrix and not even two of these monomers are directly chemically bonded to each other in these CSPs.

Recently, two new synthetic polymeric CSPs, based on *trans*-1, 2-diamino cyclohexane (commercial name = P-CAP)^{67a, b, 67d} and *trans*-diphenylethylenediamine (commercial name = P-CAP-DP)^{67c}, have been developed by Gasparri's group and our group, respectively. The "P-CAP" chiral stationary phase is prepared from radical initiated polymerization of the N, N'-diacryloyl derivative of *trans*-1, 2-diaminocyclohexane (DACH), while the "P-CAP-DP" CSP was made from the N, N'-diacryloyl derivative of *trans*-1, 2-diphenylethylenediamine (DPEDA). In the first case, the free radical initiator was bonded to the silica gel; while in the second case, the initiator was dissolved in the bulk reaction solution. Both CSPs were stable and can be used in multiple mobile phase modes such as normal phase mode and polar organic mode. Many racemates with different structures have been separated on these two synthetic polymeric CSPs. These two CSPs are known to have high sample capacities and thus have considerable potential as preparative columns, also both enantiomeric forms of these CSPs are available. Finally, these two columns are complementary to one another. Some analytes are only separated on one or the other of these two columns, and the enantiomeric selectivities are usually different for the racemates, which can be separated on both columns.

The P-CAP CSP contains a chiral selector that is relatively rigid ring that has no aromatic moieties, while P-CAP-DP CSP has aromatic units, and the conformation of the monomer is flexible. A new chiral monomer presented here has structural features of both of the two commercial CSPs. *Trans*-9,10-dihydro-9,10-ethanoanthracene-(11S, 12S)-11, 12-dicarboxylic acid provides the possibility of making a new synthetic polymeric CSP with different enantiomeric selectivities in comparison with the P-CAP and P-CAP-DP columns. In this paper, we reported a new synthetic polymeric CSP prepared via radical initiated polymerization of the bis-4-vinylphenylamide derivative of this molecule. The synthesis of the chiral selectors, its enantiomeric resolution, bonding chemistry, and chromatographic evaluation of its

enantiomeric separation abilities in the normal phase mode, and polar organic mode are presented. The effect of the polar modifier in the mobile phase, mobile phase additives, and complementary nature to related polymeric columns also are discussed.

6.3 Experimental

6.3.1 Materials

Spherical silica gel (partical diameter: 5 μm , pore size: 200 \AA , surface area: 213 m^2/g) functionalized with dichloride of 4,4'-azo-bis-cyanovaleric acid was obtained from Advanced Separation Technologies (Whippany, NJ, USA). Anthrance, fumaric, brucine, 4-vinylaniline, triethylamine, anhydrous chloroform, anhydrous toluene, acetone, thionyl chloride, and trifluoroacetic acid (TFA) were purchased from Aldrich (Milwaukee, WI, USA). HPLC grade methylene chloride, methanol, ethanol, acetonitrile, 2-propanol, and *n*-heptane were purchased from Fisher (Fairlawn, NJ, USA).

6.3.2 Synthesis

6.3.2.1 Preparation of *trans*-9,10-dihydro-9,10-ethanoanthracene-11,12-dicarboxylic acid [21]

6.3.2.2 Preparation of *trans*-9,10-dihydro-9,10-ethanoanthracene-(11*S*,12*S*)-11,12-dicarboxylic acid bis-4-vinylphenylamide (DEABV)

Trans-9,10-dihydro-9,10-ethanoanthracene-(11*S*,12*S*)-11,12-dicarboxylic acid (1.0 g, 3.40 mmol) and thionyl chloride (0.8 mL, 11.0 mmol) were added into 30 mL anhydrous toluene. The mixture was refluxed for 12 h. After removal of volatile components under vacuum, the residue was dissolved in 10 mL anhydrous chloroform. This solution was then added dropwise into the 40 mL chloroform solution of triethylamine (1.5 mL, 11.0 mmol) and 4-vinylaniline (1.0 g, 8.40 mmol) at 0 $^{\circ}\text{C}$ under stirring. The reaction was then raised to room temperature in 30 minutes and stirred for 12 h. The chloroform solution was washed with 1 M hydrochloric acid (2 x 20 mL), 1 M sodium bicarbonate (2 x 20 mL), and water (2 x 20 mL). The chloroform layer was dried over sodium sulfate, filtered, and the solvent was evaporated under vacuum. The product was purified by flash chromatography (Methylene chloride) to obtain 1.20 g light yellow solid (yield: 71%). ^1H NMR (300 MHz, CDCl_3): δ 8.75 (s, 2H), 7.56-7.53 (m, 2H), 7.43-7.32 (m, 10H), 7.26-7.16 (m, 4H), 6.65 (dd, $J_1 = 17.4$ Hz, $J_2 = 11.1$ Hz, 2H), 5.66 (dd, $J_1 = 17.4$ Hz, $J_2 = 0.6$ Hz, 2H), 5.18 (dd, $J_1 = 11.1$ Hz, $J_2 = 0.6$ Hz, 2H), 4.80 (s, 2H), 3.10 (s, 2H). ^{13}C NMR (75 MHz, CDCl_3)

6.3.2.3 Preparation of poly-DEABV CSP

To a heated anhydrous, degassed chloroform (50 mL) solution of DEABV (0.8 g), Silica gel functionalized with dichloride of 4,4'-azo-bis-cyanovaleric acid (3.20 g) was added under argon atmosphere. The suspension was stirred at 60 °C for 5 h and was heated to reflux for 1 h. The CSP was collected by filtration, washed with 100 mL of methanol, acetone, and chloroform respectively. The CSP was dried under vacuum at 50 °C over night and screened with 53 μm sieve and bottle to obtain 3.50 g. Loading: 9.38%. Elemental Analysis: C, 19.53%; H, 1.97%; N, 2.46%. The CSP was packed into a 250 mm x 4.6 mm (i. d.) stainless steel column.

6.3.3 Equipment

Chromatographic separations were carried out using a HP 1050 HPLC system with an auto sampler, a UV VWD detector, and computer controlled Chem-station data processing software (Agilent Technologies, Palo Alto, CA, USA). The mobile phases were degassed under helium for 7 min. UV detection was carried out at 254 nm for all analytes. All separations were carried out at room temperature ($\sim 23^\circ\text{C}$) and the flow rate of the mobile phase for all separations was 1.0 mL min^{-1} .

6.3.4 Column Evaluation

The performance of poly-DEABV chiral stationary phase was evaluated in the polar organic mode using acetonitrile/methanol mobile phase, in the normal phase mode using 2-propanol/heptane, ethanol/heptane, and methylene chloride/methanol mobile phase. Before using a new mobile phase, ten column volumes of new mobile phase were pumped through the column prior to the injection of the analyte.

6.3.5 Calculation

The dead time (t_0) was estimated using the peak resulting from the change in refractive index from the injection solvent on the poly-DEABV column. The retention factor (k) was calculated using the equation $k = (t_r - t_0) / t_0$. The enantiomeric selectivity (α) was calculated using $\alpha = k_2 / k_1$. The resolution factor (R_S) was calculated using the equation $R_S = 2 \times (t_{r2} - t_{r1}) / (w_1 + w_2)$, where t_{r2} and t_{r1} are the retention times of the second and first enantiomers, respectively, and w_1 and w_2 are the corresponding base peak widths. The efficiency (number of theoretical plates, N) was calculated using $N = 16(t_r/w)^2$.

6.4 Results and Discussion

6.4.1 Synthesis of poly-DEABV

Racemic *Trans*-9,10-dihydro-9,10-ethanoanthracene-11,12-dicarboxylic acid is easy to prepare through a simple Diels-Alder reaction between anthracene and fumaric acid. The racemic diacid can be simply resolved via recrystallization with brucine to obtain the enantiomeric pure (S, S)-enantiomer. *Trans*-9,10-dihydro-9,10-ethanoanthracene- (11S,12S)-11,12-dicarboxylic acid was transformed to diacid dichlorides and reacted with 4-vinylaniline to obtain the DEABV monomer. Figure 6.1 shows the procedure of preparation of the new synthetic polymeric CSP (See Experimental). We use the polymerization method introduced by Gasparri.^{67a, b} In this method, the radical initiator, 4, 4'-azo-bis-4-cyanopentanoic acid, is immobilized on the surface of the silica gel. This silanized support is then suspended along with the monomer, which is dissolved in the anhydrous chloroform. Thus, the radical polymerization is initiated from the surface of the silica gel and a uniform and thin polymer layer is bonded to the silica gel. The unreacted monomers can be removed by washing the CSP with various solvents. A 9.37% loading of chiral selector was obtained.

6.4.2 Column Performance of poly-DEABV CSP

Two mobile phase modes were investigated for this new poly-DEABV CSP. They are normal phase mode and polar organic mode. The major components for the normal phase are heptane/isopropanol or heptane/ethanol. For the polar organic mode, the mobile phase is acetonitrile with a small amount of methanol. One uncommon mobile phase of normal phase mode, which is composed of methylene chloride and methanol, was also assessed on this new polymeric CSP. The separation factors of the compounds resolved on this new polymeric CSP are listed in Table 6.1, Table 6.2 and Table 6.3 for the three mobile phases, respectively. In heptane/ethanol or heptane/isopropanol mobile phase, 59 enantiomeric separations and 26 baseline separations of chiral molecules were observed. The other two mobile phases were not as powerful as heptane/ethanol or heptane/isopropanol mobile phase. Only 20 enantiomeric separations and 5 baseline separations were obtained in the polar organic mode. Nineteen separations and 7 baseline separations were acquired in the methylene chloride/methanol mobile phase. Totally, this new polymeric CSP showed enantiomeric selectivities for 70 chiral molecules and 28 of them were baseline separated. The

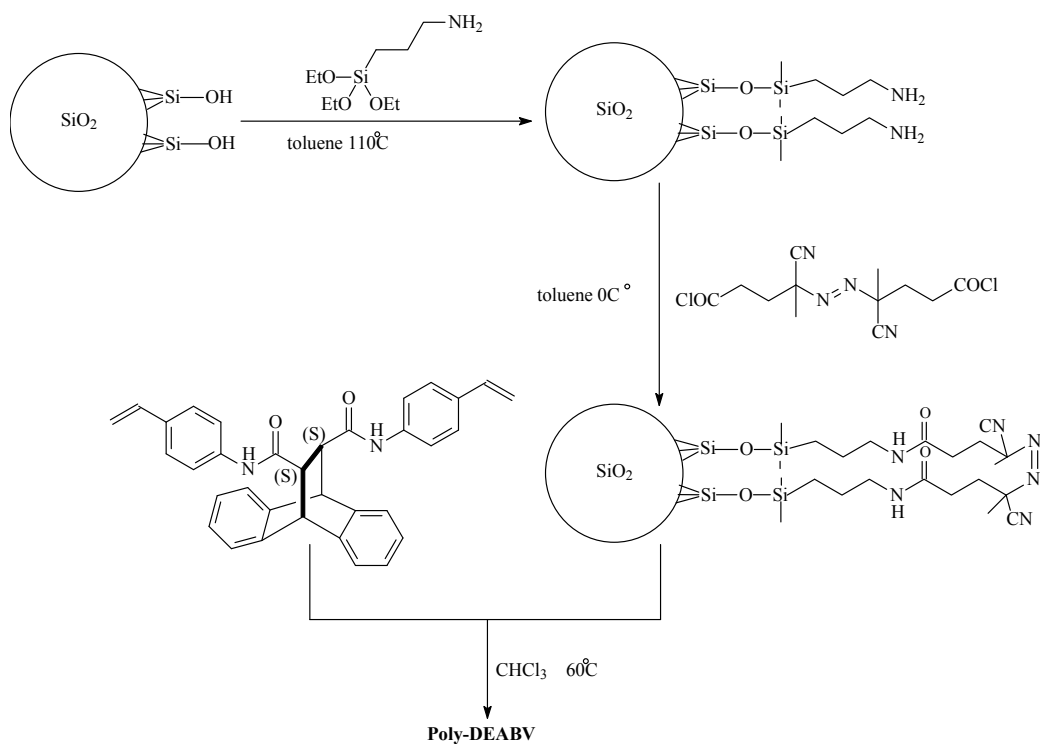


Figure 6.1 Preparation of the poly-DEABV chiral stationary phase.

Table 6.1 Retention factor of the first peak (k_1), enantioselectivity (α), and enantioresolution (R_s) of separated racemic compounds on the poly-DPAAS column in the normal phase mode

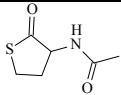
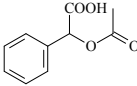
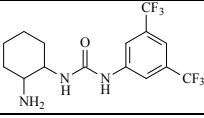
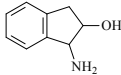
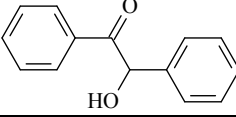
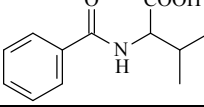
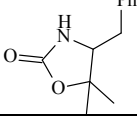
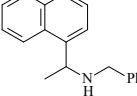
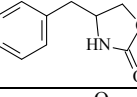
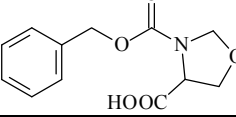
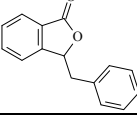
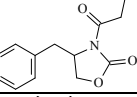
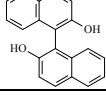
#	Compound	Structure	k_1	α	R_s	Mobile Phase (v/v) ^a
1	N-Acetylhomocysteine thiolactone		3.27	1.10	0.9	HEP/EtOH/TFA = 70/30/0.1
2	O-Acetyl-mandelic acid		3.70	1.07	0.7	HEP/EtOH/TFA = 90/10/0.1
3	1-(2-Aminocyclohexyl)-3-(3,5-bis-trifluoromethyl-phenyl)urea		3.58	1.33	1.6	HEP/EtOH/TFA = 90/10/0.1
4	cis-1-Amino-2-indanol		3.19	1.12	0.8	HEP/EtOH/TFA = 70/30/0.1
5	Benzoin		5.48	1.07	0.9	HEP/EtOH/TFA = 95/5/0.1
6	N-Benzoyl-valine		5.20	1.30	2.7	HEP/EtOH/TFA = 90/10/0.1
7	4-Benzyl-5,5-dimethyl-2-oxazolidinone		1.63	1.20	1.5	HEP/EtOH/TFA = 60/40/0.1
8	N-Benzyl-1-(1-naphthyl)-ethylamine		4.21	1.12	0.5	HEP/EtOH/TFA = 70/30/0.1
9	4-Benzyl-2-oxazolidinone		2.58	1.24	1.6	HEP/EtOH/TFA = 60/40/0.1
10	3-(Benzyloxycarbonyl)-4-oxazolidine carboxylic acid		3.79	1.06	0.4	HEP/EtOH/TFA = 80/20/0.1
11	Benzylphthalide		3.58	1.07	0.7	HEP/EtOH/TFA = 80/20/0.1
12	4-Benzyl-3-propionyl-2-oxazolidinone		6.43	1.23	1.9	HEP/EtOH/TFA = 80/20/0.1
13	1, 1'-Bi-2-naphthol		8.65	1.07	0.6	HEP/EtOH/TFA = 90/10/0.1

Table 6.1 – Continued

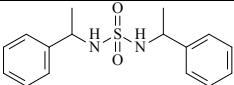
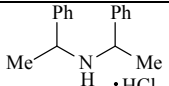
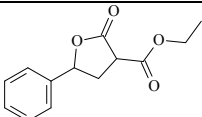
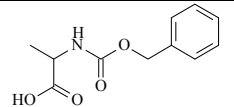
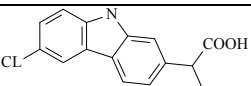
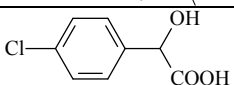
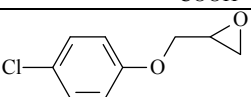
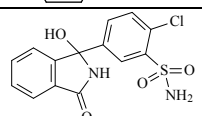
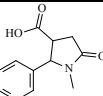
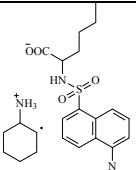
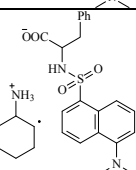
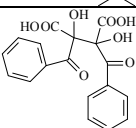
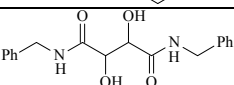
14	N,N'-Bis(2-methylbenzyl)sulfamide		4.67	1.05	0.4	HEP/EtOH/TFA = 80/20/0.1
15	Bis[1-phenylethyl]-Amine hydrochloride		4.11	1.30	1.7	HEP/EtOH/TFA = 80/20/0.1
16	2-Carboethoxy-γ-phenyl-γ-butyrolactone		6.67	1.12	1.5	HEP/EtOH/TFA = 90/10/0.1
17	Carbobenzyloxy-alanine		2.33	1.33	2.5	HEP/EtOH/TFA = 80/20/0.1
18	Carprofen		3.72	1.09	0.5	HEP/EtOH/TFA = 80/20/0.1
19	4-Chloromandelic acid		11.3	1.03	0.4	HEP/EtOH/TFA = 95/5/0.1
20	4-Chlorophenyl-2,3-epoxypropyl ether		3.51	1.04	0.6	HEP/EtOH/TFA = 100/1/0.1
21	Chlorthalidone		5.48	1.12	0.6	HEP/EtOH/TFA = 60/40/0.1
22	trans-4-Cotinine-carboxylic acid		4.63	1.13	0.6	HEP/EtOH/TFA = 60/40/0.1
23	Dansyl-norleucine cyclohexylammonium salt		4.37	1.24	1.5	HEP/EtOH/TFA = 80/20/0.1
24	Dansyl-phenylalanine cyclohexylammonium salt		2.60	1.49	1.8	HEP/EtOH/TFA = 60/40/0.1
25	2,3-Dibenzoyl-tartaric acid		7.41	1.23	1.5	HEP/EtOH/TFA = 80/20/0.1
26	N,N'-Dibenzyl-tartramide		4.42	1.33	1.6	HEP/EtOH/TFA = 70/30/0.1

Table 6.1 – Continued

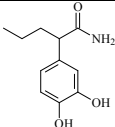
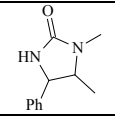
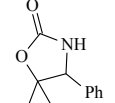
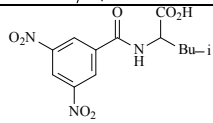
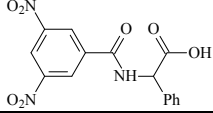
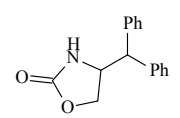
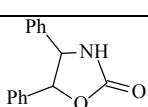
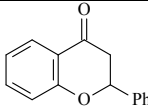
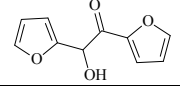
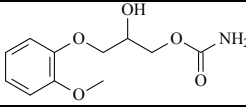
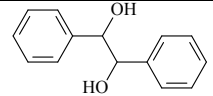
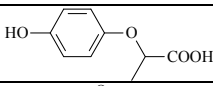
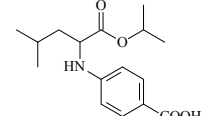
27	3,4-Dihydroxyphenyl- α -propylacetamide		5.99	1.05	0.4	HEP/EtOH/TFA = 80/20/0.1
28	1,5-Dimethyl-4-phenyl-2-imidazolidinone		2.67	1.08	0.8	HEP/EtOH/TFA = 80/20/0.1
29	5,5-Dimethyl-4-phenyl-2-oxazolidinone		3.63	1.18	1.5	HEP/EtOH/TFA = 80/20/0.1
30	N-(3,5-Dinitrobenzoyl)-leucine		1.79	3.93	5.1	HEP/EtOH/TFA = 60/40/0.1
31	N-(3,5-Dinitrobenzoyl)-phenylglycine		4.52	1.87	2.8	HEP/EtOH/TFA = 60/40/0.1
32	4-(Diphenylmethyl)-2-oxazolidinone		5.23	1.23	1.6	HEP/EtOH/TFA = 70/30/0.1
33	cis-4,5-Diphenyl-2-oxazolidinone		2.57	1.30	1.8	HEP/EtOH/TFA = 60/40/0.1
34	Flavanone		2.96	1.06	0.6	HEP/EtOH/TFA = 95/5/0.1
35	Furoin		9.29	1.03	0.4	HEP/EtOH/TFA = 90/10/0.1
36	Guaiacol glyceryl ether carbamate		1.93	1.25	1.9	HEP/EtOH/TFA = 70/30/0.1
37	Hydrobenzoin		7.03	1.04	0.4	HEP/EtOH/TFA = 95/5/0.1
38	2-(4-Hydroxyphenoxy)-propionic acid		2.89	1.09	0.8	HEP/EtOH/TFA = 80/20/0.1
39	4-((1-(Isopropoxycarbonyl)-4-methyl-butyl)amino)-Benzoic acid		1.10	2.68	3.3	HEP/EtOH/TFA = 60/40/0.1

Table 6.1 – Continued

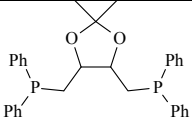
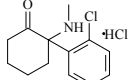
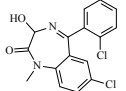
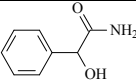
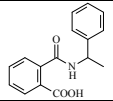
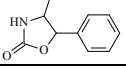
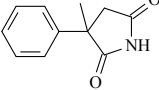
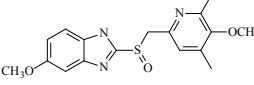
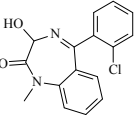
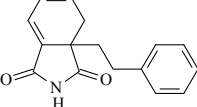
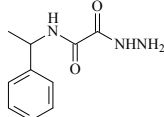
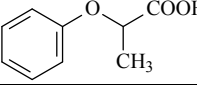
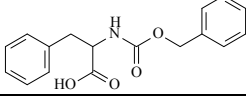
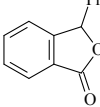
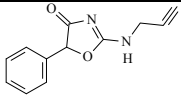
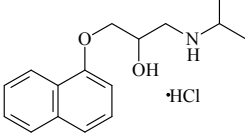
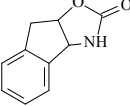
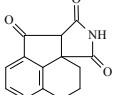
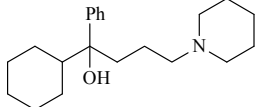
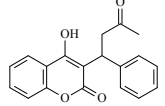
40	2,3-O-Isopropylidene-2,3-dihydroxy-1,4-bis-(disphenylphosphino)butane		3.64	1.35	1.3	HEP/EtOH/TFA = 60/40/0.1
41	Ketamine hydrochloride		8.77	1.17	0.5	HEP/IPA/TFA = 50/50/0.1
42	Lormetazepam		3.51	1.37	1.6	HEP/EtOH/TFA = 60/40/0.1
43	Mandelamide		6.67	1.17	1.7	HEP/EtOH/TFA = 85/15/0.1
44	N-(α -Methylbenzyl)phthalic acid monoamide		2.38	1.16	0.9	HEP/EtOH/TFA = 70/30/0.1
45	<i>cis</i> -4-Methyl-5-phenyl-2-oxazolidinone		11.3	1.15	1.7	HEP/EtOH/TFA = 90/10/0.1
46	α -Methyl- α -phenyl-succinimide		3.73	1.05	0.4	HEP/IPA/TFA = 70/30/0.1
47	Omeprazole		6.04	1.42	1.4	HEP/EtOH/TFA = 60/40/0.1
48	Oxazepam		18.0	1.18	0.8	HEP/EtOH/TFA = 85/15/0.1
49	Phenethyl-phthalimide		2.75	1.04	0.3	HEP/EtOH/TFA = 95/5/0.1
50	5-(α -Phenethyl)-semioxamazide		2.77	1.13	0.5	HEP/EtOH = 60/40
51	2-Phenoxypropionic acid		3.66	1.07	0.7	HEP/EtOH/TFA = 95/5/0.1
52	Z-Phenylalanine		1.09	1.58	2.2	HEP/EtOH/TFA = 60/40/0.1
53	3-Phenylphthalide		10.0	1.10	1.5	HEP/EtOH/TFA = 95/5/0.1

Table 6.1 – Continued

54	5-Phenyl-2-(2-propynylamino)-2-oxazolin-4-one		5.04	1.21	1.5	HEP/EtOH/TFA = 70/30/0.1
55	Propranolol hydrochloride		4.02	1.11	0.4	HEP/EtOH/TFA = 70/30/0.1
56	(3a-cis)-3,3a,8,8a-Tetrahydro-2H-indenol[1,2-d]oxazol-2-one		12.4	14.0	1.5	HEP/EtOH/TFA = 85/15/0.1
57	3a,4,5,6-Tetrahydro-succininido[3,4-b]-acenaphthen-10-one		6.96	1.16	0.9	HEP/EtOH/TFA = 60/40/0.1
58	Trihexyphenidyl		7.72	1.08	0.4	HEP/EtOH/TFA = 80/20/0.1
59	Warfarin		14.1	1.05	0.3	HEP/EtOH/TFA = 90/10/0.1

^a HEP: *n*-heptane. EtOH: ethanol. IPA: isopropanol. TFA: trifluoroacetic acid

Table 6.2 Retention factor of the first peak (k_1), enantioselectivity (α), and enantioresolution (R_s) of separated racemic compounds on the poly-DPAAS column in the polar organic mode

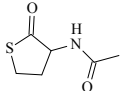
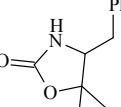
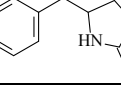
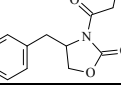
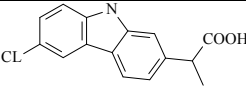
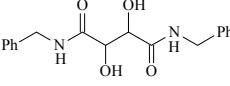
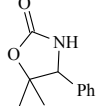
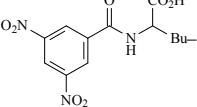
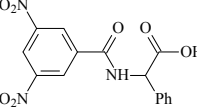
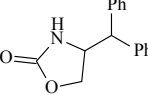
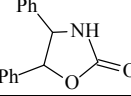
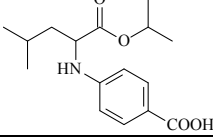
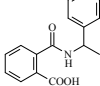
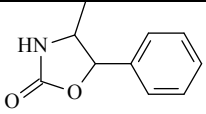
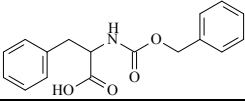
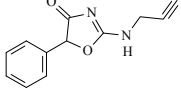
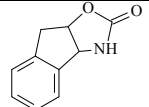
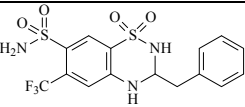
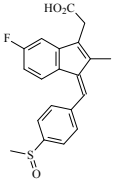
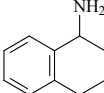
#	Compound	Structure	k_1	α	R_s	Mobile Phase (v/v) ^a
1	N-Acetylhomocysteine thiolactone		0.27	1.07	0.3	ACN /TFA = 100/0.1
7	4-Benzyl-5,5-dimethyl-2-oxazolidinone		0.18	1.28	0.7	ACN/TFA =100/0.1
9	4-Benzyl-2-oxazolidinone		0.24	1.32	1.3	ACN/TFA =100/0.1
12	4-Benzyl-3-propionyl-2-oxazolidinone		0.25	1.32	1.4	ACN/TFA =100/0.1
18	Carprofen		0.85	1.06	0.3	ACN/TFA =100/0.1
26	N,N'-Dibenzyl-tartramide		0.68	1.48	2.0	ACN/MeOH/TFA =100/1/0.1
29	5,5-Dimethyl-4-phenyl-2-oxazolidinone		0.23	1.43	1.4	ACN/ TFA=100/0.1
30	N-(3,5-Dinitro-benzoyl)-leucine		0.30	2.31	2.6	ACN/MeOH/TFA =100/1/0.1
31	N-(3,5-Dinitrobenzoyl)-phenylglycine		0.50	1.40	1.4	ACN/MeOH/TFA =100/1/0.1
32	4-(Diphenylmethyl)-2-oxazolidinone		0.29	1.38	1.6	ACN/TFA =100/0.1
33	cis-4,5-Diphenyl-2-oxazolidinone		0.26	1.54	1.9	ACN/TFA =100/0.1
39	4-((1-(Isopropoxycarbonyl-4-methyl)-butyl)amino)-Benzoic acid		0.04	6.06	3.0	ACN/TFA =100/0.1
44	N-(α -Methylbenzyl)phthalic acid monoamide		0.46	1.15	0.5	ACN/MeOH/TFA =100/1/0.1

Table 6.2 – Continued

45	<i>cis</i> -4-Methyl-5-phenyl-2-oxazolidinone		0.24	1.25	0.8	ACN/TFA =100/0.1
52	Z-Phenylalanine		0.33	1.33	1.0	ACN/TFA =100/0.1
54	5-Phenyl-2-(2-propynylamino)-2-oxazolin-4-one		0.31	1.16	0.4	ACN/MeOH/TFA =100/1/0.1
56	(3a-cis)-3,3a,8,8a-Tetrahydro-2H-indenol[1,2-d]oxazol-2-one		0.38	1.24	1.3	ACN/TFA =100/0.1
60	Bendroflumethiazide		0.10	1.40	0.3	ACN/TFA =100/0.1
61	Sulindac		1.38	1.05	0.3	ACN/MeOH/TFA =100/1/0.1
62	1,2,3,4-Tetrahydro-1-naphthylamine		0.38	1.24	1.4	ACN/TFA =100/0.1

^a ACN: acetonitrile. MeOH: methanol. TFA: trifluoroacetic acid.

Table 6.3 Retention factor of the first peak (k_1), enantioselectivity (α), and enantioresolution (R_s) of separated racemic compounds on the poly-DPEDA column in the normal-phase mode with halogenated solvent

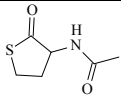
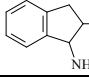
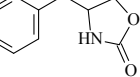
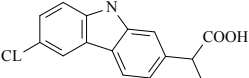
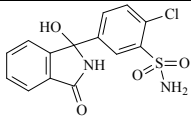
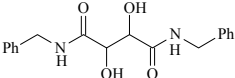
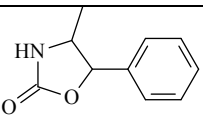
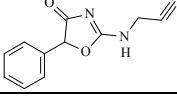
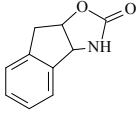
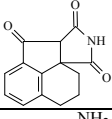
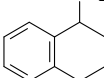
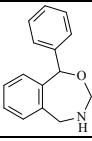
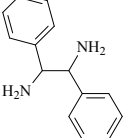
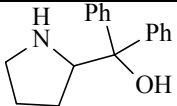
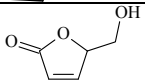
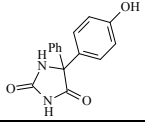
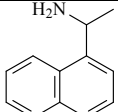
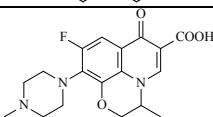
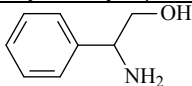
#	Compound	Structure	k_1	α	R_s	Mobile Phase (v/v) ^a
1	N-Acetylhomocysteine thiolactone		0.93	1.22	1.3	CH ₂ Cl ₂ /MeOH /TFA = 99/1/0.1
4	Cis-1-Amino-2-indanol		3.62	1.13	0.8	CH ₂ Cl ₂ /MeOH /TFA = 95/5/0.1
9	4-Benzyl-2-oxazolidinone		0.11	2.04	1.8	CH ₂ Cl ₂ /MeOH /TFA = 95/5/0.1
18	Carprofen		1.65	1.10	0.5	CH ₂ Cl ₂ /MeOH /TFA = 97/3/0.1
21	Chlorthalidone		2.77	1.21	1.4	CH ₂ Cl ₂ /MeOH /TFA = 95/5/0.1
26	N,N'-Dibenzyl-tartramide		0.26	1.43	1.5	CH ₂ Cl ₂ /MeOH /TFA = 95/5/0.1
45	cis-4-Methyl-5-phenyl-2-oxazolidinone		1.18	1.32	2.2	CH ₂ Cl ₂ /MeOH /TFA = 99/1/0.1
54	5-Phenyl-2-(2-propynylamino)-2-oxazolin-4-one		0.96	1.18	1.4	CH ₂ Cl ₂ /MeOH /TFA = 97/3/0.1
56	(3a-cis)-3,3a,8,8a-Tetrahydro-2H-indenol[1,2-d]oxazol-2-one		0.36	0.62	2.6	CH ₂ Cl ₂ /MeOH /TFA = 95/5/0.1
57	3a,4,5,6-Tetrahydro-succininido[3,4-b]-acenaphthen-10-one		0.95	1.30	2.0	CH ₂ Cl ₂ /MeOH /TFA = 97/3/0.1
62	1,2,3,4-Tetrahydro-1-naphthylamine		0.40	1.70	2.7	CH ₂ Cl ₂ /MeOH /TFA = 95/5/0.1
63	N-Desmethyl-nefopam		0.94	1.26	1.1	CH ₂ Cl ₂ /MeOH /TFA = 95/5/0.1
64	1,2-Diphenylethylene-diamine		0.69	1.39	1.1	CH ₂ Cl ₂ /MeOH /TFA = 95/5/0.1

Table 6.3 – Continued

65	α, α -Diphenylprolinol		0.95	1.26	1.4	CH ₂ Cl ₂ /MeOH /TFA = 95/5/0.1
66	5-Hydroxymethyl-2(5H)-furanone		1.75	1.28	2.0	CH ₂ Cl ₂ /MeOH /TFA = 99/1/0.1
67	5-(4-Hydroxyphenyl)-5-phenylhydantoin		4.85	1.13	0.8	CH ₂ Cl ₂ /MeOH /TFA = 95/5/0.1
68	1-(1-Naphthyl)ethylamine		3.20	1.08	0.5	CH ₂ Cl ₂ /MeOH /TFA = 95/5/0.1
69	Ofloxacin		0.83	1.10	0.9	CH ₂ Cl ₂ /MeOH /TFA = 95/5/0.1
70	2-Phenylglycinol		3.75	1.12	0.7	CH ₂ Cl ₂ /MeOH /TFA = 95/5/0.1

^a MeOH: methanol. TFA: trifluoroacetic acid.

number of enantiomeric separations in every mobile phase was summarized in Figure 6.3.

Since the polymeric chiral selectors are covalently bonded to the surface of silica gel, high stability of the new CSP was observed in the column evaluation process. After more than 1500 injections and several times of mobile phase mode change, no decrease in retention or enantiomeric selectivities were observed, which indicated that no degradation of CSP occurred.

6.4.3 Comparison of Separation in Three Mobile Phases

Although polar organic mode and methylene chloride/methanol mobile phase are not as powerful as heptane/ethanol mobile phase for the separation of chiral molecules, these two mobile phases have their own advantages. First, 11 new separations of racemates were obtained from these two mobile phases (Figure 6.3). Second, the separations in these two mobile phases are fast. Most separations in these two mobile phases are in 10 minutes. Finally, for some analytes such as compound **1**, **21**, **26**, **45**, **56**, and **57**, better separations were achieved in either polar organic mode or methylene chloride/methanol mobile phase compared with the separations in the heptane/ethanol or heptane/isopropanol mobile phase.

6.4.4 Effect of Polar Modifiers in Normal Phase Mode

Two polar modifiers, ethanol and isopropanol were assessed in the normal phase mode. Generally, ethanol is a better polar modifier compared with isopropanol. For most analytes, better efficiency and resolution were observed in ethanol/heptane mobile phase than ones in isopropanol/heptane mobile phase. The typical examples are the separations of compound **6** and **24** (Figure 6.2). Although enantioselectivities of compound **6** and **24** decreased a little bit from the ethanol/heptane mobile phase to isopropanol/heptane mobile phase, the resolutions increased greatly due to the significant improvement of peak efficiency. For compound **6**, N_1 (Theoretical plate numbers of the first peak) was 2600 when ethanol was used as polar modifier, while N_1 was just 700 when isopropanol was used. For compound **24**, N_1 also increased from 200 to 800 when the mobile phase was changed from isopropanol/heptane mobile phase to ethanol/heptane mobile phase. The reason of this phenomenon is because the viscosity of ethanol is lower than that of isopropanol. The low viscosity of mobile phase improves mass transfer, thus increases efficiency and resolution. However, for a few analytes such as compound **41** and **46**, better resolutions were achieved in isopropanol/heptane mobile phase than ones in ethanol/heptane mobile phase (data not showed) due to the

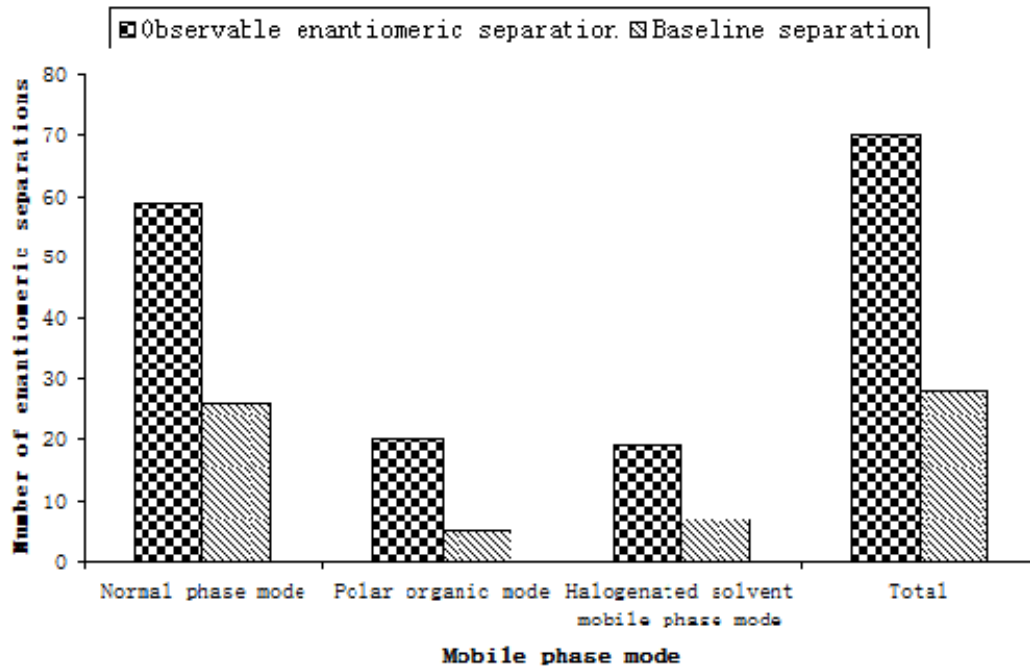


Figure 6.3 Summary of the number of observable and baseline separations achieved on the poly-DEABV CSP.

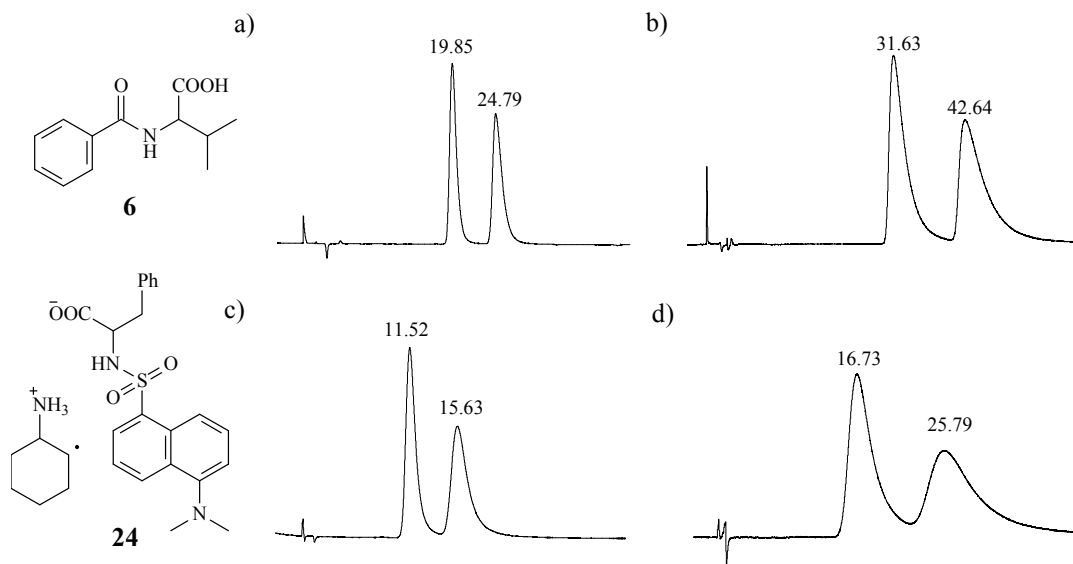


Figure 6.2 The effect of polar modifier on the enantiomeric separations of compounds **6** (a, b) and **24** (c, d) in the normal phase mode. Mobile phase: a) Heptane/Ethanol/TFA = 90/10/0.1, b) Heptane/Isopropanol/TFA = 90/10/0.1, c) Heptane/Ethanol/TFA = 60/40/0.1, d) Heptane/Isopropanol/TFA = 50/50/0.1. Enantioselectivity α : a) $\alpha = 1.30$, b) $\alpha = 1.39$, c) $\alpha = 1.49$, d) $\alpha = 1.67$. Resolution R_s : a) $R_s = 2.7$, b) $R_s = 1.8$, c) $R_s = 1.8$, d) $R_s = 1.4$. Number of theoretical plates of the first peak N_1 : a) $N_1 = 2600$, b) $N_1 = 700$, c) $N_1 = 800$, d) $N_1 = 200$.

better enantiomeric selectivities when isopropanol was used as polar modifier.

6.4.5 *Effect of Mobile Phase Additive: TFA*

A small amount of trifluoroacetic acid is important for the enantiomeric separation on this new polymeric CSP. The effect of TFA depends on the structural characteristics of the analytes. For the neutral analytes without ionizable groups, Addition of TFA into mobile phase has no or little effect on the enantiomeric separations. For example, no difference has been observed on the retention, enantiomeric selectivity, and resolution on the separation of compound **33** (Figure 6.4a and b). However, for the separation of acidic analytes, addition of TFA into the mobile phase can decrease the retention and increase the efficiency, enantiomeric selectivities and resolutions in some cases. The typical example is the separation of compound **31** (Figure 6.4c and d). Better efficiency, enantiomeric selectivity, and resolution were obtained when 0.1% TFA was added into the mobile phase versus ones observed in the mobile phase without TFA. Another advantage of TFA is the decrease of separation time. Similar phenomenon has also been observed on the P-CAP column [8]. A small amount of TFA in the mobile phase can cover the residual amino groups on the stationary phase, thus prevent the strong acid-base interaction between the acidic analytes and basic sites on the stationary phase. Therefore, efficiency increases and retention decreases.

6.4.6 *Sample Loading Study*

This new polymeric CSP showed high sample loading ability for some analytes with high enantiomeric selectivities. For example, when 1 μg of compound **30** was injected into the column, an excellent separation with a resolution 5.1 was achieved (Figure 6.5a). However, a satisfactory separation with a resolution of 2.4 was obtained when 1000 μg of analyte was injected (Figure 6.5b). Considering that the baseline separation of such a large amount of analyte was achieved on an analytical size column (250 x 4.6 mm), this new polymeric CSP has the potential to be an excellent preparative CSP.

6.4.7 *Complementary Nature to P-CAP and P-CAP-DP Columns*

As a column in the same family, poly-DEABV CSP is complementary to the other two polymeric CSPs, P-CAP and P-CAP-DP CSPs. It is clearly to see this phenomenon from the two examples below (Figure 6.6). For the separation of compound **30**, enantiomeric selectivities increased from P-CAP column to DEABV column. However, for the separation of compound **13**, the best separation was achieved on the P-CAP CSP

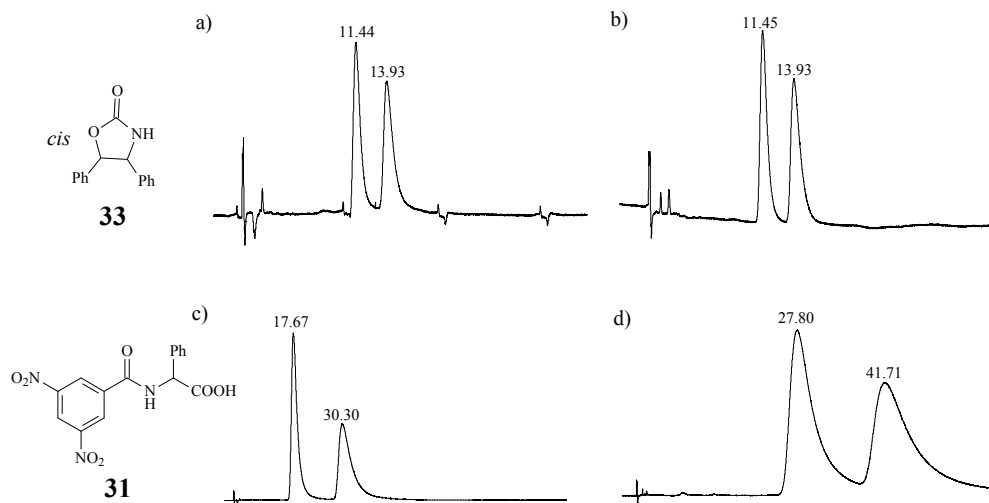


Figure 6.4 The effect of the acidic additive on the enantiomeric separations of compound **33** (a, b)) and **31** (c, d)) in the normal phase mode. Mobile phase: a, c) Heptane/Ethanol/TFA = 60/40/0.1, b, d) Heptane/Isopropanol/TFA = 60/40. Enantioselectivity α : a), b) $\alpha = 1.30$, c) $\alpha = 1.87$, d) $\alpha = 1.54$. Resolution R_s : a), b) $R_s = 1.8$, c) $R_s = 2.8$, d) $R_s = 1.4$.

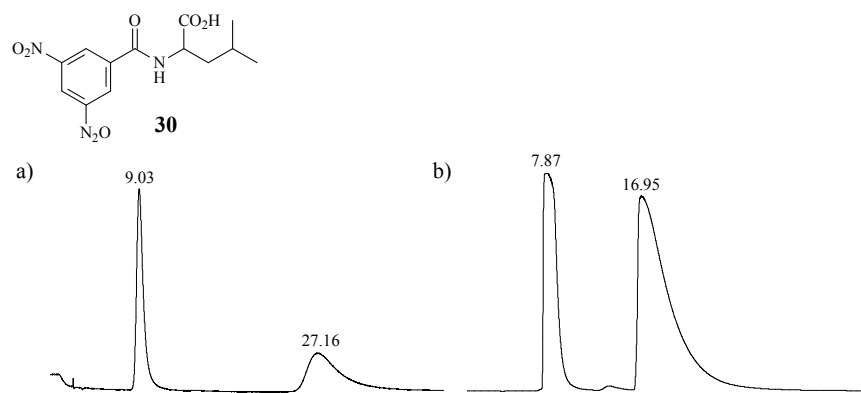


Figure 6.5 The effect of sample loading on the enantiomeric separation of compound **30** with a) 1.0 μg and b) 1000 μg of compound injected on the poly DEABV CSP. Mobile phases: a), b) Heptane/Ethanol/TFA = 60/40/0.1. Enantioselectivity α : a) $\alpha = 4.11$, b) $\alpha = 2.94$. Resolution R_s : a) $R_s = 5.1$, b) $R_s = 2.4$.

and the worst separation was obtained on the poly-DEABV CSP. The new polymeric CSP extends the concept of the P-CAP column family.

6.5 Conclusions

A new polymeric CSP based on a new monomer, *trans*-9, 10-dihydro-9, 10-ethanoanthracene-(11S, 12S)-11, 12-dicarboxylic acid bis-4-vinylphenylamide, was prepared via the surface initiated free radical polymerization method. The new CSP was stable and showed enantiomeric selectivities for many chiral compounds in multiple mobile phases. Most chiral separations were achieved in the ethanol/heptane mobile phase, while better separations for some analytes were obtained in the polar organic mode and halogenated solvent mobile phase. In the normal phase mode, ethanol is the better polar modifier compared with isopropanol. The acidic mobile phase additive is important for the separations of some compounds with ionizable groups. This new polymeric CSP showed its potential for preparative scale application. All in all, the poly-DEABV CSP enriches the family of former synthetic polymeric CSPs such as P-CAP and P-CAP-DP CSPs.

6.6 Acknowledgements

We gratefully acknowledge the support of this work by the National Institutes of Health, NIH RO1 GM53825-11.

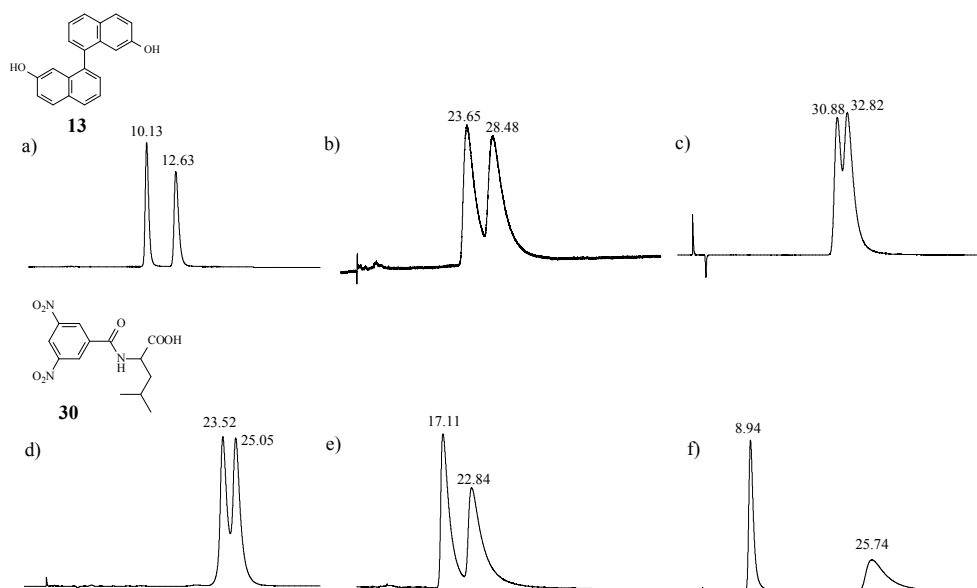


Figure 6.6 Comparison of the enantiomeric separations of compound 13 (a), b), c)) and 30 (d), e), f)) on the P-CAP (a), d)), poly-DPEDA (b), e)), and poly-DEABV (c), f)) CSPs. Mobile phase: a) Heptane/Ethanol/TFA = 90/10/0.1, b) Heptane/Isopropanol = 80/20, c) Heptane/Isopropanol = 50/50, d) Heptane/Ethanol/TFA = 80/20/0.1, e) Heptane/Isopropanol/TFA = 70/30/0.1, f) Heptane/Ethanol/TFA = 60/40/0.1. Enantioselectivity α : a) $\alpha = 1.36$, b) $\alpha = 1.23$, c) $\alpha = 1.07$, d) $\alpha = 1.07$, e) $\alpha = 1.41$, f) $\alpha = 3.93$.

CHAPTER 7

SUPER/SUBCRITICAL FLUID CHROMATOGRAPHY SEPARATIONS WITH FOUR SYNTHETIC POLYMERIC CHIRAL STATIONARY PHASES

7.1 Abstract

New synthetic polymeric chiral stationary phases were tested with supercritical fluid mobile phases made of CO₂ plus an alcohol modifier and 0.2% v/v trifluoroacetic acid. The polymeric N, N'-(1S, 2S)-1, 2-cyclohexanediyl-bis-2-propenamide (P-CAP), the polymeric N,N'-[(1R,2R)]-1,2-diphenyl-1,2-ethanediyl] bis-2-propenamide (P-CAP-DP), the polymeric *trans*-9,10-dihydro-9,10-ethanoanthracene-(11S,12S)-11,12-dicarboxylic acid bis-4-vinylphenylamide (DEABV) and the polymeric N,N'-[(1R,2R)-1,2-diphenyl-1,2-ethanediyl] bis-4-vinylbenzamide (DPEVB) were bonded to 5 μm silica particles and used to prepare four columns that were tested with a set of 88 chiral compounds with a wide variety of chemical functionalities. All 88 test compounds were separated on one or more of these “related” polymeric CSPs. Forty three enantiomeric pairs were separated in SFC conditions by only one of the CSPs. Twenty pairs were separated by two CSPs and eighteen and seven enantiomeric pairs were separated by three and all four CSPs, respectively. The three P-CAP, P-CAP-DP and DEABV CSPs have equivalent success being able to separate 49 enantiomeric pairs of the studied set with respectively 12, 14 and 20 at baseline (R_s > 1.5). The DPEVB CSP was significantly less efficient separating only 18 chiral compounds with only one at baseline. The great advantage of the SFC mobile phases is the rapid separation, with most achieved in less than 5 min. Xinxin Han, Alain Berthod, Chunlei Wang, Ke Huang, and Daniel W. Armstrong. *Chromatographia* (2007), 65(7/8), 381-400. Copyright © 2007 with permission from the Springer, LLC.

7.2 Introduction

LC chiral stationary phases (CSPs) can be used for analytical and preparative enantiomeric separations. However, the effectiveness of different classes of CSPs at each task can vary widely. Modern chiral

selectors include π -complex, ligand exchange, chiral crown ethers, cyclodextrins, polysaccharides, proteins and macrocyclic glycopeptide chiral selectors.^{31a, 73} All these chiral selectors were found to be very useful in separating enantiomers on an analytical scale (microgram to milligram amounts). One of the important challenges in enantiomeric separations is enhancing production, i.e. going to gram, kilogram and even to greater amounts in a facile manner. Many polymeric chiral selectors have a significant higher loading capability than smaller chiral selectors.^{25a} An exception to this statement are the protein CSPs which have very low capacities. Successful polymeric chiral stationary phases (CSP) include natural polymers such as polysaccharide derivatives, cellulose and amylose carbamates, or synthetic polymers such as polyamides, vinyl polymers, polyurethanes and polyacetylene derivatives.^{66b, 67d} Recent polymeric chiral selectors based on *trans*-1,2-diaminocyclohexane were found very useful when used to prepare CSPs for normal phase liquid chromatography (NPLC).^{48e, 67d, 74}

The need for preparative enantiomeric separations is driving the renewed interest in supercritical fluid chromatography (SFC). In the 1980s, some studies overestimated the solvent strength of supercritical CO₂ and this led to some disappointments especially in the applicability of capillary SFC.⁷⁵ It became clear that some percentage of a more polar cosolvent, like methanol, was needed to elute most analytes. With the increased interest in high throughput separations, preparative separations and solvent disposal concerns, SFC with packed columns underwent a rebirth as a potential replacement for NPLC.⁷¹

Enantiomeric separations using SFC with packed columns were first performed by Mourier et al. separating phosphine oxide enantiomers on a π -complex based CSP.^{67c} Supercritical CO₂, almost exclusively used in its subcritical state associated with significant amounts of organic modifier, was found to increase dramatically the preparative productivity of enantiomeric separations.^{67b, 76} Many different CSPs have been used in packed column SFC.⁷⁷

In this work, the capabilities of the recently introduced synthetic polymeric CSPs^{67c, d} will be evaluated in SFC. Two new related polymeric CSPs will also be evaluated with the same set of solutes and SFC mobile phases. The results obtained with the four CSPs will be discussed and compared. A set of 88 chiral compounds with a wide variety of functionalities was used to test the four CSPs. Experimental conditions

were deliberately selected to favor fast rather than efficient separations. The results obtained on the four CSPs are compared and discussed in terms of enantio-recognition capabilities.

7.3 Experimental

7.3.1 Chemicals

Eighty eight enantiomeric pairs with a wide variety of functionalities were evaluated on four different polymeric CSPs. All the test compounds could be placed into one of four classes: i) compounds with a sp^2 hybridized carbon directly attached to the asymmetric center; ii) compounds whose asymmetric center is part of a ring; iii) chiral acids and derivatized amino-acids; iv) other compounds including atropoisomers, alcohols, and stereogenic phosphorous and sulfoxide compounds. All analytes were obtained from Sigma (St. Louis, MO, USA) or Aldrich (Milwaukee, WI, USA). Stock solutions of 1 mg/mL of each compound were prepared and injected individually on the four polymeric CSPs.

7.3.2 Chiral Stationary Phases

Figure 7.1 shows the chiral monomers used to prepare the four synthetic polymeric CSPs evaluated in this work. All chiral selectors were bonded on spherical 5 μm porous silica gel (Akzo Nobel, EKA Chemicals AB, Sweden, pore size 20 nm, pore volume 0.9 ml/g, specific surface area 210 m^2/g). The bonded particles were used to fill 250 x 4.6 mm columns. The P-CAP, from “poly Cyclic Amine Polymer”, is actually a polymer of *trans*-1,2-cyclohexanediyl-bis-acrylamide (Figure 7.1a). The P-CAP denomination comes from the Astec trade name (Astec, Whippany, NJ, USA). This stationary phase was fully described recently.^{67d} The P-CAP-DP, also an Astec trade name, is a polymer of N,N' -[(1R,2R)-1,2-diphenyl-1,2-ethanediyl] bis-2-propenamide (Figure 7.1b). It was prepared as fully described in.^{67c} Figure 7.1c shows the monomer *trans*-9,10-dihydro-9,10-ethanoanthracene-(11S,12S)-11,12-dicarboxylic acid bis-4-vinylphenylamide that was used to prepare the DEABV stationary phase. This molecule was synthesized in our group using a chiral dicarboxylic acid originally reported by Thunberg and Allenmark and then coupled to *p*-vinylphenylamine. The chiral selector and the phase preparation were fully described in a recent article.⁷⁸ Figure 7.1d shows the N,N' -[(1R,2R)-1,2-diphenyl-1,2-ethanediyl] bis-4-vinylbenzamide monomer, a variation of Figure 7.1b, used to prepare the DPEVB stationary phase according to a procedure similar to those described previously.^{67c, d}

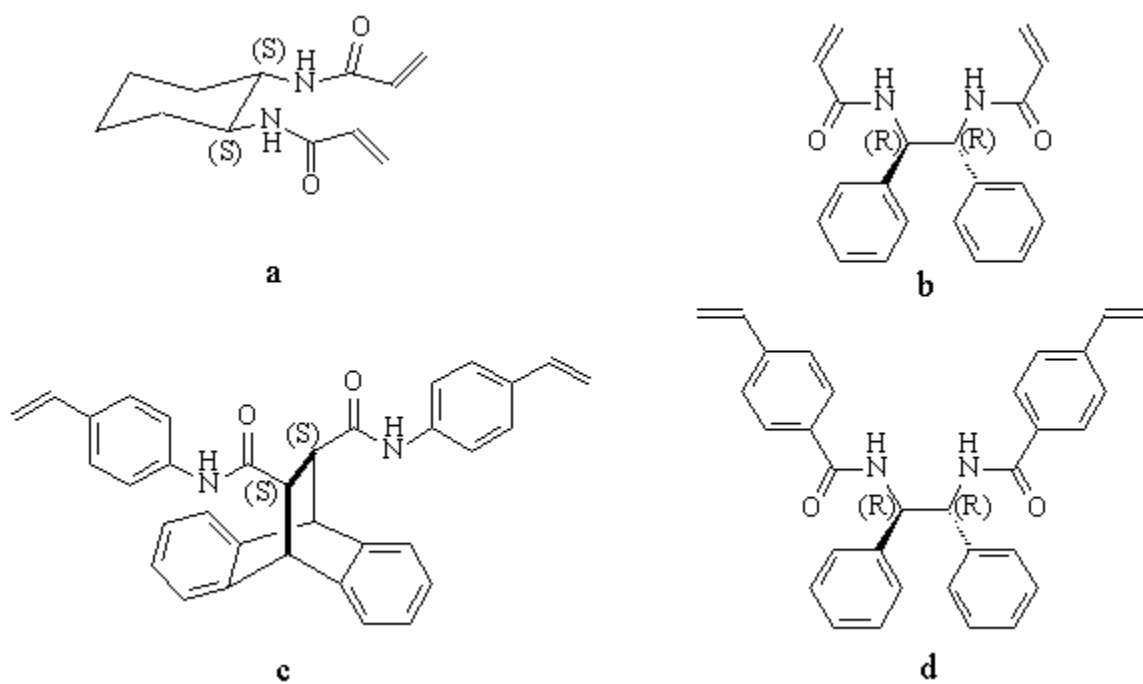


Figure 7.1 The monomer of the polymeric chiral stationary phases used. **a**- P-CAP (*trans*-1,2-cyclohexanediyl-bis acrylamide), **b**- P-CAP-DP (*N,N'*-[(1*R*,2*R*)-1,2-diphenyl-1,2-ethanediyl] bis-2-propenamide), **c**-DEABV (*trans*-9,10 dihydro-9,10-ethanoanthracene-(1*S*,12*S*)-11,12-dicarboxylic acid bis-4-vinylphenylamide), **d**-DPEVB (*N,N'*-[(1*R*,2*R*)-1,2-diphenyl-1,2-ethanediyl] bis[4-vinylbenzamide]).

7.3.3 *Supercritical Fluid Chromatography*

The SFC apparatus was from Thar Technologies, Inc. (Pittsburgh, PA). The SFC system includes a fluid delivery module (liquid CO₂ pump and cosolvent pump) an auto sampler with a 48 sample tray, a column oven with column selection and an auto back pressure regulator, a UV VWD detector, and the SuperChrom™ software for data treatment. SFC-grade CO₂ was from Air Liquide America (Houston, TX).

7.3.4 *Operating Conditions*

All studies of the effect of temperature in enantiomeric separations have shown that the enantioselectivity factors decrease as the temperature increases.⁷⁹ So a constant and low temperature of 31°C (CO₂ critical temperature is 31.3°C) was selected for all analyses. Similarly, raising the pressure does produce faster analyses, but it is associated with a poorer enantioselectivity.⁸⁰ Consequently, a constant outlet pressure of 100 bar (1430 p.s.i.) was used in all cases.

The polarity of pure CO₂ mobile phase can be compared to that of pentane. It is not high enough to perform useful separations. Therefore, significant amounts of polar organic modifier were added in all mobile phases used.⁸¹ Trifluoroacetic acid (TFA) was also added at a concentration of 0.2% v/v in the organic modifier (unless otherwise indicated) used in all mobile phases to protonate the solutes and any stationary phase basic sites. The total flow rate (CO₂ + MeOH) was always 4 ml/min at the column inlet.

The amount of methanol (MeOH) added to CO₂ was selected so that the solute peaks elute in less than 8 min. When a particular solute was not separated on all four CSPs, another mobile phase was tested either with first another MeOH concentration and next another organic modifier (ethanol, EtOH, or isopropyl alcohol, IPA) keeping the CO₂ pressure at 100 bar and the TFA concentration at 0.2% v/v in the organic modifier until the solute's enantiomers are separated by at least one CSPs. This procedure shows that the listed results are certainly not the best results that could be obtained working with the studied polymeric CSPs. Further optimization of the mobile phase composition for each individual compounds could be done if desired.

7.4 **Results and Discussion**

Table 7.1 gives the number code used to identify the 88 compounds; along with their names, chemical structures and chromatographic parameters obtained on the four polymeric CSPs. All blank entries

correspond to non-observable enantiomeric separation (a single peak, enantioselectivity and resolution factors are respectively 1 and 0).

7.4.1 Overall CSP Effectiveness

Figure 7.2 (top) shows the number of enantiomeric separations obtained on each polymeric CSP. It clearly shows that the DPEVB CSP is less effective than the three other CSPs and is able to baseline separate only one compound (Compound **58**, $R_s = 1.6$, Table 7.1). By chance, the other three CSPs, P-CAP, P-CAP-DP and DEABV, were able to separate exactly the same number of compounds (49). The DEABV CSP baseline separated 20 compounds (41% of the 49 separations, Table 7.1). Fifteen of the 49 fully or partially enantioseparated compounds were separated only on the DEABV-CSP. The number of baseline separations for the P-CAP and P-CAP-DP CSPs was, respectively, 12 and 14 compounds. The number of unique separations for the P-CAP and P-CAP-DP CSPs was eleven compounds. With the 6 compounds uniquely separated by the DPEVB CSP, a total of 43 compounds or 49% of the selected set were separated by only one CSP. Figure 7.2 (bottom) shows that 20 compounds were separated by two CSPs, 18 by three CSPs and 7 compounds were enantioseparated by all four CSPs. These later compounds are **6**, **22**, **23**, **26**, **45**, **52** and **63** (Table 7.1).

Figure 7.3 presents an overall view of the Table 7.1 listed results. A solid vertical bar over the compound number means that an observable separation of the enantiomers of that compound was obtained ($R_s > 0.3$). The bar with horizontal stripes indicates baseline separations ($R_s > 1.5$). The light color bar containing wavy lines indicates that this particular compound was only separated on that specific polymeric CSP and none of the others. The DEABV-CSP seems to be somewhat better than the other two P-CAP CSPs in terms of the number of baseline separations and separations of compounds which contain the stereogenic center in a ring.

7.4.2 Compound Structure and Polymer CSP Enantioselectivity

In our recent work studying the behavior of the macrocyclic glycopeptide CSPs in subcritical chromatography, strong difference in enantioselectivity was found between the different related CSPs.⁸¹ Chiral acid and amino-acid enantiomers were significantly better separated by the teicoplanin aglycone (TAG) CSP while the chiral amino alcohols (β -blockers) were better separated on the native teicoplanin

Table 7.1 Enantiomeric separations on four polymeric CSPs by SFC.

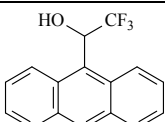
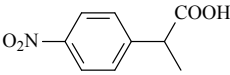
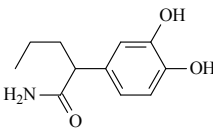
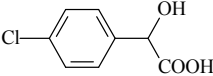
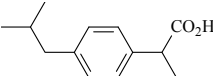
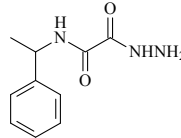
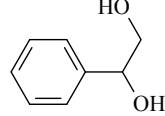
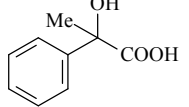
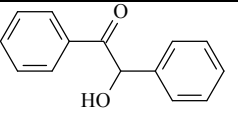
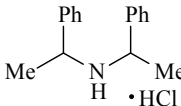
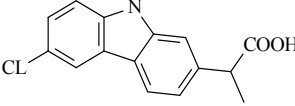
No.	Compound name and formula	CSP	t ₁ min	α	Rs	Additive M/TFA	N plates
Compounds with sp² hybridized carbon on the asymmetric center							
1	1-(9-Anthryl)-2,2,2-trifluoroethanol 	P-CAP P-CAP-DP DEABV DPEVB	2.64 3.54	1.07 1.07	0.7 0.7	30%/0.2% 15%/0.2%	4900 3700
2	2-(4-Nitrophenyl)-propionic acid 	P-CAP P-CAP-DP DEABV DPEVB	7.62	1.05	0.8	5%E/0.2%	7200
3	3,4-Dihydroxyphenyl-2-propylacetamide 	P-CAP P-CAP-DP DEABV DPEVB	7.27 7.31 6.18	1.16 1.03 1.04	1.6 0.3 0.3	25%/0.2% 20%/0.2% 20%/0.2%	2900 2200 2100
4	4-Chloromandelic acid 	P-CAP P-CAP-DP DEABV DPEVB	2.96	1.08	0.3	20%/0.2%	600
5	4-Isobutyl- α -methylphenylacetic acid 	P-CAP P-CAP-DP DEABV DPEVB	4.75	1.05	0.5	5%/0.2%	3400
6	5-(α -Phenethyl)-semioxamizide 	P-CAP P-CAP-DP DEABV DPEVB	2.19 3.58 1.73 3.69	1.13 1.05 1.21 1.22	0.8 0.4 1.1 1.1	30%/0.2% 15%/0.2% 40%/0.2% 10%/0.2%	2200 2400 3000 1000
7	1-Phenyl-1,2-ethanediol 	P-CAP P-CAP-DP DEABV DPEVB	6.63 11.2	1.16 1.06	1.8 1.4	15% I/0.2% 5%/0.2%	3500 9000
8	Atrolactic acid 	P-CAP P-CAP-DP DEABV DPEVB	4.02	1.05	0.6	10%/0.2%	3900
9	Benzoin 	P-CAP P-CAP-DP DEABV DPEVB	3.31 3.81 4.93	1.07 1.18 1.07	0.9 2.0 1.1	10%/0.2% 5%/0.2% 10%/0.2%	6900 4700 7700
10	Bis[1-phenylethyl]-Amine hydrochloride 	P-CAP P-CAP-DP DEABV DPEVB	7.34 3.02 4.30	1.09 1.16 1.28	1.1 0.9 2.0	5%/0.2% 15%/0.2% 20%/0.2%	4000 1400 2000
11	Carprufen 	P-CAP P-CAP-DP DEABV DPEVB	4.54 4.19 4.81	1.07 1.08 1.08	0.8 0.5 0.7	25%/0.2% 40%/0.2% 30%/0.2%	4400 1300 2400

Table 7.1 – Continued

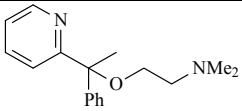
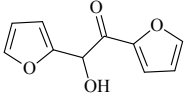
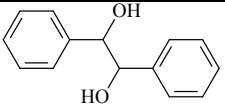
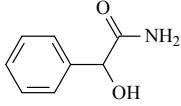
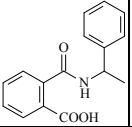
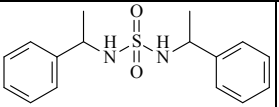
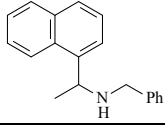
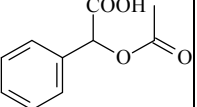
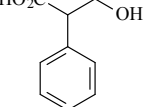
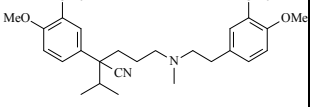
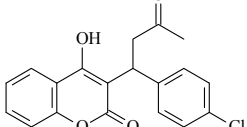
12	Doxylamine 	P-CAP P-CAP-DP DEABV DPEVB	3.06	1.07	0.3	15%/0.2%	700
13	Furoin 	P-CAP P-CAP-DP DEABV DPEVB	2.48 4.15 3.91	1.25 1.04 1.03	2.0 0.4 0.5	10%/0.2% 10%/0.2% 5%/0.2%	3800 2800 8000
14	Hydrobenzoin 	P-CAP P-CAP-DP DEABV DPEVB	5.12 5.23 7.18	1.12 1.06 1.03	1.8 0.9 0.5	15%E/0.5% 10%/0.5% 10%/0.5%	6500 5400 5000
15	Mandelamide 	P-CAP P-CAP-DP DEABV DPEVB	3.25	1.13	1.5	20%/0.5%	5300
16	N-(α -Methylbenzyl) phthalic acid monoamide 	P-CAP P-CAP-DP DEABV DPEVB	6.29 7.06	1.08 1.14	0.8 1.4	15%/0.2% 25%/0.2%	2800 2800
17	N,N'- Bis(2- methyl- benzyl) sulfamide 	P-CAP P-CAP-DP DEABV DPEVB	6.92 3.01 3.31	1.06 1.70 1.09	0.7 3.4 0.7	15%/0.2% 20%/0.2% 30%/0.2%	3800 1800 2200
18	N-Benzyl-1-(1- naphthyl)- ethylamine 	P-CAP P-CAP-DP DEABV DPEVB	5.31	1.12	0.6	35%E/0.2%	700
19	O-Acetyl mandelic acid 	P-CAP P-CAP-DP DEABV DPEVB	5.33 3.75	1.06 1.04	0.7 0.3	5%/0.2% 10%/0.2%	3300 1500
20	Tropic acid 	P-CAP P-CAP-DP DEABV DPEVB	4.44	1.15	1.6	15%E/0.2%	3700
21	Vera pami l 	P-CAP P-CAP-DP DEABV DPEVB	4.10	1.06	0.4	10%/0.2%	1300
22	Coumachl or 	P-CAP P-CAP-DP DEABV DPEVB	5.48 4.66 5.96 5.10	1.12 1.06 1.06 1.07	1.4 0.6 0.4 0.7	15%/0.2% 15%/0.2% 30%/0.2% 20%/0.2%	3600 2600 1000 2100

Table 7.1 – Continued

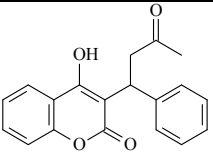
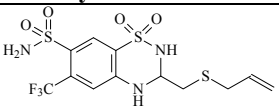
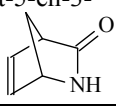
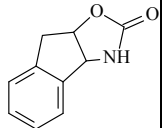
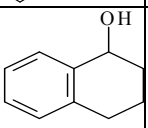
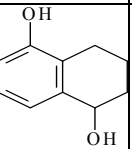
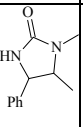
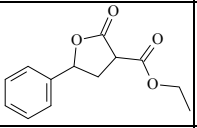
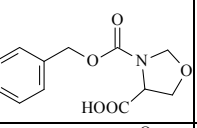
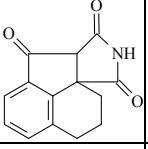
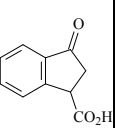
23	Warfarin		P-CAP P-CAP-DP DEABV DPEVB	4.50 4.08 4.89 4.30	1.11 1.07 1.07 1.11	1.3 0.8 0.5 1.1	15%/0.2% 15%/0.2% 30%/0.2% 20%/0.2%	4500 4200 1400 3100
Compounds whose asymmetric center is part of a ring								
24	Althia zide		P-CAP P-CAP-DP DEABV DPEVB	4.00	1.31	1.4	40%/0.2%	900
25	2-Azabicyclo[2.2.1]-hept-5-en-3-one		P-CAP P-CAP-DP DEABV DPEVB	5.17	1.10	1.4	3%/0.2%	5300
26	(3a-cis)-3,3a,8,8a-Tetrahydro-2H-indenol[1,2-d]oxazol-2-one		P-CAP P-CAP-DP DEABV DPEVB	4.31 4.35 5.8 2.95	1.16 1.12 1.13 1.06	1.5 1.1 1.5 0.8	20%/0.2% 15%/0.2% 20%/0.5% 20%/0.2%	2900 2700 4100 5700
27	1,2,3,4-Tetrahydro-1-naphthol		P-CAP P-CAP-DP DEABV DPEVB	4.25	1.05	0.9	5%E/0.2%	8000
28	1,5-Dihydroxy-1,2,3,4-tetrahydronaphthalene		P-CAP P-CAP-DP DEABV DPEVB	4.6	1.08	1.3	15%/0.2%	7000
29	1,5-Dimethyl-4-phenyl-2-imidazolidinone		P-CAP P-CAP-DP DEABV DPEVB	3.40 2.94 6.15	1.08 1.07 1.09	1.0 0.8 1.2	10%/0.2% 20%/0.2% 5% E/0.2%	5100 5000 5000
30	2-Carboethoxy-γ-phenyl-γ-butyrolactone		P-CAP P-CAP-DP DEABV DPEVB	3.59	1.07	0.9	10%/0.2%	5100
31	3-(Benzyloxy carbonyl)-4-oxazolidine carboxylic acid		P-CAP P-CAP-DP DEABV DPEVB	7.07	1.05	0.5	10%/0.5%	2400
32	3a,4,5,6-Tetrahydro-succininido[3,4-b]-acenaphthen-10-one		P-CAP P-CAP-DP DEABV DPEVB	6.08 5.60	1.04 1.13	0.5 1.0	15%/0.2% 35%E/0.2%	3300 1800
33	3-Oxo-1-indancarboxylic acid		P-CAP P-CAP-DP DEABV DPEVB	4.79	1.05	0.6	10%E/0.2%	4000

Table 7.1 – Continued

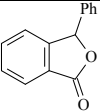
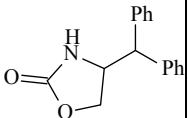
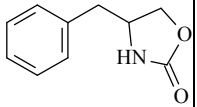
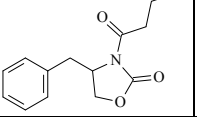
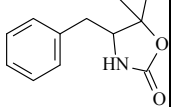
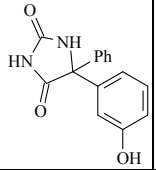
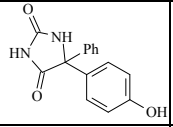
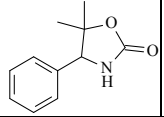
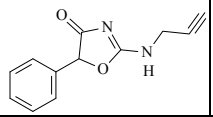
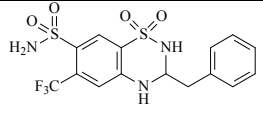
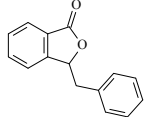
34	3-Phenylphthalide		P-CAP P-CAP-DP DEABV DPEVB	6.87	1.08	1.5	10%/0.5%	8000
35	4-(Diphenylmethyl)-2-oxazolidinone		P-CAP P-CAP-DP DEABV DPEVB	6.00 6.86 2.97	1.08 1.04 1.18	1.3 0.4 1.5	10%/0.2% 10%/0.2% 40%/0.2%	6300 2400 3000
36	4-Benzyl-2-oxazolidinone		P-CAP P-CAP-DP DEABV DPEVB	2.85	1.18	1.5	30%/0.2%	3300
37	4-Benzyl-3-propionyl-2-oxazolidinone		P-CAP P-CAP-DP DEABV DPEVB	4.44	1.18	2.0	20%/0.2%	4300
38	4-Benzyl-5,5-dimethyl-2-oxazolidinone		P-CAP P-CAP-DP DEABV DPEVB	3.17	1.17	1.5	25%E/0.2%	3300
39	5-(3-Hydroxyphenyl)-5-phenylhydantoin		P-CAP P-CAP-DP DEABV DPEVB	7.34	1.04	0.3	40%/0.2%	1300
40	5-(4-Hydroxyphenyl)-5-phenylhydantoin		P-CAP P-CAP-DP DEABV DPEVB	4.88	1.05	0.3	40%/0.2%	900
41	5,5-Dimethyl-4-phenyl-2-oxazolidinone		P-CAP P-CAP-DP DEABV DPEVB	3.08	1.14	1.5	20%/0.5%	4800
42	5-Phenyl-2-(2-propynylamino)-2-oxazolin-4-one		P-CAP P-CAP-DP DEABV DPEVB	4.52 4.73 3.15	1.06 1.08 1.25	0.7 0.7 1.5	15%/0.2% 15%/0.2% 35%E/0.2%	4000 2400 1700
43	Bendroflumethiazide		P-CAP P-CAP-DP DEABV DPEVB	8.91 3.90	1.11 1.31	0.8 1.3	40%/0.2% 35%/0.2%	1200 800
44	Benzylphthalide		P-CAP P-CAP-DP DEABV DPEVB	3.94	1.05	0.7	20%/0.2%	5100

Table 7.1 – Continued

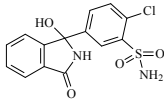
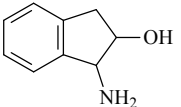
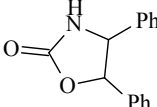
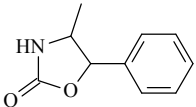
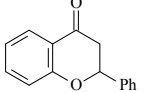
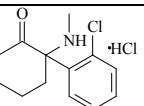
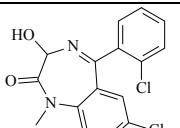
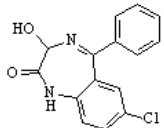
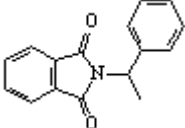
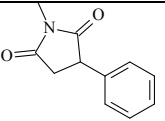
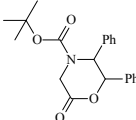
45	Chlorthalidone		P-CAP P-CAP-DP DEABV DPEVB	7.08 4.38 3.79 5.27	1.21 1.09 1.09 1.07	1.5 0.4 0.5 0.6	40%/0.2% 40%/0.2% 40%/0.2% 30%/0.2%	1600 600 1100 2000
46	<i>cis</i> -1-Amino-2-indanol		P-CAP P-CAP-DP DEABV DPEVB	6.38	1.10	1.3	20%/0.2%	4400
47	<i>cis</i> -4,5-Diphenyl-2-oxazolidinone		P-CAP P-CAP-DP DEABV DPEVB	7.43 4.51 3.66	1.06 1.06 1.21	1.0 0.9 1.6	10%/0.2% 15%/0.2% 30%/0.2%	6700 6600 2400
48	<i>cis</i> -4-Methyl-5-phenyl-2-oxazolidinone		P-CAP P-CAP-DP DEABV DPEVB	4.15 4.94 3.76	1.07 1.08 1.16	0.9 1.0 1.5	15%E/0.2% 10%/0.2% 25%E/0.2%	5100 4600 3300
49	Flavanone		P-CAP P-CAP-DP DEABV DPEVB	5.11	1.31	0.4	10%/0.2%	100
50	Ketamine (hydrochloride)		P-CAP P-CAP-DP DEABV DPEVB	5.79	1.05	0.5	10%/0.2%	2300
51	Lormetazepam		P-CAP P-CAP-DP DEABV DPEVB	4.79 3.00	1.15 1.31	2.0 1.8	15%/0.2% 40%/0.2%	5800 1800
52	Oxazepam		P-CAP P-CAP-DP DEABV DPEVB	3.43 3.18 3.62 3.32	1.37 1.36 1.34 1.08	2.2 2.5 1.0 0.5	40%/0.2% 40%/0.2% 40%/0.2% 30%/0.2%	1800 2600 400 1400
53	N-(α -Methylbenzyl)-phthalimide		P-CAP P-CAP-DP DEABV DPEVB	4.48	1.02	0.3	10%/0.2%	4600
54	Phensuximide		P-CAP P-CAP-DP DEABV DPEVB	6.25	1.11	1.5	1%/0.2%	4700
55	<i>t</i> -Butyl-6-oxo-2,3-diphenyl-4-morpholine carboxylate		P-CAP P-CAP-DP DEABV DPEVB	3.66 4.85	1.04 1.16	0.3 1.5	5%/0.2% 5%E/0.2%	1700 3000

Table 7.1 – Continued

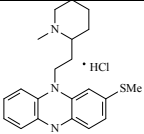
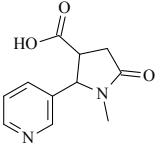
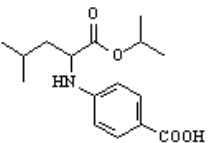
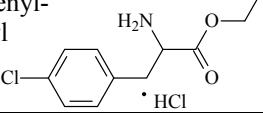
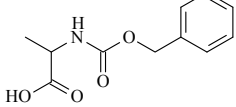
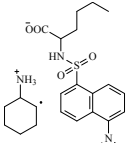
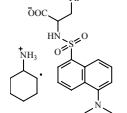
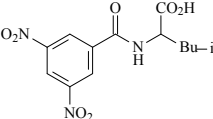
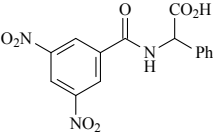
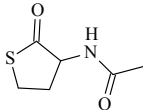
56	Thioridazine 	P-CAP P-CAP-DP DEABV DPEVB	3.9	1.09	0.4	15%/0.2%	700
57	<i>trans</i> -4-Cotinine-carboxylic acid 	P-CAP P-CAP-DP DEABV DPEVB	5.25 4.27	1.06 1.02	0.6 0.3	10%/0.2% 20%/0.2%	2800 4300
Chiral acids and amino-acid derivatives							
58	4-((1-(Isopropoxycarbonyl-4-methyl)-butyl)-amino)-benzoic acid 	P-CAP P-CAP-DP DEABV DPEVB	2.64 2.22 3.46	1.28 1.93 1.21	1.6 4.0 1.6	10%/0.2% 30%/0.2% 10%/0.2%	1800 2200 2500
59	4-Chlorophenyl-alanine ethyl ester 	P-CAP P-CAP-DP DEABV DPEVB	4.08	1.10	0.7	15%/0.2%	1700
60	Carbobenzyloxy-alanine 	P-CAP P-CAP-DP DEABV DPEVB	4.44 3.68 2.79	1.07 1.06 1.21	0.9 0.7 1.5	15%E/0.2% 10%/0.2% 20%/0.2%	5300 5100 2500
61	Dansyl-norleucine cyclohexylammonium salt 	P-CAP P-CAP-DP DEABV DPEVB	4.08 3.96	1.08 1.16	1.0 1.4	30%/0.2% 30%/0.2%	5600 2900
62	Dansyl-phenylalanine cyclohexylammonium salt 	P-CAP P-CAP-DP DEABV DPEVB	3.81 3.90	1.09 1.29	0.5 1.7	30%/0.2% 40%/0.2%	1000 1400
63	N-(3,5-Dinitro-benzoyl)-leucine 	P-CAP P-CAP-DP DEABV DPEVB	7.17 2.35 1.97 3.74	1.04 1.30 3.14 1.10	0.4 1.6 4.5 1.2	15%/0.2% 20%/0.2% 40%/0.2% 20%/0.2%	2600 1900 1200 4400
64	N-(3,5-Dinitro-benzoyl)-phenyl glycine 	P-CAP P-CAP-DP DEABV DPEVB	3.75 3.94 3.70	1.19 1.23 1.58	1.4 1.8 2.7	30%/0.2% 20%/0.2% 40%/0.2%	3100 2400 1300
65	N-Acetylhomocysteine thiolactone 	P-CAP P-CAP-DP DEABV DPEVB	7.36 4.73 3.55	1.06 1.11 1.06	0.9 1.3 0.7	5%/0.2% 10%/0.2% 20%/0.2%	5600 4600 4700

Table 7.1 – Continued

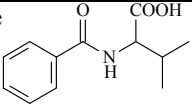
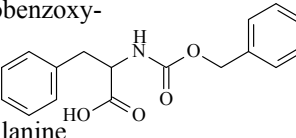
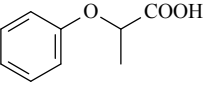
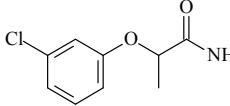
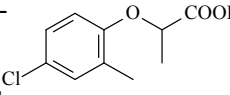
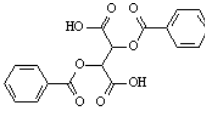
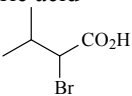
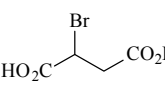
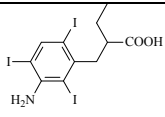
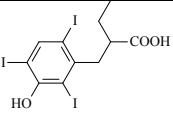
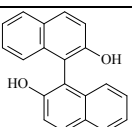
66	N-Benzoyl-valine 	P-CAP P-CAP-DP DEABV DPEVB	4.85 3.58	1.11 1.07	1.3 0.7	15%E/0.2% 10%/0.2%	4200 3800
67	N-carbobenzoxy- Phenylalanine 	P-CAP P-CAP-DP DEABV DPEVB	5.13 4.38 2.04	1.04 1.09 1.35	0.5 0.9 1.5	15%/0.2% 15%E/0.2% 40%/0.2%	4300 3000 1600
68	2-Phenoxy propionic acid 	P-CAP P-CAP-DP DEABV DPEVB	3.49	1.03	0.4	10%/0.2%	5100
69	2-(3-Chloro- phenoxy) propionamide 	P-CAP P-CAP-DP DEABV DPEVB	6.73	1.06	0.9	5%/0.2%	5300
70	2-(4-Chloro-2- methyl- phenoxy) propionic acid 	P-CAP P-CAP-DP DEABV DPEVB	4.81	1.09	1.1	5%E/0.2%	4700
71	2,3-Dibenzoyl- tartaric acid 	P-CAP P-CAP-DP DEABV DPEVB	3.80 4.61	1.15 1.03	1.3 0.3	30%/0.2% 20%/0.2%	2700 2200
72	2-Bromo-3-methylbutyric acid 	P-CAP P-CAP-DP DEABV DPEVB	4.02	1.08	0.9	5%/0.2%	4400
73	Bromosuccinic acid 	P-CAP P-CAP-DP DEABV DPEVB	5.15 5.90	1.05 1.11	0.6 1.5	20%/0.2% 10%/0.2%	3100 5100
74	Iopanoic acid 	P-CAP P-CAP-DP DEABV DPEVB	6.02	1.13	1.0	30%/0.2%	1600
75	Iophenoxic acid 	P-CAP P-CAP-DP DEABV DPEVB	5.75	1.12	0.7	30%/0.2%	1000
Atropoisomerism and miscellaneous chemical functionalities on the asymmetric center							
76	1,1'-Bi-2-naphthol 	P-CAP P-CAP-DP DEABV DPEVB	4.17 7.96	1.32 1.04	2.7 0.3	40%/0.2% 30%/0.2%	3100 1500

Table 7.1 – Continued

77	1,1'-Bi-2-naphthol bis(trifluoromethane sulfonate) 	P-CAP P-CAP-DP DEABV DPEVB	5.18	1.08	0.9	5%E/0.2%	3200
78	2,2'-Diamino-1,1'-binaphthalene 	P-CAP P-CAP-DP DEABV DPEVB	6.54	1.08	0.8	20%/0.2%	2800
79	6-(4-Chlorophenyl)-4,5-dihydro-2-hydroxybutyl)-3-(2H)-pyridazinone 	P-CAP P-CAP-DP DEABV DPEVB	6.65 11.6	1.22 1.06	2.4 1.0	10% I/0.2% 5%/0.2%	3800 6800
80	7-(2,3-Dihydroxypropyl)theophylline 	P-CAP P-CAP-DP DEABV DPEVB	6.08	1.03	0.4	10%/0.2%	3900
81	Triadimenol (Baytan) 	P-CAP P-CAP-DP DEABV DPEVB	3.94	1.20	1.6	10% I/0.2%	2500
82	N,N'-Dibenzyltartramide 	P-CAP P-CAP-DP DEABV DPEVB	2.60 3.44 2.73	1.46 1.45 1.36	2.5 2.2 1.5	30%/0.2% 20%/0.2% 40%/0.2%	2100 1300 1100
83	2-Amino-3-phenyl-1-propanol 	P-CAP P-CAP-DP DEABV DPEVB	4.61 2.90	1.09 1.07	1.3 0.4	15%/0.2% 20%/0.2%	6000 1400
84	Propranolol 	P-CAP P-CAP-DP DEABV DPEVB	7.12	1.10	0.4	20%/0.2%	400
85	3-(4-Nitrophenyl)glycidol 	P-CAP P-CAP-DP DEABV DPEVB	9.4	1.07	0.9	5%E/0.2%	4200
86	Crufomate (Ruelene) 	P-CAP P-CAP-DP DEABV DPEVB	3.27 5.72	1.06 1.14	0.5 1.7	5%/0.2% 5%E/0.2%	2700 4300

The additive is methanol (M) unless otherwise indicated: E = ethanol, I = isopropyl alcohol. The TFA percentage is added to the alcohol modifier. The plate number is the average value for the two enantiomer peaks (accuracy 20%).

CSP.⁸¹ The data in Figure 7.3 does not indicate that there is such a profound structural selectivity difference between the polymer CSPs. The 43 compounds that are enantioseparated by a single CSP are more randomly spread among the four structural classes of compounds.

However, a closer look at solute structure and CSP enantioselectivity allows one to find some structural selectivity. More specifically, the 9 oxazolidinone derivatives (Compounds **26**, **35**, **36**, **37**, **38**, **41**, **42**, **47** and **48**) with an asymmetric carbon in position 4 are all baseline separated on the DEABV CSP. Four of these compounds (**36**, **37**, **38** and **41**) are separated only on the DEABV CSP (Table 7.1). For the 5 oxazolidinone that are separated on several CSPs, the resolution factor obtained with the DEABV CSP is the highest. Clearly, there is an interaction between the oxazolidinone ring and the DEABV CSP that is very sensitive to substitution on the ring's 4-carbon.

Some general trends that have been observed with other CSPs also were observed with the polymeric CSPs studied here. First, it was observed that compounds having four very different substituents on the stereogenic center are well differentiated by many CSPs.⁸² For example, the enantiomers of Warfarin (**23**), with a hydrogen atom, a phenyl group, an acetyl group and a huge hydroxycoumarinyl group on its asymmetric center are differentiated by all four CSPs in this study. Also, it was observed that a minor change in the molecular structure of a chiral analyte can produce a dramatic change in enantioselectivity.⁸² For example, compounds **39** and **40** differ only in the position of their hydroxyl group (changing from the meta to para position). **39** is separated by the P-CAP-CSP only and **40** is separated by the P-CAP-DP CSP only (Table 7.1). Such a change in enantiomeric recognition is observed only if the minor structural change occurs on an "enantiosensitive" part of the molecule. Considering Coumachlor (**22**) and Warfarin (**23**), they differ only by a chlorine atom, but both are equally well separated by all four CSPs indicating that the chlorine atom is not located in a part of the molecule involved in any enantioselective interactions. A similar observation can be made with Benzoin (**9**) and Hydrobenzoin (**14**) whose enantiomers are equally well separated by three polymeric CSPs (Table 7.1).

7.4.3 Chiral stationary Phases and Chemical Interactions

Figure 7.1a shows that the P-CAP monomer does not contain any aromatic moieties. Consequently, π - π interactions cannot be important in the chiral recognition mechanism of this CSP. The P-CAP polymeric

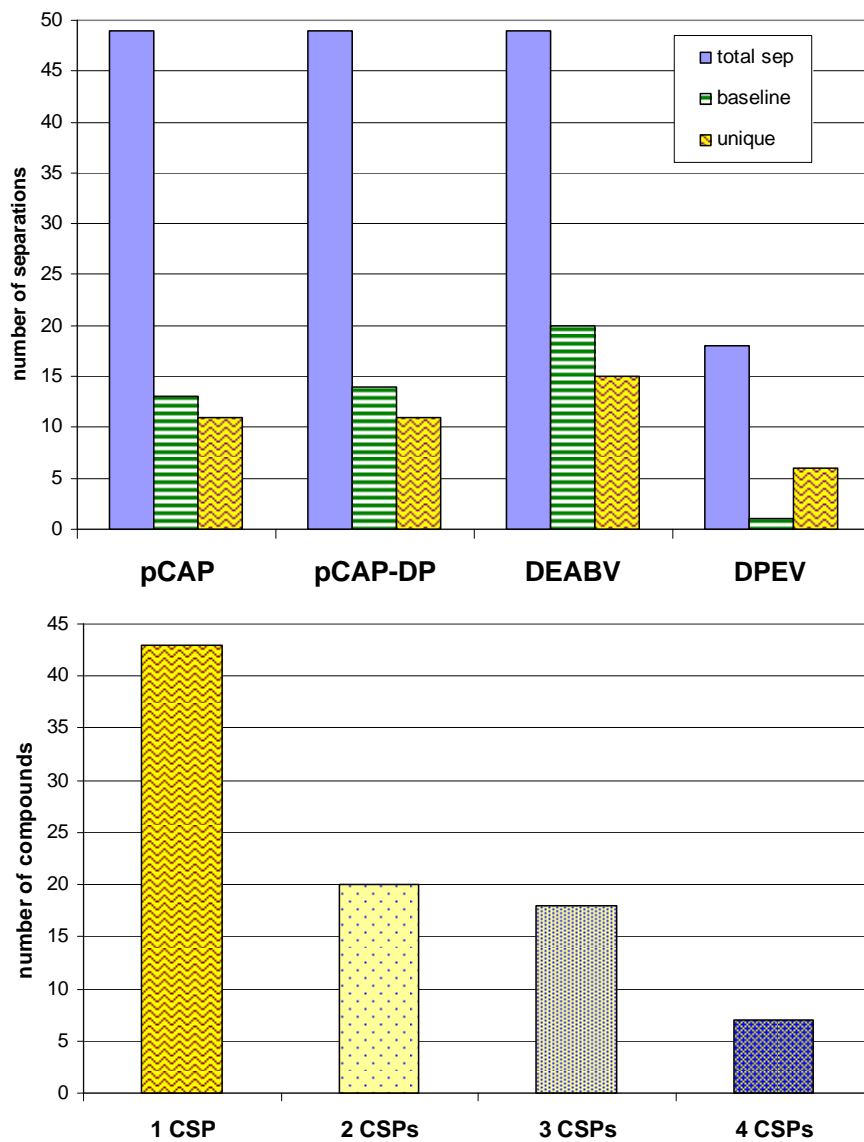


Figure 7.2 Overall results obtained with the four synthetic polymeric chiral stationary phases in subcritical mode. Top diagram: number of separations obtained on each CSPs. Bottom diagram: the number of compounds that were separated only by one single CSP or 2 or 3 or all 4 CSPs. The percentages refer to the number of compounds from the 88 compound set shown in Compound Structure and Polymer CSP Enantio-recognition

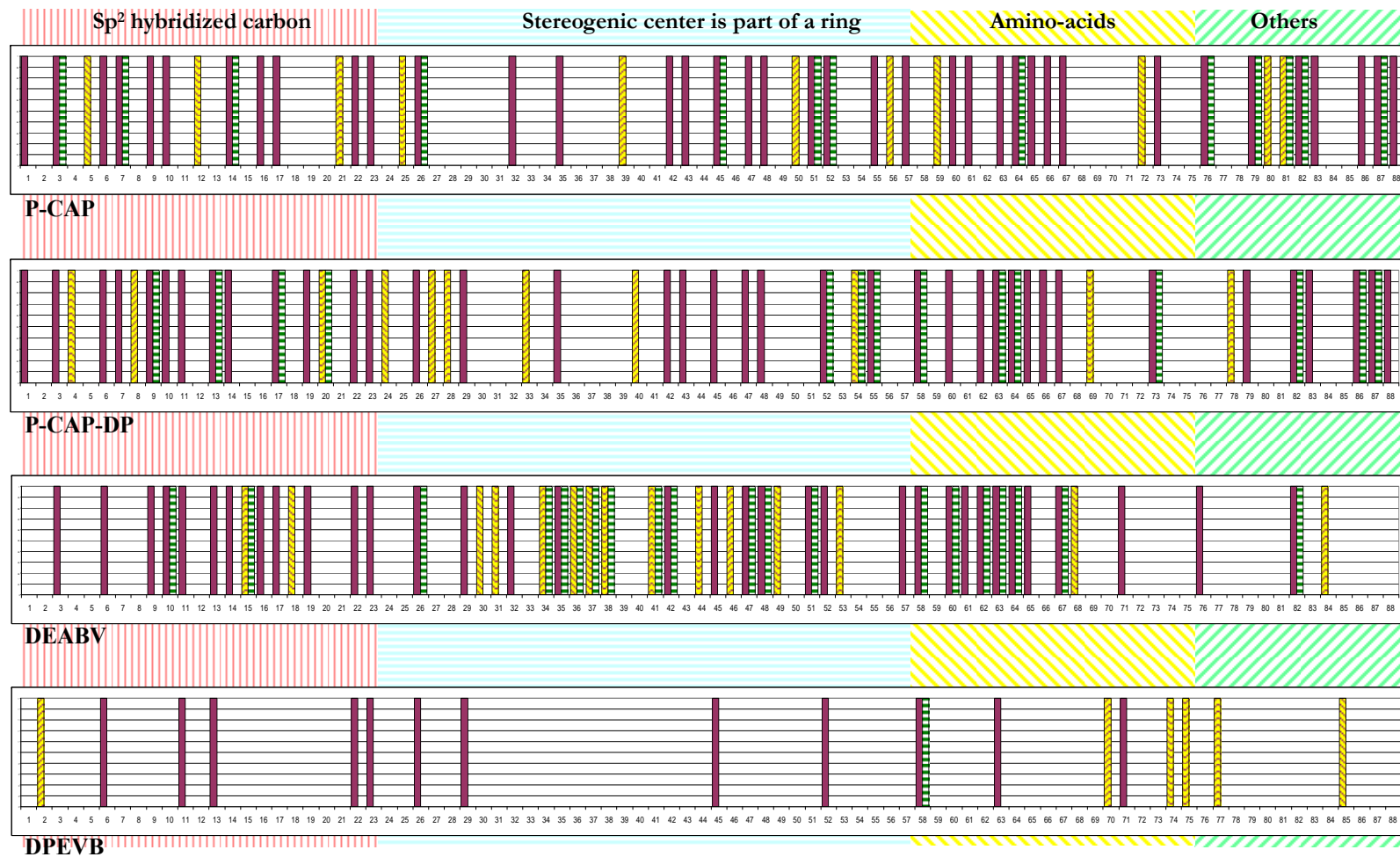


Figure 7.3 Overview of the results obtained on the four polymeric CSPs with the 88 chiral compounds evaluated in subcritical mode with CO₂/methanol/trifluoroacetic acid mobile phases, see Table 1 for full details. A solid dark vertical bar over the compound number indicates an observable separation ($R_s > 0.3$). A vertical bar with horizontal stripes doubling a bar indicates a baseline separation ($R_s > 1.4$) and a light vertical bar with wave lines indicates that the compound was only separated on that particular CSP.

CSP has a large number of amide linkages providing a wealth of sites for hydrogen bonding and dipolar interactions.^{67d} The three other CSPs do have several aromatic rings in their structures (Figure 7.1b, c, and d) along with amide linkages. They should be able to combine π - π interactions with other types of interactions for chiral recognition.⁸²

Figure 7.4 shows the separation of Compounds **63** (left) and **64** (right), respectively DNB-leucine and DNB-phenylglycine, on the three CSPs, P-CAP, P-CAP-DP and DEABV. π - π interactions are likely in the case of the DNB-leucine (**63**, Figure 7.4-left). The DNB derivative is a strongly π -acid substituent on the amine group of leucine. The two enantiomeric forms of DNB-leucine are well ($R_s = 1.6$) and extremely well ($R_s = 4.7$) separated by the π - π capable P-CAP-DP and DEABV CSPs, respectively. They are poorly separated by the P-CAP CSP which is unable to interact through π - π interactions (Figure 7.4-left).

However, the P-CAP CSP separates well ($R_s = 1.4$) the structurally related DNB-phenylglycine (Figure 7.4-right). This compound (**64**) is equally or better separated by the two other CSPs as shown. In this case, the dipolar interactions with the DNB amide group and/or the H-bond interactions with the carboxylic acid moiety are more important than the π - π interactions for enantioselective recognition of DNB-phenylglycine.

The results obtained with atropoisomers suggest that π - π interactions play little or no role in their enantioseparation. Indeed, the highest enantioselectivity factor of all atropoisomers is obtained with 1,1'-binaphthol (**76**) on the P-CAP CSP (no π - π interactions). All other three CSPs are able to separate partially ($R_s < 0.9$) the binaphthalene atropoisomers **76**, **77** and **78** (Table 7.1). However, the exact nature of the enantioselective interactions has not been identified.

7.4.4 Normal Phase LC versus SFC

The synthetic polymeric CSPs were shown to be highly efficient in normal phase liquid chromatography using heptane-alcohol, halogenated solvent or waterless acetonitrile-methanol mobile phases. The later mobile phase is used in the special mode called polar organic mode^{67c, d, 78} Most of the compounds whose enantiomers were successfully separated with a given polymeric phase in the normal or polar organic mode also produced successful enantioseparations with subcritical CO₂ + MeOH mobile phases.

The separations of N-(α -methylbenzyl) phthalic acid monoamide (**16**) and Furoin (**13**) respectively on the DEABV and P-CAP-DP CSPs will be used to illustrate the difference that can be observed between the

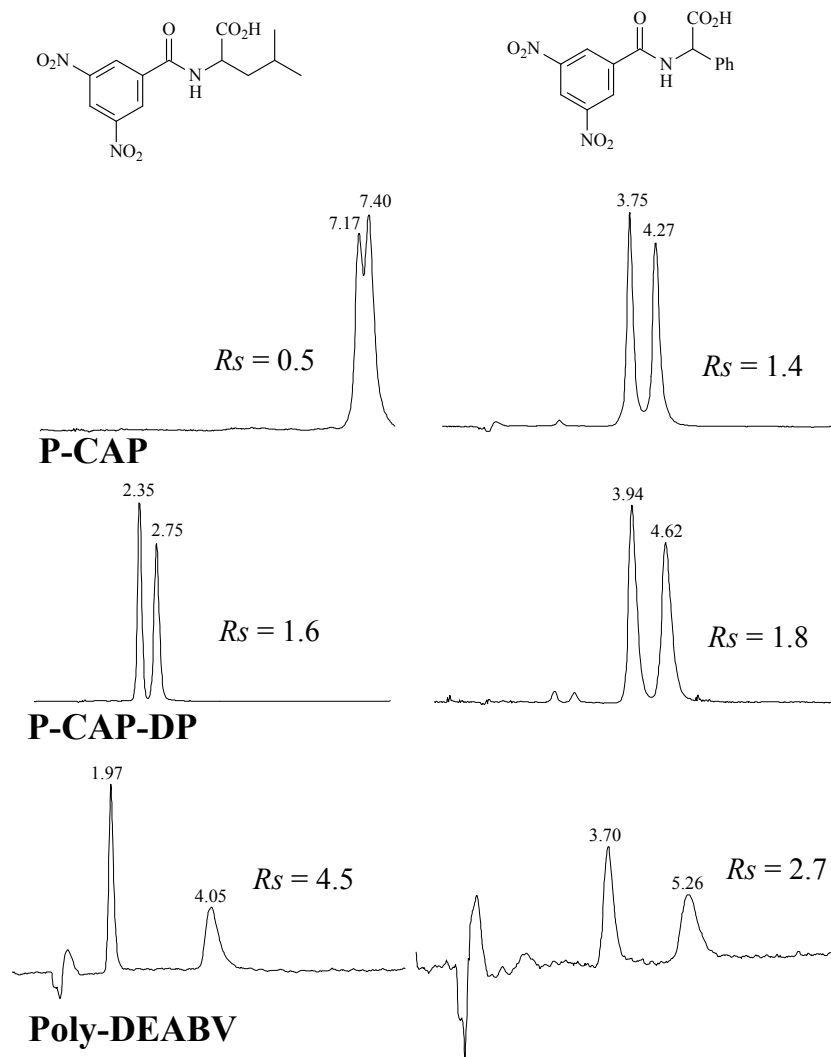


Figure 7.4 Enantioseparation of DNB-leucine (3 left chromatograms) and DNB-phenylglycine (3 right chromatograms) on the indicated polymeric chiral stationary phases. Column 250 x 4.6 mm with 5 μ m silica particles bonded by the indicated selector, subcritical mobile phase with CO₂ + methanol (+ 0.2% v/v TFA) (proportion in Table 1, Compounds **63** and **64**), 100 bar, 4 ml/min, 31°C, UV detection 254 nm.

normal phase mode and the subcritical fluid mode. The two enantiomers of **16** are partially separated ($\alpha = 1.13$, $R_s = 1.2$, Figure 7.5A) in the normal phase mode with an heptane/MeOH mobile phase in more than 12 min. They are separated with a similar enantioselectivity factors in less than 8 min in SFC with a CO₂/MeOH 75/25% v/v mobile phase (Figure 7.5B). Raising the amount of methanol to 30% halves the separation duration without losing any enantioresolution (Figure 7.5C). The two enantiomers of Furoin are very well separated ($\alpha = 1.69$, $R_s = 3.7$, Figure 7.5D) in the normal phase mode with a heptane-IPA mobile phase in about 32 min. Table 7.1 and Figure 7.5E shows the separation obtained with a SFC mobile phase, also baseline and obtained in less than 3 min. Better resolution factors were obtained in the normal phase mode compared to the Table 7.1 results in SFC for many compounds. It is recalled that the SFC separations were not optimized and all R_s -factors listed in Table 7.1 could likely be increased. However, the solute retention times were always significantly lower in the SFC mode than in both the normal phase and polar organic modes of classical liquid chromatography.

7.4.5 Kinetic Considerations

Table 7.1 lists the average plate number measured for the observed enantioseparated peaks. A huge plate count variation, with efficiencies that could be as low as 500 plates for a 25 cm column (h_{etp} = 5000 μ m or 1000 particle diameters) or reach 9000 plates (h_{etp} = 270 μ m or 50 particle diameters), could be observed on the four CSPs studied. Of course, a low efficiency is not favorable for an acceptable resolution factor as illustrated by Figure 7.6. The enantiomers of **27** are separated with a measured plate number of about 7000 plates and an enantioselectivity factor of 1.08 producing an almost baseline resolution factor ($R_s = 1.3$). With the same retention times and selectivity factor, the enantiomers of Chlorthalidone (Compound **45**) are separated with a low resolution factor of 0.4 because the observed efficiency is very low (600 plates) for this compound (Figure 7.6, bottom).

The observed efficiency is a measure of the kinetics of the solute exchange between the mobile phase and the stationary phase. This parameter is difficult to predict. It is known that strong interactions between a solute and the stationary phase may be linked to a slow adsorption-desorption process being associated with a low efficiency. In the case illustrated by Figure 7.6, Chlorthalidone has a plethora of functionality including a sulfamide group, an amide, an alcohol, a chlorinated phenyl and another aromatic ring. These

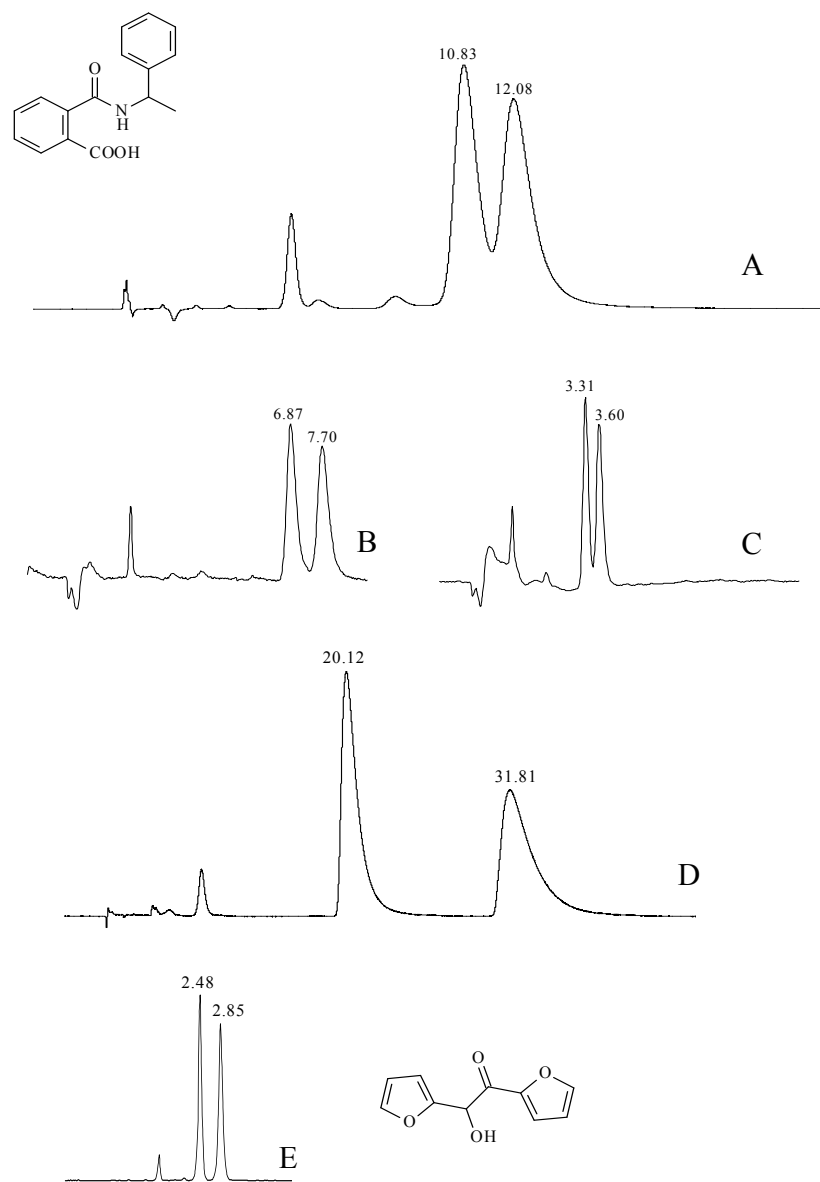


Figure 7.5 Separation of the enantiomers of N-(α -methylbenzyl) phthalic acid monoamide (**16**) on the DEABV CSP. Chromatogram **A**: normal phase heptane/EtOH 70%/30% (+0.1% v/v TFA), 1 ml/min, $\alpha = 1.13$, $R_s = 1.2$; Chromatogram **B**: SFC CO₂/MeOH 75/25% v/v (+0.2% v/v TFA), 100 bar, 4 ml/min, 31°C, $\alpha = 1.14$, $R_s = 1.4$; Chromatogram **C**: SFC CO₂/MeOH 70/30% v/v (+0.2% v/v TFA), 100 bar, 4 ml/min, 31°C, $\alpha = 1.12$, $R_s = 1.3$. Separation of the enantiomers of Furoin (**13**) on the polymeric P-CAP-DP CSP. Chromatogram **D**: normal phase mode, mobile phase heptane/IPA 80/20 %v/v (with 0.1% TFA), 1 ml/min, $\alpha = 1.69$, $R_s = 3.7$; Chromatogram **E**: SFC CO₂/MeOH 90/10% v/v (+0.2% v/v TFA), 100 bar, 4 ml/min, 31°C, $\alpha = 1.25$, $R_s = 2.0$, detection UV 254 nm.

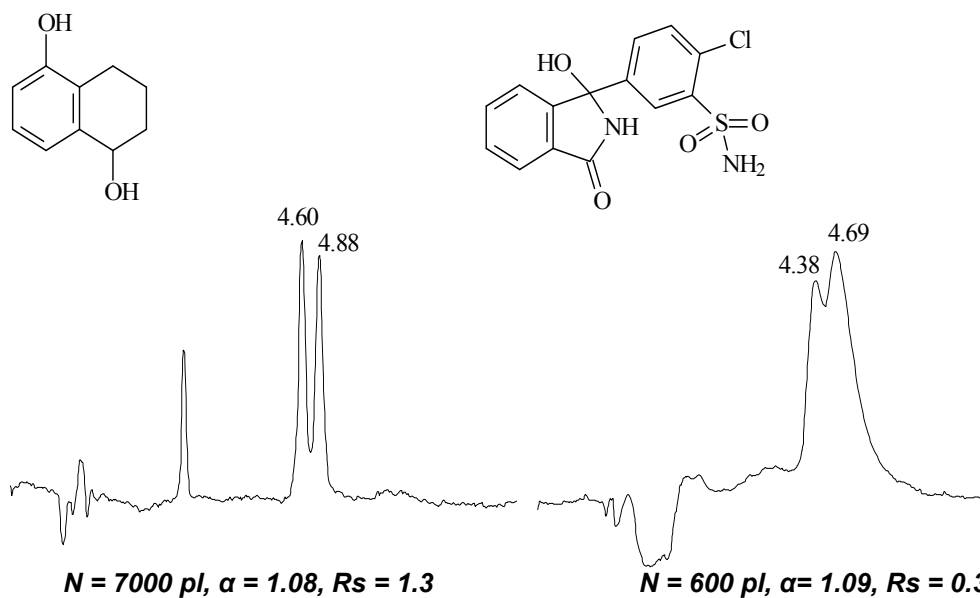


Figure 7.6 Efficiency variations on the P-CAP-DP chiral stationary phase. Left chromatogram: separation of the enantiomers of 1,5-dihydroxy-1,2,3,4-tetrahydronaphthalene (**28**), mobile phase, CO₂ + 15% v/v (MeOH + 0.2% v/v TFA); right chromatogram: enantioseparation of Chlorthalidone (**45**), mobile phase, CO₂ + 40% v/v (MeOH + 0.2% v/v TFA). Total flow rate 4 mL/min, 31°C, 100 bar, UV detection 254 nm.

numerous functionalities are subject to a variety of different interactions with the polymeric P-CAP-DP stationary phase. At least one of these possible interactions is slow, producing the observed poor peak shape. Compound **28** has less functionalities (phenol and alcohol). It interacts rapidly with the CSP producing sharper peaks. The kinetics of a particular solute-stationary phase interaction can be completely independent of the solute's chiral recognition interactions. In some cases, a strong interaction with slow adsorption/desorption kinetic may be critical for enantioselectivity. In other cases, the strong interaction may play no role.⁸¹

The observed peak efficiency of a particular solute separated on a given CSP is very dependent on the experimental conditions. The nature of the alcohol modifier used is especially important. However quantitative comparison is difficult because most often the retention times and enantioselectivity factors are also changed when the organic modifier is changed. As a general trend, ethanol produced better efficiencies than methanol and isopropyl alcohol. The TFA additive has also a critical influence on efficiencies since it reduces the strong (and slow) charge-charge interactions that occur with acidic analytes.

7.5 Conclusions

The new synthetic polymeric P-CAP, P-CAP-DP, DEABV and DPEVB CSPs are all capable of producing effective enantioseparations with supercritical fluid mobile phases. The DPEVB CSP is significantly less successful than the three other CSPs in separating a large number of compounds with a variety of functionalities. The DEABV CSP seems to be the most broadly applicable and useful of these CSPs. The biggest advantage of the SFC mobile phase is the short separation times observed compared to those in the normal phase mode. Retention times lower than 5 min, with 25 cm columns, were obtained for 90% of the separations presented in this work. The second advantage of SFC mobile phases is the easy recovery of the separated solutes. There is no hindrance to injecting large amounts of sample on these columns and maintaining the enantiomeric separations as was demonstrated in the normal phase mode,^{67c, d, 78} however the SFC loading capability was not evaluated in this study.

7.6 Acknowledgements

The support of this work by the National Institute of Health, NIH RO1 GM53825-11 is gratefully acknowledged.

CHAPTER 8

STUDY OF COMPLEXATION BETWEEN CYCLOFRUCTANS AND ALKALI METAL CATIONS BY ELECTROSPRAY IONIZATION MASS SPECTROMETRY AND DENSITY FUNCTIONAL THEORY CALCULATIONS

8.1 Abstract

Cyclofructans, cyclic fructofuranose oligomers, form complexes with a variety of metal cations in solution. ESI-MS was used to investigate both solution and gas phase selectivities of cyclofructans for alkali metal cations. In the gas phase, cyclofructans bind to alkali metal cations in the order of $\text{Li}^+ > \text{Na}^+ > \text{K}^+ > \text{Rb}^+ > \text{Cs}^+$. The gas phase selectivity, obtained by competitive dissociation of ternary complexes between one cyclofructan and two different metal cations, was confirmed with density functional theory calculations. The calculated binding strength is from -99 to -383 kJ mol^{-1} for cyclofructan 6 and the alkali metal cations. The cyclofructan's 3-position oxygens are the most likely interaction points for the alkali metals. Surprisingly, the crown ether oxygens are barely involved in the complexation process. For the solution phase study, sodium and potassium complexes of cyclofructans were the most abundant species in the ESI-MS spectra. Compared with previous solution phase studies of cyclofructans, ESI-MS produced higher abundance of complexes with Li^+ and lower abundance of complexes with larger metal cations. The relative intensities of different cyclofructan-metal cation complexes observed in the ESI-MS spectra was a reflection of both the solution phase and gas phase stability of different complex ions. Chunlei Wang, Samuel H. Yang, Jianguang Wang, Peter Kroll, Kevin A Schug, Daniel W Armstrong. Submitted to International Journal of Mass Spectrometry. Unpublished work Copyright © 2009 with permission from Elsevier.

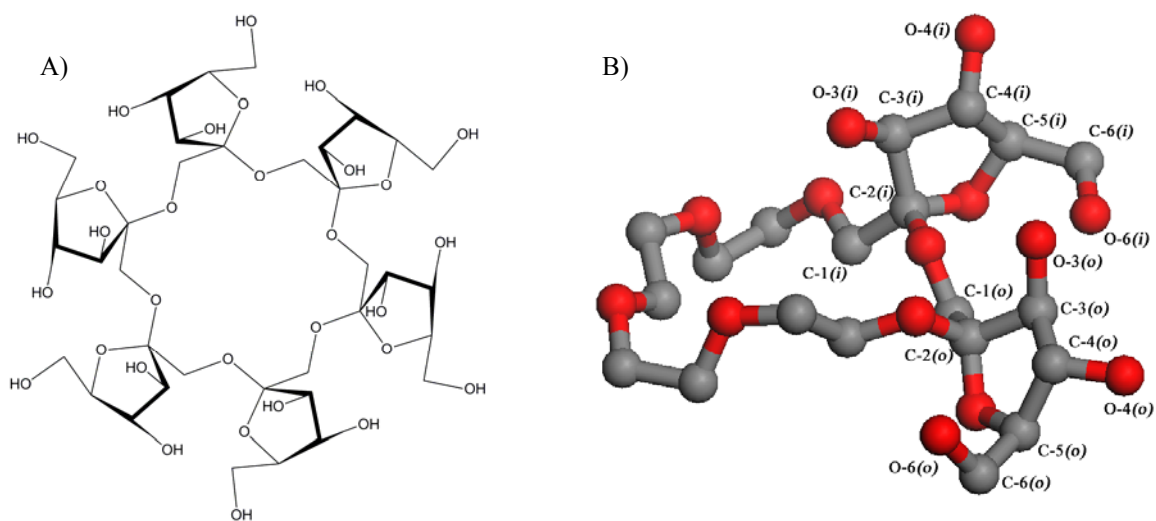
8.2 Introduction

Cyclofructans are β -(2 \rightarrow 1)-linked cyclic fructofuranose oligomers that have unique crown ether cores (see Figure 8.1).^{60g, 83} Native and derivatized cyclofructans have been found to complex with a variety of metal

cations,^{60c, 84} and have been used as ion trapping agents in various applications.⁸⁵ The X-ray structure of permethylated cyclofructan 6 (CF6) and barium isothiocyanate,^{84d} along with NMR studies,^{84b, 84d} revealed that the crown ether moiety in permethylated CF6 did not participate directly in metal complexation as did other synthetic crown ether analogues. However, the selectivities of permethylated cyclofructans for alkali metals are found to be identical to their counterpart crown ethers: i.e., permethylated CF6 binds to alkali metals in the decreasing order of $K^+ > Rb^+ > Cs^+ > Na^+ > Li^+$.^{84b, 84d} Surprisingly, there are only limited host-guest studies for native cyclofructans.^{84a, 84c, f}

ESI-MS has been widely used for host-guest studies of many crown ethers and their related analogues in solution and in the gas phase.⁸⁶ The Brodbelt group has extensively studied the selectivity of crown ether type hosts for different metal cations with known stability constants in solution using ESI-MS.^{86b} Generally, the selectivity of a host for different guests, predicted from ion intensity in the mass spectrum, correlated well with that in solution. On the other hand, the Liu group reported that corrections for ionization efficiency of different complex ions were necessary when studying the alkali metal complexes of a series of lariat ethers.⁸⁷ ESI-MS also has been used to study complexation between oligosaccharides and alkali metal cations. Reale et al. studied the metal complexation of β -cyclodextrin (β -CD), an isomer of cyclofructan 7 (CF7).⁸⁸ With competitive binding ESI-MS experiments, they found that sodium, among the alkali metals, had the highest affinity for β -CD in solution.⁸⁸ Both 1:1 and 1:2 β -CD-metal cation complexes were observed in the ESI-MS spectra. Shizuma et al. studied the complexation between permethylated cyclofructans with alkali metal cations using ESI-MS along with other approaches.^{84b} According to their results, relative peak intensities in ESI mass spectra were not always a true reflection of the distribution of species in the solution. Surprisingly, there is no reported ESI-MS study of complexation by native cyclofructans.

In this paper, we study the complexation of native cyclofructans with alkali metal cations using ESI-MS, and compare the solution phase selectivity deduced from ESI-MS spectra with previous results from a thin layer chromatography study.^{84c} In addition, the gas phase selectivity of cyclofructans for alkali metal cations is studied using both the competitive dissociation method and density functional theory calculations.



8.3 Experimental

8.3.1 Materials

All chloride salts of alkali metal cations were purchased from Sigma-Aldrich (Milwaukee, WI, USA). LC-MS grade methanol and water were purchased from VWR (Bridgeport, NJ, USA). Cyclofructans were generous gifts from Mitsubishi Kagaku Co. (Tokyo, Japan): CF6 was used as received whereas CF7 was purified before use according to a previously published method.⁸⁹

8.3.2 Methods

All mass spectrometry experiments were performed with a Thermo Finnigan LXQ mass spectrometer equipped with a syringe pump, an ESI source and a linear ion trap mass analyzer. The syringe pump flow rate was set at 5.0 $\mu\text{l}/\text{min}$. Compound mixtures were sprayed in 50% aqueous methanol solution at a source voltage of 3.5 kV. The vacuum chamber was operated at a pressure of 1 mTorr with helium. Each spectrum was sampled for 1 min (~ 300 scans). Triplicate spectra were averaged for each experimental data point. The collisional induced dissociation study was carried out with 30 ms activation time, a 0.25 Q value, and the normalized collisional energy between 5% and 30% for different species. Density functional theory calculations were computed using Gaussian 03 program.^{38b}

8.4 Results and Discussion

Figure 8.1A shows the molecular structure of CF6. The 18-crown-6 ring serves as the skeleton as core of CF6, with six fructofuranose units attached on its rim. The fructofuranose units are alternatively pointing towards and away from the molecular center, which are described as “inward-inclined” and “outward-inclined” by Immel et al., respectively.⁹⁰ These two types of fructofuranose units are depicted in Figure 8.1B. The numberings of C and O atoms on the fructofuranose units are also labeled in Figure 8.1B.

The complexes between cyclofructans and metal cations are sufficiently stable to be observed directly by ESI-MS. Figure 8.2 shows the mass spectrum of 1×10^{-4} M CF6 and equimolar NaCl in 50% aqueous methanol solution. The m/z 995 and m/z 509 peaks correspond to the 1:1 and 1:2 complexes between CF6 and Na^+ . Minor peaks at m/z 1011 ($\text{CF}_6 + \text{K}^+$) and m/z 506 ($\text{CF}_6 + \text{K} - \text{H}^+$) were also observable due to trace amounts of potassium present in the MS system. In order to establish the solution concentration for our study, the dependence of the signal intensity (characterized by the peak area of all isotope peaks) on the

solution concentration was examined over the range from 1×10^{-8} M to 3×10^{-4} M. As shown in Figure 8.3, a linear response was observed for the studied range of concentrations ($R^2 = 0.9841$ for the fitted linear line passing the origin point). The linear range is comparable to the reported range for crown ethers.⁹¹ As a result, a working concentration of 1×10^{-4} M was chosen for our study.

8.4.1 Complexation Ratio

Crown ethers form stable complexes with metal cations. Both 2:1 and 1:1 crown ether-metal complexes have been observed by mass spectrometry.⁹² However, crown ethers do not typically complex with multiple metal cations, with an exception of a few bis-crowned hosts.⁹³ In our study, a substantial abundance of 1:2 cyclofructan-metal cation complexes was observed for small alkali metals even at a solution host-to-guest concentration ratio of 1:1 (Figure 8.2). Cyclofructans have a crown ether macrocycle as the core/skeleton. The formation of 1:2 cyclofructan-metal cation complexes implies that at least one other structured feature of cyclofructan is responsible for its complexation with metal cations, if the crown ether moiety is even responsible at all.

Table 8.1 lists the relative intensities observed for 1:1 and 1:2 cyclofructan-metal cation complexes. The 1:2 complexes were observed for Li^+ and Na^+ with CF6, and for Li^+ , Na^+ , and K^+ with CF7. Clearly, the extent of 1:2 complex formation depends on the sizes of the hosts and guests. The larger CF7 is able to complex with two larger metal cations (i.e., K^+). For the same alkali metal cation, the relative intensities of 1:2 complexes, compared to 1:1 complexes, is always higher for CF7 versus CF6.

For both CF6 and CF7 hosts, Na^+ has the highest tendency among the alkali metals to form 1:2 rather than 1:1 host-guest complexes. β -cyclodextrins, which are isomers of CF7, also have the capability to complex with 2 Li^+ or 2 Na^+ .⁸⁸ Unlike CF7, $(\beta\text{-CD} + 2\text{Li})^{2+}$ has a higher relative intensity (to its 1:1 complexes) than that of $(\beta\text{-CD} + 2\text{Na})^{2+}$ (Figure 8.4) and $\beta\text{-CD}$ does not form 1:2 complexes with K^+ .

8.4.2 Solution Phase Selectivity

Figure 8.5 shows the mass spectrum of an equimolar solution of cyclofructan and every alkali metal chloride salts in 50% aqueous methanol solvent. The relative intensities of these cyclofructan-alkali metal cation peaks (based on the peak area of all isotopic peaks) are listed in Table 8.2.

Uchiyama et al. studied the relative complexation strength between alkali metal cations and cyclofructans

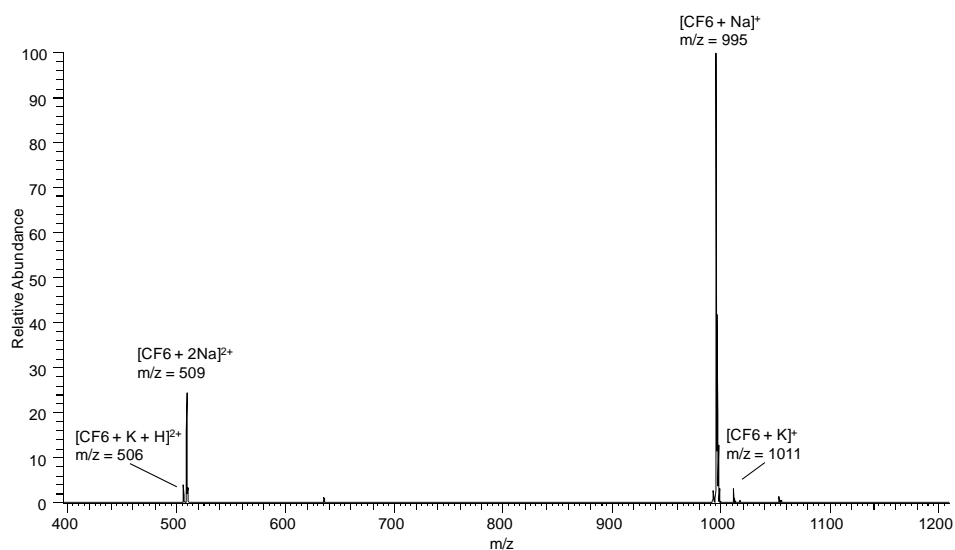


Figure 8.2 Sample mass spectrum obtained by electrospraying 50% aqueous methanol solution of 1:1 (1.0×10^{-4} M each) CF6 and NaCl.

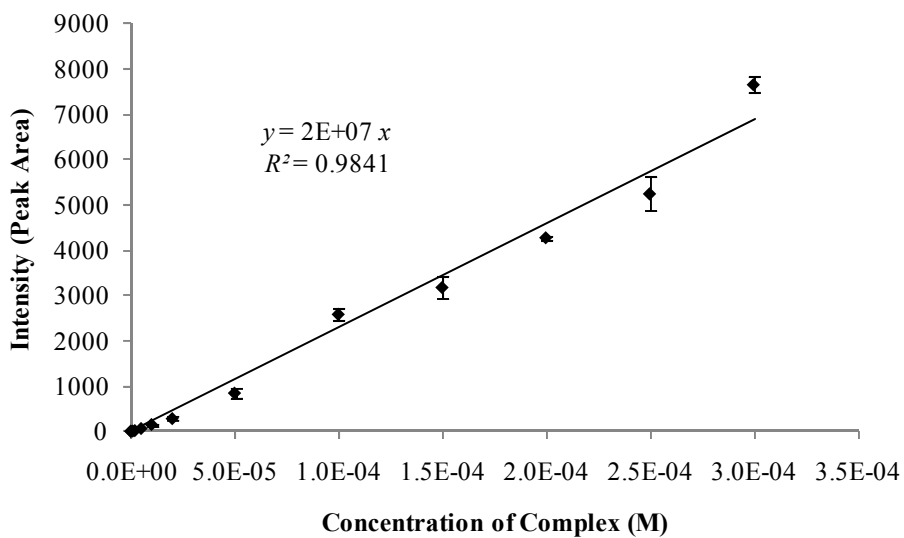


Figure 8.3 The linear fit of ESI-MS peak intensity vs. concentration of 1:1 CF6 and NaCl in 50% aqueous methanol solution. Error bars represent one standard deviation from the mean.

by a thin layer chromatographic (TLC) method.^{84c} There seemed to be a size dependence aspect to the complexation strength: CF6 was found to bind the strongest to Rb⁺, while the CF7 binds the strongest to Cs⁺, among all of the alkali metal cations. Interestingly, Reijenga et al. reported the opposite relative binding strength for CF6-Rb⁺ and CF6-K⁺ complexes, based on their apparent mobility in a capillary electrophoresis study.^{84a} These are the only two systematic complexation studies between native cyclofructans and alkali metal cations which can be found in literature. In our study, by directly comparing the complex ion intensities in the ESI mass spectra, the apparent cationic selectivity for CF6 was Na⁺ > K⁺ > Rb⁺ > Li⁺ > Cs⁺, and the selectivity for CF7 was Na⁺ > K⁺ > Li⁺ > Rb⁺ > Cs⁺ (as shown in Table 8.2). The Na⁺ and K⁺ complexes of cyclofructans were the two most abundant species detected for both CF6 and CF7 hosts. The Li⁺ was found to have negligible binding towards cyclofructans according to the TLC study by Uchiyama et al.^{84c} However, a substantial abundance of cyclofructan-Li⁺ complexes (~40% of the most abundant species) were detected in our ESI-MS study for both CF6 and CF7. On the other hand, the Rb⁺ and Cs⁺ complexes were among the least abundant species in the ESI-MS spectra, whereas Rb⁺ and Cs⁺ were reported to bind strongly to cyclofructans in the previous TLC study.

Shizuma et al. studied the alkali metal cation preference of permethylated cyclofructans using similar ESI-MS methods.^{84b} Permethylated CF6 was found to bind to alkali metal cations in the decreasing order of K⁺ > Rb⁺ > Cs⁺ > Na⁺ (Li⁺ was not studied), which correlated well with that observed in the solution phase via a NMR study. On the other hand, there was an underestimation of the CF7-Cs⁺ complex abundance by the ESI-MS technique, compared to the NMR study. The cesium cation was found to form the second strongest complex (right after Rb⁺) with permethylated CF7, yet the (CF7 + Cs)⁺ ion peak was observed as the least abundant signal in the mass spectrum.

The ability of the ESI mass spectra to accurately portray the equilibrium of ionized species in solution is still an issue of heated debate.^{86b, 94} In addition to spray efficiency differences among complex ions, the relative stabilities of the ions in the mass spectrometer may also dictate the relative peak intensities. The gas phase stability of cyclofructan-alkali metal complexes was thus studied in an attempt to explain the differences observed between our ESI-MS studies and the previous TLC study.

Table 8.1 The ratios between 1:2 and 1:1 cyclofructan-metal cation complexes electrosprayed from 1:1 solutions of cyclofructan and metal chloride salts. The peak intensities are scaled relative to the 1:1 cyclofructan-metal complexes within each set. “NA” represents less than 1% of 1:2 complexes observed. Standard deviation for three measurements are given.

	CF6	CF7
Li	$(7 \pm 1) : 100$	$(46 \pm 6) : 100$
Na	$(18 \pm 1) : 100$	$(58 \pm 5) : 100$
K	NA	$(8 \pm 1) : 100$
Rb	NA	NA
Cs	NA	NA

Table 8.2 Relative abundance of cyclofructan-alkali metal cation complexes obtained from ESI-MS experiment for the equimolar (10^{-4} M) solution of cyclofructan, alkali metal and ammonium chloride salts (refer to Figure 5 for mass spectra). Standard deviation for three measurements are given.

	CF6	CF7
Li	41 ± 1	38 ± 1
Na	100	100
K	88 ± 1	61 ± 1
Rb	44 ± 1	24 ± 1
Cs	8 ± 1	4 ± 1
NH ₄	2 ± 1	1 ± 1

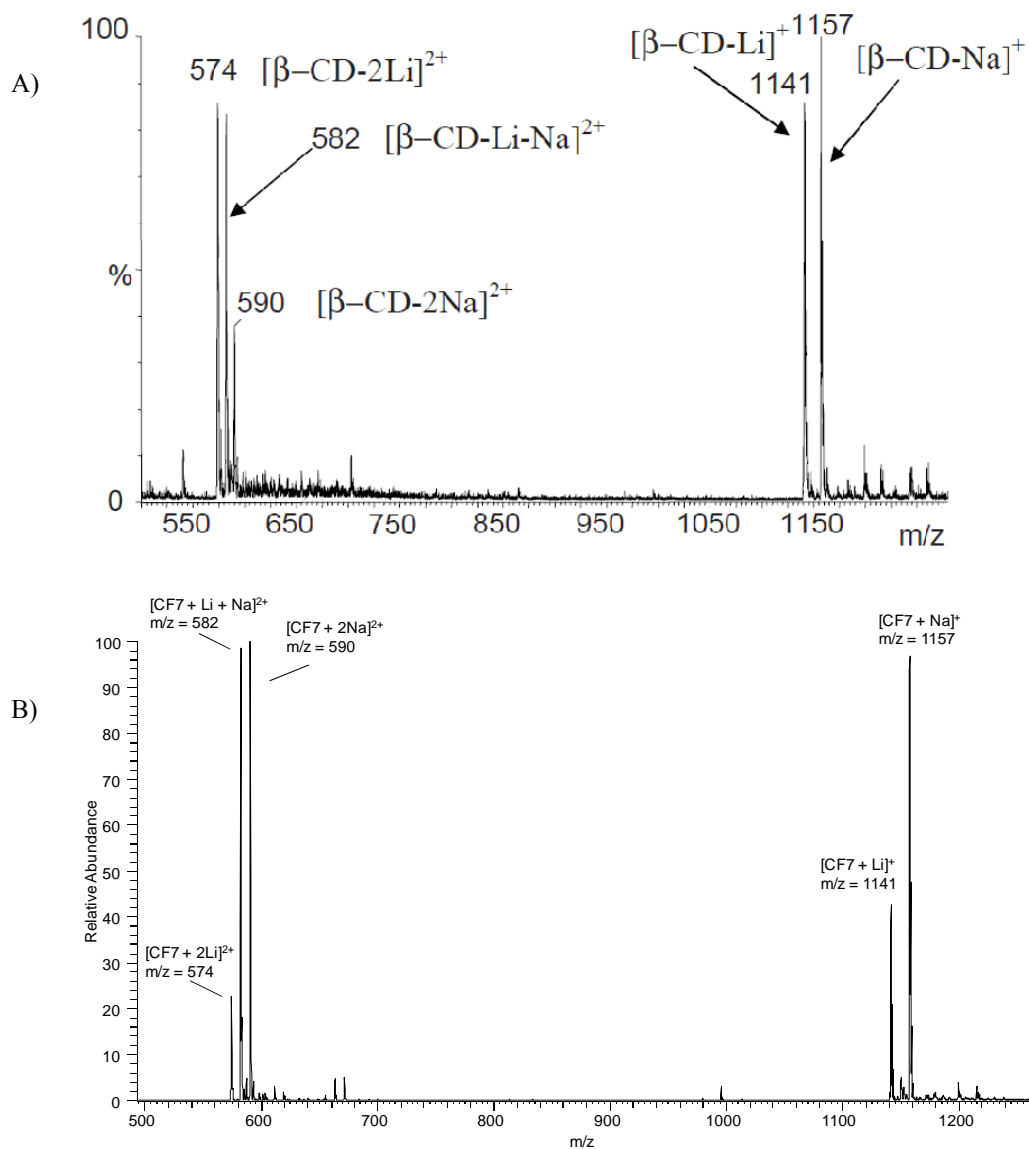


Figure 8.4 Comparison of ESI-MS spectra between the β -CD and CF7 when complexing with Li^+ and Na^+ . (A) 1:2 complexes is more favorable for Li^+ than for Na^+ ; (B) CF7 gives the opposite trend, i.e., 1:2 complexes is more favorable for Na^+ than for Li^+ . Figure A is reprinted from reference 88 with permission.

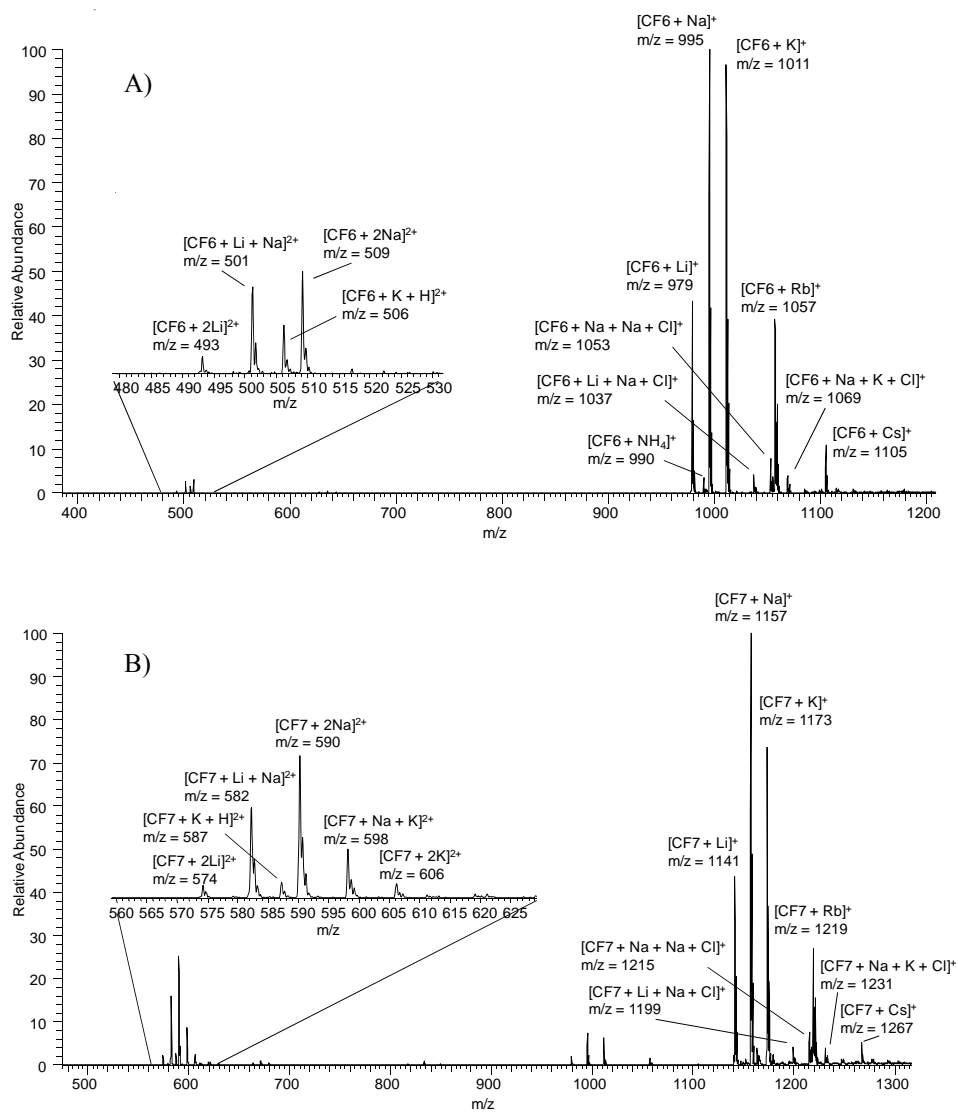


Figure 8.5 Competitive binding of (A) CF6 and (B) CF7 with all alkali metal cation and ammonium chlorides.

8.4.3 Gas Phase Selectivity

The gas phase selectivities of cyclofructans for the alkali metal cations were studied by competitive dissociation of ternary complexes, in a manner similar to the kinetic method.^{86e, 95} As shown in Figure 8.6A, the parent ion $(\text{CF6} + \text{Na} + \text{K})^{2+}$, subjected to collision induced dissociation, produced almost exclusively a $(\text{CF6} + \text{Na})^+$ fragment by loss of a potassium cation. Consequently, the Na^+ was determined to have a higher affinity than K^+ for cyclofructan in the gas phase. Because both dissociation channels ($(\text{CF6} + \text{Na})^+$ and $(\text{CF6} + \text{K})^+$) were not observed, calculations of product ratios, typically recorded using the kinetic method, could not be evaluated. The data did however show conclusive binding preferences. The large alkali metal rubidium and cesium cations form negligible doubly charged complexes with cyclofructans. Instead, the complex of cyclofructan with Rb^+ , Cs^+ and one Cl^- was isolated for the CID study (as shown in Figure 8.6B). Three fragment ions were observed: $(\text{CF6} + \text{Rb} + \text{Cs} - \text{H})^+$, $(\text{CF6} + \text{Cs})^+$, and $(\text{CF6} + \text{Rb})^+$, corresponding to the parent ion losing one HCl , one RbCl , and one CsCl , respectively. The significantly higher abundance of the $(\text{CF6} + \text{Rb})^+$ signal compared to the $(\text{CF6} + \text{Cs})^+$ signal was interpreted as the result of the preferential binding of CF6 towards Rb^+ in the gas phase. By mixing cyclofructan with all possible combinations of two alkali metal complexes, the selectivity of both CF6 and CF7 for alkali metal ions is determined to be $\text{Li}^+ > \text{Na}^+ > \text{K}^+ > \text{Rb}^+ > \text{Cs}^+$. Similar studies have been conducted for synthetic crown ethers: 18-crown-6 and 21-crown-7 bind the most strongly to Na^+ and K^+ cations, respectively.^{86e} Only small crown ethers (e.g., 15-crown-5) have a similar gas phase preference for alkali metal cations to the cyclofructans.^{86e} Our findings provide strong evidence that the crown ether core of the cyclofructan does not directly participate in binding the alkali metal cations.

The gas phase complexation between CF6 and alkali metals also was studied by B3LYP density functional theory calculations using the cc-pVDZ basis for C, H, and O,⁹⁶ and the SDD (Stuttgart/Dresden) ECP basis set⁹⁷ for metal cations. The input coordinates of CF6 were obtained from the X-ray structure.^{60g} The side and top view of the central 18-crown-6 plane in CF6 are illustrated in Figure 8.7. Metal cations, in principle, can approach CF6 from either side of the CF6 central plane. However, previous computational results showed that the two sides are dramatically different in their electrostatic potential profiles. One side is aligned with 1- and 6-methylene moieties of fructofuranose units, and is “pronouncedly electropositive”,

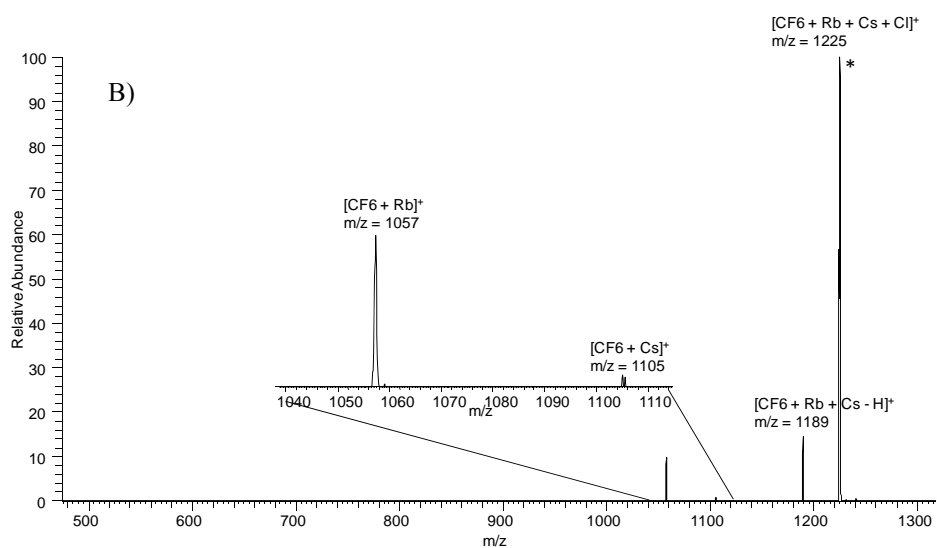
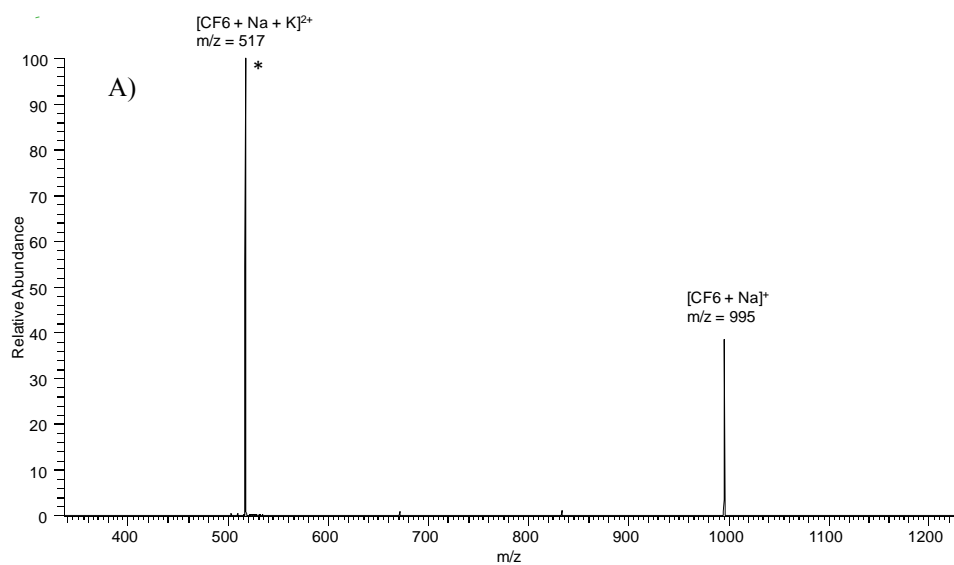


Figure 8.6 Collision induced dissociation mass spectra of complexes formed by ESI-MS: (A) $(CF_6 + Na + K)^{2+}$ and (B) $(CF_6 + Rb + Cs + Cl)^+$.

whereas the other side is occupied with hydroxyl groups in the 3- and 4-positions of the fructofuranose units (top side in Figure 8.7A), and is “distinctly electronegative”.⁹⁰ Previous NMR studies of metal complexation of native and derivatized cyclofructans also revealed that the 3-OH and 4-OH groups are responsible for cyclofructan-metal cation interactions.^{84f} In addition, the X-ray structure analysis of permethylated CF6 complexed with Ba²⁺ showed that the cation (Ba²⁺) is positioned on the molecular rotational axis on the electronegative side (top side in Figure 8.7A) of the molecule.^{84d} Consequently, we placed metal cations on the electronegative side of CF6, right above the plane defined by three O-3(*i*) atoms (which will be referred to as the O-3(*i*) plane in following discussions), as shown in Figure 8.7. There was no obvious structure relaxation of CF6 after energy minimization of the complex. The calculated binding energies are between -99 and -383 kJ mol⁻¹ (Table 8.3, column 4) for the studied complexes. Our results compare well with experimental data obtained by threshold CID studies for the binding energies between crown ethers and alkali metal cations (see Table 8.3).⁹⁸ According to our calculations, CF6 binds to alkali metal cations in the decreasing order of Li⁺ > Na⁺ > K⁺ > Rb⁺ > Cs⁺, which is in good agreement with the results obtained by the MS study.

By comparing the optimized complex structures, it can be inferred that the gas phase selectivity of CF6 is dictated by the size of the metal cations. Table 8.4 lists the elevation of metal cations above the O-3(*i*) plane (shaded plane in Figure 8.7): The distance increases with increasing size of the metal cation. The small Li⁺ ion is able to nestle inside the plane, whereas larger cations can only perch above the plane. The relative position of the metal cations to the O-3(*i*) plane bears important consequences. Firstly, the distances between metal cations and the three O-3(*i*) atoms increase as the metal cations perch higher above the plane. Secondly, according to the “best fit” model developed for crown ether and metal complexes,¹⁰⁰ the nestling provides stronger binding than perching. Finally, the crown ether ring in CF6 is located on the side opposite to the metal cations. The Li⁺, nestling inside the O-3(*i*) plane, is closer to the crown ether ring in CF6 than a larger metal cation perching above the plane. As a result, the electrostatic interaction between oxygen atoms on the crown ether ring in CF6 is stronger with Li⁺ than with larger metal cations. All these three factors contribute to a gas phase selectivity for CF6 of Li⁺ > Na⁺ > K⁺ > Rb⁺ > Cs⁺.

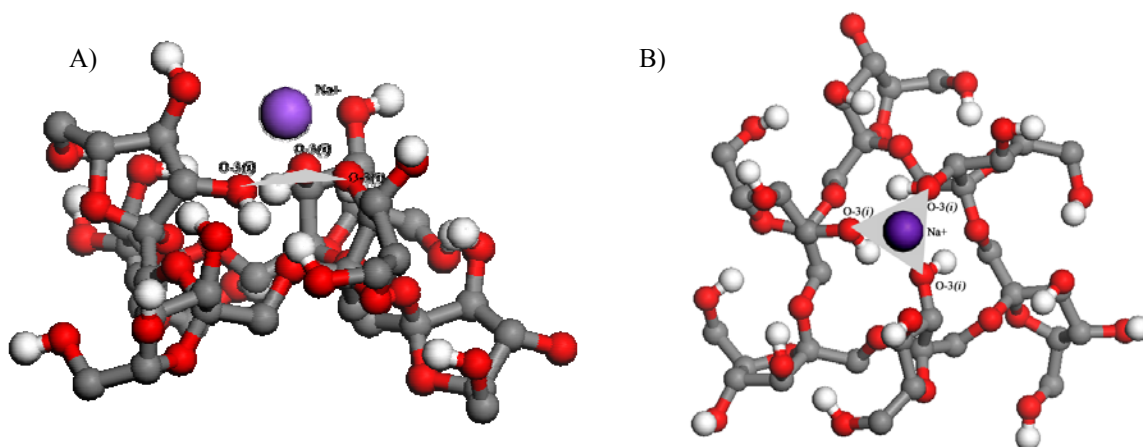


Figure 8.7 Ball and stick model of optimized CF6-Na⁺ complex: (A) side view; (B) top view. Color coding: sodium, blue; carbon, gray; oxygen, red; hydrogen, white. The plane defined by three O-3(*i*) atoms is shaded light gray. The size of sodium is enlarged in order to differentiate from C, H, and O atoms. Hydrogen atoms attached to the carbons have been removed for visual clarity.

Table 8.3 Binding energy (kJ mol⁻¹) between alkali metal cations and crown ethers and CF6. Values for crown ethers are obtained from threshold CID experiments,⁹⁸ and values for CF6 are obtained from DFT calculations.

	18-crown-6	15-crown-5	12-crown-4	CF6
Li ⁺	NA	NA	-372	-383
Na ⁺	-296	-294	-252	-234
K ⁺	-235	-205	-189	-152
Rb ⁺	-191	-114	-93	-121
Cs ⁺	-168	-100	-85	-99

Table 8.4 Optimized structural parameters for complexes between CF6 and alkali metal cations.

	d,plane ^a	M-O1 ^b	M-O2 ^b	M-O3 ^b	$r_{M^+} + r_{O2^-}$ ^c
Li ⁺	0.56	1.92	1.87	1.88	2.16
Na ⁺	1.76	2.36	2.28	2.44	2.42
K ⁺	2.26	2.74	2.71	2.86	2.78
Rb ⁺	2.51	3.03	2.95	2.93	2.92
Cs ⁺	2.81	3.53	3.12	3.13	3.07

^a between neighboring distance (in the unit of Å) between metal cations to the plane consisting of three 3-position oxygen atoms; ^b bond length (in the unit of Å) between metal cations (M) and three 3-position oxygen atoms (O1, O2, and O3); ^c sum ionic radius (in the unit of Å) of metal cation and oxygen anion.⁹⁹

8.5 Conclusions

Complexes of one cyclofructan and two guest cations were observed for small alkali metals using ESI-MS. The larger size CF7 is more likely to form 1:2 complexes with alkali metal cations than CF6. By direct inference from the ESI-MS spectra, both CF6 and CF7 favor the mid-size alkali metal cations (e.g., Na⁺ and K⁺) in solution. Our ESI-MS results differ from the previous TLC results by overestimating the Li⁺ complexes and underestimating the Rb⁺ and Cs⁺ complexes, which could be explained by relative gas phase stabilities of complex ions.

The gas phase selectivity of both CF6 and CF7 is determined to be Li⁺ > Na⁺ > K⁺ > Rb⁺ > Cs⁺ by the competitive dissociation method. The density functional theory calculations of CF6-alkali metal cation complexes reveal that the gas phase selectivity of CF6 is determined by the size of metal cations: smaller size metal cations better fit the interaction plane, and are able to form stronger electrostatic-dipole interactions with CF6.

8.6 Acknowledgement

We gratefully thank Robert A. Welch Foundation (Y.0026) for financial support of the work and Mitsubishi Kagaku Co. for providing us cyclofructans.

CHAPTER 9

SEPARATIONS OF CYCLOINULOOLIGOSACCHARIDES VIA HYDROPHILIC INTERACTION CHROMATOGRAPHY (HILIC) AND LIGAND-EXCHANGE CHROMATOGRAPHY

9.1 Abstract

A homologous series of three cyclinooligosaccharides were separated on the β -cyclodextrin and on the silica based strong cation exchange columns using high organic content aqueous solvents. The elution order on the cyclodextrin column was from low DP to high DP of oligosaccharides, whereas the elution order on the cation exchange column was mixed and determined by both the metal cations on the stationary phases and the organic solvent in the mobile phases. In comparison, α -, β - and γ -cyclodextrin were also separated using the same or similar mobile phases on these columns. With no exception, the elution order was from α - to γ -cyclodextrins. Chunlei Wang, Zachary S. Breitbach, and Daniel W. Armstrong. Separation Science and Technology, in press. Copyright © 2009 with permission from the Taylor & Francis Group, LLC.

9.2 Introduction

Cyclinooligosaccharides (cyclofructans) are β -(2 \rightarrow 1)-linked cyclic fructofuranose oligomers (Figure 9.1). They are produced via fermentation of inulin by *Bacillus circulans* or alternatives from the enzyme cyclinooligosaccharide fructanotransferase which can be isolated from this culture.^{83,101} The major cyclofructans (CF) produced is cyclinulohexaose (CF6), although both cyclinuloheptaose (CF7) and cyclinulooctaose (CF8) also are produced in smaller amounts.⁸³ CFs have a unique crown ether skeleton as the center core.^{60g, 102} The crown ether core for CF6 is 18-crown-6, which makes CF6 attractive for CF6-metal complexation. In addition, CF6 \cdot 3H₂O forms crystals in MeOH, and can be easily purified.⁸³ Many host-guest studies of CF6 and derivatized CF6 thus have been carried out since its first discovery in 1989.^{60c, 84b, 84d, e, 103} On the other hand, CF7 and CF8 are far less studied, largely due to the lack of facile purification methods. The purification of CF7 was briefly reported on the QAE-Toyopearl 550C strong

purification methods. The purification of CF7 was briefly reported on the QAE-Toyopearl 550C strong cation exchange (SCX) resin using 70% aqueous ethanol solvents. Unfortunately no information was provided on the counter cation employed.^{83, 84d} Shizuma et al. briefly mentioned purifying CF7 with a potassium (K⁺)/calcium (Ca²⁺) charged cation exchange resin.^{84b} In a recent study, Jiang et al. reported different chiral discriminating capability between sulfated-CF6 and sulfated-CF7.¹⁰⁴ In their study, 72% pure CF7 was used (with CF6 as the major impurity). To better study the host-guest chemistry of CFs, both appropriate analytical and preparative separation methods for CFs are needed.

Separations of other carbohydrates were achieved on ion-exchange columns mainly in the following three modes¹⁰⁵: (a) They were either ionized in very basic mobile phases (pH > 13) or complexed with borate anions to adopt an anionic form, and were subsequently separated on anion-exchange columns;¹⁰⁶ (b) carbohydrates were separated via a ligand-exchange mechanism on calcium or lanthanum cation charged cation-exchange columns;¹⁰⁷ (c) carbohydrates were separated using high ACN (or ethanol) aqueous solvents on cation- or anion-exchange columns (HILIC mode).¹⁰⁸ Many other polar stationary phases have also been used to separate carbohydrates in the HILIC mode.¹⁰⁹ In HILIC, the polar stationary phases provide more retention for carbohydrates than reversed-phase stationary phases. In this paper, we present the HILIC and/or ligand-exchange separation of CFs on a β -cyclodextrin column and a silica based SCX column charged with different metal cations. Possible separation mechanisms are discussed.

9.3 Experimental

9.3.1 Materials

Lithium chloride, sodium acetate, potassium chloride, rubidium nitrate, silver nitrate, barium acetate, α -, β - and γ -cyclodextrins were purchased from Sigma-Aldrich (Milwaukee, WI, USA). LC-MS grade acetonitrile (ACN), methanol (MeOH) and water were purchased from VWR (Bridgeport, NJ, USA). The β -cyclodextrin column CYCLOBOND I 2000 250 x 4.6 mm, 5 μ m was provided by Astec (Whippany, NJ, USA). The silica based SCX column TSK-Gel SP-2SW 250 x 4.6 mm, 5 μ m was purchased via VWR. Mixture of cyclofructan 6, cyclofructan 7 and cyclofructan 8 are generous gift from Mitsubishi Kagaku Co. (Tokyo, Japan).

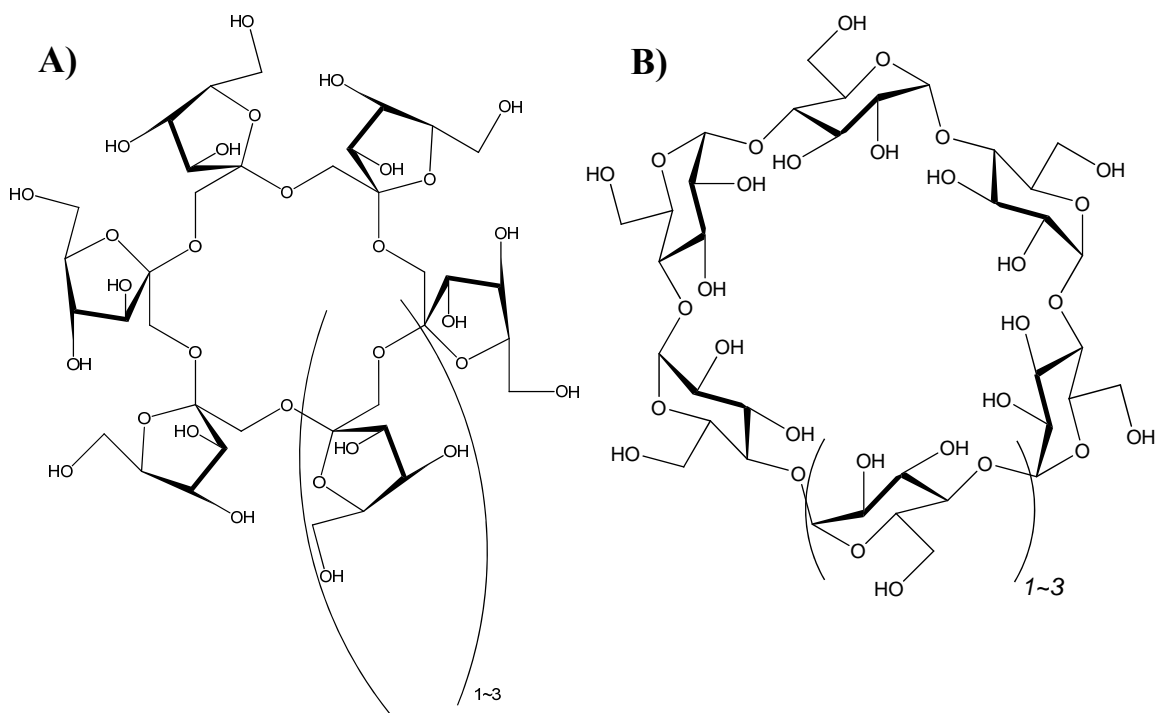


Figure 9.1 Chemical structure of (A) cyclofructans and (B) cyclodextrins.

9.3.2 Instrumentation

All LC-ESI-MS experiments were performed on a Thermo Finnigan (San Jose, CA, USA) Surveyor LC system coupled to a Thermo Finnigan LXQ Advantage API ion-trap mass spectrometer with ESI ion source. A Shimadzu LC-6A pump was used to charge the SCX column with different cations.

9.3.3 Methods

The mixture of CF6, CF7 and CF8 were used directly for analytical separations as it was received from Mitsubishi Kagaku Co. Samples were prepared at 0.5 mg/ml using water or ACN/water 70/30 (v/v, all solvents are indicated in volume percentage unless otherwise noted) as solvents. All separations were carried out at room temperature with 0.4 ml/min flow rate. To enhance the ionization of oligosaccharides, 0.1% w/v sodium acetate dissolved in water/ACN 10/90 was added into the mobile phase post column via a Y-type mixing tee at 4 μ l/min using a syringe pump. The ESI-MS conditions were as following: spray voltage 3.2 kV; sheath gas flow rate, 37 arbitrary units (AU); auxiliary gas flow rate, 6 AU; capillary voltage 11 V; capillary temperature, 350 C; tube lens voltage 105 V; and all oligosaccharides were detected in the SIM mode for $[M+Na]^+$ cations. The Xcalibur software was used for data analysis.

9.4 Results and Discussion

9.4.1 Separation of CFs in the HILIC Mode

The separation of α -cyclodextrin (CD6), β -cyclodextrin (CD7), and γ -cyclodextrin (CD8) on cyclodextrin columns has been reported previously.¹¹⁰ Cyclofructans are isomers of cyclodextrins, and are readily separated on a β -cyclodextrin column using hydro-organic mobile phases with high percentages of ACN (Figure 9.2A). The retention and separation factors decrease as the amount of water increases in the mobile phase (Figure 9.3).

In addition, the mixture of CD6-8 and CF6-8 can be separated simultaneously on the β -cyclodextrin column as shown in Figure 9.2B. CFs and CDs of the same degree of polymerization (DP) have the same number of hydroxyl groups, but cyclofructan isomers are less retained than their cyclodextrin counterparts (Figure 9.2B). Despite of the same total number of hydroxyl groups for CF and CD isomers, all hydroxyl groups are not equally available for solute-stationary phase interactions (e.g., hydrogen-bonding). The separation of CF and CD isomers can be attributed to their different numbers of simultaneously available

hydroxyl groups for solute-stationary phase interactions. As a matter of fact, the separation of isomers of oligosaccharides has been reported on the β -cyclodextrin columns before.^{109a-d}

HPLC separation of CFs was also demonstrated on a silica based strong cation exchange column, TSK-Gel SP-2SW. The retention of CFs and CDs follow the typical HILIC mechanism: the higher the DP, the greater the retention (Figure 9.4A); retention increases as acetonitrile percentage increases in the aqueous mobile phase (Figure 9.4B).

9.4.2 Separation of CFs via Ligand-Exchange Mechanism

The possession of a crown ether skeleton makes CFs different from other oligosaccharides. Uchiyama et al. studied the complexation of CFs with different metals via thin-layer chromatography.^{84c} They also obtained complexation coefficient in 50% aqueous MeOH solvents based on the equation (Eq. (3)) derived by Briggs et al.¹¹¹

$$K = 1/RF' - 1 \quad (\text{Eq. (3)})$$

where K is the complexation coefficient, and RF' is the real migration rate relative to solvent front. Table 9.1 summarizes the complexation coefficients between CFs and selected metal cations in 50% aqueous MeOH. The differences of the complexation coefficients between CFs of different DPs and metal cations are also listed in Table 9.1.

Figure 9.5A shows the separation of CFs using a neat water mobile phase. The retention of all CFs and the separation between CF7/8 and CF6 increases with increasing amounts of ACN in the mobile phase. When using a 40% aqueous ACN mobile phase, the CF7 and CF8 coelute at 8.6 min, whereas the CF6 is retained for 107.5 min (chromatogram not shown). In all aqueous ACN mobile phases tested, the CF6 is always much more strongly retained. The strong retention of CF6 is attributed to its strong binding to the Ba^{2+} on the stationary phase surface.

Our HPLC separations are in good accordance with the complexation difference between CFs obtained by TLC. Ba^{2+} binds CF6 much stronger than CF7 and CF8, and the Ba-SCX provides greatest retention for CF6. In this case, the direct interaction between the CFs and Ba^{2+} on the solid support, instead of hydrophilic partitioning, plays the dominant role in the separation.

Furthermore, compared with other metal cations, the Ba^{2+} provides the largest binding difference between

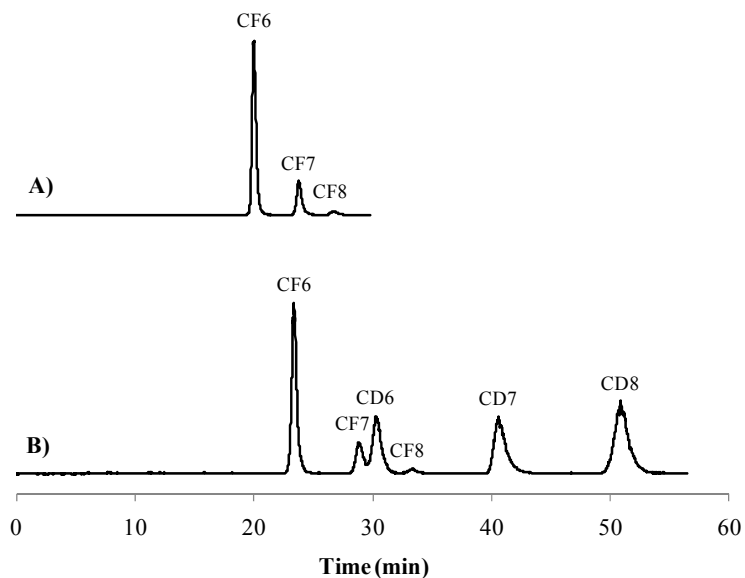


Figure 9.2 Separation of (A) CFs and (B) CFs and CDs on the β -cyclodextrin column. Mobile phases: (A), ACN/water 70/30; (B) ACN/water 72/28.

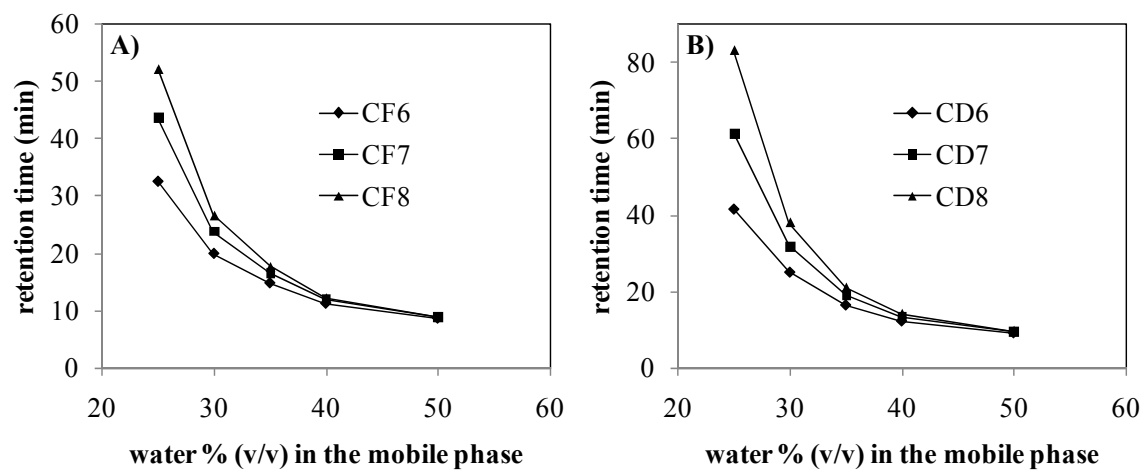


Figure 9.3 Plots of retention time of (A) CFs and (B) CDs vs. water percentage in the aqueous ACN mobile phases on the β -cyclodextrin column.

CF6 and CF7/CF8, and correspondingly, Ba-SCX produces the best separation between CF6 and CF7/CF8. Silver cation (Ag^+) provides the largest binding difference between CF8 and CF7 (refer to Table 9.1), and Ag^+ charged SCX column provides best separation for CF7 and CF8 (Figure 9.5B). Using aqueous MeOH mobile phases, CF8 is retained less than CF7 and CF6 due to its weaker affinity for Ag^+ .

9.4.3 *Mixed Mode Separation of CFs*

Rubidium cation (Rb^+) provides a minimal binding difference between CF7 and CF8, whereas it binds strongly to CF6. Figure 9.6 shows the separation of the cyclofructans on the Rb-SCX column using a 65% aqueous ACN mobile phase. The longer retention of CF6 is the result of the stronger CF6- Rb^+ interaction, whereas relative retention of CF8 and CF7 follow a more conventional HILIC mechanism like that shown in Figure 9.4A. In this case, both the hydrophilic interaction and CFs-metal cation complexation are reflected in the chromatogram. In fact, the relative importance of these two interactions can be affected by simply modifying the mobile phase composition as demonstrated on the K-SCX column below (Figure 9.7).

Potassium cation (K^+) binds strongest to CF6, and it also binds slightly more to CF7 than CF8. In aqueous ACN mobile phases, CF6 always elutes last on the K-SCX column. The elution order of CF7 and CF8 can be manipulated by changing mobile phase compositions as shown in Figure 9.7. In the 40% aqueous ACN mobile phase, the direct CF- K^+ complexation determines the elution order, and CF8 is eluted first (Figure 9.7A). With a 65% aqueous ACN mobile phase, however, the hydrophilic interaction is a more important contributor to the elution order, and CF7 elutes first (Figure 9.7B).

9.4.4 *Separation of CDs on the SCX Column*

Carbohydrates are in general good ligands for metal cations, and ligand-exchange chromatography has been used for separation of carbohydrates using aqueous mobile phases.¹¹² However, most carbohydrate-metal cation complexation is much weaker than that of CF-metal complexation. In our study, the elution order of cyclofructans were greatly affected by the counter cations on the SCX column, whereas the elution order of cyclodextrins is, with no exception, from CD6 to CD8 under all tested chromatographic conditions (Figure 9.8).

Table 9.1 Complexation coefficients between CFs and different metal cations (summarized from reference 84e).

	K_{CF6}	K_{CF7}	K_{CF8}	$\Delta K_{CF6,7}$	$\Delta K_{CF7,8}$
Li^+	0.00	0.00	0.00	0.00	0.00
Ba^{2+}	4.65	0.06	0.01	4.59	0.05
Ag^+	1.66	0.84	0.33	0.82	0.51
Rb^+	1.40	0.09	0.09	1.31	0.00
K^+	1.18	0.11	0.04	1.07	0.07

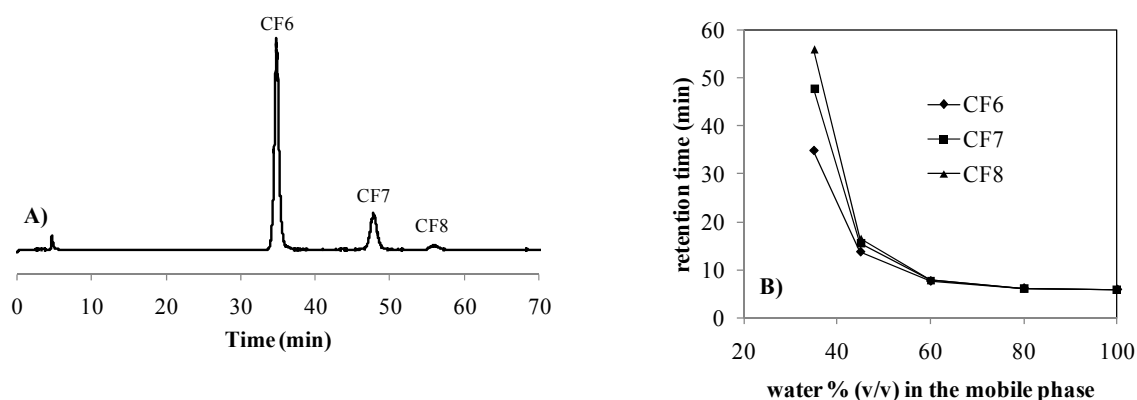


Figure 9.4 (A) Separation of CFs on the Li-SCX column using an ACN/water 65/35 mobile phase. (B) Plot of retention time of CFs vs. water percentage in the aqueous ACN mobile phases on the Li-SCX column.

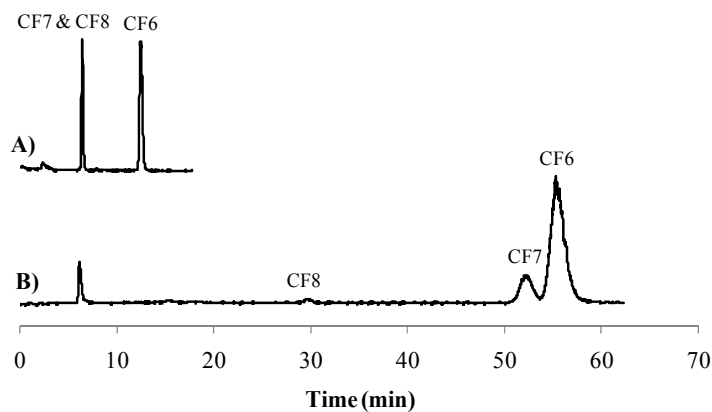


Figure 9.5 Separations of CFs on (A) the Ba-SCX column and (B) the Ag-SCX column. Mobile phases: (A) water; (B) MeOH/water 80/20.

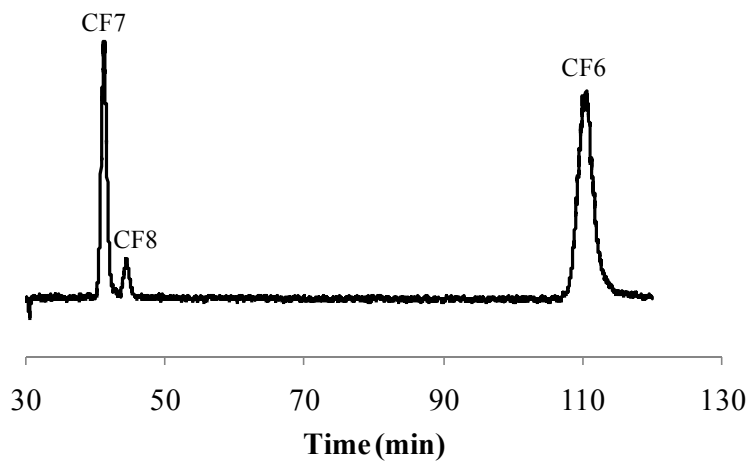


Figure 9.6 Separation of CFs on the Rb-SCX column using an ACN/water 65/35 mobile phase.

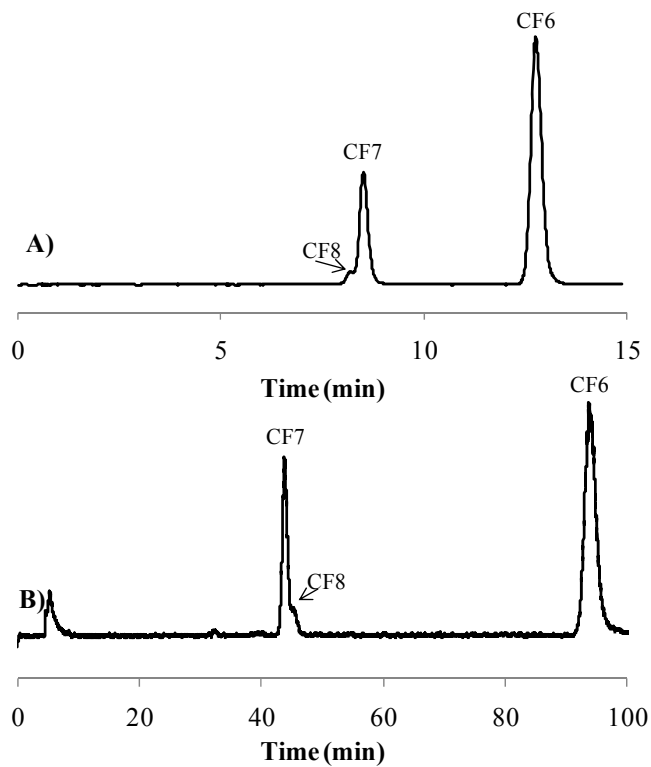


Figure 9.7 Separation of CFs on the K-SCX column using different mobile phases: (A) ACN/water 40/60; (B) ACN/water 65/35.

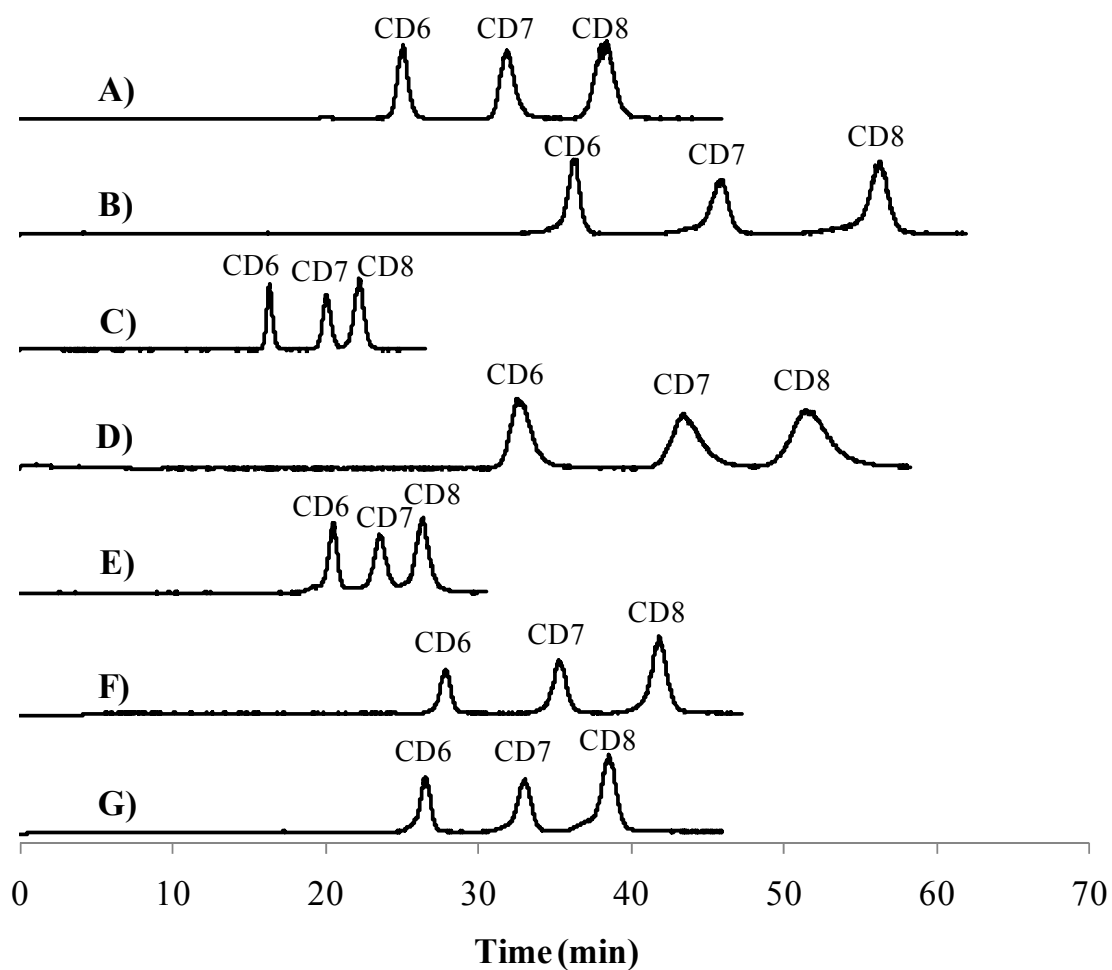


Figure 9.8 Separation of CDs under various tested conditions: (A) β -cyclodextrin column, ACN/water 65/35; (B) Li-SCX column, ACN/water 65/35; (C) Ba-SCX column, ACN/water 55/45; (D) Ag-SCX column, MeOH/water 97/3; (E) Ag-SCX column, ACN/water 70/30; (F) Rb-SCX column, ACN/water 65/35; and (G) K-SCX column, ACN/water 65/35.

9.5 Conclusions

The separation of CF6, CF7 and CF8 were achieved on both the β -cyclodextrin column and various metal cation charged silica based SCX columns by HILIC and/or ligand-exchange mechanisms. Typical HILIC elution order, i.e, from CF6 to CF8, was observed on the cyclodextrin column. On the SCX column however, the complexation between CFs and the counter cation on the column (ligand-exchange mechanism) played an important role in the retention and separation. The elution order of CFs can be manipulated by changing both counter cations on the column and the organic solvent in the mobile phase. The ligand-exchange separation of CFs based on their specific complexation differences with metal cations provide higher selectivity than the separations based on simple generic hydrophilic interactions. In comparison, cyclodextrins were eluted in the order of CD6 < CD7 < CD8 in all chromatographic conditions tested.

9.6 Acknowledgement

We gratefully thank Robert A. Welch Foundation (Y.0026) for financial support of the work and Mitsubishi Kagaku Co. for providing us cyclofructans.

CHAPTER 10

CYCLOFRUCTANS, A NEW CLASS OF CHIRAL STATIONARY PHASE

10.1 Introduction

Cyclofructans are cyclic oligosaccharides consisting of β -2, 1 linked D-fructofuranose units (Figure 10.1). As first reported by Karvamura and Uchiyama in 1989, they are produced by fermentation of inulin using an extracellular enzyme from a strain of *Bacillus circulans* OKUMZ31B.⁸³ In 1994, Kushibe et al. reported a different strain of *Bacillus circulans* (MCI-2554), which enabled more efficient cyclofructan production.¹⁰¹ Cyclofructans with degrees of polymeration from six to eight have been produced, and they are commonly abbreviated as CF6, CF7, and CF8, respectively. CF6 can be crystallized from aqueous methanol solutions,^{60g, 102} and is available with high purity. Analytical separation methods for cyclofructans of different degrees of polymerization have been reported,⁸⁹ and high purity CF7 (>99%) can be produced via preparative separation using methods slightly modified from the reported analytical approaches.

There are two general types of applications of cyclofructans. First, they have been used as bulk additives in various industrial formulations, in much the same manner as another cyclic oligosaccharide (cyclodextrin) has. For example, cyclofructans have been used as the coating material for inkjet recording media¹¹³ and silver halide photographic materials,¹¹⁴ as the food additives,^{54-55, 115} and as excipients in pharmaceutical applications.¹¹⁶ Secondly, cyclofructans have been used as ion trapping reagents due to their ability to form complexes with many metal cations.⁸⁵

The first study on chiral recognition of cyclofructans was reported by Sawada et al. in 1998.¹¹⁷ They found that permethylated CF6 and CF7 were able to discriminate between several enantiomers of amino acid esters in the gas phase using a direct FAB mass spectrometric approach. The highest enantioselectivity, 1.38, was observed for D,L-tryptophan isopropyl esters using permethylated CF6. There was no follow up on this topic. Nor were there any other reports on any type of “chiral applications” of cyclofructans in the following 11 years. It was not until very recently that Armstrong et al. employed native and/or derivatized

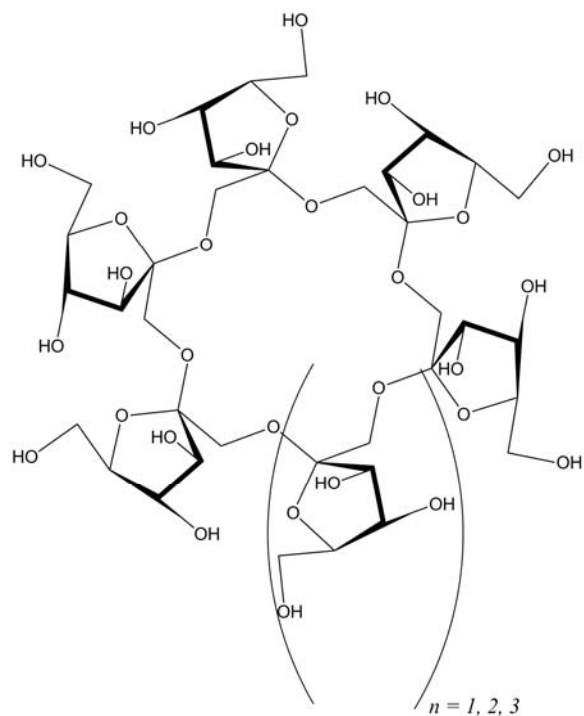


Figure 10.1 Molecular structure of cyclofructans.

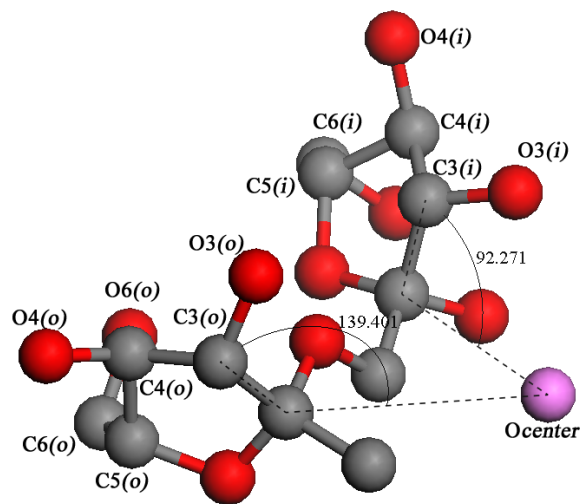


Figure 10.2 Inward and outward included fructofuranose units on the crown ether rim of CF6. The angle $O_{center}-C2-C3$ is 92° and 139° for inward and outward included fructofuranose units, respectively. O_{center} is the average position of six oxygen atoms on the crown ether rim, and is colored pink. Only two fructosefuranose units and part of the crown ether rim are shown for clarity reason. Carbon atoms are colored gray, oxygen atoms red. The suffix “(i)” and “(o)” are included in atom labels to indicate that the atom is in the “inward” inclined and “outward” inclined fructofuranose units, respectively.

cyclofructans as chiral selectors for the capillary electrophoresis (CE), gas chromatography (GC), high performance liquid chromatography (HPLC), and supercritical fluid chromatography (SFC) separations of enantiomers. In this chapter, we examine the enantiomeric separations obtained using cyclofructan-based selectors by all of the aforementioned approaches, and then examine possible chiral recognition mechanisms for this new class of chiral selectors with the help of computational tools.

10.2 Structural Characteristics of Native Cyclofructan 6

Cyclofructans are isomers of cyclodextrins of the same degree of polymerization. However, their structures are substantially different. Cyclofructans do not have hydrophobic cavities. Cyclodextrins are linked via α -1, 4 glycosidic bonds, and α -cyclodextrin (α -CD) has a 30-atom macrocyclic ring (24 carbon and 6 oxygen atoms). In contrast, cyclofructans are linked via β -2, 1 glycosidic bonds, and there are only 18 atoms (12 carbon and 6 oxygen atoms) in the center macrocycle of cyclofructan 6 (CF6).^{60g, 102} The distance between opposing oxygens on the macrocyclic ring is 6.1 Å for CF6 as compared to 8.5 Å for α -CD.¹¹⁸ In addition, the six glucose units in α -CD are uniformly tilted towards the molecular center, whereas the six fructofuranose units in CF6 are oriented alternatively towards (“inward” inclination) and away from (“outward” inclination) the molecular center to minimize steric repulsion on the macrocyclic rim (Figure 10.2).⁹⁰ The alternating inward/outward inclination of fructofuranose units are more like chiral propellers attached to the CF6 central macrocycle.

The CF6 central macrocycle is a natural 18-crown-6. However, the conformation of macrocycle is different from that of synthetic crown ethers. When crown ethers are complexed with potassium ion, the six -O-C-C-O- units adopt a gggggg (g stands for gauche) conformation (Figure 10.3A),¹¹⁹ and are evenly distributed above and below the crown ether mean plane. In CF6, the six oxygen atoms are all aligned towards one side of the macrocycle due to the gtgtgt (g stands for gauche; t trans) configuration of the six -O-C-C-O- units in the center 18-crown-6 core as shown in Figure 10.3B.^{60g} In addition, all 3-OH and 4-OH groups also are aligned on the same side of the macrocycle, making this side “pronouncedly hydrophilic”.⁹⁰ The other side of the macrocycle is “distinctly hydrophobic” due to occupation of ethylene groups in the 18-crown-6 core, 6-methylene groups, and the O5-C5-H5 fragments.⁹⁰

Figure 10.4A shows the space filling model viewed from hydrophobic side of CF6. It is clear that the

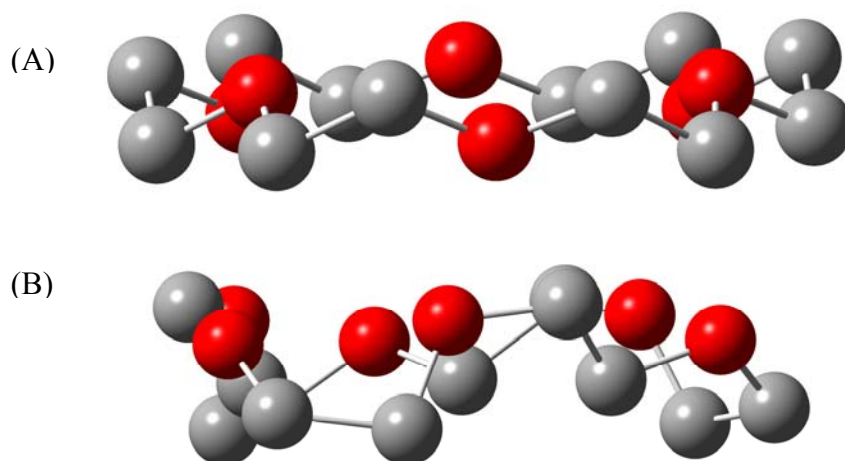


Figure 10.3 Comparison of the macrocycle in CF6 with that in 18-crown-6: (A) the oxygen atoms are in the gggggg conformation in 18-crown-6 and K^+ complexes. (B) the oxygen atoms are alternatively in the gtgtgt conformation in the macrocycle in CF6; Color coding: carbon, gray, oxygen, red. Hydrogen atoms are left out for clarity purpose.

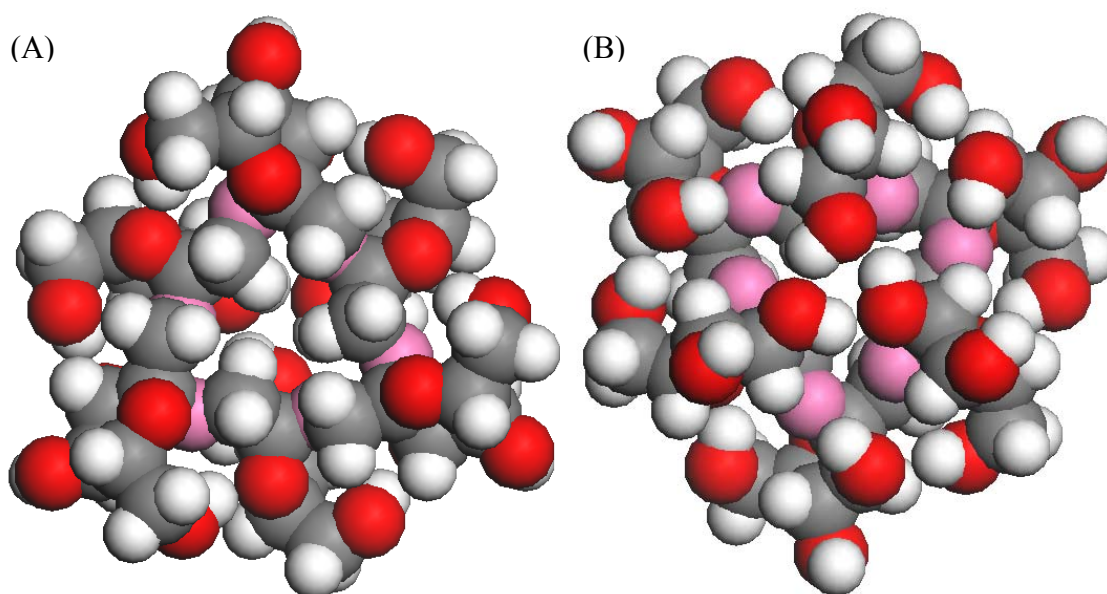


Figure 10.4 Space filling model of CF6: (A) view from the hydrophobic side; (B) view from the hydrophilic side. Color coding: carbon, gray, oxygen, red; oxygen on the crown ether ring, pink; hydrogen, white.

oxygen atoms are all hidden by the ethylene groups in the 18-crown-6 core, and the inner diameter of the macrocycle is around 1.5 Å (as compared to 2.6 Å in 18-crown-6¹²⁰). Consequently, any solute interaction with the six oxygen atoms on the 18-crown-6 moiety from the hydrophobic side of CF6 is not likely. On the hydrophilic side, 3-OH groups from the three inward-inclined fructofuranose units (the O3(*i*) groups in Figure 10.2) are hydrogen bonding with each other and effectively block access to the macrocycle cavity from this side (Figure 10.4B). Consequently, the 18-crown-6 core of the native CF6 is cavity is effectively folded inside the molecule and relatively inaccessible.

Overall, CF6 has distinctively different hydrophilic and hydrophobic surfaces on the two sides of the central macrocycle, and propeller-oriented fructofuranose units along the rim of the macrocycle. These loci are three possible docking sites for molecular recognition of CF6.

10.3 Chiral Recognition of Native Cyclofructan 6

The native CF6 chiral stationary phase produced chiral separations of a few primary amines and binaphthyl type molecules using organic solvents as mobile phases (as shown in Figure 10.5). The fact that no enantiomeric separations were observed in the reversed-phase mode indicates that effective chiral recognition at the hydrophobic surface of CF6 is not prevalent. Previous NMR studies of metal complexation of native and permethylated cyclofructans also reveal that the 3-OH and 4-OH groups are responsible for cyclofructan-metal cation interactions.^{84b, 84d, 84f} In the X-ray structure of permethylated CF6 with Ba²⁺, the Ba²⁺ is positioned on the molecular rotational axis on the top side of the molecule.^{84d} Protonated primary amines could approach CF6 in a similar way. In fact, the three O3(*i*) atoms form a triangular plane, which is similar to the three alternating oxygen atoms in 18-crown-6. Primary amines are likely to form tripodal hydrogen bonding with these O3(*i*) atoms as they do with 18-crown-6. However, these three oxygen atoms are much closer together (2.8 Å, as compared to 4.9 Å in 18-crown-6; see Figure 10.6A and B) and they are hydrogen bonding with one another. As a result, the tripodal hydrogen bonding with three O3(*i*) atoms in CF6 is much weaker than that with 18-crown-6. As will be discussed in the following sections, partial derivatization of native CF6 very likely disrupts the CF6 internal hydrogen bonding thereby causing the remaining free hydroxyl groups to reorient to different geometries. In addition, the hydroxyl groups in CF6 can also act as hydrogen bonding donors, and enantiomeric separation of

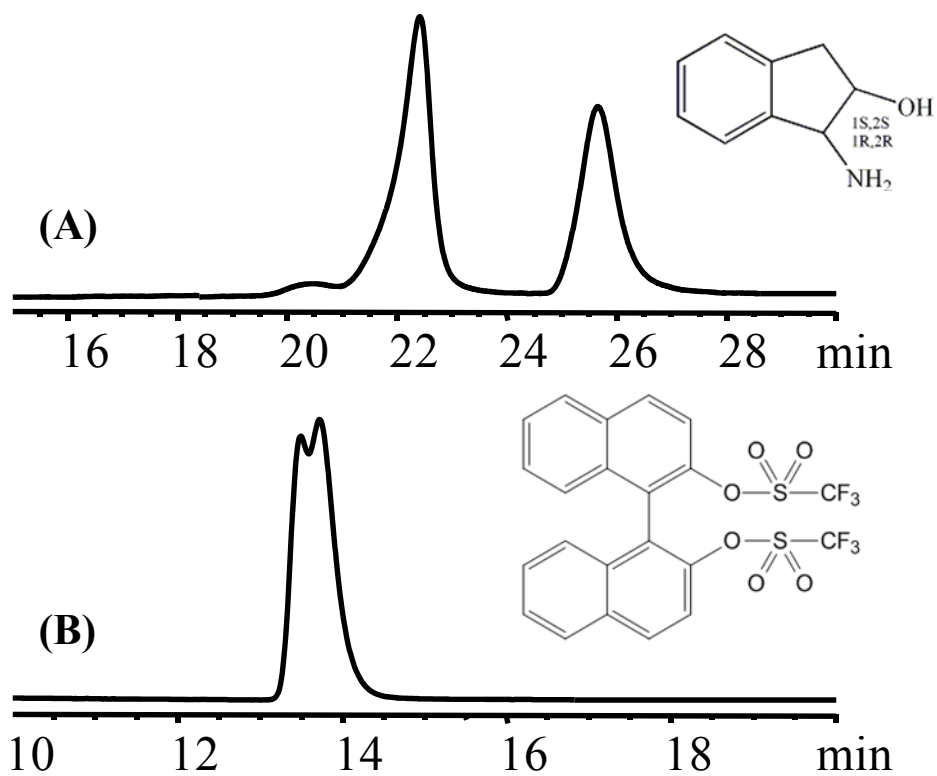


Figure 10.5 Two out of a few enantiomeric separations observed on a native CF6 CSP: (A) primary amine type compound; (B) binaphthyl type compound. Mobile phases: (A) heptan/ethanol/trifluoroacetic acid 70/30/0.1; (B) heptane 100.

secondary and tertiary amines are common on cyclofructan based CSPs, whereas crown ether based CSPs separate almost exclusively primary amines. Tripodal hydrogen bonding alone is not sufficient for chiral recognition. After the docking of amines by the tripodal hydrogen bonding with 3-OH groups, surrounding chiral interaction sites and/or simply chiral barriers (i.e., C3-C4-O4 fragments on fructofuranose units) would provide enantioselective interactions for chiral amines.

There are totally 18 hydroxyl groups in CF6, two thirds of which are attached to chiral centers and are able to provide different hydrogen bonding with chiral analytes. In addition, some of these oxygen atoms adopt a similar geometry to 18-crown-6. As shown in Figure 10.6C and D, the triage formed by O4(*i*)-O3'(*o*)-O3''(*i*) and O3(*o*)-O6(*o*)-O4'(*i*) are more similar to 18-crown-6 than the three O3(*i*) atoms are in the respective of O-O distances among each other. Density theory functional theory calculations at the 6-31g level were employed to validate the binding of potassium cations at these sites. Surprisingly, these two triangular planes provide stronger binding than do the O3(*i*) triangular plan (refer to Figure 10.6 caption). When a potassium cation approaches these two sites (Figure 10.6C and D), it is also able to have electrostatic-dipole interaction with one oxygen atom on the crown ether skeleton of CF6. Despite the energetically favorite binding at these two sites (Figure 10.6C and D), there are not many chiral interaction sites/barriers above these triangular planes in native CF6 to afford chiral recognition. Derivatization could provide extra interactions surrounding those triangular planes for chiral recognitions. One thing to note is that, the hydroxyl groups can also reorient themselves upon interacting with a guest molecule. This “induced-fit” by hydroxyl groups could possibly provide even more interaction sites between cyclofructans and amine compounds. The abundance of hydroxyl groups and suitable interaction sites may account for the high loading capacity that is observed for cyclofructan based CSPs as will be discussed in Section 10.5.

10.4 Chiral Recognition of Derivatized Cyclofructan 6

Despite the limited success of native CF6 as a chiral selector in both HPLC and CE, certain derivatized CF6s show great potential as chiral selectors. During the discussion of structural properties of native CF6, several advantages of derivatization have already been mentioned: (1) derivatization could disrupt the hydrogen bonding between 3-OH groups (as shown in Figure 10.6B) and increase their hydrogen bonding interaction with guest molecules; (2) derivatized groups could provide additional interaction sites

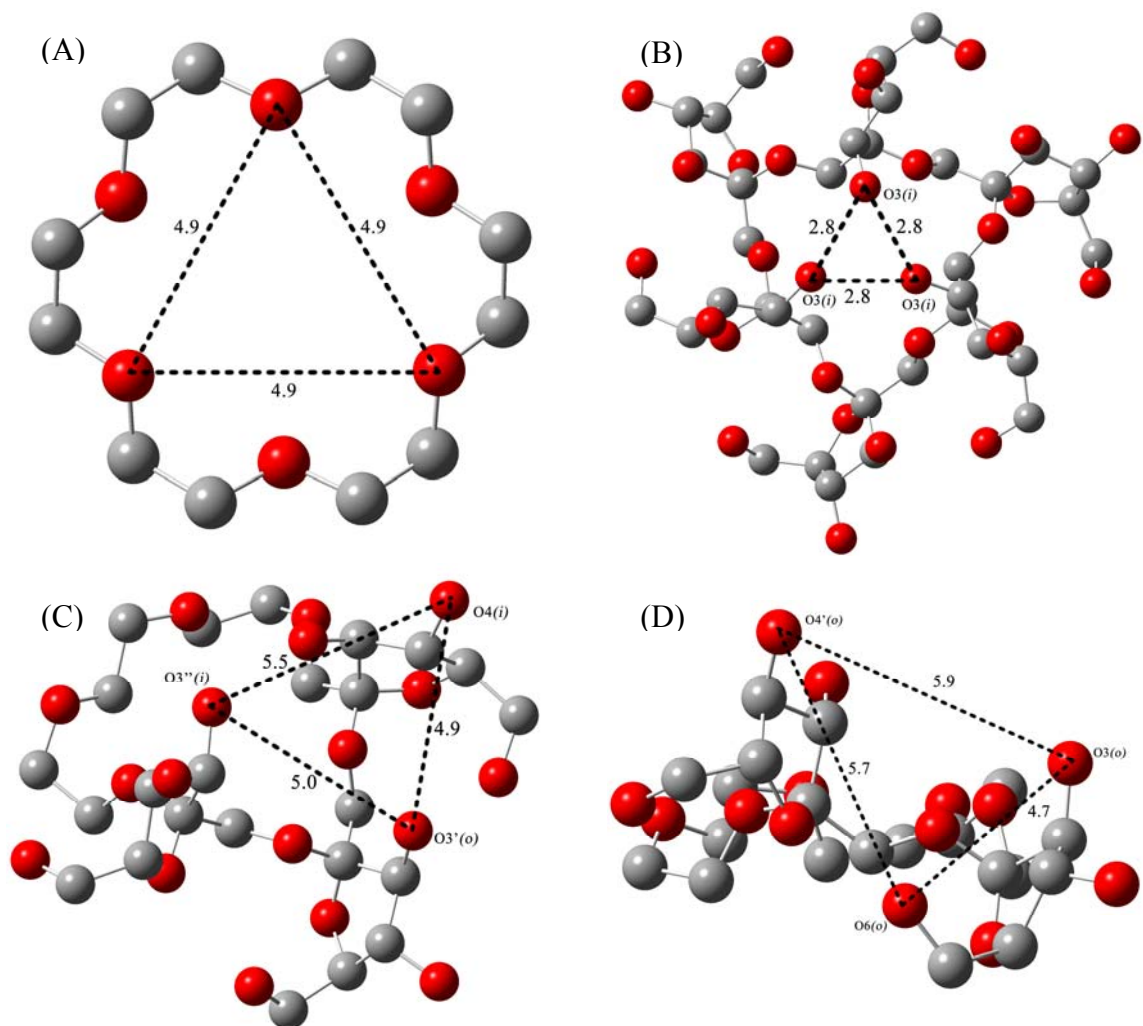


Figure 10.6 Possible tripodal hydrogen bonding sites for ammonium cations: (A) alternating oxygen atoms in 18-crown-6; (B) three alternating O3 on inward-included fructofuranose units (O3(*i*) atoms); (C) O4(*i*), O3'(*o*) and O3''(*i*) on three neighboring fructofuranose units; (D) O3(*o*), O6(*o*) and O4'(*i*) on two neighboring fructofuranose units. The distance between those oxygen atoms are labeled on the figures in the unit of Å. The binding energy of potassium cation (having similar size as ammonium cation) at these sites (calculated at B3LYP/6-31g level) are -364, -195, -261, and -210 kJ mol⁻¹, respectively. Color coding: carbon, gray, oxygen, red. Hydrogen atoms are left out for clarity purpose.

surrounding effective amine binding sites, i.e. sites as shown in Figure 10.6C and D. In addition, the C3 symmetry of native CF6 could be broken. Finally, addition of aromatic groups to CF6 can increase π - π and steric interactions, which are important for many successful chiral selectors.^{49b, 62c, 121}

10.4.1 Aliphatic-Derivatized CF6

Cyclofructan 6 derivatized with only a few aliphatic groups showed exceptional enantioselectivity for primary amine containing compounds.¹²² Organic solvents are the best mobile phases for these types of separations. As discussed in section 10.3, hydrogen bonding is considered to be the most important primary interaction for chiral recognition of amines. This type of interaction is known to be enhanced in solvents of low dielectric constants. It is also observed experimentally that better enantioselectivity is observed in the normal phase mode (heptane/alcohol solvents) than in the polar organic mode (acetonitrile/alcohol solvents) (Figure 10.7). The efficiency, however, is typically better in the polar organic mode as indicated by the sharp and symmetric peaks observed, as compared to usually broad and fronting peaks in the normal phase mode. Overall, faster separations and better enantiomeric resolution (due to enhanced efficiency) is obtained in the polar organic mode (Figure 10.7). In contrast, Crown ether based CSPs operate almost exclusively in the reversed phase mode using acidic aqueous solvents.

Additives are often necessary in order for the elution of chiral primary amines from aliphatic-derivatized CF6 in the normal phase mode. Figure 10.8 shows the separation of *trans*-1-amino-2-indanol with different additives in a heptane/ethanol 70/30 (v/v) solvent. Without additives, the analyte was strongly retained and did not elute in 2 hr. In mobile phases with acidic additives, peaks were eluted and enantiomeric separation was observed. The retention decreases with the decrease of pK_a of acidic additives: the first peak was eluted at 91 min when using 0.1% acetic acid (chromatogram not shown), and was decreased to 31 min when using 0.1% trifluoroacetic acid (Figure 10.8A). Basic additives caused a more dramatic decrease in the retention times, yet enantioseparation was still observed when 0.1% triethylamine was used (Figure 10.8B). The enantiomeric separation of a primary amine in its free form (when only basic additives are used) implies that the prevalent hydroxyl groups in CF6 could effectively act as hydrogen bond donors when interacting with free primary amines. In contrast, there are no hydrogen bonding donating groups on crown ether rings and strong acidic additives, i.e., sulfuric and perchloric acid, are necessary to protonate

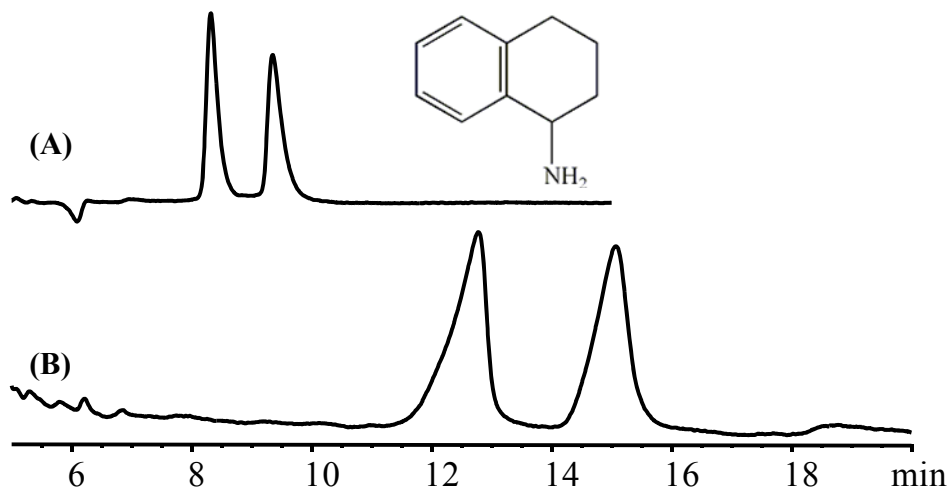


Figure 10.7 The polar organic mode (A) and the normal phase (B) mode separations of a chiral primary amine on a methylated CF6 CSP. Chromatographic parameters: (A) acetonitrile/methanol/acetic acid/triethylamine 60/40/0.3/0.2, $k_1 = 1.77$, $\alpha = 1.19$, $N = 8750$, $R_s = 2.8$; (B) heptane/ethanol/trifluoroacetic acid 70/30/0.1, $k_1 = 4.33$, $\alpha = 1.22$, $N = 3110$, $R_s = 2.2$.

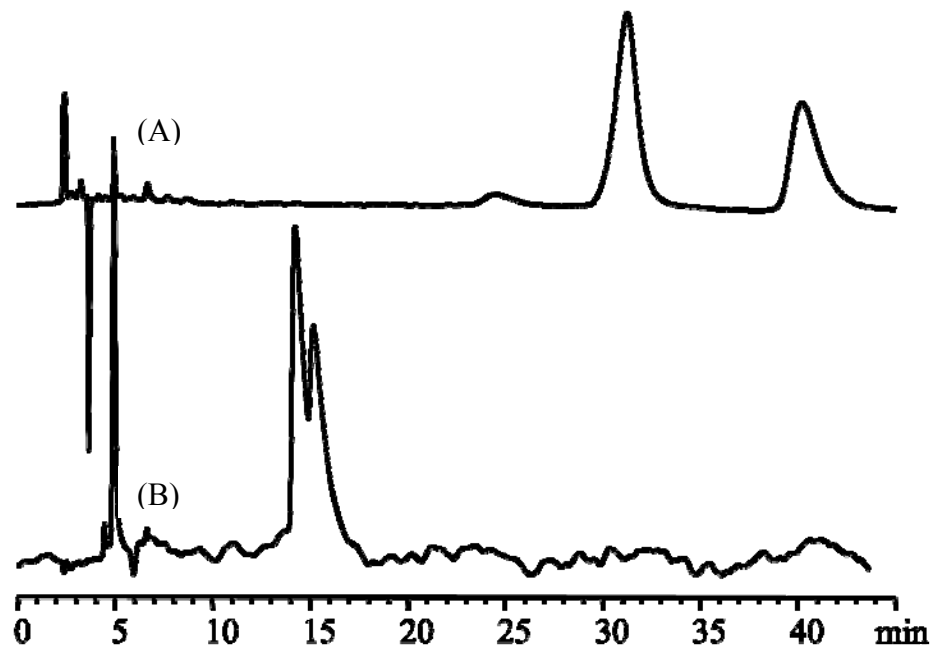


Figure 10.8 Separation of *trans*-1-amino-2-indanol on a methyl carbamate CF6 CSP in a heptanes/ethanol 70/30 mobile phase with different additives: (A) 0.1% trifluoroacetic acid; (B) 0.1% triethylamine.

primary amines to afford enantiomeric separation on synthetic crown ether based CSPs.

A combination of acidic and basic additives is used for the separation of primary amines in the polar organic mode. Table 10.1 lists the chromatographic data obtained using different combinations of acidic and basic additives. The optimized additive composition is 0.3%/0.2% (v/v) acetic acid/triethylamine, which happens to be the recommended buffer for the polar organic phase separation on cyclodextrin based CSPs.^{73a, 123}

Different aliphatic groups, i.e., methyl, ethyl, isopropyl, and tert-butyl groups, have been used to derivatize CF6. Slightly different separations are observed for these four aliphatic-derivatized CF6 CSPs due to the bulkiness and geometry of different aliphatic groups. Overall, the isopropyl-derivatized CF6 produced the best enantiomeric separations for primary amines.

10.4.2 Aromatic-Derivatized CF6

Derivatization of native chiral molecules with aromatic moieties is a common strategy used to enhance their chiral recognition abilities. Examples are oligo- and poly-saccharide based selectors that lack of delocalized π electrons, e.g., (R or S)-naphthylethyl derivatized cyclodextrins, 3,5-dimethylphenyl, along with many other different aromatic moieties, derivatized cellulose and amylose. The optimal derivatization degree is usually different for different type of native selectors. A low degree of derivatization, i.e., 6, was found to be the best for β -cyclodextrins because these aromatic groups were able to effectively provide extra interactions while not completely blocking the cyclodextrin cavity or removing all free hydroxyl groups.^{62c} On the other hand, cellulose and amylose based CSPs favors high degrees of derivatization, and even complete derivatization of all hydroxyl groups.¹²⁴

Aromatic-derivatized CF6 was thus prepared in both low and high degrees of derivatization. Interestingly, low and high degree derivatized CF6 showed dramatically different chiral recognition properties. When CF6 is derivatized with 3 to 5 aromatic groups, the general enantioselectivity for primary amines were also observed, quite analogous to that found on aliphatic-derivatized CF6. The CF6 aromatic moieties play essentially the same role as the aforementioned aliphatic moieties did to enhance chiral recognition for primary amine compounds. Figure 10.9A and B compares the separation of *trans*-1-amino-2-indanol on similarly substituted aliphatic- and aromatic-derivatized CF6 columns. Higher enantiomeric selectivity,

Table 10.1 The effect of acidic and basic additives on the chromatographic separation of (\pm) *trans*-1-amino-2-indanol in the polar organic mode on an isopropyl carbamate derivatized CF6 column.

No.	Additives (in volumn percentages)	k_1	α	R_s
1	Acetic acid (0.30%) / trimethylamine (0.13%)	3.36	1.29	5.3
2	Acetic acid (0.30%) / ethanolamine (0.08%)	1.97	1.14	2.6
3	Acetic acid (0.30%) / butylamine (0.14%)	2.36	1.16	2.3
4	Acetic acid (0.30%) / diethylamine (0.14%)	3.67	1.29	1.6
5	Acetic acid (0.30%) / triethylamine (0.20 %)	2.85	1.31	4.0
6	Acetic acid (0.20%) / triethylamine (0.30 %)	2.69	1.24	3.9
7	Acetic acid (0.25%) / triethylamine (0.25%)	3.24	1.27	4.4

The mobile phase is composed of 60%acetonitrile/40%methanol (v/v). Different volume percentages of basic additives in entry 1-5 are chosen to afford same molar concentration (14 mM) of basic additives.

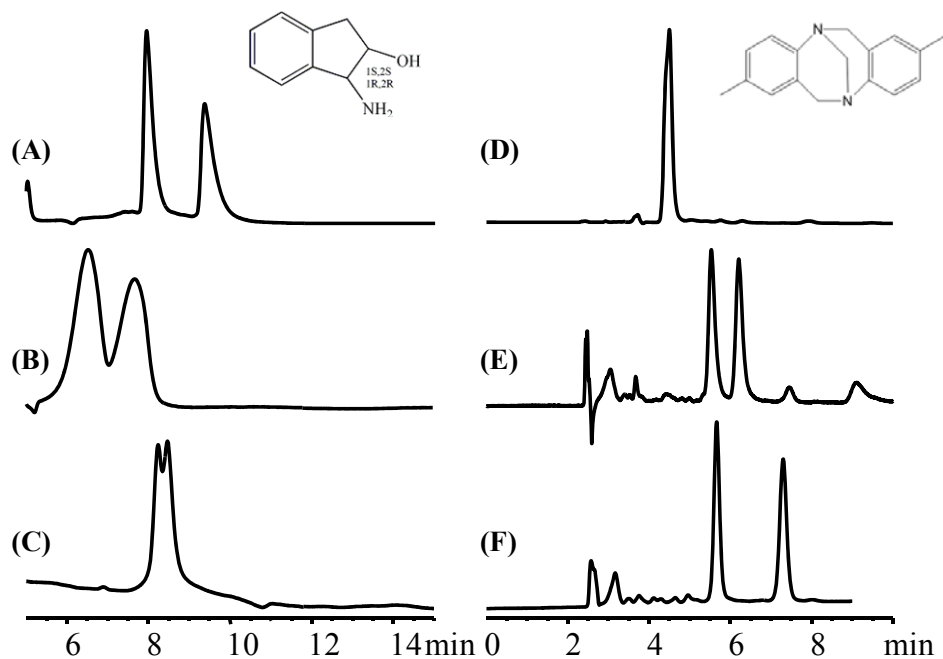


Figure 10.9 Separation of *trans*-1-amino-2-indanol (left) and Troger's base (right) on CF6 CSPs derivatized in three different ways: (A) and (D), low degree methyl carbamate derivatization; (B) and (E), low degree 3,5-dimethylphenyl carbamate derivatization; (C) and (F), high degree 3,5-dimethylphenyl carbamate derivatization. Mobile phases: left, acetonitrile/methanol/acetic acid/triethylamine 60/40/0.3/0.2 (70/30/0.3/0.2 for (C)); right, heptane/ethanol 70/30.

efficiency, and better separation were always observed on aliphatic-derivatized CF6 columns for primary amines. However, in addition to primary amines, other types of racemic compounds were starting to show enantioselectivity on the aromatic-derivatized CF6 CSPs (Figure 10.9D and E).

When most of the accessible hydroxyl groups in CF6 are derivatized with aromatic groups, however, the general enantioselectivity for primary amines is almost completely lost (Figure 10.9C), whereas enhanced separations of a great variety of other chiral compounds can be obtained (Figure 10.9F). These observations are readily explained by looking at the optimized (at HF/6-31g level) structure of the all-O-3,5-dimethylphenyl carbamate-derivatized CF6 as shown in Figure 10.10. The bulky aromatic groups block the access to the tripodal hydrogen bonding sites (shown in Figure 10.6), and negate the chiral recognition for primary amines. On the other hand, the propeller side arm along the crown ether rim of CF6 was not only preserved but also extended in the space to adopt chiral helical geometry with polar oxygen and nitrogen moieties aligned in the helical grooves. Similar chiral helical groove motifs have been proposed to contribute to high enantioselectivity observed for highly aromatic-derivatized polysaccharide-type CSPs.^{48e, 121d} They are likely to play a similar role in chiral recognition for a variety of compounds in the highly aromatic-derivatized CF6.

Ten different aromatic derivatizations of CF6 were made. Examples of the enantiomeric separation of different classes of racemates are shown in Figure 10.11. Most of the observed enantiomeric separations could be obtained on several different aromatic-derivatized CSPs¹²². In addition, the same elution order is generally obtained for chiral compounds on R- and S-naphthylethyl carbamate derivatized CSPs. These observations suggest that the enantiomeric selectivities of the aromatic-functionalized CF6 CSPs are more dependent on the chirality of the base CF6 than the chirality of substituent groups. However, aromatic moieties play an indispensable role in chiral recognitions because the separations of non-primary amine compounds on aromatic-derivatized CF6 CSPs are generally better than those on aliphatic-derivatized ones.

10.4.3 Derivatized CF6 for CE

Capillary electrophoresis is usually carried out in aqueous solutions. However, the interactions (mainly hydrogen bonding) between native CF6 and amino compounds are greatly attenuated in aqueous solvents. Minimal interactions between native CF6 and amine compounds were observed in aqueous CE. On the

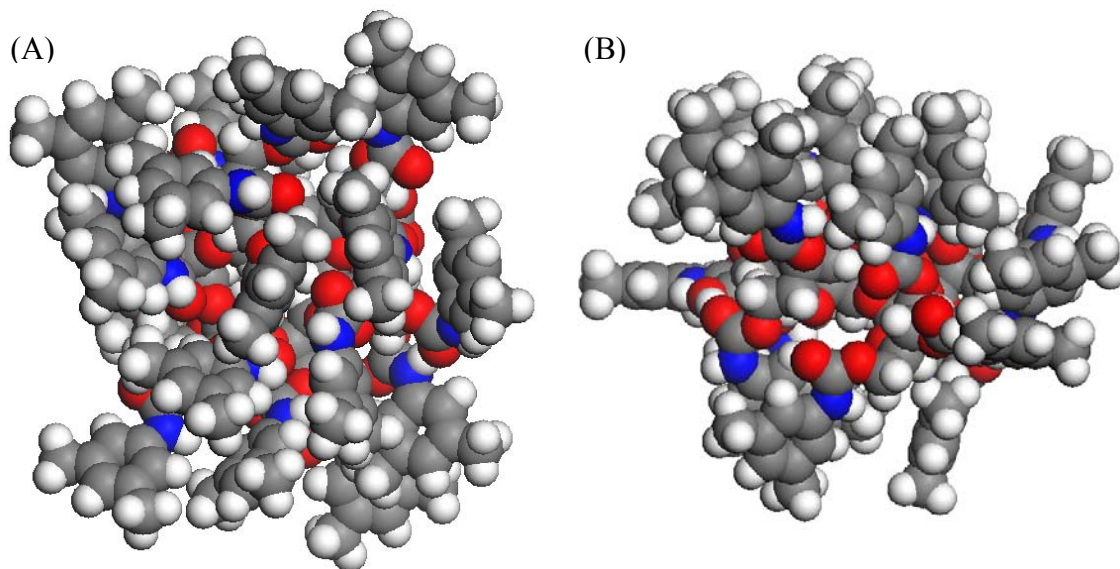


Figure 10.10 Space filling model of all-O-3,5-dimethylphenyl carbamate CF6 calculated at HF/6-31g level: (A) top view from the hydrophilic side of CF6; (B) side view.

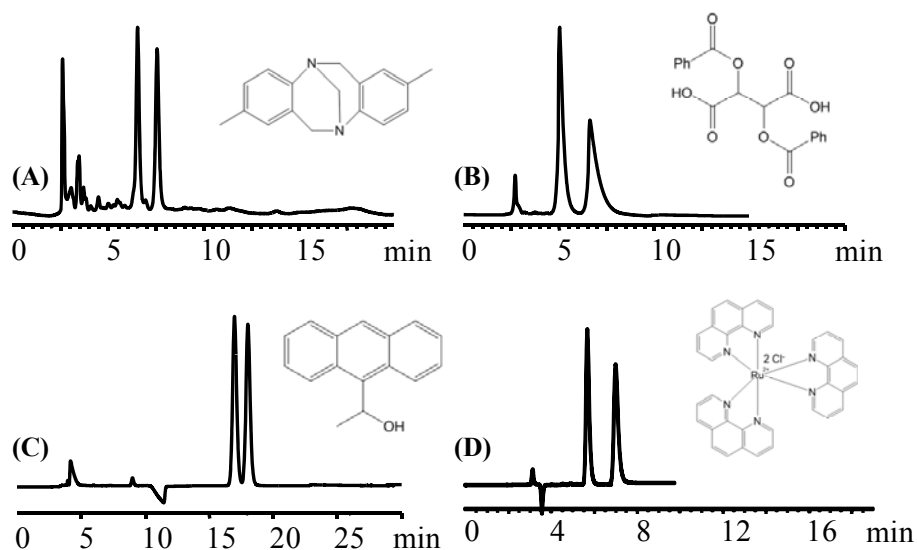


Figure 10.11 Separation of different class of compounds on aromatic-derivatized CF6 CSPs. Aromatic derivatization groups: (A) 3,5-dichlorophenyl carbamate; (B) 3,5-bis(trifluoromethyl)phenyl carbamate; (C), and (D) R-naphthylethyl carbamate. Mobile phases: (A) heptane/ethanol 80/20; (B) acetonitrile/methanol/acetic acid/triethylamine 75/25/0.3/0.2; (C) heptane/isopropanol/trifluoroacetic acid 98/2/0.1; (D) acetonitrile/methanol 40/60 with 25 mM ammonium nitrate.

other hand, sulfated CF6 was able to bind to basic analytes via strong electrostatic interactions in aqueous solvents at appropriate pHs.¹⁰⁴ This electrostatic interaction may not only facilitate initial docking of basic analytes, but also contributes to their chiral separation, along with hydrogen bonding interactions. Figure 10.12 shows the enantiomeric separation of p-chloroamphetamine using sulfated CF6. The separation was virtually unaffected when 20% methanol was added to the background electrolyte (BEG) (Figure 10.12). This was different from what was observed for enantiomeric separations using sulfated cyclodextrins, where methanol in the BGE competes for the hydrophobic cavity of cyclodextrin-based selectors and usually diminishes their enantiomeric separations.¹²⁵ The fact that methanol has minimal effects on enantiomeric separations by sulfated CF6 indicates that the hydrophobic side of CF6 is not responsible for the chiral recognitions, which is in accordance with the mechanisms deduced from HPLC separations. Sulfated CF6 showed excellent enantioselectivity towards primary, secondary, tertiary, and quaternary amines.¹⁰⁴ Enantiomeric separations can be obtained in both normal and reverse polarity modes, although the reversed polarity mode usually produced electropherograms with better peak shapes.¹⁰⁴ In addition, 25 native amino acids were also separated in the reversed polarity mode.¹⁰⁴

10.4.4 Derivatized CF6 for GLC

Permethylated and partially pentylated CF6 have been used as chiral selectors for gas-liquid chromatography (GLC).¹²⁶ The geometry of these chiral selectors was optimized using Hartree-Fock theory calculations at the 6-31g level. Computational studies showed that the high degree alkylation of CF6 changed the alternating inward/outward arrangements on the CF6 macrocyclic rim. As shown in Figure 10.2, the O_{center} -C2-C3 angle is 92° and 139° for inward and outward inclined fructofuranose units, respectively. After alkylation, the C3 symmetry of native CF6 is lost, the O_{center} -C2-C3 angles becomes larger on average (Table 10.2), the distances among the O3(*i*) atoms increases and thus original intramolecular hydrogen bonding of the native CF6 is disrupted, and the crown ether skeleton becomes more exposed (Figure 10.13). These structural changes after derivatization are also likely for other type derivatizations of CF6. Racemic compounds separated using alkylated CF6 as the selector in GCL includes: β -lactams, trifluoroacetyl derivatized amino acids and tartaric acid esters.¹²⁶ Hydrogen bonding is of critical

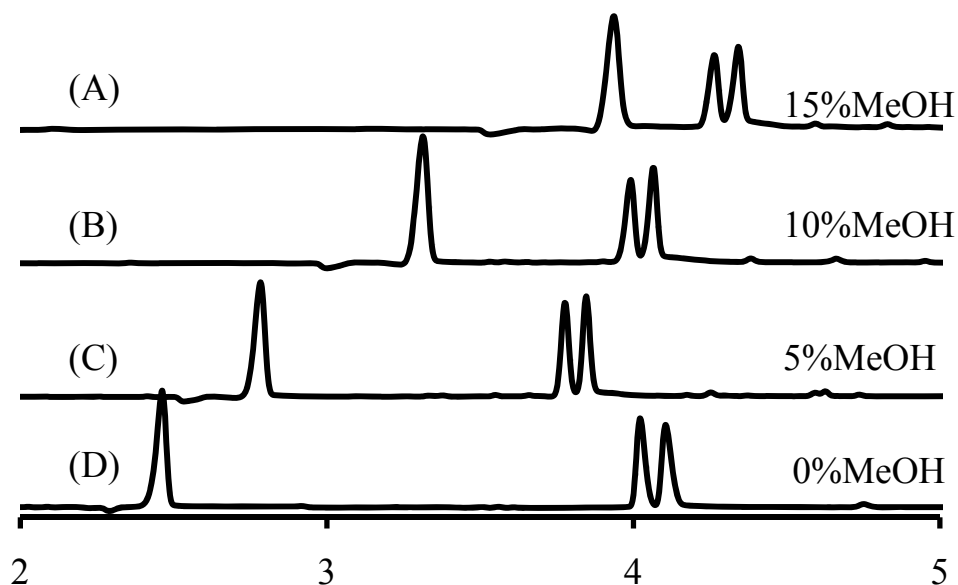


Figure 10.12 Effect of MeOH addition (in volume percentages) on the separation of *p*-chloroamphetamine using 5 mM sulfated cyclofructan as the chiral selector. CE conditions: buffer, 20 mM ammonium acetate; pH, 4.7; voltage, +25 kV; capillary length, 30/40 cm; capillary i.d., 50 μ m. First peak is EOF marker. The unit for the time axis (horizontal axis) is minute. Reprinted from reference 104 with permission.

Table 10.2 O_{center} -C2-C3 angles (as shown in Figure 10.2) for each of the six fructofuranose ring in native and derivatized CF6. a, X-ray structure of CF6 (obtained from reference 60g); b, structures calculated at B3LYP/cc-pVDZ level; c, X-ray structure of permethylated CF6 when crystallized with $Ba(SCN)_2$ (obtained from reference 84d); d, structures calculated at HF/b-31g level; e, all-4-O-all-6-O-pentylated CF6.

Fructose ring index	CF6(X-ray) ^a	CF6 ^b	PM-CF6(X-ray with $Ba(SCN)_2$) ^c	PM-CF6 ^d	PT-CF6 ^{d,e}
1	93.9	92.6	98.1	103.4	79.4
2	139.2	139.4	121.3	124.6	130.6
3	93.9	92.3	139.2	152.2	101.6
4	139.2	139.2	98.1	101.2	105.9
5	93.8	92.4	121.3	126.1	106.9
6	139.2	138.6	139.2	159.6	117.6

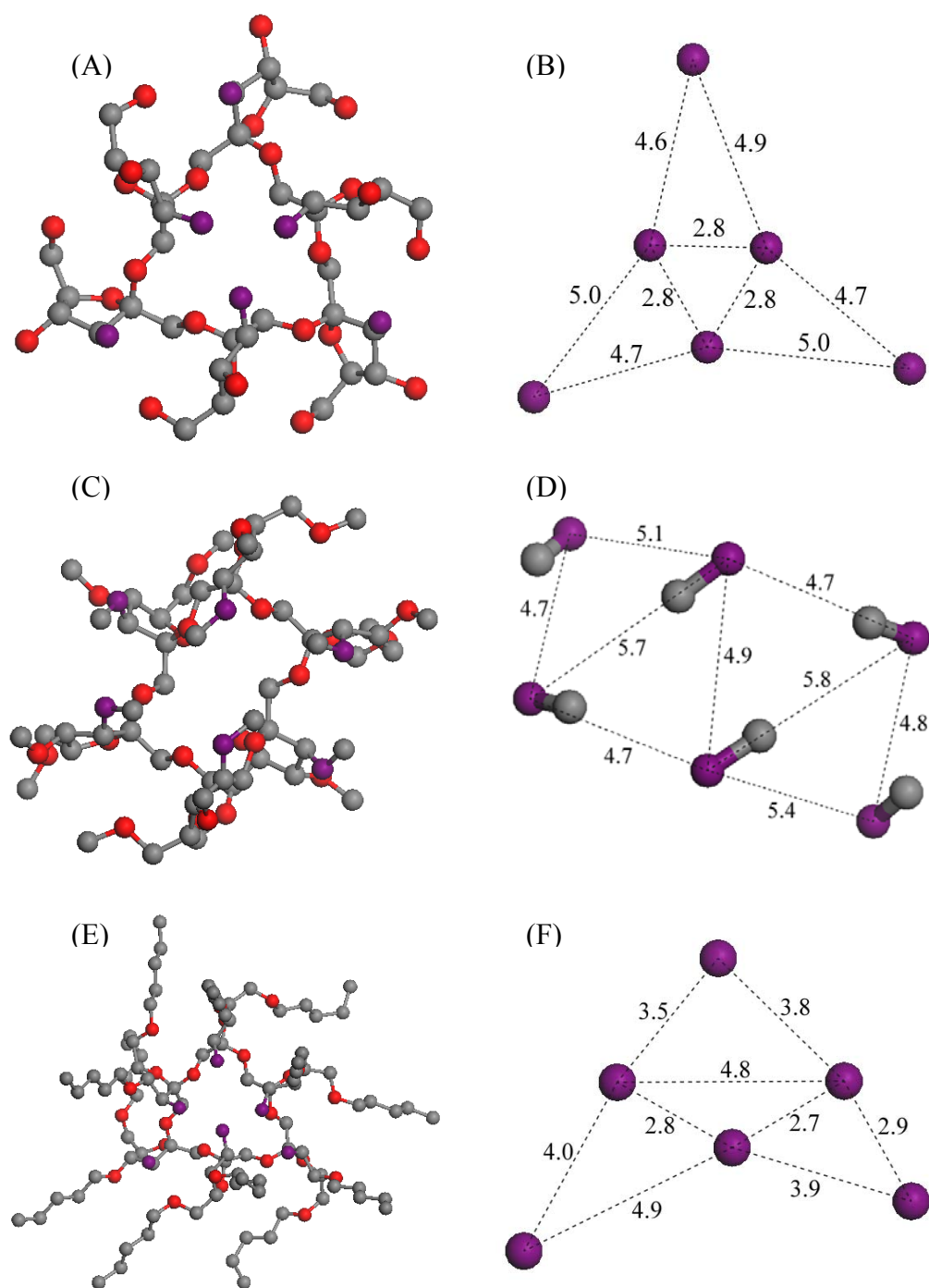
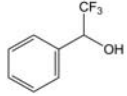
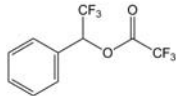
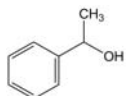


Figure 10.13 Top view of native and alkylated CF6: (A) and (B), native CF6 optimized at B3LYP/6-31g level; (C) and (D), permethylated CF6 optimized at HF/6-31g level; (E) and (F), all-4-O-all-6-O-pentylated CF6 optimized at HF/6-31g level. Figures on the right side are displaying relative positions of O3 atoms on each fructofuranose units. The distance between neighboring oxygen atoms are labeled in the unit of Å. Color coding: gray, carbon; oxygen, red; O3 oxygen atoms, purple. Hydrogen atoms are left out for clarity purpose.

Table 10.3 Chromatographic data for three structurally similar compounds on permethylated-CF6 chiral GLC phase at the same chromatographic condition. Data from reference 126.

No.	Compound	Structure	k_1'	α
1	α -(trifluoromethyl)benzyl alcohol		93.2	1.05
2	trifluoacetyl α -(trifluoromethyl)benzyl alcohol		4.2	1.00
z3	α -methylbenzyl alcohol		34.4	1.00

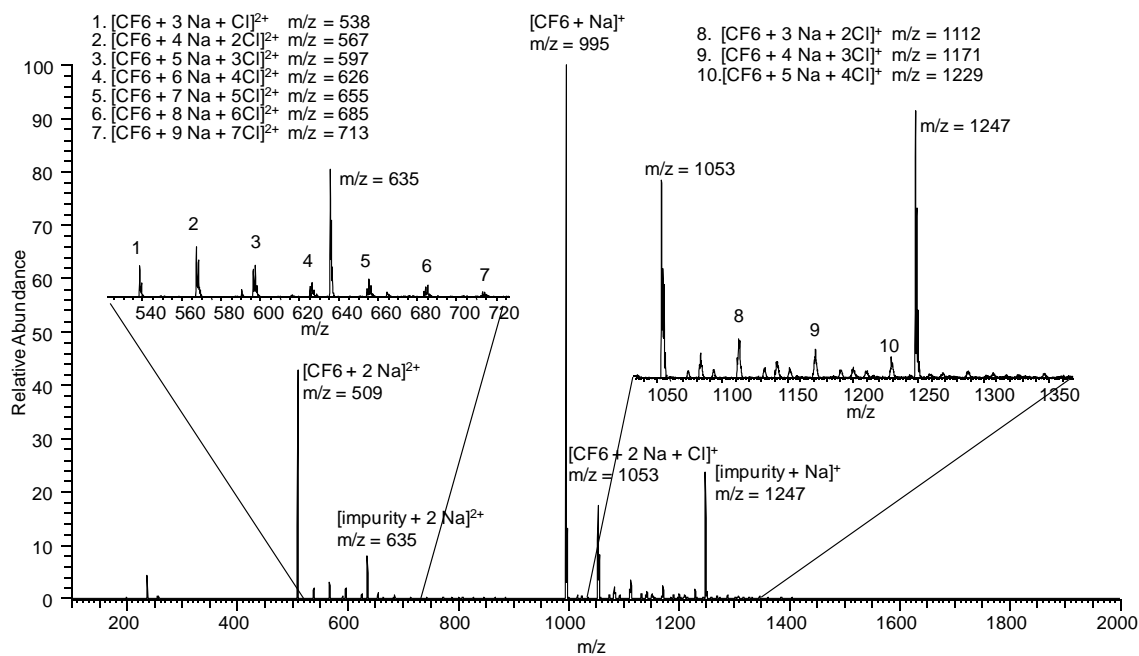


Figure 10.14 ESI-MS spectrum showing adduct ions of one CF6 with multiple sodium cations (see reference 127 for detail experimental conditions).

importance for enantiomeric separations in GLC. On permethylated CF6, α -(trifluoromethyl)-benzyl alcohol was baseline separated, whereas esters of this alcohol were less retained and no separation was observed (Table 10.3). Furthermore, no separation was observed for native α -methylbenzyl alcohol, which is a weaker hydrogen bond donor than α -(trifluoromethyl)benzyl alcohol. Likewise, enantiomers of N-acetylated amino acids were poorly separated or not separated, whereas N-trifluoroacetylated amino acids are very well separated.¹²⁶

10.5 Loading Tests on Cyclofructan Based CSPs

The loading capability of a CSP is related to the available number of selector-analyte interaction sites. For example, protein-based CSPs are vulnerable to overloading because protein selectors generally interact enantioselectively with only one analyte at a time. On the other hand, polymeric CSPs usually have high loading capabilities because its repeating units can provide multiple interaction sites for chiral recognition. Cyclofructans are oligomers. As shown in Figure 10.6, cyclofructans and derivatized cyclofructans can interact with chiral primary amines via tripod hydrogen bonding through at least several interaction sites. In addition, adducts of one CF6 with two metal cations, or multiple metal chloride salts were observed in ESI-MS (Figure 10.14). In contrast, crown ethers can only interact with one guest molecule at a time, and only 1:1 crown ether-metal cation complexes were observed in ESI-MS.¹²⁷ Consequently, cyclofructan-based CSPs are expected to have superior loading capabilities than crown ether-based CSPs. Loading test experiment was performed on a methylcarbamate CF6 CSP with *trans*-1-amino-2-indanol in the polar organic mode. As shown in Figure 10.15, 3.37 mg of the primary amine can be baseline separated in 20 min on an analytical column (250 \times 4.6 mm). Furthermore, cyclofructan type CSPs operates best in organic solvents and supercritical fluid solvents as well, which makes the sample recovery much easier than with aqueous mobile phases. These characteristics make the cyclofructan type of CSPs viable candidates for the preparative separations of primary amines. In addition, high loading of N-blocked amino acids were also reported on aromatic-derivatized CF6 CSPs.¹²²

10.6 Conclusions

Cyclofructans are a new class of chiral selectors. Despite the fact that they are cyclic oligosaccharides and have a crown ether core, their chiral recognition capabilities are completely different from either

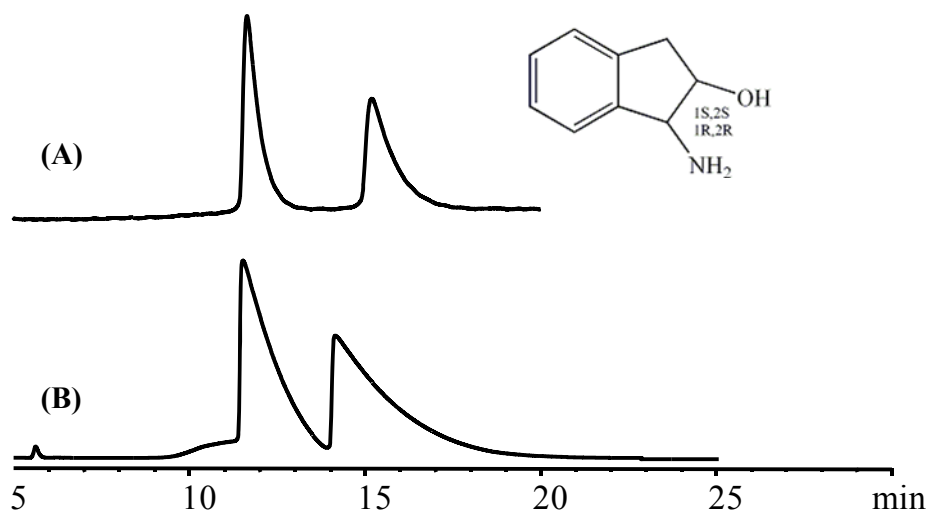


Figure 10.15 Loading test of a methyl carbamate CF6 CSP in the polar organic mode. (A) 13.5 μ g and (B) 3.37 mg of *trans*-1-amino-2-indanol were injected on a 250 x 4.6 mm column. Mobile phase: acetonitrile/methanol/acetic acid/triethylamine 75/25/0.3/0.2.

cyclodextrins or crown ethers. Two chiral recognition mechanisms are proposed for cyclofructan CSPs. Tripodal hydrogen bonding between the hydroxyl groups on the hydrophilic side of CF6 and hydrogen bonding donor and/or acceptors in analytes is of critical importance for enantiomeric separations of primary amine type compounds. On the other hand, chiral helical grooves on the side of CF6, along with the carbamate linked aromatic substituents, can provide steric and π - π interactions between the CSP and analytes. These interactions contribute to chiral recognition for aromatic non-primary amine compounds separated on the aromatic-derivatized CF6 CSPs.

While native CF6 showed only limited enantioselectivity to a few compounds, derivatized CF6 appeared to be versatile chiral selectors and can be tuned for the best HPLC separation of different types of compounds. Aliphatic-derivatized cyclofructans operating in the polar organic mode provide best enantiomeric separations for primary amines. On the other hand, extensively aromatic-derivatized CF6 were able to separate a variety of different classes of enantiomers. Cyclofructans are the newest types of chiral selectors, and their further development and their applications in both analytical and preparative enantiomeric separations are expected to grow in the future.

CHAPTER 11

CONCLUSIONS AND REMARKS

11.1 Conclusions

11.1.1 Part One (Chapter 2 and 3)

All 12 β -lactams were successfully separated on cyclodextrin-based CSPs. The 3,5-dimethylphenyl derivatized β -cyclodextrin column (Cyclobond I 2000 DMP) operating in the reversed phase mode (acetonitrile/water solvents) is the preferred chromatographic approach for their enantiomeric separation. The first efficient baseline separation of all-*trans*-astaxanthin stereoisomers was obtained on an immobilized 3,5-dichlorophenyl derivatized cellulose column (Chiralpak IC) using methyl t-butyl ether and acetonitrile as mobile phase solvents. In addition, stereoisomers of several structurally related compounds were also separated in the same chromatographic conditions. As a result, Chiralpak IC is recommended for the separation of astaxanthin type compounds.

11.1.2 Part Two (Chapter 4, 5, 6 and 7)

Boromycin is a specific chiral selector for primary amine compounds: 52 out of 53 tested chiral primary amines were separated successfully. The boromycin CSP is most selective in the presence of polar organic solvents. Because of the strength of the CSP-amine complex, mM concentrations of a competitive binding additive (i.e., tetramethylammonium nitrate) profoundly enhances efficiency and decreases retention. Most separations are completed in 4-10 minutes.

Cyclofructans are a new class of chiral selectors. Their mass production is possible via fermentation of inulin. There are 18 to 24 of hydroxyl groups in cyclofructans that can be functionalized to afford different chiral selectors. While native cyclofructan 6 has limited capabilities as a chiral selector, specific, derivatized cyclofructans appear to be exceptional chiral selectors which can be “tuned” to separate enantiomers of different types of molecules. When partially derivatized with aliphatic functionalities, CF6 becomes an excellent selector for chiral primary amines in organic mobile phases. When CF6 is extensively

functionalized with aromatic moieties, it no longer effectively separates primary amine racemates.

However, it does separate a broad variety of other enantiomers.

The polymeric CSP based on a new monomer, *trans*-9, 10-dihydro-9, 10-ethanoanthracene-(11S, 12S)-11, 12-dicarboxylic acid bis-4-vinylphenylamide, is a valuable addition to the commercially available polymeric type of P-CAP and P-CAP-DP CSPs. The new CSP (DEABV) showed competitive performance with P-CAP and P-CAP-DP CSPs. Totally 70 out of 200 random selected chiral compounds were separated on the new polymeric CSP. The CSP operates best in the normal phase mode using heptane/ethanol solvents with acidic additives. Its high loading property was demonstrated by the separation of 1 mg of N-(3,5-dinitrobenzoyl)-phenylglycine at a resolution of 2.6 on an analytical column (250 x 4.6 mm). These polymeric CSPs also were tested and compared in SFC. The normal phase separations on these polymeric CSPs were successfully transferred into SFC separations. The advantages of SFC over HPLC separations are: short separation times, i.e., usually less than 5 min; low consumption of organic solvents; and easy recovery of the separated solutes. Overall, the DEABV CSP is the most broadly applicable and useful of these polymeric CSPs.

11.1.3 Part Three (Chapter 8, 9, and 10)

Part three of the thesis studied the host-guest chemistry of cyclofructans and its applications. In addition, theoretical computations were carried out to help understanding of the chiral recognition mechanism of cyclofructan-based CSPs.

The complexation between cyclofructans and alkaline metal cations was studied by ESI-MS. In the gas phase, cyclofructans bind to alkali metal cations in the order of $\text{Li}^+ > \text{Na}^+ > \text{K}^+ > \text{Rb}^+ > \text{Cs}^+$. The gas phase selectivity, obtained by competitive dissociation of ternary complexes between one cyclofructan and two different metal cations, was confirmed with density functional theory calculations. For the solution phase study, sodium and potassium complexes of cyclofructans were the most abundant species in the ESI-MS spectra. Compared with previous solution phase studies of cyclofructans, ESI-MS produced a higher abundance of complexes with smaller metal cations and lower abundances of complexes with larger metal cations. The relative intensities of different cyclofructan-metal cation complexes observed on ESI-MS spectra was a reflection of both solution phase and gas phase stability of different complex ions.

Cyclofructans form complexes with metal cations. We designed ligand-exchange separations of cyclofructans (CF6, CF7, and CF8) based on their specific complexation differences with metal cations. The separation was performed on a silica based SCX column charged with metal cations. A barium charged SCX column provides the best separation between CF6 and CF7, whereas a silver charged SCX column provides the greatest separation between CF7 and CF8. The analytical methods could be scaled up for mass production of CF7 with high purity.

The chiral recognition mechanism was studied using computational methods in combination with chromatographic data obtained experimentally. Despite the fact that cyclofructans are cyclic oligosaccharides and that they have a crown ether central macrocyclic core, the chiral recognition mechanism of cyclofructans are completely different from that of either cyclodextrins or synthetic crown ethers. Two chiral recognition mechanisms are proposed for cyclofructan CSPs. Hydrogen bonding between the hydroxyl groups on the hydrophilic side of CF6 and hydrogen bonding donor and/or acceptors in chiral analytes is of critical importance for chiral separations of amine type compounds. On the other hand, chiral helical grooves on the side of CF6, along with the carbamate linked aromatic derivatization moieties, can provide steric and π - π interactions between these CSPs and aromatic analytes. These interactions are responsible for chiral recognition of aromatic non-primary amine compounds separated on high aromatic-derivatized CF6 CSPs.

11.2 Remarks

We have demonstrated three major approaches to facilitate chiral methods development. Firstly, trial-and-error is still the most commonly adopted approach. Chiral method development in pharmaceutical companies relies on automated column screening approaches. A series of complementary CSPs, with the highest success rates, are screened at predetermined chromatographic conditions. Although time consuming, an overall success rate of 80% to 90% can be achieved on a well-established screening strategy.¹²⁸

Secondly, the continuous development of new CSPs that specifically separate a class of compounds is attractive. These types of CSPs can provide a “yes or no” answer to whether a compound will be separated even without any scouting HPLC injections. In addition, the same class of compounds is usually separated

in the same or similar chromatographic conditions on a specific CSP. As a result, minimal effort would be needed for method development on this type of CSP. Crown ether CSPs and the boromycin CSP belong to this type. They were initially discovered to have specific host-guest chemistry for primary amines, and based on this characteristic, they were extended to applications as CSPs for enantiomeric separation of chiral primary amines with high success rates. From the examples of crown ether and boromycin, it is clear that molecules with specific host-guest chemistry are potentially successful CSPs for a specific class of compounds. With this approach in mind, the discovery of new host molecules, being natural products or synthetic compounds, would provide a good source for new CSPs.

Thirdly, a clear understanding the chiral recognition mechanism would help to pin-point the starting chromatographic conditions or even predict the separation conditions for certain analytes. This is only possible with large amount of chromatographic data collected for a specific CSP. By comparing the separation of structural similar compounds or the separation of same compounds under different chromatographic conditions, the general properties of a CSP can sometimes be revealed. Computational tools are starting to play a role in understanding chiral recognition. The geometry of chiral selector and analytes, and possible binding sites can be examined by energy minimization computations. The adsorption of analytes on CSP surfaces can be studied by molecular dynamics methods. However, this type of application is still at a rudimentary stage, but is expected to grow with the continuous development of both computational methodologies and computer hardware.

In addition to these three approaches, computers are going to play a more important role in chiral method development as they do in almost every scientific field. With almost thirty years' development of chiral HPLC separations, there are huge amounts of chromatographic data available. Data mining tools using modern algorithms would help us to use the huge chromatographic database more creatively, and to extract useful information for further guidance into chiral method development. This is a fast expanding field. Several applications have already emerged. For example, with a new chiral compound, a structural similarity search can be used to isolate all separations achieved on structurally similar molecules. This would help to establish a starting condition for method development of the new chiral compound. Classification algorithms can help to give a "yes or no" answer as to whether a compound can be separated

on a certain CSP. Quantitative structure-retention relationships (QSRR) methods can even predict retention times, elution order and enantioselectivity of a pair of enantiomers at a specified chromatographic condition.

REFERENCES

1. Ariëns, E. J. *Drug Metab. Rev.* **1984**, *15* (3), 425-504.
2. MacDermott, A. J.; Barron, L. D.; Brack, A.; Buhse, T.; Drake, A. F.; Emery, R.; Gottarelli, G. et al. *Planet. Space Sci.* **1996**, *44* (11), 1441-1446.
3. *Science* **2005**, *309* (5731), 78b-102.
4. (a) Maher, T. J.; Johnson, D. A. *Drug Dev. Res.* **1991**, *24* (2), 149-156; (b) Owens, J. M. M. J. *Prim Care Companion J. Clin. Psychiatry* **2003**, *5* (2), 70-73.
5. (a) *Chirality* **1992**, *4* (5), 338-340; (b) Rauws, A. G.; Groen, K. *Chirality* **1994**, *6* (2), 72-75.
6. Caner, H.; Groner, E.; Levy, L.; Agranat, I. *Drug Discovery Today* **2004**, *9* (3), 105-110.
7. Armstrong, D. W.; Zhang, B. *Anal. Chem.* **2001**, *73* (19), 557 A-561 A.
8. (a) Ojima, I.; Lin, S. *J. Org. Chem.* **1998**, *63* (2), 224-225; (b) Yang, Y.; Wang, F.; Rochon, F. D.; Kayser, M. M. *Can. J. Chem.* **2005**, *83* (1), 28-36.
9. (a) Agami, C.; Dechoux, L.; Hebbe, S.; Menard, C. *Tetrahedron* **2004**, *60* (25), 5433-5438; (b) Madan, S.; Milano, P.; Eddings, D. B.; Gawley, R. E. *J. Org. Chem.* **2005**, *70* (8), 3066-3071; (c) Ojima, I. *Acc. Chem. Res.* **1995**, *28* (9), 383-389.
10. (a) Cirilli, R.; Del Giudice, M. R.; Ferretti, R.; La Torre, F. *J. Chromatogr. A* **2001**, *923* (1-2), 27-36; (b) Ficarra, R.; Calabro, M. L.; Tommasini, S.; Costantino, D.; Carulli, M.; Melardi, S.; Di Bella, M. R.; Casuscelli, F.; Romeo, R.; Ficarra, P. *Chromatographia* **1996**, *43* (7/8), 365-368; (c) Peter, A.; Arki, A.; Forro, E.; Fueleop, F.; Armstrong, D. W. *Chirality* **2005**, *17* (4), 193-200; (d) Pirkle, W. H.; Finn, J. M.; Schreiner, J. L.; Hamper, B. C. *J. Am. Chem. Soc.* **1981**, *103* (13), 3964-3966; (e) Pirkle, W. H.; Spence, P. L. *Chirality* **1998**, *10* (5), 430-433; (f) Pirkle, W. H.; Tsipouras, A.; Hyun, M. H.; Hart, D. J.; Lee, C. S. *J. Chromatogr.* **1986**, *358* (2), 377-384.
11. (a) Armstrong, D. W.; DeMond, W. *J. Chromatogr. Sci.* **1984**, *22* (9), 411-415; (b) Armstrong, D. W.; DeMond, W.; Czech, B. P. *Anal. Chem.* **1985**, *57* (2), 481-484; (c) Armstrong, D. W.; Ward, T. J.; Armstrong, R. D.; Beesley, T. E. *Science* **1986**, *232* (4754, Pt. 1), 1132-1135; (d) Armstrong, D. W.; Zukowski, J. *J. Chromatogr. A* **1994**, *666* (1-2), 445-448; (e) Mitchell, C.; Desai, M.; McCulla, R.; Jenks, W.; Armstrong, D. *Chromatographia* **2002**, *56* (3/4), 127-135; (f) Soukup, R. J.; Rozhkov, R. V.; Larock, R. C.; Armstrong, D. W. *Chromatographia* **2005**, *61* (5/6), 219-224.
12. (a) Higuera-Ciapara, I.; Felix-Valenzuela, L.; Goycoolea, F. M. *Crit. Rev. Food Sci. Nutr.* **2006**, *46* (2), 185-96; (b) Olaizola, M. *Nutraceutical Sci. and Technol.* **2007**, *7*, 321-343.
13. Miki, W. *Pure Appl. Chem.* **1991**, *63* (1), 141-146.
14. Chew, B. P.; Park, J. S. *J. Nutr.* **2004**, *134* (1), 257S-261S.
15. Chew, B. P.; Park, J. S.; Wong, M. W.; Wong, T. S. *Anticancer Res.* **1999**, *19* (3A), 1849-1853.
16. Misawa, N.; Satomi, Y.; Kondo, K.; Yokoyama, A.; Kajiwara, S.; Saito, T.; Ohtani, T.; Miki, W. *J. Bacteriol.* **1995**, *177* (22), 6575-6584.
17. (a) Choi, S.-K.; Matsuda, S.; Hoshino, T.; Peng, X.; Misawa, N. *Appl. Microbiol. Biotechnol.* **2006**, *72* (6), 1238-1246; (b) Ye, R. W.; Yao, H.; Stead, K.; Wang, T.; Tao, L.; Cheng, Q.; Sharpe, P. L.; Suh, W.; Nagel, E.; Arcilla, D.; Dragotta, D.; Miller, E. S. *J. Ind. Microbiol. Biotechnol.* **2007**, *34* (4), 289-299.
18. Britton, G. *FASEB J.* **1995**, *9* (15), 1551-1558.
19. Johnson, E. A.; An, G. H. *Crit. Rev. Biotechnol.* **1991**, *11* (4), 297-326.
20. Parajo, J. C.; Santos, V.; Vazquez, M. *Alimentacion, Equipos y Tecnologia* **1996**, *15* (1), 153-160.
21. Grewe, C.; Menge, S.; Griehl, C. *J. Chromatogr. A* **2007**, *1166* (1-2), 97-100.
22. Lura, H.; Saegrov, H. *Can. J. Fish. Aquat. Sci.* **1991**, *48* (3), 429-433.
23. Vecchi, M.; Mueller, R. K. *HRC & CC, J. High Resolut. Chromatogr. & Chromatogr. Commun.* **1979**, *2* (4), 195.

24. (a) Abu-Lafi, S.; Turujman, S. A. *Enantiomer* **1997**, *2* (1), 17-25; (b) Abu-Lafi, S.; Turujman, S. A. *J. Chromatogr. A* **1999**, *855* (1), 157-170; (c) Maoka, T.; Komori, T.; Matsuno, T. *J. Chromatogr.* **1985**, *318* (1), 122-124.
25. Turujman, S. A. *J. Chromatogr.* **1993**, *631* (1-2), 197-199.
26. Misawa, N.; Satomi, Y.; Kondo, K.; Yokoyama, A.; Kajiwara, S.; Saito, T.; Ohtani, T.; Miki, W. *J. Bacteriol.* **1995**, *177* (22), 6575-6584.
27. (a) Yuan, J. P.; Chen, F. *J. Agric. Food Chem.* **1999**, *47* (9), 3656-60; (b) Yuan, J.-P.; Chen, F. *J. Agric. Food Chem.* **1999**, *47* (9), 3656-3660.
28. Renströma, B.; Borchb, G.; Skulbergc, O. M.; Liaaen-Jensen, S. *Phytochem.* **1981**, *20* (11), 2561-2564.
29. (a) He, L.; Beesley, T. E. *J. Liq. Chromatogr. Related Technol.* **2005**, *28* (7-8), 1075-1114; (b) Schurig, V. *J. Chromatogr. A* **2001**, *906* (1-2), 275-299.
30. (a) Vigh, G.; Sokolowski, A. D. *Electrophoresis* **1997**, *18* (12-13), 2305-2310; (b) Ward, T. J.; Hamburg, D.-M. *Anal. Chem.* **2004**, *76* (16), 4635-4644.
31. (a) Armstrong, D. W.; Zhang, B. *Anal. Chem.* **2001**, *73* (19), 557A-561A; (b) Maier, N. M.; Franco, P.; Lindner, W. *J. Chromatogr. A* **2001**, *906* (1-2), 3-33; (c) Stalcup, A. M.; Chang, S. C.; Armstrong, D. W. *J. Chromatogr.* **1991**, *540* (1-2), 113-128; (d) Davankov, V. A. *Enantiomer* **2000**, *5* (3-4), 209-223; (e) Ward, T. J.; Farris, A. B. *J. Chromatogr. A* **2001**, *906* (1-2), 73-89; (f) Lammerhofer, M.; Lindner, W. *J. Chromatogr. A* **1996**, *741*, 33-48; (g) Okamoto, Y.; Yashima, E., *Angew. Chem., Int. Ed.* **1998**, *37*, 1020-1043.
32. (a) Anderson, S.; Allenmark, S. G., *J. Biochem. Biophys. Methods* **2002**, *54*, 11; (b) Francotte, E. R., *J. Chromatogr. A* **2001**, *906*, 379-397.
33. (a) Brocks, D. R., *Biopharm. Drug Dispos.* **2006**, *27*, 387-406; (b) Desai, M. J.; Gill, M. S.; Hsu, W. H.; Armstrong, D. W., *Chirality* **2005**, *17*, 154-162; (c) Lu, X.; Liu, P.; Chen, H.; Qin, F.; Li, F., *Biomed. Chromatogr.* **2005**, *19*, 703-708; (d) Miura, M.; Uno, T.; Tateishi, T.; Suzuki, T., *Chirality* **2007**, *19*, 223-227.
34. (a) Han, X.; Berthod, A.; Wang, C.; Huang, K.; Armstrong, D. W. *Chromatographia* **2007**, *65*, 381-400; (b) Liu, Y.; Berthod, A.; Mitchell, C. R.; Xiao, T. L.; Zhang, B.; Armstrong, D. W., *J. Chromatogr. A* **2002**, *978*, 185-204; (c) Schurig, V.; Fluck, M., *J. Biochem. Biophys. Methods* **2000**, *43*, 223-240; (d) Terfloth, G., *J. Chromatogr. A* **2001**, *906*, 301-307; (e) Villeneuve, M. S.; Anderegg, R. J., *J. Chromatogr. A* **1998**, *826*, 217-225.
35. (a) Bakhtiar, R.; Ramos, L.; Francis, L. S., *Chirality* **2001**, *13*, 63-74; (b) Desai, M.; Armstrong, D., *W. J. Chromatogr., A* **2004**, *1035*, 203-210; (c) Ding, J.; Desai, M.; Armstrong, D. W., *J. Chromatogr. A* **2005**, *1076*, 34-43; (d) Xia, Y. Q.; Liu, D. Q.; Bakhtiar, R., *Chirality* **2002**, *14*, 742-749.
36. (a) Armstrong, D. W.; Demond, W., *J. Chromatogr. Sci.* **1984**, *22*, 411-415; (b) Armstrong, D. W.; Tang, Y.; Chen, S.; Zhou, Y.; Bagwill, C.; Chen, J. R., *Anal. Chem.* **1994**, *66*, 1473-1484; (c) Armstrong, D. W.; Ward, T. J.; Armstrong, R. D.; Beesley, T. E., *Science* **1986**, *232*, 1132-1135; (d) Berthod, A.; Chen, X.; Kullman, J. P.; Armstrong, D. W.; Gasparrini, F.; D'Acquarica, I.; Villani, C.; Carotti, A., *Anal. Chem.* **2000**, *72*, 1767-1780.
37. Whiteside, I. R. C.; Worsfold, P. J., *Anal. Chim. Acta* **1988**, *212*, 155-163.
38. (a) Macrae, C. F.; Edgington, P. R.; McCabe, P.; Pidcock, E.; Shields, G. P.; Taylor, R.; Towler, M.; van de Streek, J., *J. Appl. Crystallogr.* **2006**, *39*, 453-457; (b) Frisch, M. J. T., G. W.; Schlegel, H. B.; Scuseria, G. E.; Robb, M. A.; Cheeseman, J. R.; Montgomery, Jr., J. A. et al. *Gaussian 03*, Revision C.02; Gaussian, Inc., Wallingford CT: 2004.
39. Hutter, R.; Keller-Schierlein, W.; Knusel, F.; Prelog, V.; Rodgers, G. C.; Jr, n.; Vogel, G.; Voser, W.; Zahner, H., *Helv. Chim. Acta* **1967**, *50*, 1533-1539.
40. Waksman, S. A.; Woodruff, H. B., *J. Bacteriol.* **1941**, *42*, 231-249.
41. (a) Pache, W., *Antibiotics* **1975**, *3*, 585-587; (b) White, J. D.; Avery, M. A.; Choudhry, S. C.; Dhingra, O. P.; Gray, B. D.; Kang, M. C.; Kuo, S. C.; Whittle, A., *J. Am. Chem. Soc.* **1989**, *111*, 790-792.
42. Kohno, J.; Kawahata, T.; Otake, T.; Morimoto, M.; Mori, H.; Ueba, N.; Nishio, M.; Kinumaki, A.; Komatsubara, S.; Kawashima, K., *Biosci. Biotechnol. Biochem.* **1996**, *60*, 1036-1037.
43. Lakatos, B.; Kaiserova, K.; Simkovic, M.; Orlicky, J.; Knezl, V.; Varecka, n., *Mol. Cell. Biochem.* **2002**, *231*, 15-22.

44. Arai, M.; Koizumi, Y.; Sato, H.; Kawabe, T.; Suganuma, M.; Kobayashi, H.; Tomoda, H.; Mura, S., *J. Antibiot.* **2004**, *57*, 662-668.
45. Boeseken, J.; Vermaas, N., *J. Phys. Chem.* **1931**, *35*, 1477-1489.
46. (a) Dunitz, J. D.; Hawley, D. M.; Miklos, D.; White, D. N. J.; Berlin, Y.; Marusic, R.; Prelog, V., *Helv. Chim. Acta* **1971**, *54*, 1709-1713; (b) Marsh, W.; Dunitz, J. D.; White, D. N. J., *Helv. Chim. Acta* **1974**, *57*, 10-17.
47. (a) Dotsevi Yao Sogah, G.; Cram, D. J., *J. Am. Chem. Soc.* **1979**, *101*, 3035-3042; (b) Hilton, M.; Armstrong, D. W., *J. Liq. Chromatogr.* **1991**, *14*, 9-28; (c) Hilton, M.; Armstrong, D. W., *J. Liq. Chromatogr.* **1991**, *14*, 3673-3683; (d) Lingenfelter, D. S.; Helgeson, R. C.; Cram, D. J., *J. Org. Chem.* **1981**, *46*, 393-406; (e) Newcomb, M.; Toner, J. L.; Helgeson, R. C.; Cram, D. J., *J. Am. Chem. Soc.* **1979**, *101*, 4941-4947; (f) Shinbo, T.; Yamaguchi, T.; Nishimura, K.; Sugiura, M., *J. Chromatogr.* **1987**, *405*, 145-153; (g) Machida, Y.; Nishi, H.; Nakamura, K.; Nakai, H.; Sato, T., *J. Chromatogr. A* **1998**, *805*, 85-92; (h) Hyun, M. H.; Jin, J. S.; Lee, W., *Bull. Korean Chem. Soc.* **1998**, *19*, 819-821.
48. (a) Oguni, K.; Oda, H.; Ichida, A. *J. Chromatogr. A* **1995**, *694* (1), 91-100; (b) Okamoto, Y.; Kaida, Y. *J. Chromatogr. A* **1994**, *666* (1-2), 403-419; (c) Okamoto, Y.; Kawashima, M.; Hatada, K. *J. Chromatogr. A* **1986**, *363* (2), 173-186; (d) Okamoto, Y.; Nakano, T. *Chem. Rev.* **1994**, *94* (2), 349-372; (e) Okamoto, Y.; Yashima, E. *Angew. Chem. Int. Ed.* **1998**, *37* (8), 1020-1043; (f) Yashima, E.; Fukaya, H.; Okamoto, Y. *J. Chromatogr. A* **1994**, *677* (1), 11-19; (g) Yashima, E.; Okamoto, Y. *Bull. Chem. Soc. Jpn.* **1995**, *68* (12), 3289-3307; (h) Yashima, E.; Okamoto, Y. *Chemical Analysis (New York)* **1997**, *142*, 345-376; (i) Yashima, E.; Sahavattapong, P.; Okamoto, Y. *Chirality* **1996**, *8* (6), 446-451; (j) Yashima, E.; Yamada, M.; Kaida, Y.; Okamoto, Y. *J. Chromatogr. A* **1995**, *694* (2), 347-354.
49. (a) Armstrong, D. W.; Rundlett, K.; Reid, G. L. *Anal. Chem.* **1994**, *66* (10), 1690-1695; (b) Armstrong, D. W.; Tang, Y.; Chen, S.; Zhou, Y.; Bagwill, C.; Chen, J.-R. *Anal. Chem.* **1994**, *66* (9), 1473-1484; (c) Berthod, A.; Valleix, A.; Tizon, V.; Leonce, E.; Caussignac, C.; Armstrong, D. W. *Anal. Chem.* **2001**, *73* (22), 5499-5508; (d) Berthod, A.; Xiao, T. L.; Liu, Y.; Jenks, W. S.; Armstrong, D. W. *J. Chromatogr. A* **2002**, *955* (1), 53-69; (e) Ekborg-Ott, K. H.; Kullman, J. P.; Wang, X.; Gahm, K.; He, L.; Armstrong, D. W. *Chirality* **1998**, *10* (7), 627-660; (f) Ekborg-Ott, K. H.; Liu, Y.; Armstrong, D. W. *Chirality* **1998**, *10* (5), 434-483; (g) Karlsson, C.; Karlsson, L.; Armstrong, D. W.; Owens, P. K. *Anal. Chem.* **2000**, *72* (18), 4394-4401; (h) Liu, Y.; Berthod, A.; Mitchell, C. R.; Xiao, T. L.; Zhang, B.; Armstrong, D. W. *J. Chromatogr. A* **2002**, *978* (1-2), 185-204; (i) Mitchell, C. R.; Armstrong, D. W.; Berthod, A. *J. Chromatogr. A* **2007**, *1166* (1-2), 70-78; (j) Péter, A.; Török, G.; Armstrong, D. W. *J. Chromatogr. A* **1998**, *793* (2), 283-296; (k) Török, G.; Péter, A.; Armstrong, D. W.; Tourwé, D.; Tóth, G.; Säpi, J. *Chirality* **2001**, *13* (10), 648-656.
50. (a) Gubitz, G.; Schmid Martin, G. *Methods Mol. Biol.* **2004**, *243*, 1-28; (b) Lämmerhofer, M.; Lindner, W. *J. Chromatogr. A* **1996**, *741* (1), 33-48; (c) Maier, N. M.; Franco, P.; Lindner, W. *J. Chromatogr. A* **2001**, *906* (1-2), 3-33; (d) Pirkle, W. H.; Welch, C. J. *Tetrahedron: Asymmetry* **1994**, *5* (5), 777-780.
51. Wang, C.; Armstrong, D. W.; Riskey, D. S. *Anal. Chem.* **2007**, *79* (21), 8125-8135.
52. (a) Kawamura, M.; Uchiyama, T. *Carbohydr. Res.* **1994**, *260* (2), 297-304; (b) Kawamura, M.; Uchiyama, T.; Kuramoto, T.; Tamura, Y.; Mizutani, K. *Carbohydr. Res.* **1989**, *192*, 83-90.
53. Armstrong, D.; Ward, T.; Armstrong, R.; Beesley, T. *Science* **1986**, *232* (4754), 1132-1135.
54. (a) Mori, H.; Nishioka, M.; Nanjo, F. JP Patent 2006067896, **2006**; (b) Mori, H.; Nishioka, M.; Nanjo, F. JP Patent 2006067895, **2006**; (c) Nishioka, M.; Mori, H.; Nanjo, F. JP Patent 2004337132, **2004**.
55. Mori, H.; Nishioka, M.; Nanjo, F. JP Patent 2006067894, **2006**.
56. Fang, Y.; Ferrie, A. M. JP Patent 2005048648, **2005**.
57. Yokoyama, H.; Ikeuchi, H.; Teranishi, Y.; Murayama, H.; Sano, K.; Sawada, K. JP Patent 2282147, **1995**.
58. Ozaki, K.; Hayashi, M. *Int. J. Pharm.* **1998**, *160* (2), 219-227.
59. Reijenga, J. C.; Verheggen, T. P. E. M.; Chiari, M. *J. Chromatogr. A* **1999**, *838* (1-2), 111-119.
60. (a) Immel, S.; Schmitt, G. E.; Lichtenthaler, F. W. *Carbohydr. Res.* **1998**, *313* (2), 91-105; (b) Kanai, T.; Ueki, N.; Kawaguchi, T.; Teranishi, Y.; Atomi, H.; Tomorbaatar, C.; Ueda, M.; Tanaka, A. *Appl. Environ. Microbiol.* **1997**, *63* (12), 4956-4960; (c) Kida, T.; Inoue, Y.; Zhang, W.; Nakatsuji, Y.; Ikeda, I. *Bull. Chem. Soc. Jpn.* **1998**, *71* (5), 1201-1205; (d) Kushibe, S.; Mitsui, K.; Yamagishi, M.; Yamada, K.;

- Morimoto, Y. *Biosci. Biotechnol. Biochem.* **1995**, *59* (1), 31-34; (e) Kushibe, S.; Sashida, R.; Morimoto, Y. *Biosci. Biotechnol. Biochem.* **1994**, *58* (6), 1136-1138; (f) Sawada, M.; Tanaka, T.; Takai, Y.; Hanafusa, T.; Hirotsu, K.; Higuchi, T.; Kawamura, M.; Uchiyama, T. *Chem. Lett.* **1990**, *19* (11), 2011-2014; (g) Sawada, M.; Tanaka, T.; Takai, Y.; Hanafusa, T.; Taniguchi, T.; Kawamura, M.; Uchiyama, T. *Carbohydr. Res.* **1991**, *217*, 7-17.
61. Zhong, Q.; He, L.; Beesley, T. E.; Trahanovsky, W. S.; Sun, P.; Wang, C.; Armstrong, D. W. *J. Chromatogr. A* **2006**, *1115* (1-2), 19-45.
62. (a) Armstrong, D. W.; Chang, C.-D.; Haing Lee, S. *J. Chromatogr. A* **1991**, *539* (1), 83-90; (b) Armstrong, D. W.; Hilton, M.; Coffin, L. *LC-GC* **1991**, *9* (9), 646, 648-652; (c) Armstrong, D. W.; Stalcup, A. M.; Hilton, M. L.; Duncan, J. D.; Faulkner, J. R.; Chang, S. C. *Anal. Chem.* **1990**, *62* (15), 1610-1615; (d) Hargitai, T.; Kaida, Y.; Okamoto, Y. *J. Chromatogr. A* **1993**, *628* (1), 11-22; (e) Stalcup, A. M.; Chang, S.-C.; Armstrong, D. W. *J. Chromatogr. A* **1991**, *540*, 113-128.
63. (a) Hilton, M.; Armstrong, D. W. *J. Liq. Chromatogr. Related Technol.* **1991**, *14* (1), 9 - 28; (b) Kuhn, R. *Electrophoresis* **1999**, *20* (13), 2605-2613; (c) Nishi, H.; Nakamura, K.; Nakai, H.; Sato, T. *J. Chromatogr. A* **1997**, *757* (1-2), 225-235; (d) Walbroehl, Y.; Wagner, J. *J. Chromatogr. A* **1994**, *680* (1), 253-261.
64. (a) Pirkle, W. H.; Pochapsky, T. C. *J. Am. Chem. Soc.* **1986**, *108* (2), 352-354; (b) Pirkle, W. H.; Pochapsky, T. C. *Chem. Rev.* **1989**, *89* (2), 347-362.
65. (a) Miller, L.; Orihuela, C.; Fronek, R.; Murphy, J. *J. Chromatogr. A* **1999**, *865* (1-2), 211-226; (b) Warnke, M. M.; Cotton, F. A.; Armstrong, D. W. *Chirality* **2007**, *19* (3), 179-183; (c) Zhang, T.; Schaeffer, M.; Franco, P. *J. Chromatogr. A* **2005**, *1083* (1-2), 96-101.
66. (a) Gasparrini, F.; Misiti, D.; Villani, C. *J. Chromatogr. A* **2001**, *906* (1-2), 35-50; (b) Yamamoto, C.; Okamoto, Y. *Bull. Chem. Soc. Jpn.* **2004**, *77* (2), 227-257.
67. (a) Gasparrini, F.; Misiti, D.; Rompietti, R.; Villani, C. *J. Chromatogr. A* **2005**, *1064* (1), 25-38; (b) Gasparrini, F.; Misiti, D.; Villani, C. European Patent 2003079002, **2003**; (c) Han, X.; He, L.; Zhong, Q.; Beesley, T. E.; Armstrong, D. W. *Chromatographia* **2006**, *63* (1-2), 13-23; (d) Zhong, Q.; Han, X.; He, L.; Beesley, T. E.; Trahanovsky, W. S.; Armstrong, D. W. *J. Chromatogr. A* **2005**, *1066* (1-2), 55-70.
68. (a) Blaschke, G.; Donow, F. *Ber.* **1975**, *108* (8), 2792-8; (b) Blaschke, G.; Donow, F. *Ber.* **1975**, *108* (4), 1188-1197.
69. Okamoto, Y.; Honda, S.; Okamoto, I.; Yuki, H.; Murata, S.; Noyori, R.; Takaya, H. *J. Am. Chem. Soc.* **1981**, *103* (23), 6971-6973.
70. (a) Okamoto, Y.; Yashima, E.; Hatada, K.; Mislow, K. *J. Org. Chem.* **1984**, *49* (3), 557-8; (b) Okamoto, Y.; Mohri, H.; Hatada, K. *Polym. J.* **1989**, *21* (5), 439-445.
71. Allenmark, S. G.; Andersson, S.; Moeller, P.; Sancher, D. *Chirality* **1995**, *7* (4), 248-56.
72. (a) Saotome, Y.; Miyazawa, T.; Endo, T. *Chromatographia* **1989**, *28* (9-10), 505-8; (b) Thunberg, L.; Allenmark, S. *J. Chromatogr. A* **2004**, *1026* (1-2), 65-76; (c) Thunberg, L.; Allenmark, S.; Friberg, A.; Ek, F.; Frejd, T. *Chirality* **2004**, *16* (9), 614-624.
73. (a) Mitchell, C. R.; Armstrong, D. W. *Method Mol. Biol.* **2004**, *243*, 61-112; (b) Armstrong, D. W.; Zhang, B. *Anal. Chem.* **2001**, *73* (19), 557A-561A.
74. (a) Aboul-Enein, H. Y. *J. Sep. Sci.* **2003**, *26* (6/7), 521-524; (b) Preinerstorfer, B.; Lindner, W.; Laemmerhofer, M. *Electrophoresis* **2005**, *26* (10), 2005-2018.
75. Lindholm, J.; Fornstedt, T. *J. Chromatogr. A* **2005**, *1095* (1-2), 50-59.
76. Gasparrini, F.; Misiti, D.; Rompietti, R.; Villani, C. *J. Chromatogr. A* **2005**, *1064* (1), 25-38.
77. Phinney, K. W., SFC of drug enantiomers. *Anal. Chem.* **2000**, *72* (5), 204A-211A.
78. Han, X.; Wang, C.; He, L.; Beesley, T.; Armstrong, D. *Anal. Bioanal. Chem.* **2007**, *387* (8), 2681-2697.
79. Berthod, A.; He, B. L.; Beesley, T. E. *J. Chromatogr. A* **2004**, *1060* (1-2), 205-214.
80. Toribio, L.; David, F.; Sandra, P. *Quim. Anal. (Barcelona)* **1999**, *18* (3), 269-273.
81. Liu, Y.; Berthod, A.; Mitchell, C. R.; Xiao, T. L.; Zhang, B.; Armstrong, D. W. *J. Chromatogr. A* **2002**, *978* (1-2), 185-204.
82. Berthod, A. *Anal. Chem.* **2006**, *78* (7), 2093-2099.
83. Kawamura, M.; Uchiyama, T.; Kuramoto, T.; Tamura, Y.; Mizutani, K. *Carbohydr. Res.* **1989**, *192*, 83-90.

84. (a) Reijenga, J. C.; Verheggen, T. P. E. M.; Chiari, M. *J. Chromatogr. A* **1999**, 838 (1-2), 111-119; (b) Shizuma, M.; Takai, Y.; Kawamura, M.; Takeda, T.; Sawada, M. *J. Chem. Soc., Perkin Trans. 2* **2001**, (8), 1306-1314; (c) Takai, Y.; Okumura, Y.; Takahashi, S.; Sawada, M.; Kawamura, M.; Uchiyama, T. *J. Chem. Soc., Chem. Commun.* **1993**, (1), 53-54; (d) Takai, Y.; Okumura, Y.; Tanaka, T.; Sawada, M.; Takahashi, S.; Shiro, M.; Kawamura, M.; Uchiyama, T. *J. Org. Chem.* **1994**, 59 (11), 2967-2975; (e) Uchiyama, T.; Kawamura, M.; Uragami, T.; Okuno, H. *Carbohydr. Res.* **1993**, 241, 245-248; (f) Yoshie, N.; Hamada, H.; Takada, S.; Inoue, Y. *Chem. Lett.* **1993**, 22 (2), 353-356.
85. (a) Imaki, S.; Takuma, J.; Aiura, M.; Hosono, E. JP Patent 06121927, 1994; (b) Uchama, T. JP Patent 05076756, **1993**.
86. (a) Blair, S. M.; Brodbelt, J. S.; Marchand, A. P.; Kumar, K. A.; Chong, H.-S. *Anal. Chem.* **2000**, 72 (11), 2433-2445; (b) Brodbelt, J. S. *Int. J. Mass spectrom.* **2000**, 200 (1-3), 57-69; (c) Kempen, E. C.; Brodbelt, J. S. *Anal. Chem.* **2000**, 72 (21), 5411-5416; (d) Liou, C.-C.; Brodbelt, J. S. *J. Am. Soc. Mass. Spectrom.* **1992**, 3 (5), 543-548; (e) Maleknia, S.; Brodbelt, J. *J. Am. Chem. Soc.* **1992**, 114 (11), 4295-4298.
87. (a) Young, D.-S.; Hung, H.-Y.; Liu, L. K. *Rapid Commun. Mass Spectrom.* **1997**, 11 (7), 769-773; (b) Young, D.-S.; Hung, H.-Y.; Liu, L. K. *J. Mass Spectrom.* **1997**, 32 (4), 432-437.
88. Reale, S.; Teixidò, E.; Angelis, F. d. *Anal. Chim.* **2005**, 95 (6), 375-381.
89. Wang, C.; Breitbach, Z. S.; Armstrong, D. W. *Sep. Sci. Technol.* **2009**, in press.
90. Immel, S.; Schmitt, G. E.; Lichtenthaler, F. W. *Carbohydr. Res.* **1998**, 313 (2), 91-105.
91. Blair, S. M.; Kempen, E. C.; Brodbelt, J. S. *J. Am. Soc. Mass. Spectrom.* **1998**, 9 (10), 1049-1059.
92. Chu, I.-H.; Zhang, H.; Dearden, D. V. *J. Am. Chem. Soc.* **1993**, 115 (13), 5736-5744.
93. Blair, S. M.; Brodbelt, J. S.; Reddy, G. M.; Marchand, A. P. *J. Mass Spectrom.* **1998**, 33 (8), 721-728.
94. Niessen, W. M. A.; Tinke, A. P. *J. Chromatogr. A* **1995**, 703 (1-2), 37-57.
95. Cooks, R. G.; Patrick, J. S.; Kotiaho, T.; McLuckey, S. A. *Mass Spectrom. Rev.* **1994**, 13 (4), 287-339.
96. (a) Becke, A. D. *J. Chem. Phys.* **1993**, 98 (7), 5648-5652; (b) Lee, C.; Yang, W.; Parr, R. G. *Phys. Rev. B* **1988**, 37, 785; (c) Thom H. Dunning, J., *J. Chem. Phys.* **1989**, 90 (2), 1007-1023.
97. Andrae, D.; Häußermann, U.; Dolg, M.; Stoll, H.; Preuß, H. *Theor. Chem. Acc.* **1990**, 77 (2), 123-141.
98. Rodgers, M. T.; Armentrout, P. B. *Mass Spectrom. Rev.* **2000**, 19 (4), 215-247.
99. Shannon, R. *Acta Crystallogr., Sect. A* **1976**, 32 (5), 751-767.
100. Izatt, R.; Eatough, D.; Christensen, J. *Struct. Bond.* **1973**, 16, 161-189.
101. Kushibe, S.; Sashida, R.; Morimoto, Y. *Biosci. Biotechnol. Biochem.* **1994**, 58 (6), 1136-8.
102. Sawada, M.; Tanaka, T.; Takai, Y.; Hanafusa, T.; Hirotsu, K.; Higuchi, T.; Kawamura, M.; Uchiyama, T. *Chem. Lett.* **1990**, (11), 2011-2014.
103. Reijenga, J. C.; Verheggen, T. P. E. M.; Chiari, M. *J. Chromatogr. A* **1999**, 838 (1 + 2), 111-119.
104. Jiang, C.; Tong, M.-Y.; Breitbach, Z. S.; Daniel W. A. *Electrophoresis* **2009**, in press.
105. Walton, H. F. R., Roy D., *Ion Exchange in Analytical Chemistry*. CRC Press: Boca Raton, FL, 1990.
106. (a) Khym, J. X.; Zill, L. P. *J. Am. Chem. Soc.* **1952**, 74 (8), 2090-2094; (b) Rocklin, R. D.; Pohl, C. A. *J. Liq. Chromatogr. Related Technol.* **1983**, 6 (9), 1577 - 1590.
107. Goulding, R. W. *J. Chromatogr. A* **1975**, 103 (2), 229-239.
108. (a) Kawamoto, T.; Okada, E. *J. Chromatogr. A* **1983**, 258, 284-288; (b) Samuelson, O.; Sjöstrom, E. *Sven. Kem. Tidskr.* **1952**, 64, 305-314.
109. (a) Armstrong, D. W.; Jin, H. L. *J. Chromatogr.* **1989**, 462, 219-232; (b) Berthod, A.; Chang, S. S. C.; Kullman, J. P. S.; Armstrong, D. W. *Talanta* **1998**, 47 (4), 1001-1012; (c) Liu, Y.; Urganekar, S.; Verkade, J. G.; Armstrong, D. W. *J. Chromatogr. A* **2005**, 1079 (1-2), 146-152; (d) Wang, C.; Jiang, C.; Armstrong, D. W. *J. Sep. Sci.* **2008**, 31 (11), 1980-1990; (e) Alpert, A. J. *J. Chromatogr. A* **1990**, 499, 177-196; (f) Hemström, P.; Irgum, K. *J. Sep. Sci.* **2006**, 29 (12), 1784-1821.
110. Jin, H. L.; Stalcup, A. M.; Armstrong, D. W. *J. Liq. Chromatogr. Related Technol.* **1988**, 11 (16), 3295-3304.
111. Briggs, J.; Finch, P.; Matulewicz, M. C.; Weigel, H. *Carbohydr. Res.* **1981**, 97 (2), 181-188.

112. Stefansson, M.; Westerlund, D. *J. Chromatogr. A* **1996**, 720 (1-2), 127-136.
113. (a) Matsubara, M.; Kaneko, T.; Chiba, M.; Oota, N. JP Patent 06071903, **1994**; (b) Ono, H.; Ando, O.; Takeuchi, M. JP Patent 06124002, **1994**.
114. (a) Meji, I. JP Patent 06043573, **1994**; (b) Nishio, S. JP Patent 06250347, **1994**; (c) Nishio, S. JP Patent 07064249, **1995**; (d) Nishio, S.; Komatsu, H.; Shimizu, H. JP Patent 08029927, **1996**.
115. Nishioka, M.; Mori, H.; Nanjo, F. JP Patent 2004337133, **2004**.
116. (a) Ishikawa, K.; Nanjo, F. JP Patent 2005154388, **2005**; (b) Ishikawa, T.; Nanjo, F. JP Patent 2005179195, **2005**; (c) Schoch, C.; Bizec, J.-C.; Kis, G. *J. Inclusion Phenom. Macrocyclic Chem.* **2007**, 57 (1-4), 391-394; (d) Ishikawa, K.; Nanjo, F. JP Patent 2008069095, 2008; (e) Ishikawa, K.; Nanjo, F. JP Patent 2008069094, **2008**.
117. (a) Sawada, M.; Takai, Y.; Yamada, H.; Hirayama, S.; Kaneda, T.; Tanaka, T.; Kamada, K.; Mizooku, T.; Takeuchi, S. *J. Am. Chem. Soc.* **1995**, 117 (29), 7726-7736; (b) Sawada, M.; Takai, Y.; Shizuma, M.; Takeda, T.; Adachi, H.; Uchiyama, T. *Chem. Commun. (Cambridge)* **1998**, (14), 1453-1454.
118. Harata, K. *Bull. Chem. Soc. Jpn.* **1977**, 50 (6), 1416-1424.
119. Fehlhammer, W. P.; Schrölkamp, S.; Hoyer, M.; Hartl, H.; Beck, W. *Z. Anorg. Allg. Chem.* **2005**, 631 (15), 3025-3029.
120. Pedersen, C. *J. Am. Chem. Soc.* **1970**, 92 (2), 386-391.
121. (a) Pirkle, W. H.; Welch, C. J.; Lamm, B. *J. Org. Chem.* **1992**, 57 (14), 3854-3860; (b) Gasparini, F.; Misiti, D.; Villani, C.; La Torre, F.; Sinibaldi, M. *J. Chromatogr. A* **1988**, 457, 235-245; (c) Uray, G.; Lindner, W. *Chromatographia* **1990**, 30 (5), 323-327; (d) Okamoto, Y.; Ikai, T. *Chem. Soc. Rev.* **2008**, 37 (12), 2593-2608.
122. Sun, P.; Wang, C.; Breitbach, Z. S.; Zhang, Y.; Armstrong, D. W. *Anal. Chem.* **2009**, in press.
123. Chang, S. C.; Reid Iii, G. L.; Chen, S.; Chang, C. D.; Armstrong, D. W. *TrAC, Trends Anal. Chem.* **1993**, 12 (4), 144-153.
124. Ikai, T.; Yamamoto, C.; Kamigaito, M.; Okamoto, Y. *Polym. J.* **2006**, 38 (2), 91-108.
125. (a) Fanali, S. *J. Chromatogr. A* **2000**, 875 (1-2), 89-122; (b) Jiang, C.; Tong, M.-Y.; Armstrong, D. W.; Perera, S.; Bao, Y.; MacDonnell, F. M. *Chirality* **2009**, 21 (1), 208-217.
126. Zhang, Y.; Breitbach, Z. S.; Wang, C.; Armstrong, D. W. **2009**, in preparation.
127. Wang, C.; Yang, S. H.; Wang, J.; Kroll, P.; Schug, K. A.; Armstrong, D. W., submitted to *Int. J. Mass. Spectrom.* **2009**.
128. (a) Andersson, M. E.; Aslan, D.; Clarke, A.; Roeraade, J.; Hagman, G. *J. Chromatogr. A* **2003**, 1005 (1-2), 83-101; (b) de la Puente, M. L.; White, C. T.; Rivera-Sagredo, A.; Reilly, J.; Burton, K.; Harvey, G. *J. Chromatogr. A* **2003**, 983 (1-2), 101-114; (c) Matthijs, N.; Maftouh, M.; Heyden, Y. V. *J. Chromatogr. A* **2006**, 1111 (1), 48-61; (d) Perrin, C.; Matthijs, N.; Mangelings, D.; Granier-Loyaux, C.; Maftouh, M.; Massart, D. L.; Vander Heyden, Y. *J. Chromatogr. A* **2002**, 966 (1-2), 119-134; (e) Perrin, C.; Vu, V. A.; Matthijs, N.; Maftouh, M.; Massart, D. L.; Vander Heyden, Y. *J. Chromatogr. A* **2002**, 947 (1), 69-83.

BIOGRAPHICAL INFORMATION

Chunlei Wang obtained his Bachelor of Science degree from the University of Science and Technology of China in Applied Chemistry. He then went on to study under Dr. Daniel W. Armstrong at Iowa State University and the University of Texas at Arlington. He earned his Doctor of Philosophy in December 2009 working on research in areas such as enantiomeric separations by chromatographic methods and development of new chiral stationary phases.